Black holes, stars and cosmology in scalar-tensor theories

Timothy Anson

université
PARIS-SACLAY

Black holes, stars and cosmology in scalar-tensor theories

Trous noirs, étoiles et cosmologie dans les théories tenseur-scalaire

Thèse de doctorat de l'Université Paris-Saclay

École doctorale n° 564, École Doctorale de Physique en Île de France (EDPIF)
Spécialité de doctorat : Physique
Unité de recherche : Université Paris-Saclay, CNRS, IJCLab, 91405, Orsay, France
Référent : Faculté des Sciences d'Orsay

Thèse présentée et soutenue à Orsay, le 10/09/2021, par

Timothy ANSON

Composition du jury

Éric GOURGOULHON Directeur de Recherche, Laboratoire Univers et Théories, Observatoire de Paris	Président
Ruth GREGORY Professeure, Department of Physics, King's College London	Rapporteure & Examinatrice
David LANGLOIS Directeur de Recherche, Laboratoire AstroParticule et Cosmologie, Université Paris Diderot	Rapporteur & Examinateur
Vitor CARDOSO Professeur, Instituto Superior Técnico, Université de Lisbonne	Examinateur
Christos CHARMOUSIS Directeur de Recherche, Laboratoire de Physique des 2 Infinis Irène Joliot-Curie, Université Paris-Saclay	Examinateur
Thomas SOTIRIOU Professeur, School of Physics and Astronomy, Université de Nottingham	Examinateur

Direction de la thèse

Eugeny BABICHEV Chargé de Recherche, Laboratoire de Physique des 2 Infinis Irène Joliot-Curie, Université Paris-Saclay	Directeur de thèse

Thèse de doctorat

NNT: 2021UPASP067

Remerciements

This thesis owes a lot to many people that I've interacted with over the years. Thank you Eugeny for giving me the opportunity to carry out my PhD studies. Your guidance and ideas have been essential throughout these years, and I am very grateful for what you taught me. I am happy to have been your student. Christos, it was a pleasure to work and discuss with you. Even though you were not officially my supervisor, you were always there when I needed it and I appreciate it. Thank you Sabir and Mokhtar for enjoyable collaborations, it was nice to work with you. I am indebted to Ruth Gregory and David Langlois for accepting to referee my thesis, thank you for your valuable comments. Thank you to Vitor Cardoso and Thomas Sotiriou for being part of the committee, and for your comments on the thesis. Merci aussi à Éric Gourgoulhon d'avoir accepté de présider le jury de thèse, et pour tes commentaires sur le manuscrit. Merci Karim pour tes conseils et ton rôle de tuteur scientifique, nos discussions m'ont beaucoup aidé. Merci à Robin pour ton rôle dans le cadre du suivi de ma thèse. Thank you Marco for your tips about using Mathematica. Merci Gilles d'avoir pris le temps pour me conseiller lorsque j'étais à la recherche d'une thèse, et pour ton aide sur divers sujets scientifiques pendant ces années. Merci Sarah pour ton aide sur des questions administratives. Merci Marie-Agnès pour ta gentillesse et ton aide au quotidien pendant ma thèse, le laboratoire ne serait pas le même sans toi !

Merci à mes amis d'avoir rendu ces années bien plus agréables. Martin, Thomas, Dounia et Flo, merci pour les nombreux diners ou soirées qui m'ont permis de me changer les idées à maintes reprises. Merci aussi Martin de ton aide pour l'organisation de ma soutenance et du pot de thèse ! Merci aux autres étudiants du laboratoire pour les discussions notamment lors des pauses café: Amaury, Florentin, Gioacchino, Nicolas, Elie, Lydia, mais aussi tous les stagiaires qui sont passés plus ou moins brièvement pendant ces années. Un grand merci également à François et Quentin pour les moments conviviaux à l'IAP et dans les bars aux alentours, ainsi que pour les discussions scientifiques. Merci à mes amis de l'ENS : Alex et Cyril pour les journées de grimpe à Bleau, Jordan pour nos discussions échiquéennes, Andréane pour la découverte des plages normandes.

Merci à ma famille pour leur soutien permanent, et en particulier : Maman, Olivier et Co pour votre accueil à la campagne, qui a rendu le confinement bien plus agréable;

Papa pour ta relecture de la thèse; Marie-France pour ta générosité, ce fut une grande chance de pouvoir profiter de l'appartement à Saint-Mandé; Mémé, Bab et Lilou pour vos encouragements. Grazie mille Simone e Roberto per il vostro benvenuto in Ticino, è stato un vero piacere.

Enfin, merci Giulia d'avoir été à mes côtés, même dans les moments difficiles. Le soutien que tu m'as apporté est inestimable, et cette thèse te doit beaucoup.

Synthèse en français

Aperçu historique

La force gravitationnelle est l'une des interactions fondamentales de la nature. Pendant des siècles, le mouvement des corps célestes a été décrit dans le contexte de la physique newtonienne. Cependant, l'une des observations qui restait inexpliquée par cette théorie au début du 20e siècle est l'avance séculaire du périhélie de Mercure, qui s'écarte de la prédiction newtonienne de 43" par siècle. L'avance du périhélie dans le système solaire est principalement due à l'attraction gravitationnelle des autres planètes, puisqu'une planète seule en orbite autour du Soleil aurait une trajectoire elliptique. Un problème similaire s'était posé pour la planète Uranus. En 1846, Le Verrier a pu prédire l'existence et la position d'un corps perturbateur qui expliquerait les anomalies de son orbite, ce qui a conduit à la découverte de Neptune plus tard dans l'année. En 1859, il se rendit compte que le mouvement de Mercure ne pouvait être expliqué par la théorie newtonienne avec les planètes connues du système solaire. Il émit l'hypothèse qu'un nouvel objet pourrait exister encore plus près du Soleil, et ainsi expliquer ce mouvement anormal. Cependant, la prédiction était cette fois incorrecte et la nouvelle planète, qui devait être nommée Vulcain, ne fut pas trouvée. Par conséquent, l'avance du périhélie de Mercure restait inexpliquée dans la théorie de Newton. En 1915, Einstein publia sa théorie générale de la relativité (RG), dans laquelle il propose que la gravitation soit une manifestation de la courbure de l'espace-temps [1]. Dans cette description, le potentiel gravitationnel lui-même est intégré à la métrique de l'espace-temps $g_{\mu\nu}$. Le mouvement de la matière, qui est représentée par un tenseur énergie-impulsion $T_{\mu\nu}$, est directement lié à la géométrie de l'espace-temps par les équations d'Einstein :

$$R_{\mu\nu} - \frac{1}{2} R\, g_{\mu\nu} = \frac{8\pi G}{c^4} T_{\mu\nu} - \Lambda g_{\mu\nu} \,, \tag{1}$$

où G est la constante de Newton et c est la vitesse de la lumière dans le vide. En unités naturelles, nous avons $G = (8\pi M_P^2)^{-1}$, où la constante $M_P \sim 10^{18}$ GeV est la masse de Planck réduite.

Depuis sa proposition il y a plus d'un siècle, la relativité générale a passé tous les tests expérimentaux dans le système solaire, son premier triomphe étant la prédiction correcte de la précession séculaire du périhélie de Mercure. Même dans le cadre de

la physique newtonienne, il était compris que la lumière pouvait être déformée par des sources gravitationnelles. En utilisant une théorie corpusculaire de la lumière, cet effet a été calculé par Cavendish et Soldner, la première version publiée remontant à 1804 [2]. Cette prédiction a également été calculée par Einstein en 1911 en utilisant le principe d'équivalence. Cependant, dans la théorie complète de la RG, Einstein a réalisé que la déviation de la lumière devait être deux fois plus importante, et sa mesure constitue un deuxième test important de la RG. Cette déviation fut observée pour la première fois par Eddington et ses collaborateurs pendant l'éclipse solaire de 1919 [3], et ils ont conclu que la prédiction d'Einstein était correcte (bien que la faible précision de la mesure ait conduit à une controverse, voir par exemple Ref. [4]). Un autre test de la RG proposé par Einstein est le décalage vers le rouge gravitationnel, qui prédit que les photons perdent de l'énergie (et deviennent donc rouges) lorsqu'ils s'échappent d'un puits gravitationnel. Si l'on imagine deux horloges, l'une proche d'une source gravitationnelle et l'autre éloignée, un observateur fixe constate que la fréquence de la première est plus basse. En 1959, Pound et Rebka ont mesuré cet effet en tirant des rayons gamma du haut d'une tour de 22 mètres, montrant que les photons étaient décalés vers le bleu lors de leur chute. En plus des expériences du système solaire dans le régime de champ faible, la découverte des pulsars binaires en 1974 [5] a permis de tester la RG dans des environnements de champ fort [6].

La relativité générale peut également être appliquée à de très grandes échelles, en cosmologie. Dans ce cas, l'espace-temps est décrit par la métrique isotrope et homogène de Friedmann-Lemaître-Robertson-Walker (FLRW), qui s'écrit :

$$\mathrm{d}s^2 = -\mathrm{d}t^2 + a^2(t)\left(\frac{\mathrm{d}r^2}{1-\kappa r^2} + r^2\mathrm{d}\theta^2 + r^2\sin^2\theta\mathrm{d}\varphi^2\right) , \tag{2}$$

où la fonction a est appelée le facteur d'échelle et la constante κ est la courbure de l'espace. Elle peut prendre les valeurs $\kappa \in \{-1, 0, 1\}$, correspondant respectivement à un Univers ouvert, plat ou fermé. Nous supposons que le contenu énergétique de l'Univers peut être décrit par un fluide parfait de densité énergétique ρ et de pression P, auquel cas le tenseur énergie-impulsion prend la forme suivante :

$$T^{\mu}{}_{\nu} = \mathrm{diag}\left(-\rho, P, P, P\right) . \tag{3}$$

En substituant ces expressions dans l'Eq. (16), on obtient les équations de Friedmann

$$\frac{\ddot{a}}{a} = \frac{\Lambda}{3} - \frac{\rho + 3P}{6M_P^2} , \tag{4}$$

$$H^2 = \frac{\Lambda}{3} + \frac{\rho}{3M_P^2} - \frac{\kappa}{a^2} , \tag{5}$$

où le point représente la dérivée par rapport au temps cosmique t, et $H = \dot{a}/a$ est le paramètre de Hubble. Ces équations montrent que l'Univers n'est pas statique, c'est-à-dire que $H \neq 0$. En voulant que l'Univers soit statique à tout prix, conformément à la

compréhension traditionnelle, Einstein a essayé d'imposer $H = 0$ dans l'équation (5), sans se rendre compte que cet équilibre finement ajusté est de toute façon instable. Hubble a montré que l'Univers était en expansion en 1929 [7]. En combinant les équations de Friedmann, on obtient une troisième relation correspondant au fait que le tenseur énergie-impulsion a une divergence nulle, c'est-à-dire que $\nabla_\mu T^{\mu\nu} = 0$. Cela découle de l'identité géométrique $\nabla_\mu G^{\mu\nu} = 0$, où le tenseur d'Einstein $G_{\mu\nu}$ est défini comme suit :

$$G_{\mu\nu} = R_{\mu\nu} - \frac{1}{2} R g_{\mu\nu} \,. \tag{6}$$

Pour un fluide parfait, l'équation de continuité s'écrit

$$\dot{\rho} + 3H\left(\rho + P\right) = 0 \,. \tag{7}$$

Si nous considérons une équation d'état de la forme $P = w\rho$, avec w constant, alors il découle de l'équation (7) que

$$\rho\, a^{3(1+w)} = \text{const.} \tag{8}$$

Par conséquent, les différents types de matière se diluent différemment au fur et à mesure de l'expansion de l'Univers. La matière ordinaire correspond à $w = 0$, et la densité de matière ρ_m évolue comme $\rho_\text{m} \sim 1/a^3$, alors que pour le rayonnement nous avons $w = 1/3$ et la densité correspondante ρ_r décroît comme $\rho_\text{r} \sim 1/a^4$. Un autre cas intéressant est $w = -1$, qui correspond à l'énergie noire, ou une constante cosmologique. En effet, on peut considérer la constante cosmologique comme un fluide de densité $\rho_\Lambda = \Lambda M_P^2$ et de pression $P_\Lambda = -\Lambda M_P^2$, et donc $w = -1$. En fixant $\rho = P = 0$ dans l'équation (4), on voit qu'un Univers dominé par une constante cosmologique positive Λ correspond à une expansion accélérée de la forme $a \sim \exp(t\sqrt{\Lambda/3})$. L'expansion accélérée actuelle de l'Univers a été démontrée en 1998 [8,9] en utilisant des supernovae de type Ia (ces objets sont des chandelles standard, c'est-à-dire que leur pic de luminosité est connu et qu'ils fournissent donc un moyen précis de mesurer les distances à grande échelle). Ceci peut être expliqué dans le modèle standard de la cosmologie en introduisant une petite constante cosmologique $\Lambda_\text{eff} \sim 10^{-65}\,\text{GeV}^2$. De plus, puisque la valeur mesurée de la courbure spatiale de l'Univers est très faible, nous fixerons par la suite $\kappa = 0$ dans l'équation (2). Le contenu énergétique de l'Univers est aujourd'hui constitué de 3 composants majeurs : l'énergie noire ($\sim 68\%$), la matière noire froide ($\sim 27\%$), et la matière baryonique ($\sim 5\%$) [10].

Une autre prédiction fascinante de la RG est l'existence des trous noirs, qui sont des objets si compacts que même les rayons lumineux sont piégés en leur sein. Ces trous noirs avaient été conceptualisés même dans le contexte de la physique newtonienne, notamment par Michell et Laplace au 19e siècle. Quelques mois après la publication de la RG, Schwarzschild trouva une solution statique aux équations d'Einstein dans le vide, à savoir $R_{\mu\nu} = 0$. Nous discuterons de quelques propriétés de cette solution plus en détail dans le chapitre 7, ainsi que de la métrique de Kerr [11] pour un trou noir en rotation. Alors que l'on a longtemps pensé que de tels objets présentaient un

intérêt purement mathématique, de plus en plus de mesures expérimentales montrent que les trous noirs existent dans la nature, et ils seront au cœur de la dernière partie de cette thèse. Contrairement à la théorie newtonienne, la RG prédit l'existence d'ondes gravitationnelles. De telles ondes ont été détectées en 2015 à l'aide d'interféromètres terrestres [12] provenant de la coalescence lointaine de deux trous noirs, bien que des preuves indirectes de leur existence aient déjà été obtenues par l'étude de pulsars binaires [13]. Il s'agit à nouveau d'un succès de la RG, qui a ouvert la voie à une nouvelle ère de tests expérimentaux de la théorie dans le régimes de champ fort.

Malgré tous les triomphes de la RG que nous avons évoqués, il reste quelques phénomènes inexpliqués qui ont encouragé les physiciens à envisager des théories alternatives de la gravitation. Tout d'abord, il est bien connu que la relativité générale n'est pas renormalisable, ce qui signifie qu'elle perd son pouvoir prédictif à des énergies élevées. L'énergie qui correspond à cette coupure est la masse de Planck $m_P = \sqrt{8\pi} M_P \sim 10^{19}$ GeV. De nombreux efforts ont été déployés au cours des dernières décennies pour construire une théorie de la gravité complète dans l'ultraviolet, la tentative la plus célèbre étant la théorie des cordes. Un autre problème est lié à la faible valeur expérimentale de la constante cosmologique. Dans une théorie quantique des champs, on s'attend à une correction quantique $\delta\Lambda$ qui s'ajoute à la valeur nue pour former la contante mesurée $\Lambda_{\text{eff}} = \Lambda + \delta\Lambda$. En supposant une coupure à l'échelle de Planck m_P, les corrections quantiques sont estimées de l'ordre de $\delta\Lambda \sim 10^{37}\text{GeV}^2$, ce qui signifie que les deux contributions à Λ_{eff} devraient s'annuler avec une précision de plus de 100 ordres de grandeur. Un calcul différent utilisant la régularisation dimensionnelle atténue le problème, mais il reste une divergence d'environ 50 ordres de grandeur (voir Ref. [14] pour une revue). C'est ce que l'on appelle le problème de la naturalité, qui se produit de manière similaire (mais pas aussi radicale) pour la masse du boson de Higgs en physique des particules. Il existe d'autres problèmes liés à la cosmologie, l'un d'eux étant le problème de la platitude. On peut le comprendre facilement en introduisant la densité critique $\rho_{\text{c}} = 3M_P^2 H^2$ et en réécrivant l'équation (5) avec $\Lambda = 0$ comme suit :

$$\left(\frac{\rho_{\text{c}}}{\rho} - 1\right) \rho a^2 = -3\kappa M_P^2 \,.$$

Puisque le côté droit de l'équation précédente est constant, le côté gauche doit également rester constant tout au long de l'évolution de l'Univers. Cependant, étant donné que pendant la domination de la matière et du rayonnement, la combinaison ρa^2 diminue, le deuxième terme du côté gauche doit augmenter. Les mesures actuelles montrent que $|1 - \rho_{\text{c}}/\rho|$ est très petit aujourd'hui, ce qui implique qu'il était extrêmement petit (environ 10^{-62}) aux premiers instants de l'Univers, et il n'y a pas de mécanisme permettant d'expliquer cet ajustement fin. Un autre problème est celui dit de l'horizon. Le satellite Planck [10] a pu mesurer la température du fond diffus cosmologique avec une grande précision, et des régions du ciel qui n'auraient pas pu être en contact causal dans le passé ont une température très proche, ce qui laisse perplexe. Heureusement, une explication possible de ces deux problèmes a été proposée

dans les années quatre-vingt, et repose sur une période d'expansion accélérée au tout début de l'histoire de l'Univers, appelée l'inflation [15–22]. Pendant cette période, le facteur d'échelle a croît exponentiellement (au moins d'un facteur e^{60}), et cela permet d'expliquer les deux problèmes précédents. Une autre caractéristique intrigante de l'Univers est qu'environ 85% de la matière est invisible, en ce sens qu'elle n'émet pas de lumière, d'où le nom de matière noire. L'analyse des courbes de rotation des galaxies spirales (c'est-à-dire la distribution de la vitesse des étoiles), suggère l'existence de matière invisible qui interagit gravitationnellement et expliquerait les profils plats observés. À plus grande échelle, la masse des amas de galaxies peut être déterminée à l'aide de techniques de lentilles gravitationnelles, et fournit également une motivation pour l'existence de la matière noire (voir Ref. [23] pour une revue récente). La compréhension de sa nature est l'un des défis principaux de la physique moderne.

Théories tenseur-scalaire

Introduisons maintenant les théories tenseur-scalaire, qui fournissent un cadre général pour les travaux présentés dans cette thèse. Les théories alternatives de la gravitation nous permettent de prédire et de tester les déviations à la RG, ce qui est déjà une raison suffisante pour motiver leur étude. De plus, les défauts de la RG discutés précédemment fournissent une incitation supplémentaire à considérer ces théories alternatives, dans l'espoir d'obtenir des réponses aux questions que nous avons mentionnées. Les équations d'Einstein peuvent être obtenues à partir de l'action d'Einstein-Hilbert :

$$S = \frac{M_P^2}{2}\int \mathrm{d}^4x\sqrt{-g}(R-2\Lambda) + S_\mathrm{m}\left[g_{\mu\nu},\psi_\mathrm{m}\right] \ , \tag{9}$$

où ψ_m désigne les champs de matière qui sont couplés minimalement à la métrique $g_{\mu\nu}$. Le tenseur énergie-impulsion $T_{\mu\nu}$ est défini en utilisant l'action de matière de la manière suivante :

$$T_{\mu\nu} = -\frac{2}{\sqrt{-g}}\frac{\delta S_\mathrm{m}}{\delta g^{\mu\nu}} \ . \tag{10}$$

Le principe de moindre action appliqué à cette théorie conduit aux équations d'Einstein. Selon un théorème de Lovelock [24, 25], les seuls 2-tenseurs en 4 dimensions ayant une divergence nulle, et construits avec la métrique et ses dérivées premières et secondes uniquement sont la métrique $g_{\mu\nu}$ elle-même et le tenseur d'Einstein $G_{\mu\nu}$. Par conséquent, pour obtenir des équations du mouvement différentes de celles de la RG, il est nécessaire de briser l'une des hypothèses du théorème de Lovelock. Par exemple, on peut considérer des champs supplémentaires médiateurs de la gravité, changer la dimension de l'espace-temps ou introduire des dérivées supérieures dans l'action. La façon la plus simple de modifier la RG est de construire une théorie avec un champ scalaire en plus de la métrique, qui s'appelle une théorie tenseur-scalaire. La détection du boson de Higgs en 2012 a montré que les champs scalaires peuvent exister dans la nature [26]. De plus, on s'attend à ce qu'ils apparaissent dans les actions effectives

quadri-dimensionnelles des théories des cordes, après compactification des dimensions supplémentaires (voir Réf. [27]). On s'attend également à ce que les champs scalaires participent à la phase inflationnaire de l'Univers. Pour ces raisons, il semble naturel de considérer les théories tenseur-scalaire comme des extensions de la RG et d'étudier leurs propriétés. Nous nous concentrerons sur ce type de modification tout au long de la thèse, bien qu'il existe de nombreuses autres théories de gravité modifiée (voir Refs. [28, 29] pour des revues). En 1961, Brans et Dicke [30], s'appuyant notamment sur les travaux antérieurs de Jordan [31], ont proposé une théorie qui inclut un champ scalaire supplémentaire ϕ pouvant être interprété comme une constante de Newton variable. L'action de la théorie de Jordan-Brans-Dicke est la suivante :

$$S_{\rm JBD} = \frac{M_P^2}{2}\int \mathrm{d}^4\sqrt{-g}\left[\phi R - \frac{\omega_0}{\phi}\left(\partial\phi\right)^2\right] \ , \tag{11}$$

où ω_0 est une constante. Cette action a été étendue plus tard en remplaçant la constante ω_0 par une fonction $\omega(\phi)$, et en ajoutant un terme potentiel pour le champ scalaire [32]. Ces extensions sont habituellement appelées théories tenseur-scalaire, bien que nous utilisions ce terme dans un sens plus large dans cette thèse, comme nous allons le discuter. En effet, les théories tenseur-scalaire standard ne contiennent que les dérivées premières du scalaire dans l'action. Dans les années soixante-dix, Horndeski a déterminé l'action la plus générale contenant un scalaire ϕ et la métrique qui conduit à des équations d'Euler-Lagrange du second ordre [33], et le lagrangien contient les dérivées secondes du champ scalaire. Cette classe de théories a été redécouverte récemment lors de l'extension du modèle des galileons [34] à un espace-temps courbe [35–37], et il a été démontré qu'elle est équivalente à la théorie de Horndeski [38]. Dans la formulation moderne, le lagrangien de Horndeski s'écrit

$$\begin{aligned}\mathcal{L}_{\rm H} &= f(\phi,X)R + K(\phi,X) - G_3(\phi,X)\Box\phi - 2f_X\left(\{\Box\phi\}^2 - \phi_{\mu\nu}\phi^{\mu\nu}\right)\\ &\quad + G_5(\phi,X)G_{\mu\nu}\phi^{\mu\nu} + \frac{1}{3}G_{5X}\left(\{\Box\phi\}^3 - 3\Box\phi\,\phi^{\mu\nu}\phi_{\mu\nu} + 2\phi_{\mu\alpha}\phi^{\alpha\nu}\phi^{\mu}{}_{\nu}\right) \ ,\end{aligned} \tag{12}$$

où $X = \partial_\mu\phi\partial^\mu\phi$, $f_X = \partial f/\partial X$, et nous utilisons les notations abrégées $\phi_\mu = \nabla_\mu\phi$, $\phi_{\mu\nu} = \nabla_\mu\nabla_\nu\phi$. Le fait d'exiger que les équations de champ soient du second ordre permet d'éviter l'apparition d'un fantôme d'Ostrogradsky [39, 40], qui est un degré de liberté avec une énergie ne possédant pas de borne inférieure. Bien qu'avoir des équations du second ordre soit une condition suffisante pour obtenir une théorie ne contenant pas de fantôme d'Ostrogradsky, ce n'est pas une condition nécessaire. En effet, le théorème d'Ostrogradsky ne s'applique qu'aux Lagrangiens non dégénérés, ce qui signifie qu'il est possible qu'une théorie aux dérivées supérieures soit saine (dans le sens qu'elle ne contient pas de fantôme d'Ostrogradsky) si elle est également dégénérée. Par conséquent, des théories tenseur-scalaire au-delà de la classe de Horndeski ont été recherchées. Le premier pas dans cette direction a été obtenu en effectuant une transformation disforme du tenseur métrique [41] :

$$\tilde{g}_{\mu\nu} = C(\phi,X)g_{\mu\nu} + D(\phi,X)\phi_\mu\phi_\nu \ . \tag{13}$$

Il a été montré dans la Réf. [42] que l'action de Horndeski est stable sous cette transformation si les fonctions C et D ne dépendent pas du terme cinétique X. Cependant, si les fonctions C et D dépendent de X mais sont choisies de manière à ce que la transformation soit inversible, alors la relation précédente est simplement un changement de variable, et une théorie devrait rester saine sous une telle transformation même si les équations d'Euler-Lagrange contiennent des dérivées d'ordre supérieur. Cette propriété intéressante a été soulignée pour la première fois dans la Réf. [43]. Elle a conduit au développement de théories au-delà de la classe de Horndeski, et des extensions des termes G_4 et G_5 ont été trouvées dans la Ref. [44], qui peuvent être obtenues par transformation purement disforme de la théorie de Horndeski. La classe la plus générale des théories tenseur-scalaire saines a ensuite été isolée en imposant certaines conditions de dégénérescence sur le Lagrangien, permettant de réduire les équations de champ d'ordre supérieur à un système du second ordre et donc d'éviter la propagation d'un fantôme d'Ostrogradsky. Ces théories ont été appelées Extended Scalar-Tensor (EST) [45], ou Degenerate Higher-Order Scalar-Tensor (DHOST) theories [46, 47], et nous utiliserons ce dernier nom dans la thèse. Le Lagrangien DHOST quadratique, c'est-à-dire contenant des termes au plus quadratiques en les dérivées secondes du champ scalaire ϕ, s'écrit

$$S = \frac{M_P^2}{2}\int \mathrm{d}^4x\sqrt{-g}\left(f(\phi,X)R + K(\phi,X) - G_3(\phi,X)\Box\phi + \sum_{i=1}^{5}\mathcal{L}_i\right) , \tag{14}$$

où les densités scalaires $\mathcal{L}_i$ sont données par

$$\begin{aligned}
\mathcal{L}_1 &= A_1(\phi,X)\,\phi_{\mu\nu}\phi^{\mu\nu} ,\\
\mathcal{L}_2 &= A_2(\phi,X)\,(\Box\phi)^2 ,\\
\mathcal{L}_3 &= A_3(\phi,X)\,\phi_{\mu\nu}\phi^{\mu}\phi^{\nu}\Box\phi ,\\
\mathcal{L}_4 &= A_4(\phi,X)\,\phi_{\mu\alpha}\phi^{\alpha\nu}\phi^{\mu}\phi_{\nu} ,\\
\mathcal{L}_5 &= A_5(\phi,X)\,\left(\phi_{\mu\nu}\phi^{\mu}\phi^{\nu}\right)^2 .
\end{aligned} \tag{15}$$

Plusieurs sous-classes de théories DHOST peuvent être obtenues à partir de cette action. Dans chaque classe, des conditions de dégénérescence spécifiques sont supposées afin d'éviter l'apparition du fantôme d'Ostrogradsky.

Structure et principaux résultats de la thèse

Dans cette thèse, je présente plusieurs sujets dans le contexte général des théories tenseur-scalaire de la gravitation. La première partie de la thèse est consacrée à la cosmologie des théories présentant une scalarisation spontanée des objets compacts. Je décris le mécanisme de scalarisation dans le chapitre 1, à la fois dans le contexte des théories tenseur-scalaire standard et dans le cas d'un couplage non trivial au scalaire de Gauss-Bonnet. Il repose sur une masse effective tachionique acquise par le champ

scalaire, et je montre dans le chapitre 2 que cela conduit génériquement à une instabilité des modes scalaires pendant l'inflation. Ceci est vrai dans les deux cas que nous considérons, c'est-à-dire le modèle de Damour et Esposito-Farèse (DEF) et les théories avec un couplage au terme de Gauss-Bonnet. Un mécanisme pour résoudre cette instabilité dans le cas du modèle DEF, reposant sur un couplage du champ scalaire à l'inflaton, est proposé dans le chapitre 3. Ce couplage induit une masse effective pour le scalaire, qui permet de le stabiliser pendant la période inflationnaire. Bien que l'amplitude du scalaire croisse durant les phases ultérieures de l'expansion de l'Univers (comme dans le modèle DEF), sa valeur actuelle est suffisamment faible pour passer les tests expérimentaux actuels de la RG.

Dans la deuxième partie, j'étudie l'écrantage de Vainshtein pour les étoiles en rotation lente dans les théories tenseur-scalaire. Les tests de la gravité dans le système solaire sont tous compatibles avec les RG. Il est donc important qu'une théorie modifiée de la gravité dispose d'un mécanisme qui rétablisse la RG à proximité des sources gravitationnelles, et l'écrantage de Vainshtein est l'un des moyens d'y parvenir. Il a été beaucoup étudié dans le cas de sources à symétrie sphérique, mais les objets astrophysiques réalistes sont en rotation, et l'objectif était d'étudier cet effet dans le cas d'étoiles en rotation lente. Pour ceci, j'utilise le formalisme de Hartle, qui nécessite d'introduire une fonction supplémentaire ω dans le tenseur métrique. Celle-ci est responsable de l'effet Lense-Thirring prédit par la théorie de la relativité. Notez que dans certains cas, l'équation satisfaite par ω dans le vide est la même que pour la RG, ce que je montre dans l'annexe II.A. Dans le chapitre 4, j'écris l'équation satisfaite par la fonction ω traduisant la rotation lente de la source. Je me place ensuite dans l'approximation de champ faible et écris les solutions pour ω dans ce cas, montrant qu'en général le mécanisme d'écrantage peut être étendu à la fonction ω en dehors de la source. Cependant, il est possible que ω reçoive des corrections d'ordre supérieur à l'intérieur de la source. Dans le chapitre 5, j'étudie l'écrantage dans le cas d'un champ scalaire dépendant du temps, et donne des exemples dans différentes classes de théories. Je montre que même si l'écrantage de Vainshtein fonctionne en symétrie sphérique, il n'est pas nécessaire que les corrections pour ω soient atténuées par des puissances du rayon de Vainshtein r_V. Dans ces cas, bien que l'écrantage fonctionne également pour ω, il est moins efficace que pour les potentiels de la métrique. L'écrantage dans le cas d'un champ scalaire statique est ensuite étudié dans le chapitre 6. Je considère une certaine classe de théories de Horndeski permettant d'échapper au théorème de calvitie pour les étoiles. Dans ce cas, les résultats sont similaires au cas du scalaire dépendant du temps.

La dernière partie de la thèse porte sur les trous noirs, et je commence par passer en revue les solutions (non chargées) de la RG dans le chapitre 7, en rappelant certaines propriétés importantes des solutions de Schwarzschild et de Kerr. Dans le chapitre 8, des solutions de trous noirs en rotation dans des théories tenseur-scalaire sont construites en effectuant une transformation disforme de la métrique de Kerr, et j'explique les propriétés de ces espaces-temps. Ces solutions axisymétriques sont similaires à celle de

Kerr à certains égards : la même singularité ; une expansion asymptotique similaire ; l'existence d'une ergorégion. Cependant, elles sont très différents de l'espace-temps de Kerr sous d'autres aspects : absence de circularité ; $R_{\mu\nu} \neq 0$; pas de tenseur de Killing non trivial ; la limite stationnaire est distincte de l'horizon ; ce dernier n'est pas un horizon de Killing et a un profil dépendant de θ. Il est important de noter que ces espaces-temps restent causaux même après une petite perturbation des cônes de lumière, ce qui permet d'éviter les pathologies telles que les courbes temporelles fermées dans la région située en dehors de l'horizon. Des exemples intéressants de métriques de trous noirs non circulaires sont obtenus dans les limites $D \to -1$ (quasi-Weyl) et $D \to \infty$ (Schwarzschild non circulaire), où D est le paramètre disforme. En raison de leur simplicité par rapport au cas générique, une analyse détaillée de ces métriques pourrait être utile pour comprendre les propriétés des espaces non circulaires. Après avoir présenté la métrique de Schwarzschild non circulaire, je montré qu'elle est du type I de Petrov. Bien que le calcul explicite ne soit présenté que dans ce cas simple, le résultat est valable pour des $D \neq 0$ et $a \neq 0$ génériques. L'orbite des étoiles autour d'un trou noir de Kerr déformé est analysée dans le chapitre 9. J'y calcule la variation séculaire des paramètres orbitaux jusqu'au deuxième ordre post-newtonien pour différentes limites du paramètre disforme D. De manière générale, les métriques disformes ne satisfont pas le théorème de calvitie de la RG, qui stipule que les multipôles d'ordre supérieur sont déterminés de manière unique par la masse et le moment angulaire du trou noir. En particulier, la mesure simultanée du spin et du quadrupôle de Sgr A*, permettra de tester cette propriété dans le futur. Dans une limite particulière de D, il est possible d'obtenir une prédiction différente de la RG pour la précession du péricentre au premier ordre post-newtonien. Ceci constitue une prédiction venant d'une théorie de gravité modifiée, et permet de contraindre le paramètre disforme en utilisant les observations actuelles provenant de l'orbite de l'étoile S2 autour de Sgr A*.

Cette thèse a donné lieu aux publications suivantes :

- T. Anson, E. Babichev and C. Charmousis, *Deformed black hole in Sagittarius A*, *Phys. Rev. D* **103** no. 12, (2021) 124035,
- T. Anson, E. Babichev, C. Charmousis and M. Hassaine, *Disforming the Kerr metric*, *JHEP* **01** (2021) 018,
- T. Anson and E. Babichev, *Vainshtein screening for slowly rotating stars*, *Phys. Rev. D* **102** no. 4, (2020) 044046,
- T. Anson, E. Babichev, and S. Ramazanov, *Reconciling spontaneous scalarization with cosmology*, *Phys. Rev. D* **100** no. 10, (2019) 104051,
- T. Anson, E. Babichev, C. Charmousis, and S. Ramazanov, *Cosmological instability of scalar-Gauss-Bonnet theories exhibiting scalarization*, *JCAP* **06** (2019) 023.

Contents

Remerciements i

Synthèse en français iii

Introduction 1
Historical overview 1
Scalar-tensor theories 5
Structure of the thesis 9

I Cosmology of theories exhibiting spontaneous scalarization 11

Introduction to Part I 12

1 Scalarization of compact objects 13
1.1 The Damour–Esposito-Farèse model of scalarization 13
1.2 Coupling to the Gauss-Bonnet scalar 15

2 Cosmological instability of the scalar mode 19
2.1 Cosmology and scalar fluctuations 19
2.2 Instability of the perturbations on an FLRW background 23
2.3 Catastrophic instability of the scalar field during inflation 25

3 Quenching the cosmological instability in the DEF model 31
3.1 Setting the problem: cosmological instability of the scalar 31
3.2 Cosmological relaxation of the field ϕ to zero 35

Conclusion to Part I 42

II Vainshtein screening for slowly rotating stars 45

Introduction to part II 46

4 Setup and weak-field approximation **51**
4.1 Equations of motion for slow rotation 51
4.2 Frame-dragging function in the weak-field approximation 54

5 Slow rotation with a time-dependent scalar field **59**
5.1 General equations 59
5.2 Outside the Vainshtein radius 61
5.3 Case 1: $C_3 \neq 0$ and $\Gamma_1 \neq 0$, inside the Vainshtein radius 62
5.4 Case 2: $C_3 = \Gamma_1 = 0$ and $C_2 \neq 0$ inside the Vainshtein radius 65

6 Slow rotation with a static scalar field **71**
6.1 K-essence 72
6.2 Cubic Galileon 74
6.3 Quadratic sector of Horndeski theory 76

Conclusion to Part II **79**

Appendices **81**
II.A Relativistic sources in shift-symmetric theories 81
II.B List of coefficients 83

III Disforming the Kerr metric **87**

Introduction to Part III **88**

7 Black holes in general relativity **91**
7.1 Schwarzschild black hole and definitions 91
7.2 The Kerr spacetime 95

8 The disformed Kerr metrics **103**
8.1 Construction of the disformed Kerr metrics 103
8.2 Properties of the disformed Kerr metrics 107
8.3 Interesting limiting cases 119
8.4 Petrov type of the disformed metrics 123

9 Orbit of stars in the disformed Kerr spacetime **127**
9.1 Comparison of different metrics asymptotically 127
9.2 Two-timescale analysis for the secular variation of orbital elements . . . 131
9.3 Orbital perturbations for the disformed Kerr metric 135

Conclusion to Part III **146**

Appendices **149**
III.A Polynomials Q_i 149
III.B Secular shifts for the EKD metric 149
III.C Leading-order pericenter precession using the textbook method 151

Summary **155**

Bibliography **157**

Abstract **177**

Introduction

Historical overview

The gravitational force is one of the fundamental interactions of Nature. For centuries, the motion of celestial bodies was understood in the context of Newtonian physics. However, one of the observations that remained unexplained by this theory at the beginning of the 20th century is the secular advance of the perihelion of Mercury, which deviates from the Newtonian prediction by 43" per century. The perihelion advance in the Solar System is mainly caused by the gravitational pull of other planets, since a lone planet orbiting the Sun would have an elliptic trajectory. A similar problem had occurred for the planet Uranus. In 1846, Le Verrier was able to predict the existence and position of a perturbing body which would explain the discrepancies in its orbit, and this led to the discovery of Neptune later that year. In 1859, he realized that the motion of Mercury could not be explained by Newtonian theory with the known planets in the Solar System. He suggested that a new object may exist even closer to the Sun, and that it could explain this anomalous motion. However, this time the prediction was incorrect and the new planet, which was to be named Vulcan, was not found. Hence, Mercury's perihelion advance remained unexplained in Newton's theory. In 1915, Einstein published his general theory of relativity (GR), in which he proposed that gravitation is a manifestation of spacetime curvature [1]. In this description, the gravitational potential itself is part of the spacetime metric $g_{\mu\nu}$. The movement of matter, which is represented by a stress-energy tensor $T_{\mu\nu}$, is directly linked to the geometry of spacetime through Einstein's equations:

$$R_{\mu\nu} - \frac{1}{2} R\, g_{\mu\nu} = \frac{8\pi G}{c^4} T_{\mu\nu} - \Lambda g_{\mu\nu} \,, \tag{16}$$

where G is Newton's constant and c is the velocity of light in vacuum.[1] In natural units, we have $G = (8\pi M_P^2)^{-1}$, where the constant $M_P \sim 10^{18}$ GeV is the reduced Planck mass. We will use it instead of G in most of the thesis.

[1] We will follow the conventions of Misner-Thorne-Wheeler [48] throughout the thesis, and in particular we use the mostly-plus metric signature $(-,+,+,+)$. We will also employ natural units where $c = \hbar = 1$. Furthermore, each part of this thesis is independent, and the same letter may have a different meaning depending on the part.

Since its proposal more than a century ago, general relativity has passed all experimental tests in the Solar System, the first triumph being the correct prediction of the secular perihelion precession of Mercury. It was understood even in Newtonian physics that light could be bent by gravitational sources. Using a corpuscular theory of light, this effect was calculated by Cavendish and Soldner, the first published version dating back to 1804 [2]. This prediction was also calculated by Einstein in 1911 using the principle of equivalence. However, in the full theory of GR Einstein realized that the deflection of light should be twice as large, and its measurement constitutes a second important test of GR. The light bending effect was first observed by Eddington and his collaborators during the solar eclipse of 1919 [3], and they concluded that Einstein's prediction was correct (though the low accuracy of the measurement led to controversy, see for instance Ref. [4]). Another test of GR proposed by Einstein is the gravitational redshift, which predicts that photons lose energy (and hence become red) when escaping a gravitational well. If one imagines two clocks, one near a gravitational source and the other far away, then the former would be seen to tick slower from the point of view of a fixed observer. In 1959 Pound and Rebka measured this effect by shooting gamma rays from the top of a 22 meter tower, showing that the photons were blueshifted as they fell [49]. A useful framework to test general relativity is the so-called parametrized post-Newtonian (PPN) formalism, the first version of which was written by Eddington in 1923. The metric for a spherically symmetric source of mass M in isotropic coordinates and in the nonrelativistic limit can be parametrized as

$$\begin{aligned} \frac{g_{tt}}{c^2} &= -1 + \frac{2GM}{rc^2} - 2\beta_{\rm PPN}\left(\frac{GM}{rc^2}\right)^2 + \mathcal{O}\left(\frac{1}{c^6}\right) , \\ g_{ti} &= 0 , \\ g_{ij} &= \delta_{ij}\left(1 + 2\gamma_{\rm PPN}\frac{GM}{rc^2}\right) + \mathcal{O}\left(\frac{1}{c^4}\right) . \end{aligned} \tag{17}$$

The 2 parameters $\{\beta_{\rm PPN}, \gamma_{\rm PPN}\}$ quantify the deviations from GR, for which we have $\beta_{\rm PPN} = \gamma_{\rm PPN} = 1$. This formalism was later extended, notably by Nordtvedt and Will, and now includes 10 parameters which can be confronted with experiments (see Ref. [50] for a review). In addition to the Solar System experiments in the weak field regime, the discovery of binary pulsars in 1974 [5] provided the possibility to test GR in strong field environments [6].

General relativity can also be applied on very large scales, in cosmology. In this case spacetime is described by the isotropic and homogeneous Friedmann-Lemaître-Robertson-Walker (FLRW) metric, which is given by the following line element:

$$\mathrm{d}s^2 = -\mathrm{d}t^2 + a^2(t)\left(\frac{\mathrm{d}r^2}{1-\kappa r^2} + r^2\mathrm{d}\theta^2 + r^2\sin^2\theta\mathrm{d}\varphi^2\right) , \tag{18}$$

where the time-dependent function a is called the scale factor and the constant κ is the curvature of space. It can take the values $\kappa \in \{-1, 0, 1\}$, corresponding respectively to

an open, flat or closed Universe. We assume that the energy content of the Universe can be described by a perfect fluid of energy density ρ and pressure P, in which case the energy-momentum tensor takes the form

$$T^{\mu}{}_{\nu} = \mathrm{diag}\left(-\rho, P, P, P\right) \ . \tag{19}$$

Substituting these expressions in Eq. (16), we obtain the Friedmann equations

$$\frac{\ddot{a}}{a} = \frac{\Lambda}{3} - \frac{\rho + 3P}{6M_P^2} \ , \tag{20}$$

$$H^2 = \frac{\Lambda}{3} + \frac{\rho}{3M_P^2} - \frac{\kappa}{a^2} \ , \tag{21}$$

where a dot stands for differentiation with respect to cosmic time t, and $H = \dot{a}/a$ is the Hubble parameter. These equations show that the Universe is not static, i.e. $H \neq 0$. By wanting the Universe to be static at all cost, in line with the traditional understanding, Einstein famously tried to enforce $H = 0$ in Eq. (21), not realizing that this fine-tuned equilibrium is unstable anyway. The Universe was shown to be expanding by Hubble in 1929 [7]. By combining the Friedmann equations, we obtain a third relation corresponding to the fact that energy-momentum tensor is divergence-less, i.e. $\nabla_\mu T^{\mu\nu} = 0$. This follows from the geometric identity $\nabla_\mu G^{\mu\nu} = 0$, where the Einstein tensor $G_{\mu\nu}$ is defined as

$$G_{\mu\nu} = R_{\mu\nu} - \frac{1}{2} R g_{\mu\nu} \ . \tag{22}$$

For a perfect fluid, the continuity equation reads

$$\dot{\rho} + 3H\left(\rho + P\right) = 0 \ . \tag{23}$$

If we assume an equation of state of the form $P = w\rho$, with w constant, then it follows from Eq. (23) that

$$\rho\, a^{3(1+w)} = \text{const.} \tag{24}$$

Hence, different types of matter are diluted differently as the Universe expands. Ordinary matter corresponds to $w = 0$, and the matter density ρ_m evolves as $\rho_\mathrm{m} \sim 1/a^3$, while for radiation we have $w = 1/3$ and the corresponding density ρ_r decays as $\rho_\mathrm{r} \sim 1/a^4$. Another interesting case is $w = -1$, which corresponds to dark energy, or the cosmological constant. Indeed, one can view the cosmological constant as a fluid with density $\rho_\Lambda = \Lambda M_P^2$ and pressure $P_\Lambda = -\Lambda M_P^2$, and hence $w = -1$. By setting $\rho = P = 0$ in Eq. (20), we see that a Universe dominated by a positive cosmological constant Λ corresponds to an accelerated expansion of the form $a \sim \exp(t\sqrt{\Lambda/3})$. The current expansion of the Universe was shown to be accelerated in 1998 [8,9] using type Ia supernovae (these objects are standard candles, i.e. their peak brightness is known and hence they provide an accurate way to measure distances on large scales). The

expansion can be explained in the standard model of cosmology by introducing a small cosmological constant $\Lambda_{\text{eff}} \sim 10^{-65}\,\text{GeV}^2$. In addition, the curvature of the Universe is measured to be extremely small, so we will set $\kappa = 0$ in Eq. (18). The energy content of the Universe in the present day is made up of 3 major components: dark energy ($\sim 68\%$), cold dark matter ($\sim 27\%$), and baryonic matter ($\sim 5\%$) [10].

Another fascinating prediction of GR is the existence of black holes, which are objects so compact that even light rays are trapped in their interior. These had been conceptualized even in the context of Newtonian physics, notably by Michell and Laplace in the 19th century.[2] A few months after Einstein published his theory of gravitation, Schwarzschild found a static solution to the vacuum field equations $R_{\mu\nu} = 0$. We discuss this solution in more detail in Chapter 7, along with its rotating counterpart, the Kerr metric [11]. While such objects were thought for a long time to be of purely mathematical interest, there has been increasing experimental evidence that black holes do exist in Nature, and they will be central to the final part of this thesis. Unlike the Newtonian theory, GR predicts the existence of gravitational waves. Such waves were directly detected in 2015 using ground-based interferometers [12] coming from the distant merger of two black holes, though indirect evidence of their existence had already been obtained from the study of binary pulsars [13]. This was yet again a success of GR, and paved the way for a new era of strong field tests .

Despite all the triumphs of GR that we have discussed, there remain some unexplained phenomena which have encouraged physicists to consider alternative theories of gravitation. Firstly, it is well-known that general relativity is not renormalizable, which means that it loses its predictability at high energies. The mass scale which represents this cutoff is the Planck mass $m_P = \sqrt{8\pi} M_P \sim 10^{19}$ GeV. There has been a lot of effort in the past decades to construct a UV-complete theory of gravity, the most famous attempt being string theory. Another issue is linked to the small measured value of the cosmological constant. In a quantum field theory, the bare constant Λ is expected to be corrected by a quantum correction $\delta\Lambda$ arising from loop contributions, combining into the observed value $\Lambda_{\text{eff}} = \Lambda + \delta\Lambda$. Assuming a cutoff at the Planck scale m_P, the quantum corrections are estimated to be of order $\delta\Lambda \sim 10^{37}\text{GeV}^2$, meaning that the two contributions to Λ_{eff} would have to cancel out with a precision of more than 100 orders of magnitude. A different calculation using dimensional regularization alleviates the issue, but there remains a discrepancy of around 50 orders of magnitude (see Ref. [14] for a review). This is known as the naturalness problem, and occurs in a similar way (though not as drastically) for the mass of the Higgs boson in particle physics. There are additional problems linked to cosmology, one of them being the flatness problem. This can be understood easily by introducing the critical density $\rho_{\text{c}} = 3M_P^2 H^2$ and rewriting Eq. (21) with $\Lambda = 0$ as

$$\left(\frac{\rho_{\text{c}}}{\rho} - 1\right) \rho a^2 = -3\kappa M_P^2 \,. \tag{25}$$

[2] An English translation of Laplace's essay can be found in the book by Hawking and Ellis [51].

Since the right-hand side of the previous equation is constant, the left-hand side must also remain constant throughout the evolution of the universe. However, because during matter and radiation domination the combination ρa^2 decreases, the second term on the left-hand side must increase. Current measurements show that $|1 - \rho_c/\rho|$ is very small today, which implies that it was extremely small (around 10^{-62}) in the early stages of the Universe, and there is no explanation for this fine-tuning. Another issue is the so-called horizon problem. The Planck satellite [10] was able to measure the temperature of the cosmic microwave background (CMB) with high accuracy, and regions of the sky which could not have been in causal contact in the past have almost the same temperature, which is puzzling. Fortunately, a possible explanation for both of these problems has been proposed in the eighties, and relies on a period of accelerated expansion in the very early Universe called inflation [15–22]. During that period, the scale factor a grows by about 60 e-folds, and this allows to explain the two previous problems. If one assumes initial conditions $|1 - \rho_c/\rho| \sim 1$, this value will be diluted to a very small value during inflation (since ρa^2 increases in this case). This can explain the fine-tuning discussed above, and even if this value grows from the end of inflation until the present day, it is still consistent with the present day observations. A similar picture holds for the horizon problem: two points in spacetime can be in causal contact before inflation, and lose contact by the end of it. A simple way to model the inflationary stage is to introduce a scalar field χ, called the inflaton, slowly-rolling at the top of its potential. This mimics a fluid with equation of state $w_\chi \simeq -1$ (at least during the early stages of inflation), and hence the expansion is accelerated. Once the slow roll approximation breaks down, the scalar field oscillates at the bottom of its potential and decays into the standard model particles during a stage called (p)reheating. This acts as an apparent (nonsingular) Big Bang, and the Universe then proceeds with the three usual stages, i.e. radiation domination followed by matter domination and finally a dark energy dominated stage which we are currently living in. Another intriguing feature of the Universe is that around 85% of the matter content is invisible, in the sense that it doesn't emit light, hence the name dark matter. The analysis of rotation curves of spiral galaxies (i.e. the velocity distribution of stars), suggests the existence of invisible matter which interacts gravitationally and would explain the flat profiles. On larger scales, the mass of galaxy clusters can be determined using gravitational lensing techniques, and also provides a motivation for the existence of dark matter (see Ref. [23] for a recent review). The understanding of its nature is one of the challenges of modern physics.

Scalar-tensor theories

Let us now introduce scalar-tensor theories, which provide a general context for the work presented in this thesis. Alternative theories of gravitation allow us to predict and test deviations from GR, which is already a sufficient reason to motivate their study. Furthermore, the shortcomings of GR discussed previously provide an addi-

tional incentive to consider such alternative theories, in the hope of obtaining answers to the issues we mentioned. The Einstein field equations can be obtained from the Einstein-Hilbert action:

$$S = \frac{M_P^2}{2} \int \mathrm{d}^4x\sqrt{-g}(R - 2\Lambda) + S_\mathrm{m}\left[g_{\mu\nu}, \psi_\mathrm{m}\right] \ , \tag{26}$$

where ψ_m denotes the matter fields which are minimally coupled to the metric g. The energy-momentum tensor $T_{\mu\nu}$ is defined using the matter action as

$$T_{\mu\nu} = -\frac{2}{\sqrt{-g}}\frac{\delta S_\mathrm{m}}{\delta g^{\mu\nu}} \ . \tag{27}$$

The principle of least action applied to this theory yields the Einstein equations (16). According to a theorem by Lovelock [24, 25], the only 2-tensors in 4 dimensions that are divergence-less and constructed with the metric and its first and second derivatives only are the metric $g_{\mu\nu}$ itself and the Einstein tensor $G_{\mu\nu}$. Hence, in order to obtain field equations which are different from those of GR, it is necessary to break one of the hypotheses of Lovelock's theorem. For instance, one can consider additional fields mediating gravity, change the spacetime dimension or introduce higher derivatives in the action. The simplest way to modify GR is to construct a theory with a scalar field in addition to the metric, which is called a scalar-tensor theory. The detection of the Higgs boson in 2012 showed that scalar fields can exist in Nature [26]. Furthermore, they are expected to arise in the 4-dimensional effective action of string theories, which is obtained upon compactifying extra dimensions (see Ref. [27]). As we discussed above, scalar fields are also expected to participate in the inflationary stage of the Universe. For these reasons, it seems natural to consider scalar-tensor theories as extensions to GR and study their properties. We will focus on this type of modification throughout the thesis, though there exist many other modified gravity theories (see Refs. [28, 29] for reviews). In 1961, Brans and Dicke [30], building notably on previous work by Jordan [31], proposed a theory which includes an additional scalar field ϕ that can be interpreted as a varying Newton constant. The action for the Jordan-Brans-Dicke theory reads

$$S_\mathrm{JBD} = \frac{M_P^2}{2} \int \mathrm{d}^4\sqrt{-g}\left[\phi R - \frac{\omega_0}{\phi}\left(\partial\phi\right)^2\right] \ , \tag{28}$$

where ω_0 is a constant. This action was later extended by replacing the constant ω_0 by a function $\omega(\phi)$, and adding a potential term for the scalar field [32]. These extensions are usually called scalar-tensor theories, though we use this term in a broader sense in this thesis, as we will discuss. Indeed, the standard scalar-tensor theories only contain first derivatives of the scalar in the action. In the seventies, Horndeski determined the most general action containing a scalar ϕ and the metric which leads to second order Euler-Lagrange equations [33], and it contains second derivatives of the scalar field. This class of theories was recently rediscovered when extending the Galileon

model [34] to curved spacetime [35–37], and was shown to be equivalent to Horndeski theory [38]. In the modern formulation, the Horndeski Lagrangian reads

$$\begin{aligned}\mathcal{L}_{\rm H} &= f(\phi,X)R + K(\phi,X) - G_3(\phi,X)\Box\phi - 2f_X\left(\{\Box\phi\}^2 - \phi_{\mu\nu}\phi^{\mu\nu}\right)\\ &\quad + G_5(\phi,X)G_{\mu\nu}\phi^{\mu\nu} + \frac{1}{3}G_{5X}\left(\{\Box\phi\}^3 - 3\Box\phi\,\phi^{\mu\nu}\phi_{\mu\nu} + 2\phi_{\mu\alpha}\phi^{\alpha\nu}\phi^{\mu}{}_{\nu}\right)\ ,\end{aligned} \tag{29}$$

where $X = \partial_\mu\phi\partial^\mu\phi$, $f_X = \partial f/\partial X$, and we use the shorthand notation $\phi_\mu = \nabla_\mu\phi$, $\phi_{\mu\nu} = \nabla_\mu\nabla_\nu\phi$. The requirement that the field equations be of second order is to avoid the appearance of an Ostrogradsky ghost [39, 40], which is a degree of freedom with an energy that is unbounded from below. While having second-order equations is a sufficient condition avoid the Ostrogradsky ghost , it is not a necessary one. Indeed, the Ostrogradsky theorem only applies to nondegenerate Lagrangians, meaning that it is possible for a theory with higher derivatives to be healthy (in the sense that there is no Ostrogradsky ghost) if it is also degenerate. Hence, scalar-tensor theories going beyond the Horndeski class were sought out. The first step in that direction was obtained by performing a disformal transformation of the metric tensor [41]:

$$\tilde{g}_{\mu\nu} = C(\phi,X)g_{\mu\nu} + D(\phi,X)\phi_\mu\phi_\nu\ . \tag{30}$$

It was shown in Ref. [42] that the Horndeski action is stable under the disformal map[3] if the functions C and D do not depend on the kinetic term X. However, if the functions C and D depend on X but are chosen so that the disformal map is invertible, then the previous relation is simply a field redefinition, and a theory should remain healthy under such a transformation even if the Euler-Lagrange equations contain higher-order derivatives. This interesting property was first pointed out in Ref. [43]. It led to the development of theories beyond the Horndeski class, and extensions of the G_4 and G_5 terms were found in Ref. [44], which can be obtained by purely disformal transformation of the Horndeski theory. The most general class of healthy scalar-tensor theories were then isolated by imposing certain degeneracy conditions on the Lagrangian, allowing to reduce higher-order field equations to a second-order system and hence avoid the propagation of an Ostrogradsky ghost. Theses theories were called Extended Scalar-Tensor (EST) [45], or Degenerate Higher-Order Scalar-Tensor (DHOST) theories [46, 47], and we will use the latter name in this thesis. The quadratic DHOST Lagrangian, i.e. containing terms at most quadratic in the second derivatives of the scalar field ϕ, reads

$$S = \frac{M_P^2}{2}\int \mathrm{d}^4x\sqrt{-g}\left(f(\phi,X)R + K(\phi,X) - G_3(\phi,X)\Box\phi + \sum_{i=1}^{5}\mathcal{L}_i\right)\ , \tag{31}$$

where the scalar densities $\mathcal{L}_i$ are given by

$$\mathcal{L}_1 = A_1(\phi,X)\,\phi_{\mu\nu}\phi^{\mu\nu}\ ,$$

[3] We use the word "stable" in the sense that starting from a Horndeski theory and performing such a disformal transformation, we obtain a theory that also belongs to the Horndeski class.

$$\begin{aligned}
\mathcal{L}_2 &= A_2(\phi, X)\,(\Box\phi)^2\,, \\
\mathcal{L}_3 &= A_3(\phi, X)\,\phi_{\mu\nu}\phi^\mu\phi^\nu\Box\phi\,, \\
\mathcal{L}_4 &= A_4(\phi, X)\,\phi_{\mu\alpha}\phi^{\alpha\nu}\phi^\mu\phi_\nu\,, \\
\mathcal{L}_5 &= A_5(\phi, X)\,\left(\phi_{\mu\nu}\phi^\mu\phi^\nu\right)^2\,.
\end{aligned} \tag{32}$$

Several subclasses of DHOST theories can be obtained from this action. In each class, specific degeneracy conditions are assumed, ensuring that the theory is free from the Ostrogradsky ghost. In most of this thesis, the theories will belong to the class Ia, which is obtained by imposing the following constraints on the Lagrangian functions, assuming $f - XA_1 \neq 0$:

$$\begin{aligned}
A_2 &= -A_1\,, \\
A_4 &= \frac{1}{8(f-XA_1)^2}\left[-16XA_1^3 + 4A_1^2(3f+16Xf_X) + 4A_3A_1(3Xf-4X^2f_X)\right. \\
&\qquad \left. -X^2fA_3^2 - 16f_XA_1(3f+4Xf_X) + 8fA_3(Xf_X-f) + 48ff_X^2\right] \\
A_5 &= \frac{(2A_1 - XA_3 - 4f_X)(2A_1^2 + 3XA_1A_3 - 4f_XA_1 - 4fA_3)}{8(f-XA_1)^2}\,,
\end{aligned} \tag{33}$$

The quadratic Horndeski class [33] is given by the relations

$$A_3^{\rm H} = 0 \qquad \text{and} \qquad A_1^{\rm H} = 2f_X^{\rm H}\,. \tag{34}$$

Note that there also exist cubic DHOST theories [52], which generalize the cubic Horndeski terms in the Lagrangian (29), i.e. the terms which contain the function G_5. In the following, we limit ourselves to quadratic actions. The only exception is when considering the scalar-Gauss-Bonnet theories in the first part of the thesis, which can be written as a cubic Horndeski theory [38]. Though other classes of DHOST theories exist, they have been found to present a gradient instability of cosmological perturbations [53–55], and hence the type Ia subclass is the most interesting one from a phenomenological point of view. However, there are also constraints on the dark energy models in the Ia subclass, due to the detection of gravitational waves coming from the merger of a binary neutron star along with its electromagnetic counterpart [56, 57]. This measurement allowed to compare the speed of propagation c_T of gravitational waves to the speed of light, leading to the constraint $|c_T - 1| \sim 10^{-15}$. In order to obtain a theory with $c_T = 1$, one must set $A_1 = 0$ in the DHOST Lagragian (and hence $A_2 = 0$ to impose the degeneracy of the theory) [54, 58–61].[4] It was later argued that that one should also set $A_3 = 0$ in order to avoid the decay of the scalar field into gravitational waves, which would be in contradiction with the measurements [63]. If we assume all of these constraints, then using Eq. (33) we obtain that the only quadratic term remaining in the action (31) is $A_4 = 6f_X^2/f$. In particular, the quadratic terms of the Horndeski theory are ruled out by these observations.

[4] See however Ref. [62] for a critical discussion of the implications of the LIGO/Virgo measurement in the context of effective field theories.

Structure of the thesis

In this thesis, I will present various topics in the general context of scalar-tensor theories belonging to the Horndeski class and beyond. Part I deals with theories exhibiting spontaneous scalarization around compact objects. After explaining how this mechanism works in Chapter 1, we focus on the cosmology of these models, and more precisely the inflationary epoch. In Chapter 2, we show that an instability of the scalar mode generically develops in such models during inflation. In Chapter 3, we present a mechanism which relies on a coupling of the scalar field to the inflaton and allows to quench the instability in a particular class of models.

In Part II, we study the Vainshtein screening for slowly rotating stars, and start by briefly describing how this mechanism operates in spherically symmetric configurations. The aim of this part is to examine the validity of the Vainshtein screening for slowly rotating stars, since astrophysical objects typically rotate. In Chapter 4 the formalism is introduced, and general solutions for the frame-dragging function (which is added to the metric to account for slow rotation) are discussed. We then give explicit examples of the screening for slowly rotating sources, both in the case of a time-dependent scalar field in Chapter 5 , and a static scalar in Chapter 6.

Finally, Part III is devoted to axisymmetric black hole solutions in scalar-tensor theories. In Chapter 7, we start by reviewing the properties of (uncharged) black holes in GR. In Chapter 8, we construct disformed versions of these spacetimes by applying the disformal map to the Kerr metric, and discuss their many interesting properties. Astrophysical implications are examined in Chapter 9, where we study the post-Newtonian orbit of stars around a disformed Kerr black hole.

I will end the manuscript by summarizing the main results. This thesis gave rise to the publications listed below:

- T. Anson, E. Babichev and C. Charmousis, *Deformed black hole in Sagittarius A*, *Phys. Rev. D* **103** no. 12, (2021) 124035,
- T. Anson, E. Babichev, C. Charmousis and M. Hassaine, *Disforming the Kerr metric*, *JHEP* **01** (2021) 018,
- T. Anson and E. Babichev, *Vainshtein screening for slowly rotating stars*, *Phys. Rev. D* **102** no. 4, (2020) 044046,
- T. Anson, E. Babichev, and S. Ramazanov, *Reconciling spontaneous scalarization with cosmology*, *Phys. Rev. D* **100** no. 10, (2019) 104051,
- T. Anson, E. Babichev, C. Charmousis, and S. Ramazanov, *Cosmological instability of scalar-Gauss-Bonnet theories exhibiting scalarization*, *JCAP* **06** (2019) 023.

Part I

Cosmology of theories exhibiting spontaneous scalarization

Introduction to Part I

In this part, we will focus on scalar-tensor theories exhibiting the spontaneous scalarization of compact objects. This interesting effect was first discovered for neutron stars by Damour and Esposito-Farèse (DEF) in the nineties [64]. In this model, the coupling of the scalar field to curvature acts as an effective tachyonic mass in the strong field region inside the star. For a certain range of coupling parameters and for high enough curvature, the GR branch with a constant scalar becomes unstable in favor of the scalarized branch which accommodates a nontrivial scalar profile. Because of the coupling to the Ricci curvature R, this phenomenon only operates for stars, where $R \neq 0$. More recently, it was observed that scalarization could arise in scalar-Gauss-Bonnet theories, where the scalar field is nontrivially coupled to the Gauss-Bonnet invariant [65, 66]. Interestingly, since the latter is nonzero even in vacuum, this led to the extension of scalarization to black holes. We will briefly review these models in Chapter 1, since we will use them in the following chapters. We will limit ourselves to these models in the following, i.e. DEF and scalar-Gauss-Bonnet, but it is worth pointing out that scalarization has since been shown to work in a more general class of theories. The most general terms which can lead to the onset of scalarization were found in Refs. [67, 68]. While the examples we will treat are for spherically symmetric uncharged objects, scalarization was shown to work for charged objects as well [65, 69]. Interestingly, the instability can also be triggered for a rapidly rotating black hole [70–72].

Our main interest lies in the cosmology of such models, and in particular the inflationary stage. As we have said, the scalarization effect relies on a tachyonic effective mass for the scalar field that destabilizes the GR solution. In Chapter 2, we examine the influence of the tachyonic mass on the cosmology of a certain class of scalar-Gauss-Bonnet theories. We will argue that theories leading to the scalarization of compact objects generically present an instability during the inflationary stage, which is also present for the DEF model, as we show in Chapter 3. In that case however, we propose a mechanism to quench the instability which relies on a coupling of the scalar field ϕ to the inflaton χ. As we will explain, the inflationary stage is not broken in that case, and the current Solar System constraints are satisfied for the scalar field.

Chapter 1

Scalarization of compact objects

In this first chapter, we review the process of spontaneous scalarization for spherically symmetric compact objects in the case of the DEF model and for theories with a nontrivial coupling of the scalar field to the Gauss-Bonnet invariant.

1.1 The Damour–Esposito-Farèse model of scalarization

We begin by presenting the Damour–Esposito-Farèse (DEF) model leading to the scalarization of neutron stars [64]. We write the action in the so-called Einstein frame, where matter is nonminimally coupled to the metric:

$$S_{\rm E} = \frac{M_P^2}{2}\int {\rm d}^4x\sqrt{-g}\left[R - 2\partial_\mu\phi\partial^\mu\phi - 2V(\phi)\right] + S_{\rm m}\left[A^2(\phi)g_{\mu\nu}, \psi_{\rm m}\right] \ , \tag{1.1}$$

where $\psi_{\rm m}$ is the collective notation for matter fields, and the function $A(\phi)$ is defined as

$$A(\phi) = e^{\frac{\beta\phi^2}{2}} \ , \tag{1.2}$$

with β constant. Following the notations of Ref. [64], we have chosen the field ϕ to be dimensionless. In the original DEF model, the potential $V(\phi)$ is absent, but we keep it here because it plays a crucial role in our discussion later on. The previous action can also be written in the Jordan frame, where the matter fields follow geodesics. It is obtained by redefining the metric as $\tilde{g}_{\mu\nu} = A^2(\phi)g_{\mu\nu}$. The corresponding action is of the form (31) and reads

$$S_{\rm J} = \frac{M_P^2}{2}\int {\rm d}^4x\sqrt{-\tilde{g}}\left[\tilde{\phi}\tilde{R} - \frac{\omega(\tilde{\phi})}{\tilde{\phi}}\tilde{g}^{\mu\nu}\partial_\mu\tilde{\phi}\partial_\nu\tilde{\phi} - \Pi(\tilde{\phi})\right] + S_{\rm m}\left[\tilde{g}_{\mu\nu}, \psi_{\rm m}\right] \ , \tag{1.3}$$

where $\tilde{\phi}$, ω and Π are defined as

$$\left(\frac{{\rm d}\ln A}{{\rm d}\phi}\right)^2 = \left[2\omega(\tilde{\phi}) + 3\right]^{-1} \ , \tag{1.4}$$

$$\tilde{\phi} = A^{-2}(\phi) \,, \tag{1.5}$$

$$\Pi(\tilde{\phi}) = 2\tilde{\phi}^2 V(\phi(\tilde{\phi})) \,. \tag{1.6}$$

In the following, we will work in the Einstein frame since the field equations are simpler in that case. Let us now describe the essence of scalarization. The equation of motion for the field ϕ derived from the action (1.1) reads

$$\Box\phi + \frac{\alpha(\phi)T}{2M_P^2} - \frac{1}{2}\frac{\partial V}{\partial \phi} = 0 \,, \tag{1.7}$$

where

$$\alpha(\phi) \equiv \frac{\mathrm{d}\ln A(\phi)}{\mathrm{d}\phi} = \beta\phi \tag{1.8}$$

plays the role of the coupling constant to the matter fields and $T = g^{\mu\nu}T_{\mu\nu}$. One can see that $\phi = 0$ solves this equation for the potential $V(\phi) = 0$. For $\beta < 0$ and $T < 0$, the scalar acquires a tachyonic effective mass, which hints at the existence of other, stable solutions of Eq. (1.7). This is indeed the case when $\beta \lesssim -4$ for massive enough neutron stars [64]. The field ϕ acquires a nontrivial profile which matches the constant cosmological value $\phi_0 \equiv \phi(t_0)$, where $t_0 \approx 13.8 \cdot 10^9$ years is the present time. However, the parameter β is greatly constrained by the observation of binary pulsars, which imposes the bound $\beta > -4.5$ [73, 74]. Hence, this parameter is practically fixed for the scalarization models, and we will set $\beta \simeq -4.5$ in the following.

In the theory given by the action (1.1), the parametrized post-Newtonian (PPN) parameters (17) are given by [75]

$$\gamma_{\mathrm{PPN}} - 1 = \frac{-2\alpha^2(\phi_0)}{1+\alpha^2(\phi_0)} \qquad \beta_{\mathrm{PPN}} - 1 = \frac{\beta\alpha^2(\phi_0)}{[1+\alpha^2(\phi_0)]^2} \,. \tag{1.9}$$

In the limit $\alpha(\phi_0) \to 0$, the PPN parameters coincide with those of GR. From the definition of α in Eq. (1.8), one sees that this limit corresponds to $\phi_0 \to 0$. Using the constraint on the PPN parameter γ_{PPN} from the Shapiro time-delay measurement

$$\gamma_{\mathrm{PPN}} = 1 \pm (2.1 \pm 2.3) \times 10^{-5}$$

given in Ref. [76], we get for $|\beta| \simeq 4.5$ the following upper bound on ϕ_0:

$$\phi_0 \lesssim 10^{-3} \,. \tag{1.10}$$

For these values, the DEF model is indistinguishable from GR in the weak-field and quasi-static regimes. However, even with a vanishing value of the field ϕ at cosmological scales, neutron stars experience scalarization, leading to testable deviations from GR in the strong field regime [77, 78]. On the other hand, as we will discuss in Chapter 3, the values (1.10) are not realistic in the original DEF model with $V(\phi) = 0$. Indeed, the tachyonic instability triggers runaway cosmological solutions for the field ϕ, so that $\phi_0 \gg 1$, which is in direct conflict with the Solar System constraints [79–81].

1.2 Coupling to the Gauss-Bonnet scalar

The standard scalarization model of the previous section relies on a coupling of the scalar field to the Ricci scalar, as seen from the action (1.3) written in the Jordan frame. Outside of matter, the Ricci scalar vanishes, and hence the DEF model is only valid for neutron stars. Recently, it was found that scalarized solutions may also arise when the scalar field couples nonminimally to the Gauss-Bonnet invariant [65,66,82–85]

$$\hat{G} = R_{\mu\nu\sigma\alpha}R^{\mu\nu\sigma\alpha} - 4R_{\mu\nu}R^{\mu\nu} + R^2 \,.$$

This scalar is nonzero even for black holes, which makes scalarization possible in these cases as well. Let us now explain how scalarized solutions arise in these theories. We consider the following action, which includes a coupling term $F(\phi)$ between a scalar field ϕ and the Gauss-Bonnet invariant $\hat{G}$:

$$S = \frac{M_P^2}{2}\int \mathrm{d}^4x\sqrt{-g}\left[R - 2\Lambda - g^{\mu\nu}\partial_\mu\phi\partial_\nu\phi + 2F(\phi)\hat{G}\right] \,, \tag{1.11}$$

where Λ is the cosmological constant. Even though this action is not immediately of the form (31), one can check that the field equations are of second order, which means that this theory belongs to the Horndeski class (29). It contains cubic terms, i.e. $G_5 \neq 0$ in the Lagrangian (29), which is why it is not part of the quadratic DHOST theories. The explicit expressions for the functions appearing in the Horndeski Lagrangian corresponding to this theory can be found in Ref. [38]. By varying the previous action, we see that the Gauss-Bonnet scalar provides a source term in the scalar field equation, which reads

$$\Box\phi + F'(\phi)\hat{G} = 0 \,. \tag{1.12}$$

The variation of Eq. (1.11) with respect to the metric yields the following modified Einstein equations:

$$M_P^2\left(G_{\mu\nu} + \Lambda g_{\mu\nu}\right) = \nabla_\mu\phi\nabla_\nu\phi - \frac{1}{2}g_{\mu\nu}\nabla_\alpha\phi\nabla^\alpha\phi - 8P_{\mu\lambda\nu\alpha}\nabla^\alpha\left[F'(\phi)\nabla^\lambda\phi\right] \,. \tag{1.13}$$

We have introduced the tensor $P_{\alpha\beta\mu\nu}$, which is the double dual of the Riemann tensor. It is defined using the antisymmetric Levi-Civita tensor $\varepsilon_{\mu\nu\alpha\beta}$ in the following way:

$$\begin{aligned} P_{\alpha\beta\mu\nu} &= -\frac{1}{4}\varepsilon_{\alpha\beta\rho\sigma}R^{\rho\sigma\gamma\delta}\varepsilon_{\mu\nu\gamma\delta} \\ &= R_{\alpha\beta\mu\nu} + g_{\alpha\nu}R_{\beta\mu} - g_{\alpha\mu}R_{\beta\nu} + g_{\beta\mu}R_{\alpha\nu} - g_{\beta\nu}R_{\alpha\mu} + \frac{1}{2}\left(g_{\alpha\mu}g_{\beta\nu} - g_{\alpha\nu}g_{\beta\mu}\right)R \,. \end{aligned} \tag{1.14}$$

Under certain conditions on the coupling function $F(\phi)$, namely

$$F'(\phi_0) = 0 \qquad \text{and} \qquad F''(\phi_0) > 0 \tag{1.15}$$

for some constant ϕ_0, such theories were shown to exhibit spontaneous scalarization around black holes and neutron stars [65, 66, 82–85].

The first condition on the coupling function ensures that $\phi = \phi_0$ satisfies the equations of motion, in which case we recover the solution of GR with a constant scalar field. The second condition is crucial, as it implies that the scalar field acquires a negative effective mass squared, which is responsible for the appearance of scalar hair via a tachyonic instability. Indeed, one may study a scalar perturbation $\phi = \phi_0 + \delta\phi$ on a fixed Schwarzschild geometry, as was done in Ref. [65]. Notably, the equations for the scalar and metric fluctuations are decoupled at first order for a constant ϕ_0. The equation describing scalar perturbations is given by

$$\left(\Box + F''(\phi_0)\hat{G}\right)\delta\phi = 0 \,, \tag{1.16}$$

where the d'Alembert operator and the Gauss-Bonnet invariant are calculated using the Schwarzschild metric. We now decompose the scalar perturbation on the static and spherically symmetric background as

$$\delta\phi = \frac{u(r)}{r} e^{-i\omega t} Y_{lm}(\theta, \varphi) \,, \tag{1.17}$$

where $Y_{lm}(\theta, \varphi)$ are the spherical harmonics. One can rewrite Eq. (1.16) in the form of a Schrödinger equation by introducing the tortoise coordinate $\mathrm{d}r_* = \mathrm{d}r\,(1 - \frac{r_S}{r})^{-1}$, where r_S is the Schwarzschild radius of the black hole:

$$\frac{\mathrm{d}^2 u}{\mathrm{d}r_*^2} + \omega^2 u = V_{\text{eff}}(r) u \,. \tag{1.18}$$

For $l = 0$ the effective potential $V_{\text{eff}}(r)$ reads

$$V_{\text{eff}}(r) = \left(1 - \frac{r_S}{r}\right)\left(\frac{r_S}{r^3} - \frac{12 r_S^2}{r^6} F''(\phi_0)\right) \,. \tag{1.19}$$

A sufficient condition on the effective potential for the existence of an unstable mode is [86]

$$\int_{r_g}^{\infty} \mathrm{d}r \frac{V_{\text{eff}}(r)}{1 - \frac{r_S}{r}} < 0 \,. \tag{1.20}$$

This condition, which can be satisfied if $F''(\phi_0) > 0$, translates to

$$r_S^2 < \frac{24}{5} F''(\phi_0) \,. \tag{1.21}$$

Hence the Schwarzschild solution becomes unstable for small enough masses (the value depends on the coupling function F), and one expects scalar hair to appear in that case. Bearing in mind the possible redefinition $\phi \to \phi + \phi_0$, the function $F(\phi)$ can be expanded around $\phi_0 = 0$,

$$F(\phi) = \frac{1}{8}\lambda^2\phi^2 + \mathcal{O}\left(\frac{\lambda^2\phi^4 M_P^2}{M_1^2}\right) \,. \tag{1.22}$$

Here M_1 is some scale normally taken to be of order of the Planck mass M_P, and the sign of the quadratic term is chosen so that the effective mass is tachyonic. The value of λ sets the upper bound of the mass of a black hole or a star at which scalarization may happen, $\lambda \gtrsim r_S$. For physically interesting objects like neutron stars, one easily finds

$$\lambda \sim \frac{M_\odot}{M_P^2} \sim 10^{19}\text{GeV}^{-1} \,. \tag{1.23}$$

Different branches of scalarized solutions were shown to exist by a numerical analysis, for specific bands of λ/r_S. Each branch may be labeled by an integer $n \in \mathbb{N}$ corresponding to the number of nodes of the radial scalar profile. It was shown in Ref. [87] that none of the branches are stable for a theory with a purely quadratic coupling function, $F(\phi) \propto \phi^2$. However, for the theory with $F(\phi) \propto (1 - e^{-\phi^2/M_P^2})$ the fundamental branch $n = 0$ is stable for a specific range of parameters. The same can be achieved by adding a quartic term to the purely quadratic coupling function [88,89].

Chapter 2

Cosmological instability of the scalar mode

In this chapter, which is based on Ref. [90], we show that the tachyonic mass leading to the scalarization of black holes and stars is potentially dangerous on a cosmological background, and may result in a catastrophic instability of scalar modes during inflation.

2.1 Cosmology and scalar fluctuations

We start by introducing some aspects of cosmology that will be useful to us in the following. Everything which is described in this section can be found in more detail in any modern cosmology textbook, as for instance Ref. [91]. The Universe is homogeneous and isotropic on very large scales, and in the context of GR it can be described by the flat FLRW metric

$$\mathrm{d}s^2 = -\mathrm{d}t^2 + a(t)^2 \delta_{ij} \mathrm{d}x^i \mathrm{d}x^j \ , \tag{2.1}$$

where a is the scale factor and we define $H = \dot{a}/a$. We saw in Eq. (18) that the FLRW spacetime also depends on the spatial curvature κ, but we set it to 0 in the following as this value is consistent with experiments. In this case, the Friedmann equations (20) and (21) become

$$\frac{\ddot{a}}{a} = -\frac{1}{6M_P^2} \sum_i \rho_i \left(1 + 3w_i\right) \ , \tag{2.2}$$

$$H^2 = \frac{1}{3M_P^2} \sum_i \rho_i \ , \tag{2.3}$$

where $w_i = P_i/\rho_i$. The main species that constitute the universe are matter ($w_\mathrm{m} = 0$), radiation ($w_\mathrm{r} = 1/3$) and dark energy ($w_\Lambda = -1$). Using the conservation equation (23)

for each species, one can write the total energy density as

$$\rho = \frac{\rho_{\rm r}^0}{a^4} + \frac{\rho_{\rm m}^0}{a^3} + \rho_\Lambda^0 \ , \tag{2.4}$$

where the ρ_i^0 represent the densities for each species today, and we have set the present day scale factor $a_0 = 1$. From this expression, one sees that the energy densities for each species decays differently as the Universe expands. The matter is simply diluted as a grows, which explains the factor a^3. For radiation, there is an additional factor of a because photons are also redshifted due to the expansion. The dark energy density, on the other hand, remains constant. In the Big Bang model, the scale factor $a \to 0$ as $t \to 0$, in which case the Universe is a point with infinite density. We actually don't know what happens at very early times $t < t_P$, where $t_P \sim 10^{-43}$ s is the Planck time, since GR would break down at these high energies. Keeping this in mind, one can single out three periods in the history of the Universe in standard GR, each corresponding to the dominance of one of the species in Eq. (2.4). Radiation dominates when a is small in the early Universe, and this period lasts until the densities of matter and radiation become comparable. This happens at the time $t_{\rm eq} \sim 5 \cdot 10^4$ years. We then enter the matter dominated epoch, which constitutes the major part of the history of the Universe. During this period, the photons of the cosmic microwave background (CMB) are emitted at a time called recombination, around $t \sim 4{\cdot}10^5$ years. The matter domination ends around 10 billion years after the Big Bang, and we live today in a dark energy dominated Universe. This means that the current expansion is accelerated, i.e. $\ddot{a} > 0$.

As we saw in the previous chapter, the tachyonic instability for the scalar field which leads to the scalarization of compact objects is due to a coupling to curvature. In the DEF model, the scalar is coupled to the Ricci tensor. Since we work in the Einstein frame, given by the action (1.1), the scalar field equation contains the trace T of the energy-momentum tensor instead of the Ricci scalar. If we neglect the backreaction of the scalar on the metric, then by taking the trace of the Einstein equations we obtain $M_P^2 R = -T$. Hence one can view the effective tachyonic mass as coming either from R or T, though notice that their signs are different. For the flat FLRW metric (2.1), the Ricci scalar is given by

$$R = 6\left(\frac{\ddot{a}}{a} + H^2\right) \ .$$

Using Eqs. (2.2) and (2.3), this can be written in terms of the densities of the different perfect fluids as

$$R = \frac{1}{M_P^2}\sum_i \rho_i \left(1 - 3w_i\right) \ .$$

Hence, we have $R \geq 0$ for fluids verifying $w_i \leq 1/3$. This is true for the three different species that we consider. In the case of radiation, we have an equation of state parameter $w_{\rm r} = 1/3$, and hence $R = 0$. However, this relation is only approximate due to the trace anomaly which arises in gauge theories [92–94], and we have $R \simeq 0$

	Radiation	Matter	Inflation/Dark Energy
$a(t)$	$\sqrt{t}$	$t^{2/3}$	e^{Ht}
R	$\simeq 0$	> 0	> 0
$\hat{G}$	< 0	< 0	> 0

Table 2.1: Time-dependence of the scale factor, along with the signs of the Ricci scalar and Gauss-Bonnet invariant for different epochs of an FLRW Universe.

instead. Another curvature invariant that we will need is the Gauss-Bonnet scalar, which has the following expression in terms of the scale factor:

$$\hat{G} = 24H^2\frac{\ddot{a}}{a} \,. \tag{2.5}$$

This shows that the sign of $\hat{G}$ is directly related to $\ddot{a}$, and changes depending on whether the expansion of the Universe is accelerating or decelerating. In Table 2.1, we summarize the time dependence of the scale factor and the signs of R and $\hat{G}$ in the different epochs, i.e. radiation, matter and dark energy (this case also applies to the early stages of inflation, as we will explain).

As we mentioned already, the standard Big Bang model in GR suffers from several issues. The fact that the Universe is (very close to) flat today implies that the curvature density in the early Universe had to be fine-tuned to 0 with a high precision, as we discussed after Eq. (25). This is known as the flatness problem. Another issue that we mentioned is the horizon problem. The temperature of the CMB has been measured to a high accuracy and shows that up to small fluctuations it has a uniform value $\Theta_{\rm CMB} \simeq 2.7$ K. The puzzling issue is that regions of the sky which weren't in causal contact at the time of recombination (when the CMB photons were emitted) have the same temperature. According to the modern understanding of cosmology, these issues are solved by introducing an inflationary stage in the very early Universe, during which the expansion is accelerated. A simple way to achieve this is to introduce a scalar field χ, called the inflaton, which evolves inside a potential U. The corresponding action reads

$$S_\chi = \int \mathrm{d}^4x\sqrt{-g}\left[-\frac{1}{2}g^{\mu\nu}\partial_\mu\chi\partial_\nu\chi - U(\chi)\right] \,.$$

From the Friedmann equations with $\chi = \chi(t)$, one can identify the energy density ρ_χ and pressure P_χ of the inflaton, and deduce the following equation of state parameter:

$$w_\chi = \frac{P_\chi}{\rho_\chi} = \frac{\dot{\chi}^2 - 2U}{\dot{\chi}^2 + 2U} \,. \tag{2.6}$$

If the potential energy dominates the kinetic energy of the inflaton, i.e. $U \gg \dot{\chi}^2$, then we obtain $w_\chi \simeq -1$. This can be achieved in a Universe dominated by the

inflaton which is slowly slowly rolling at the top of its potential. More precisely, one can introduce the slow-roll parameters $\epsilon_{\rm sr} = -\dot{H}/H^2$ and $\eta_{\rm sr} = -\ddot{\phi}/(H\dot{\phi})$. If these parameters are small, i.e. $\{\epsilon_{\rm sr}, \eta_{\rm sr}\} \ll 1$, we obtain a quasi-de Sitter expansion where the scale factor takes the form $a(t) \simeq e^{Ht}$. Inflation ends when the slow-roll parameters become of $\mathcal{O}(1)$. In order to solve the flatness and horizon problems, one must have

$$N = \ln \frac{a_{\rm end}}{a_{\rm start}} \geq 60 \, , \tag{2.7}$$

where N is the number of e-folds that the scale factor has grown by from its starting value $a_{\rm start}$ to its value $a_{\rm end}$ at the end of inflation. Once the slow-roll approximation breaks down, the scalar field oscillates at the bottom of its potential and decays into the Standard Model particles in a period called (p)reheating. This acts as an apparent nonsingular Big Bang, which marks the transition between inflation and the radiation dominated Universe. In the following, we will only be interested in the quasi-de Sitter phase of inflation, and we will assume that the scale factor reads $a = e^{Ht}$ with a constant Hubble rate H.

Let us now discuss the dynamics of a scalar field in a de Sitter Universe, since we will be interested in the scalar fluctuations during inflation. We consider for simplicity a free massless scalar ψ with the Lagrangian

$$\mathcal{L} = -\frac{1}{2} g^{\mu\nu} \partial_\mu \psi \partial_\nu \psi \, . \tag{2.8}$$

The corresponding field equation for a time dependent scalar $\psi(t)$ reads

$$\ddot{\psi} + 3H\dot{\psi} - \Delta\psi = 0 \, . \tag{2.9}$$

We now introduce the variable $u = a\psi$ (which has a canonical kinetic term on the de Sitter background), and use the conformal time η given in terms of the cosmic time t as

$$\mathrm{d}t = a \, \mathrm{d}\eta \, . \tag{2.10}$$

The field u can be quantized in the standard way by promoting the Fourier coefficients to operators:

$$\hat{u}(\eta, \mathbf{x}) = \int \frac{\mathrm{d}^3\mathbf{k}}{(2\pi)^{3/2}} \left[u_{\mathbf{k}}(\eta) e^{i\mathbf{k}\cdot\mathbf{x}} A_{\mathbf{k}} + u^*_{\mathbf{k}}(\eta) e^{-i\mathbf{k}\cdot\mathbf{x}} A^\dagger_{\mathbf{k}} \right] \, , \tag{2.11}$$

where $*$ denotes complex conjugation, and $\{A_{\mathbf{k}}, A^\dagger_{\mathbf{k}}\}$ are the annihilation and creation operators, respectively. They verify the following commutation relations:

$$\begin{aligned} &[A_{\mathbf{k}}, A_{\mathbf{k}'}] = [A^\dagger_{\mathbf{k}}, A^\dagger_{\mathbf{k}'}] = 0 \, , \\ &[A_{\mathbf{k}}, A^\dagger_{\mathbf{k}'}] = \delta(\mathbf{k} - \mathbf{k}') \, . \end{aligned} \tag{2.12}$$

Using Eq. (2.9), one can show that the mode functions $u_{\mathbf{k}}(\eta)$ satisfy the equation

$$u_{\mathbf{k}}'' + \left(k^2 - \frac{a''}{a}\right) u_{\mathbf{k}} = 0 \,, \tag{2.13}$$

where a prime denotes differentiation with respect to conformal time. In Minkowski space, when $a'' = 0$, the modes satisfy $u_k \sim e^{-ik\eta}$. It is clear from the previous equation that when $a'' \neq 0$, the scalar acquires an effective mass due to the expansion. For a de Sitter spacetime where H is constant, we have $\eta = -1/(aH)$. This implies that $a''/a = 2/\eta^2$, and in this case the general solution to Eq. (2.13) reads

$$u_k(\eta) = \lambda(k) e^{ik\eta}\left(1 + \frac{i}{k\eta}\right) + \mu(k) e^{-ik\eta}\left(1 - \frac{i}{k\eta}\right) \,, \tag{2.14}$$

where λ and μ are integration constants. The inspection of Eq. (2.13) shows that in the limit $k|\eta| \to \infty$, the mode functions satisfy the same equation as in Minkowski space. This is to be expected, as these very short-wavelength modes don't "see" the spacetime curvature. Hence, it is natural to assume that in this limit we recover $u_k \sim e^{-ik\eta}$ as in Minkowski space. This allows us to set $\lambda = 0$ in Eq. (2.14). Furthermore, canonical quantization imposes the following constraint on the u_k (in natural units $\hbar = 1$):

$$u_k u_k'^{\,*} - u_k^* u_k' = i \,. \tag{2.15}$$

This determines the function μ, and we obtain

$$u_k(\eta) \underset{k|\eta|\to\infty}{\sim} \frac{e^{-ik\eta}}{\sqrt{2k}} \,. \tag{2.16}$$

With this choice, the vacuum state $|0_{\mathrm{BD}}\rangle$ annihilated by $A_{\mathbf{k}}$ is called the Bunch-Davies vacuum [95], i.e. we have $A_{\mathbf{k}}|0_{\mathrm{BD}}\rangle = 0$. In the following, we will assume that the scalar fluctuations are initially in the Bunch-Davies vacuum (i.e. when $\eta \to -\infty$), meaning that the corresponding modes u_k satisfy Eq. (2.16). In the case of a massless scalar in de Sitter space, the solution for u_k is then simply

$$u_k = \frac{e^{-ik\eta}}{\sqrt{2k}}\left(1 - \frac{i}{k\eta}\right) \,.$$

When $k|\eta| \ll 1$, using also that $\eta = -1/(aH)$, we obtain that $\psi_k = u_k/a$ is a constant. Hence, the modes stop evolving (or "freeze") as they exit the horizon, i.e. when $k \simeq aH$.

2.2 Instability of the perturbations on an FLRW background

Let us now go back to the scalar-Gauss-Bonnet theories exhibiting spontaneous scalarization (we will discuss the DEF model in the next chapter). We start with the perturbed equation of motion for the scalar field in the scalar Gauss-Bonnet theories,

which is given by Eq.(1.16):

$$\left[\Box + F''(\phi_0)\hat{G}\right]\delta\phi = 0\ , \tag{2.17}$$

where $\delta\phi$ is the perturbation of the scalar field. As we already mentioned, there are no terms involving $\delta g^{\mu\nu}$ in the above equation since the scalar field is constant on the background. This equation defines an effective mass $m_{\rm eff}$ for the scalar perturbation, where $m^2_{\rm eff} = -F''(\phi_0)\hat{G}$. Assuming the coupling given in Eq. (1.22), the effective mass can be written

$$m^2_{\rm eff} = -\frac{1}{4}\lambda^2\hat{G}\ . \tag{2.18}$$

As we have discussed in the previous chapter, the case of real λ corresponds to theories with scalarized stars and black holes. We now consider a flat Friedmann-Lemaître-Robertson-Walker (FLRW) background given by the metric (2.1). In this case, the perturbation equation (1.16) takes the form

$$\delta\ddot{\phi} + 3H\delta\dot{\phi} - \frac{1}{a^2}\Delta\delta\phi + m^2_{\rm eff}\delta\phi = 0\ , \tag{2.19}$$

where $H \equiv \dot{a}/a$ is the Hubble parameter, and we have assumed a coupling function of the form (1.22). We now expand the scalar perturbation into Fourier modes,

$$\delta\phi(t,\mathbf{x}) = \int \frac{{\rm d}\omega{\rm d}^3\mathbf{k}}{(2\pi)^2}\,\phi(\omega,\mathbf{k})e^{-i(wt-\mathbf{k}\cdot\mathbf{x})}\ ,$$

to obtain the following dispersion relation:

$$\omega^2 = \frac{k^2}{a^2} + m^2_{\rm eff}\ . \tag{2.20}$$

In the above equation, we have neglected the slow change of ω on the time scales shorter than H^{-1}. Whether the mass of the scalar perturbations is real or tachyonic depends on the sign of $\hat{G}$ for the flat FLRW metric (2.1), which is given by Eq. (2.5). This expression shows that $\hat{G}$ has the same sign as $\ddot{a}$. Thus for a decelerating Universe, $\ddot{a} < 0$, i.e. during radiation and matter dominated epochs, the mass of the scalar is real, $m^2_{\rm eff} > 0$, and no instability arises. On the other hand, for an accelerated expansion, $\ddot{a} > 0$, the mass (2.18) becomes tachyonic and the perturbations are unstable. In particular, for a de Sitter solution with constant Hubble rate $H_{\rm dS}$, one finds

$$m^2_{\rm eff} = -6\lambda^2 H^4_{\rm dS}\ . \tag{2.21}$$

The instability is extremely slow for the present-day acceleration of the Universe. Indeed, the ratio of the instability time $t_{\rm inst}$ to the age of the Universe t_0 is estimated as

$$\frac{t_{\rm inst}}{t_0} \sim \frac{H_0}{m_{\rm eff}} \sim \frac{1}{\lambda H_0} \sim 10^{23}\ , \tag{2.22}$$

so that the instability is not noticeable. However, the same estimation for inflation with the scale $H_{\rm inf} \sim 10^{13}$ GeV and $N \sim 10^2$ e-folds yields:

$$\frac{t_{\rm inst}}{t_{\rm inf}} \sim \frac{1}{N\lambda H_{\rm inf}} \sim 10^{-34} \,. \tag{2.23}$$

Thus the GR solution with $\phi = 0$ has a very short instability time. This suggests a catastrophic instability of the theory during the inflation era, unless the initial value of the field ϕ is tuned to be extremely small. Indeed, since the scalar field grows as

$$\phi \sim \phi_1 e^{|m_{\rm eff}|t}$$

starting from some initial value ϕ_1, one may choose ϕ_1 arbitrarily close to 0, so that the instability does not develop during the time of inflation. In particular, if $\phi_1 = \phi_0 = 0$, the field ϕ will stay on the top of the potential for an infinitely long time. However, even for the solution with $\phi_0 = 0$, quantum fluctuations of the scalar field rapidly grow and ultimately destroy the inflationary stage. This happens during a time which is much smaller than the duration of inflation, as we explicitly show in the next section.

2.3 Catastrophic instability of the scalar field during inflation

In this section we show that the tachyonic instability experienced by the scalar field ϕ is inconsistent with the existence of inflation in the early Universe. We approximate inflation by an exact de Sitter expansion with constant H, which is a plausible assumption away from its final stages. In this case the Friedmann equation, which is given by the (tt) component of Eq. (1.13), reads

$$3H^2 = \Lambda + \frac{\dot\phi^2}{2} - 6\lambda^2 H^3 \phi\dot\phi \,.$$

One sees that in the presence of the field ϕ coupled to the Gauss–Bonnet invariant, the Friedmann equation is modified by the term

$$\rho_{\rm GB} = -6\lambda^2 H^3 \phi\dot\phi \,. \tag{2.24}$$

We require that the previous term be negligible compared to the inflaton energy density dominating the evolution of the Universe, i.e.

$$\lambda^2 H|\phi\dot\phi| \ll 1 \,. \tag{2.25}$$

Our goal is to show that this condition gets violated quickly, namely as soon as inflation starts. Even if the field ϕ is set at the top of the effective potential initially, $\phi = 0$, its perturbations will cause a rapid instability. Perturbations of the field ϕ obey Eq. (2.19)

with an effective mass given by Eq. (2.21), where $H_{\rm dS} = H$ is the Hubble factor during inflation.

In the following, we will primarily use the conformal time η, which is defined in terms of the cosmic time in Eq. (2.10). It is negative during inflation, and the scale factor verifies $aH = 1/|\eta|$ during the quasi-de Sitter phase. We now introduce the canonical field

$$\delta\hat{\phi} = M_P \delta\phi \,,$$

and expand the perturbations into Fourier modes. We search for a solution to Eq. (2.19) of the form

$$\delta\hat{\phi}(\eta, \mathbf{x}) = \int \frac{\mathrm{d}^3\mathbf{k}}{(2\pi)^{3/2}} \left[\phi_{\mathbf{k}}(\eta) e^{i\mathbf{k}\cdot\mathbf{x}} A_{\mathbf{k}} + \phi^*_{\mathbf{k}}(\eta) e^{-i\mathbf{k}\cdot\mathbf{x}} A^\dagger_{\mathbf{k}}\right] \,, \tag{2.26}$$

where $A^\dagger_{\mathbf{k}}$ and $A_{\mathbf{k}}$ are the creation and annihilation operators. The functions $\phi_{\mathbf{k}}$ are determined by solving Eq. (2.19), which has the following expression in terms of conformal time:

$$\eta^2 \frac{\mathrm{d}^2\phi_{\mathbf{k}}}{\mathrm{d}\eta^2} - 2\eta \frac{\mathrm{d}\phi_{\mathbf{k}}}{\mathrm{d}\eta} + \left(k^2\eta^2 + \frac{m^2_{\rm eff}}{H^2}\right)\phi_{\mathbf{k}} = 0 \,. \tag{2.27}$$

This equation can easily brought to the Bessel form by performing the change of variable $\phi_{\mathbf{k}} \to (-\eta)^{3/2}\phi_{\mathbf{k}}$. The integration constants are chosen so that in the limit $k|\eta| \to \infty$, the mode $u_{\mathbf{k}} = a\phi_{\mathbf{k}}$ is in the Bunch-Davies vacuum. Under these conditions, we obtain the following expression for the scalar perturbations:

$$\delta\hat{\phi}(\eta, \mathbf{x}) = \int \frac{\mathrm{d}^3\mathbf{k}}{(2\pi)^{3/2}} \frac{\sqrt{\pi}}{2} H|\eta|^{3/2} \left[H^{(2)}_\nu(-k\eta) e^{-i\mathbf{k}\cdot\mathbf{x}} A^\dagger_{\mathbf{k}} + H^{(1)}_\nu(-k\eta) e^{i\mathbf{k}\cdot\mathbf{x}} A_{\mathbf{k}}\right] \,, \tag{2.28}$$

where $H^{(i)}_\nu(-k\eta)$ are the Hankel functions of order

$$\nu = \sqrt{\frac{9}{4} - \frac{m^2_{\rm eff}}{H^2}} \,.$$

Note that the evolution of inflaton perturbations is described by $\nu \approx 3/2$. In that case, perturbations get frozen as they exit the horizon. On the other hand, in the situation with $\nu \gg 3/2$—the case of our interest—perturbations grow fast beyond the horizon, as we will see shortly. This behavior is due to the huge tachyonic mass acquired by the scalar field. Taking the derivative of Eq. (2.28), we get

$$\frac{\partial}{\partial\eta}\delta\hat{\phi}(\eta, \mathbf{x}) = \int \frac{\mathrm{d}^3\mathbf{k}}{(2\pi)^{3/2}} \frac{H\sqrt{\pi}}{2} \left[\left\{-\frac{3}{2}|\eta|^{1/2} H^{(2)}_\nu(-k\eta) + |\eta|^{3/2} \frac{\partial}{\partial\eta}\left[H^{(2)}_\nu(-k\eta)\right]\right\} e^{-i\mathbf{k}\cdot\mathbf{x}} A^\dagger_{\mathbf{k}} + \text{h.c.}\right] \,,$$

where h.c. denotes the Hermitian conjugate, and we have used the following identity for the derivative of the Hankel functions:

$$\frac{\partial}{\partial z} H^{(1,2)}_\nu(z) = \frac{1}{2}\left[H^{(1,2)}_{\nu-1}(z) - H^{(1,2)}_{\nu+1}(z)\right] \,.$$

We are working in the large ν regime, in which case the Hankel functions take the form:

$$H_\nu^{(1,2)}(-k\eta) \underset{\nu\to+\infty}{\simeq} \mp i \left(\frac{2}{-k\eta}\right)^\nu \sqrt{\frac{2}{\pi\nu}} \left(\frac{\nu}{e}\right)^\nu , \tag{2.29}$$

(minus and plus signs correspond to the Hankel functions of the first and second kind, respectively). We see that it has a very sharp dependence on the order ν. Hence, one can keep only Hankel functions with the largest ν when calculating the relevant correlation function:

$$\langle \delta\hat{\phi}(\eta,\mathbf{x}) \frac{\partial}{\partial\eta} \delta\hat{\phi}(\eta,\mathbf{x})\rangle \simeq \int \frac{\mathrm{d}k k^3}{16\pi} H^2 |\eta|^3 H_\nu^{(1)}(-k\eta) H_{\nu+1}^{(2)}(-k\eta) , \tag{2.30}$$

where we made use of the commutation relation (2.12) and integrated over the directions of the momenta $\mathbf{k}$. As the lower limit of the above integral we choose some $k_{\min}$, which is on-horizon at some moment η_1 *during* inflation, i.e. $k_{\min}|\eta_1| = 1$, but otherwise is arbitrary. We choose $|\eta_1| > |\eta|$, so that η_1 corresponds to the past with respect to η. As for the upper limit we take $k_{\max} = 1/|\eta|$. The result, in terms of the dimensionless perturbations $\delta\phi$, is

$$\langle \delta\phi(\eta,\mathbf{x}) \frac{\partial}{\partial\eta} \delta\phi(\eta,\mathbf{x})\rangle = \frac{H^2}{8\pi^2 M_P^2 |\eta|\nu} \left(\frac{2\nu}{e}\right)^{2\nu} \left[\left|\frac{\eta_1}{\eta}\right|^{2\nu-3} - 1\right] .$$

Finally, we use that

$$\langle \delta\phi\, \delta\dot{\phi}\rangle = H|\eta| \langle \delta\phi \frac{\partial}{\partial\eta}\delta\phi\rangle ,$$

and implement condition (2.25) to obtain the ratio η_1/η at which inflation gets violated:

$$\left(\left|\frac{\eta_1}{\eta}\right|^{2\nu-3} - 1\right) \simeq \frac{8\pi^2\nu M_P^2}{\lambda^2 H^4} \cdot \left[\frac{e}{2\nu}\right]^{2\nu} , \tag{2.31}$$

or equivalently

$$\left|\frac{\eta_1}{\eta}\right| \simeq 1 + \mathcal{O}\left(\frac{M_P^2}{\lambda^2 H^4} \cdot \left[\frac{e}{2\nu}\right]^{2\nu}\right) .$$

We see that the modes with the momenta $k_1 \simeq 1/|\eta_1|$ destabilize inflation immediately after exiting the horizon. Given an essentially arbitrary choice of η_1, we conclude that inflation cannot take place in this theory.

One remark is in order here. Recall that our calculations imply the existence of modes which start from the Bunch–Davies vacuum and exit the horizon during inflation. This seemingly modest assumption requires some justification in the situation with exponentially large ν. The asymptotic expansion of the Hankel functions for large positive arguments is given by

$$H_\nu^{(i)}(z) = \left(\frac{2}{\pi z}\right)^{1/2} e^{\pm i(z-\pi\nu/2-\pi/4)} \left(1 + \mathcal{O}\left[\frac{\nu^2}{z}\right]\right) .$$

The Bunch–Davies vacuum is defined in the limit $z = -k\eta \to +\infty$, when the second term in the brackets is irrelevant. In practice, however, inflation has a finite duration. Thus, the quantity z is also large, but finite. Hence, the minimum value of momenta which are in the Bunch–Davies vacuum at the beginning of inflation is given by

$$k_{\min}|\eta_i| \simeq \nu^2 \,, \tag{2.32}$$

where η_i is the conformal time at the beginning of inflation. It is possible, in principle, that the modes with these large momenta never exit the horizon during inflation, formally invalidating our analysis. Let us show that this is not the case, unless the duration of inflation is tuned to its minimum value. By integrating Eq. (2.30) from $k_{\min}$ to infinity, we get

$$\langle \delta\phi \frac{\partial}{\partial\eta}\delta\phi \rangle = \frac{H^2}{8\pi^2 M_P^2 |\eta| \nu} \left(\frac{1}{k_{\min}|\eta|}\right)^{2\nu-3} \left(\frac{2\nu}{e}\right)^{2\nu} \,.$$

We now apply the condition (2.25), which leads to

$$k_{\min}|\eta| \gg \nu \,.$$

Combining the latter with Eq. (2.32), we obtain

$$\left|\frac{\eta_i}{\eta}\right| \ll \nu \,,$$

which should hold until the end of inflation $\eta = \eta_f$. Unless the duration of inflation is close to 60 e-folds, the ratio $|\eta_i/\eta_f|$ is very large, even compared to the huge value $\nu \simeq 10^{32}$ used for scalarization of the stars. Hence, the modes, which are in the Bunch–Davies vacuum initially and exit the horizon during inflation, *alone* destabilize inflation already 75 e-folds after it starts.

Let us now comment on a possible stabilization of the scalar field due to the presence of the quartic corrections, since one should include those anyway to make the scalarized branch of compact objects physically viable [88,89]. It is not difficult to see, however, that the quartic terms cannot stabilize the field ϕ and prevent the instability, because the destabilization occurs at tiny values of ϕ, for which the approximation $F(\phi) \propto \phi^2$ still holds. Indeed, from Eq. (2.28) we obtain

$$\langle \delta\phi^2(\eta, \mathbf{x}) \rangle = \int \frac{k^2 \mathrm{d}k}{8\pi M_P^2} H^2 |\eta|^3 |H_\nu^{(1)}(-k\eta)|^2 \,.$$

Using Eq. (2.29) and integrating over the modes in the range $\left(\frac{1}{|\eta_1|}, \frac{1}{|\eta|}\right)$, we get

$$\langle \delta\phi^2(\eta, \mathbf{x}) \rangle = \frac{H^2}{8\pi^2 M_P^2 \nu^2} \cdot \left(\frac{2\nu}{e}\right)^{2\nu} \cdot \left(\left|\frac{\eta_1}{\eta}\right|^{2\nu-3} - 1\right) \,. \tag{2.33}$$

Finally, substituting Eq. (2.31) into Eq. (2.33), we obtain the typical value of the scalar when inflation is violated:

$$\langle \delta\phi^2(\eta, \mathbf{x}) \rangle \simeq (\lambda H)^{-3} \ ,$$

where we used the relation $\nu \simeq \lambda H$. Given that $\lambda H \simeq 10^{32}$, we conclude that the instability develops at the field values $\sqrt{\langle \delta\phi^2(\eta, \mathbf{x}) \rangle} \sim 10^{-48} \lll 1$ in the theory exhibiting scalarization, i.e. well before the quartic term starts to act.

It would be interesting to find ways to stabilize the theories exhibiting scalarization during inflation. For instance, one may try to solve the problem by adding a coupling to the inflaton χ, e.g., $g^2\chi^2\phi^2$, where g is the coupling constant. In this case the inflaton expectation value serves as a stabilizing effective mass, which vanishes as inflation ends. The problem here is that the coupling constant g should be huge in this approach. Indeed, to balance the large value of $m^2_{\rm eff}$ given by Eq. (2.21), one needs to assume that

$$g^2 \gtrsim \frac{6\lambda^2 H^4}{\chi^2} \simeq 10^{53} \ ,$$

for $\chi \simeq M_P$, $\lambda H \simeq 10^{32}$, and $H \simeq 10^{13}$ GeV. Thus, the theory is deeply in the strong coupling regime, where no trustworthy predictions can be made. On the other hand, as we will explain in the next chapter, this coupling does fix a similar problem in the original DEF model of scalarization without putting the theory in the strong coupling regime.

Another idea would be to add an extra coupling of the scalar to higher powers of curvature, so that it becomes dominant during inflation. The extra term should be of order higher than 2 in curvature, otherwise one risks to spoil scalarization triggered by the coupling to the Gauss–Bonnet invariant, which is of the second order in curvature. For example, the coupling $\sim \phi^2 R^4$ with the appropriate sign stabilizes the scalar field in the high-curvature regime. In this case, similarly to $f(R)$ gravity, an extra scalar degree of freedom is effectively introduced, which is coupled to ϕ. However, the coupling between ϕ and the scalar from the gravitational sector must be huge in order to balance the term involving the Gauss–Bonnet invariant. As we have discussed above, the introduction of a strong coupling is not a viable solution.

Yet another possible way to fix the catastrophic instability during inflation is to introduce quartic terms of the scalar, $\sim \phi^4 \hat{G}$. It has been shown that such terms help to stabilize the scalarized solutions of compact objects, see, e.g., Refs. [88, 89]. However, as we have seen previously, the destabilization of inflation already happens for very small ϕ, where the quartic term does not play any role. Adding a large coupling $\tilde{g}$, i.e., writing $\tilde{g}\phi^4\hat{G}$ does not improve the situation for the following reason. We presume that the solutions for the scalarized compact objects will be indistinguishable from GR ones, since the scalar field will have values extremely close to zero due to the stabilizing quartic term. A very similar idea has been suggested recently in [96], where it has been argued that a quartic term $\sim g\phi^4$, added to the action to stabilize the scalarized solution of compact objects, may also solve the problem of instability during inflation. In [96] it has been suggested that the scalar field is in the minimum of

the effective potential during inflation. It is easy to see, however, that this mechanism cannot work either. First, the minimum should be set at a value of order of $10^{64} M_P$ (in dimensionful units), which is highly unnatural. Moreover, as inflation ends, the structure of the effective potential changes because the scalar-Gauss-Bonnet coupling changes sign, and the scalar tends to the new minimum located at zero. Carrying a tremendous initial potential energy density estimated as $\sim 10^{180} M_P^4$, the rolling scalar field again causes a large modification of the standard cosmological picture.

Finally, we comment on Ref. [97], where the authors identify a theory which allows the scalarization of compact objects while having GR as a cosmological attractor. The authors do not consider the inflationary stage, where the previously discussed instability would be problematic. They instead believe that one should not trust the theory at such high curvatures, but instead find a suitable UV completion where inflation is not broken.

Chapter 3

Quenching the cosmological instability in the DEF model

In this chapter, based on Ref. [98],[1] we examine the cosmological instability in the case of the DEF model. We propose a mechanism to quench the instability, which relies on a coupling of the scalar to the inflaton field. This new coupling term provides another contribution to the effective mass of the scalar ϕ, and allows to stabilize its perturbations during the inflationary stage.

3.1 Setting the problem: cosmological instability of the scalar

In the present section, we estimate the effect of the tachyonic instability in the DEF scenario. The presence of the instability is evident from Eq. (1.7), and it has the same origin as the instability responsible for the scalarization of neutron stars. If $V(\phi) = 0$ as in the original DEF scenario, the second term on the left-hand side of Eq. (1.7) mimics the mass term. This mass term is negative for $\beta < 0$ and thus leads to the tachyonic instability. Let us estimate the rate of this instability during the matter-dominated stage. Neglecting the backreaction of the scalar ϕ on the metric, one obtains the following expression from Eq. (1.7):

$$\ddot{\phi} + 3H\dot{\phi} + \frac{3}{2}\beta H^2\phi = 0 \, .$$

Recall that we work in the Einstein frame. Hence, the scale factor $a(t)$ and the Hubble expansion rate $H(t)$ are defined in this frame. However, in what follows we will not make a distinction between the energy-momentum tensor in the two frames, since $T_{\mu\nu} \simeq \tilde{T}_{\mu\nu}$ as long as $\phi \ll 1$. Later on, we will see that ϕ is indeed extremely close

[1] Note that the mostly minus $(+,-,-,-)$ convention for the metric was used in this reference, unlike in the present chapter.

to zero in our scenario, so this assumption is justified. The above equation has the growing solution given by

$$\phi \simeq \phi_{\rm eq} \left(\frac{t}{t_{\rm eq}}\right)^{\frac{\sqrt{1-\frac{8\beta}{3}}-1}{2}} ,$$

where $H = 2/3t$ and the subscript "eq" denotes the matter-radiation equality. From this relation, one can convert the upper bound on ϕ_0 in Eq. (1.10) into a limit on $\phi_{\rm eq}$. We substitute $t_{\rm eq} \approx 5 \cdot 10^4$ years, $t_0 \approx 13.8 \cdot 10^9$ years, $\beta = -4.5$, and obtain

$$\phi_{\rm eq} \lesssim 10^{-10} . \tag{3.1}$$

Note that we assumed that the matter-dominated stage continues up to the present day, but taking into account the current accelerated expansion of the Universe does not alter this estimate considerably.

The tachyonic instability is also present during the radiation-dominated stage. Even though the equation of state for radiation yields $T = 0$, this is only an approximation. For temperatures higher than 100 GeV, its value is given by the gauge trace anomaly [92–94]

$$T \simeq -\epsilon\rho ,$$

where $\epsilon \simeq 10^{-3}$. At lower temperatures Θ, the parameter ϵ is a function of Θ [99], but does not exceed the value 10^{-2}, see Ref. [100] for details. Hence, in order to obtain an approximate growth of the scalar in the case of maximum destabilization, we will set $\epsilon \simeq 10^{-2}$ in the following. The energy density $\rho_{\rm r}$ of radiation evolves as

$$\rho_{\rm r}(t) = \rho_{\rm r,eq} \frac{a_{\rm eq}^4}{a^4(t)} ,$$

where $\rho_{\rm r,eq}$ is the radiation density at equality. We estimate it as as

$$\rho_{\rm r,eq} \simeq 3M_P^2 H^2(t_{\rm eq}) ,$$

where $H(t_{\rm eq}) \simeq 1/2t_{\rm eq}$ is the Hubble rate at equality obtained by extrapolating the expression $H(t) = 1/2t$ during radiation domination. Putting everything together and substituting the scale factor $a(t) \propto \sqrt{t}$, we obtain the equation

$$\ddot{\phi} + \frac{3}{2t}\dot{\phi} + \frac{3\beta\epsilon}{8t^2}\phi = 0 .$$

This equation admits the growing solution:

$$\phi = \phi_{\rm r} \left(\frac{t}{t_{\rm r}}\right)^{\frac{\sqrt{1-6\beta\sigma}-1}{4}} ,$$

where $t_{\rm r}$ is the cosmic time at the beginning of the radiation dominated epoch, and $\phi_{\rm r} = \phi(t_{\rm r})$. We now set $\beta = -4.5$, $\sigma = 10^{-2}$, $t_{\rm r} \simeq 10^{-32}$ s, and use Eq. (3.1) to estimate

an upper bound on $\phi_{\rm r}$. We find that the scalar grows by a factor of about 25 during the radiation epoch, which leads approximately to:

$$\phi_{\rm r} \lesssim 10^{-11} \ . \tag{3.2}$$

This means that to achieve consistency with Solar System tests, the post-inflationary value of ϕ should be tuned to zero with high accuracy. Note that the value $\phi_{\rm r}$ is also subject to Big Bang Nucleosynthesis (BBN) constraints. However, the latter are very weak [80], typically $\phi_{\rm r} \lesssim 1$. Hence, once we manage to satisfy the constraint (3.2), the BBN limit will automatically be respected.

So far we have assumed that the scalar ϕ is homogeneous, but in practice there are small inhomogeneities due to cosmological perturbations imposed on the scalar field. These inhomogeneities evolve differently depending on their characteristic wavelength, namely there is an upper bound on the wavenumber of cosmological modes which experience the instability:

$$\frac{k}{a(t_{\rm eq})} \lesssim H(t_{\rm eq}) \ . \tag{3.3}$$

Indeed, spatial inhomogeneities of the field ϕ characterized by the wavenumber k yield the term $\sim \frac{k^2}{a^2}\phi_{\mathbf{k}}$ in the evolution equation of the corresponding mode $\phi_{\mathbf{k}}$:

$$\ddot{\phi}_{\mathbf{k}} + 3H\dot{\phi}_{\mathbf{k}} + \frac{3}{2}\beta H^2\phi_{\mathbf{k}} + \frac{k^2}{a^2}\phi_{\mathbf{k}} + ... = 0 \ . \tag{3.4}$$

Here the ellipses stand for the terms sourced by the gravitational potential and matter energy density perturbations, which give a negligible contribution. For perturbations violating the upper bound (3.3), the additional term in Eq. (3.4) screens the one of $\mathcal{O}(H^2)$, which would otherwise give rise to the tachyonic instability. As a result, short wavelength modes decay as $\phi_{\mathbf{k}} \propto 1/a$, as it should be for the case of a massless scalar field in the expanding Universe (see for instance Ref [91]). Thus, we will focus on perturbations obeying Eq. (3.3) in what follows. Note that we consider only the modes which are unstable during matter domination, although strictly speaking there is also a mild instability for the modes that re-enter the horizon during the radiation dominated epoch, as we saw above. We will discuss this in the following.

We now show that if the DEF model is not modified, the constraint given by Eq. (3.2) is violated by the end of inflation. Similarly to the previous chapter, in the case of a coupling to the Gauss-Bonnet invariant, the field ϕ is also subject to the tachyonic instability during the inflationary epoch. As a result, the field ϕ acquires large values inconsistent not only with the Solar System constraints, but also with the existence of the inflationary stage. This conclusion holds even if classically the field ϕ is set exactly at $\phi = 0$ initially. Inevitable vacuum fluctuations of the scalar field are quickly enhanced during inflation leading to a large value of ϕ. We now quantify the effect of vacuum fluctuations assuming an exact de Sitter expansion characterized by the Hubble rate H. We switch to the canonically normalized field $\hat{\phi}$ defined as

$$\delta\hat{\phi} = M_P\sqrt{2}\delta\phi \ . \tag{3.5}$$

In terms of conformal time, defined as (2.10), the perturbations $\delta\hat{\phi}$ obeying the Bunch–Davies vacuum initial conditions read:

$$\delta\hat{\phi} = \int \frac{\mathrm{d}^3\mathbf{k}}{(2\pi)^{3/2}} \frac{\sqrt{\pi}}{2} H|\eta|^{3/2} \left[H_\nu^{(2)}(k|\eta|) e^{-i\mathbf{kx}} A_\mathbf{k}^\dagger + H_\nu^{(1)}(k|\eta|) e^{i\mathbf{kx}} A_\mathbf{k} \right] ,$$

where the order of the Hankel functions is given by

$$\nu = \sqrt{\frac{9}{4} + 6|\beta|} .$$

By setting $\beta = -4.5$, we obtain $\nu \simeq 5$. The expectation value of $\delta\hat{\phi}$ can be calculated from

$$\langle \delta\hat{\phi}^2 \rangle = \int \frac{\mathrm{d}k k^2}{8\pi} H^2 |\eta|^3 \left| H_\nu^{(1)}(k|\eta|) \right|^2 .$$

We are interested in superhorizon modes, i.e. $k|\eta| \to 0$, which add up to the classical background of the field $\hat{\phi}$. In this limit, one has for the Hankel functions

$$H_\nu^{(1,2)}(k|\eta|) = \mp \frac{i\Gamma(\nu)}{\pi} \left(\frac{2}{k|\eta|} \right)^\nu .$$

The result reads

$$\langle \delta\hat{\phi}^2 \rangle_{\{k\}} = \frac{2^{2\nu}\Gamma^2(\nu) H^2}{8(2\nu-3)\pi^3} \left[(k_{\min}|\eta|)^{3-2\nu} - (k_{\max}|\eta|)^{3-2\nu} \right] .$$

Here $\{k\}$ denotes the range of momenta $(k_{\min}, k_{\max})$. Given that $\nu \simeq 5$ and assuming $k_{\max} \gg k_{\min}$, the second term in the square brackets is irrelevant. Conservatively, one can take $k_{\min} \simeq H_0$ (we set the scale factor $a_0 = 1$ today) corresponding to the largest mode which is interesting for cosmology. The final expression in terms of the original field ϕ is then given by

$$\langle \delta\phi^2 \rangle_{\{k\}} = \frac{2^{2\nu}\Gamma^2(\nu) H^2}{16(2\nu-3)\pi^3 M_P^2} \left| \frac{\eta_*}{\eta} \right|^{2\nu-3} ,$$

where η_* denotes the time when the cosmological mode with wavenumber $k_{\min}$ exits the horizon. It is evident that $\sqrt{\langle \delta\phi^2 \rangle_{\{k\}}}$ is very large for $|\eta_*| \gg |\eta|$, given the minimal duration of inflation which should last for at least $50 - 70$ e-folds. Hence, we end up with an unacceptably large ϕ which violates existing Solar System constraints and also threatens the existence of the inflationary stage. Indeed, according to Eq. (1.4) $\phi \gg 1$ corresponds to a huge $\tilde{\phi} \ggg 1$ in the Jordan frame. This means that the field $\tilde{\phi}$ quickly comes to dominate the evolution of the Universe, and inflation terminates. We conclude that the DEF scenario should be modified at least in the very early Universe, and one modification of this type is discussed in the next section.

Before that, let us briefly comment on some solutions to the problem of the tachyonic instability which exist in the literature. In Ref. [80], it was proposed to endow the

scalar with a small mass m by introducing a potential $V(\phi) = m^2\phi^2/2$. As the Hubble rate drops down to $H \simeq m$, the field ϕ starts to decay, oscillating about the minimum of its potential at $\phi = 0$. From this point on, it contributes to the dark matter content of the Universe. Given post-inflationary conditions for the field ϕ assumed in Ref. [80], $\phi_{\rm i} \simeq 1$ and $\dot{\phi}_{\rm i} \simeq 0$, the mass m should be extremely tiny, i.e. $m \lesssim 10^{-28}$ eV. For masses violating this bound, the field ϕ gives an unacceptably large contribution to the energy density of the Universe. Apart from tuning the mass m, the instability during inflation remains an issue, as discussed above. As a result of this instability, one should expect the initial condition $\phi_{\rm i} \gg 1$ rather than $\phi_{\rm i} \lesssim 1$.

In passing, we would like to point out that the instability during inflation and at later stages can be avoided by choosing the following form for the function $A(\phi)$ [81]:

$$\ln A(\phi) = \frac{\beta\phi^2}{2} + \frac{\gamma\phi^4}{4} \,. \tag{3.6}$$

Choosing the extra parameter $\gamma > 0$, one can stabilize the field ϕ during inflation, so that it evolves close to the effective minimum $\phi = \sqrt{-\beta/\gamma}$ right until present. Unfortunately, this scenario does not work, because with $\phi_0 \neq 0$ and $\gamma \neq 0$, the scalarization of neutron stars does not occur.

3.2 Cosmological relaxation of the field ϕ to zero

In this chapter, we follow another approach to the problem of consistency with Solar System tests. Namely, we will find a way to relax the field ϕ to tiny values during inflation, well below the upper bound in Eq. (3.2), while at the same time retaining the original form of the DEF model at post-inflationary times. The idea is to couple the field ϕ to the inflaton χ, by considering an interaction of the form $\sim \phi^2\chi^2$. Such a coupling induces a large effective mass for the field ϕ during inflation, so that ϕ relaxes to an exponentially small value. The effective mass term vanishes upon the inflaton decay, so that we end up with the standard DEF scenario after inflation. While the tachyonic instability during the matter-dominated stage is still present, there is not enough time for the field ϕ to grow to large values by cosmological mechanisms. In other words, the inequality (1.10) is always satisfied, in agreement with the Solar System tests.

We assume that inflation is driven by the canonical scalar field χ rolling down the slope of its (almost) flat potential $U(\chi)$. In the Einstein frame its action is given by

$$S_\chi\left[A^2(\phi)g_{\mu\nu}, \chi\right] = \int {\rm d}^4x\sqrt{-\tilde{g}}\left[-\frac{1}{2}\tilde{g}^{\mu\nu}\partial_\mu\chi\partial_\nu\chi - U(\chi)\right]|_{\tilde{g}_{\mu\nu}=A^2(\phi)g_{\mu\nu}} \,.$$

Note that unlike the field ϕ, the inflaton χ is assumed to have a canonical mass dimension. We modify the DEF model by assuming a nonzero interacting potential

$$V(\phi, \chi) = g^2\phi^2\chi^2 \,, \tag{3.7}$$

where g^2 is some dimensionless coupling. Thus the field ϕ has the effective mass $g^2\chi^2$ due to the coupling to the inflaton. We require that

$$g^2\chi^2 \gg H^2 \ . \tag{3.8}$$

Hence, the field ϕ is effectively superheavy, meaning that its effective mass is larger than the inflationary Hubble rate (but still below the Planckian scale). In this case, ϕ relaxes to zero within a few Hubble times. For the typical values $\chi \simeq M_P$ and $H \simeq 10^{13}$ GeV, the constant g^2 can be as small as $g^2 \simeq 10^{-10}$. Hence, the mechanism which cures the instabilities can operate in a very weakly coupled regime. In the Jordan frame, the potential (3.7) is transformed to

$$\Pi(\tilde{\phi},\chi) = 2g^2\phi^2(\tilde{\phi})\tilde{\phi}^2\chi^2 \ , \qquad \phi^2(\tilde{\phi}) = -\frac{\ln\tilde{\phi}}{\beta} \ .$$

Note that Eq. (1.4) implies $\tilde{\phi} > 1$ for $\beta < 0$. Hence, the Jordan frame interacting potential $\Pi(\tilde{\phi},\chi)$ is positive. We see that modulo the logarithmic correction, the interacting potential has a quadratic form in the Jordan frame as well. Therefore it is not important in which frame the coupling to the inflaton is introduced. We now list the set of equations relevant for future purposes. The metric field equations are given by

$$R_{\mu\nu} - \frac{1}{2}g_{\mu\nu}R = \frac{T^{\chi}_{\mu\nu}}{M_P^2} + T^{\phi}_{\mu\nu} \ ,$$

where

$$T^{\phi}_{\mu\nu} = 2\partial_\mu\phi\partial_\nu\phi - g_{\mu\nu}\partial_\alpha\phi\partial^\alpha\phi - g_{\mu\nu}V(\phi,\chi) \ ,$$

and

$$T^{\chi}_{\mu\nu} = A^2(\phi)\partial_\mu\chi\partial_\nu\chi - \frac{1}{2}g_{\mu\nu}A^2(\phi)\partial_\alpha\chi\partial^\alpha\chi - g_{\mu\nu}A^4(\phi)U(\chi) \ . \tag{3.9}$$

Note that the indices are raised and lowered with the Einstein metric $g_{\mu\nu}$. The equations of motion for the field ϕ is given by Eq. (1.7), where T is replaced by T^{χ}, while the equation for the inflaton reads

$$\tilde{\Box}\chi - U_\chi - \frac{M_P^2}{A^4(\phi)}V_\chi(\phi,\chi) = 0 \ .$$

3.2.1 Relaxing the background value of ϕ to zero

Let us show that the background value of the scalar relaxes to zero during inflation. The Friedmann equation is given by

$$3H^2 = \dot{\phi}^2 + V(\phi,\chi) + \frac{A^2(\phi)\dot{\chi}^2}{2M_P^2} + \frac{A^4(\phi)U(\chi)}{M_P^2} \ ,$$

and the background evolution of the scalar ϕ is governed by

$$\ddot{\phi} + 3H\dot{\phi} + \frac{\alpha(\phi)}{2M_P^2}\left[4A^4(\phi)U(\chi) - A^2(\phi)\dot{\chi}^2\right] + g^2\chi^2\phi = 0\ . \tag{3.10}$$

As usual, we assume that the inflaton potential dominates the energy density of the Universe, i.e. $3H^2 \approx A^4(\phi)U(\chi)/M_P^2$. Consequently, we drop the second term in the square brackets of Eq. (3.10). The background equation for ϕ simplifies to

$$\ddot{\phi} + 3H\dot{\phi} + m^2\phi = 0\ ,$$

where m^2 is the full effective mass of the field ϕ defined by

$$m^2 = g^2\chi^2 + 6\beta H^2\ .$$

Provided that the condition (3.8) is obeyed and $|\beta|$ is not very large, the field ϕ evolves as a superheavy field, which relaxes to zero within a few Hubble times. In the exact de Sitter space-time approximation, the solution for the field ϕ is given by

$$\phi = \frac{C}{a^{3/2}}\cos\left[\sqrt{m^2 - \frac{9H^2}{4}}\,t + \delta\right]\ ,$$

where C and δ are irrelevant constants. We conclude that starting from subplanckian values $\phi < 1$, by the end of inflation the field ϕ is relaxed to

$$\phi \lesssim 10^{-39}\ ,$$

where the upper bound corresponds to the minimal duration of inflation—about 60 e-folds. Generically, the duration of inflation is much larger, so one can safely set the background value of ϕ to zero.

The background evolution of the inflaton is given by the equation:

$$\ddot{\chi} + 3H\dot{\chi} + 2\alpha(\phi)\dot{\chi}\dot{\phi} + A^2(\phi)U_\chi + \frac{M_P^2}{A^2(\phi)}V_\chi(\phi,\chi) = 0\ .$$

As $\phi \to 0$, one has $\alpha(\phi) \to 0$, $A(\phi) \to 1$, and $V_\chi \to 0$. Therefore, the evolution of the inflaton proceeds as in GR.

3.2.2 Relaxing the perturbations $\delta\phi$ to zero

One may naively expect the field ϕ to develop superhorizon perturbations $\delta\phi \simeq H/M_P$ for each mode. Taking into account that for standard inflation scenarios

$$\frac{H}{M_P} \sim 10^{-5}\ ,$$

such perturbations would be a problem for the DEF model, cf. Eq. (3.2). Such a situation would occur for light fields during inflation, but our case is different, since the field ϕ is effectively superheavy. We will prove below that perturbations $\delta\phi$, which source the present day cosmological value of ϕ, are exponentially suppressed by the end of inflation.

In the Newtonian gauge, linear metric perturbations are given by

$$\mathrm{d}s^2 = -(1+2\Phi)\mathrm{d}t^2 + a^2(1-2\Psi)\delta_{ij}\mathrm{d}x^i\mathrm{d}x^j \ .$$

In the absence of the anisotropic stress, which is the case here, we have $\Phi = \Psi$. We are primarily interested in the linear perturbation $\delta\phi$. The relevant equation is given by

$$\begin{aligned}\delta\ddot{\phi} - \frac{1}{a^2}\partial_i\partial_i\delta\phi - 2\ddot{\phi}\Phi - 4\dot{\phi}\dot{\Phi} - 6H\dot{\phi}\Phi + 3H\delta\dot{\phi} - \frac{\delta T^\chi}{2M_P^2}\alpha(\phi) \\ - \frac{T^\chi}{2M_P^2}\frac{\partial\alpha(\phi)}{\partial\phi}\delta\phi + \frac{1}{2}\frac{\partial^2 V}{\partial\phi^2}\delta\phi + \frac{1}{2}\frac{\partial^2 V}{\partial\phi\partial\chi}\delta\chi = 0 \ ,\end{aligned} \tag{3.11}$$

where

$$\begin{aligned}\delta T^\chi = -16A^4(\phi)\alpha(\phi)U(\chi)\delta\phi - 4A^4(\phi)\frac{\mathrm{d}U}{\mathrm{d}\chi}\delta\chi \\ + 2A^2(\phi)\alpha(\phi)\dot{\chi}^2\delta\phi - 2A^2(\phi)\dot{\chi}^2\Phi + 2A^2(\phi)\dot{\chi}\delta\dot{\chi} \ .\end{aligned}$$

While this equation looks rather complicated, it is simplified upon substituting the background value $\phi = 0$. We obtain in terms of the Fourier modes $\delta\phi_{\mathbf{k}}$:

$$\delta\ddot{\phi}_{\mathbf{k}} + 3H\delta\dot{\phi}_{\mathbf{k}} + \frac{k^2}{a^2}\delta\phi_{\mathbf{k}} - \frac{T^\chi}{2M_P^2}\frac{\partial\alpha(\phi)}{\partial\phi}\delta\phi_{\mathbf{k}} + \frac{1}{2}\frac{\partial^2 V}{\partial\phi^2}\delta\phi_{\mathbf{k}} = 0 \ .$$

This is a homogeneous equation, which describes a damped oscillator with an almost constant large mass. The modes $\delta\phi_{\mathbf{k}}$ decay as $1/a^{3/2}$ in the superhorizon regime. Hence, they have negligibly small amplitudes by the end of the inflationary stage. We will make an exact estimate of the field ϕ due to its perturbations shortly.

Before going into details let us make two comments. First, note that the vanishing background value of ϕ shields the perturbations $\delta\phi$ from the metric and inflaton fluctuations $\delta\chi$. Generally, the latter source adiabatic perturbations, which turn out to be zero in our case. This is also evident from the expression for adiabatic perturbations in the superhorizon regime [101]:

$$\begin{aligned}\frac{\delta\phi_{\mathrm{ad}}}{\dot{\phi}} = \frac{\delta\chi}{\dot{\chi}} = \frac{1}{a}\cdot\left(C_1\int_0^t a\mathrm{d}t' - C_2\right) \ , \\ \chi = C_1\cdot\left(1 - \frac{H}{a}\int_0^t a\mathrm{d}t'\right) + C_2\frac{H}{a} \ .\end{aligned}$$

Here C_1 and C_2 are some constants defined by the subhorizon evolution of the gravitational potential. Independently of their values, we have $\delta\phi_{\rm ad} \to 0$, because $\dot\phi \to 0$.

Secondly, we have only considered linear perturbations $\delta\phi$. However, using the same argument as above one can show that once $\phi \to 0$ and the linear perturbation $\delta\phi \to 0$, the second-order perturbation $\delta\phi^{(2)}$ also obeys the homogeneous oscillator equation with the Hubble friction and a very large mass. Hence, it should also decay as $\delta\phi^{(2)} \propto 1/a^{3/2}$ in the superhorizon regime.

The above consideration shows that the perturbations $\delta\phi$ are indeed very small at the end of inflation. However, we still need to estimate the amplitude of perturbations in order to compare it with the constraint (3.2). We approximate inflation by an exact de Sitter stage and switch to the canonical variable $\delta\hat\phi$ related to the original field $\delta\phi$ by Eq. (3.5). The solution for the field $\delta\hat\phi$ obeying Bunch–Davies vacuum initial conditions is given by

$$\delta\hat\phi = \int \frac{{\rm d}^3\mathbf{k}}{(2\pi)^{3/2}} \frac{\sqrt{\pi}}{2} H|\eta|^{3/2} \left[e^{\frac{\pi s}{2}} H^{(2)}_{is}(k|\eta|) e^{-i\mathbf{kx}} A^\dagger_{\mathbf{k}} + e^{-\frac{\pi s}{2}} H^{(1)}_{is}(k|\eta|) e^{i\mathbf{kx}} A_{\mathbf{k}} \right] , \quad (3.12)$$

where the $H^{(1,2)}_{is}$ are Hankel functions of purely imaginary order [102] and

$$s = \sqrt{\frac{m^2}{H^2} - \frac{9}{4}} \, .$$

Note that the functions $H^{(1,2)}_{is}$ are not complex conjugate. Instead, the following relation is correct:

$$\left[H^{(1)}_{is}(k|\eta|) \right]^* = e^{\pi s} H^{(2)}_{is}(k|\eta|) \, ,$$

which explains the presence of unconventional factors $e^{\frac{\pi s}{2}}$ in Eq. (3.12). For $s \gg 1$, one obtains the following relation in the limit $k|\eta| \to 0$ [102]:

$$H^{(1,2)}_{is}(k|\eta|) = \sqrt{\frac{2}{\pi s}} e^{\pm is \ln\left[-\frac{1}{2}k\eta\right] \mp i\gamma_s \pm \frac{\pi s}{2}} \, ,$$

where $\mp\gamma_s$ are irrelevant phases. The choice of the upper or lower sign on the right-hand side of the previous corresponds to the Hankel functions of the first and the second kind, respectively. We are interested in the quantity $\langle \delta\hat\phi^2 \rangle_{\rm unstable}$, where the subscript "unstable" means that we focus on the modes which are subject to the tachyonic instability during the matter-dominated stage. These modes have the cutoff $k_{\rm max}$ defined by the condition (3.3). Strictly speaking, the modes that reenter the horizon during the radiation dominated epoch also experience an instability, but it is much milder than the one for super-horizon modes during matter domination.

By the end of inflation, at the moment η_f, the value of $\langle \delta\hat\phi^2 \rangle_{\rm unstable}$ is given by

$$\langle \delta\hat\phi^2 \rangle_{\rm unstable}(\eta_f) = \frac{H^2}{12\pi^2 s} \left| \frac{\eta_f}{\eta_\times} \right|^3 \, ,$$

where $\eta_\times$ is defined by $k_{\rm max}|\eta_\times| \simeq 1$. In terms of the original field ϕ, one finally gets

$$\langle \delta\phi^2 \rangle_{\rm unstable}(\eta_f) = \frac{H^2}{24\pi^2 s M_P^2} \left| \frac{\eta_f}{\eta_\times} \right|^3 .$$

Note that $\eta_\times$ roughly corresponds to 50-70 e-folds before the end of inflation, when cosmological modes exit the horizon. For the sake of concreteness, we assume 60 e-folds. Taking also $H \simeq 10^{-5} M_P$ (high scale inflation) and $s = 10$, we find

$$\sqrt{\langle \delta\phi^2 \rangle_{\rm unstable}(\eta_f)} \simeq 10^{-46} . \tag{3.13}$$

The field ϕ will be roughly frozen at this value during the radiation-dominated stage (modulo the enhancement by a factor of about 25 discussed in the previous section). During the matter-dominated stage, and later, it experiences the tachyonic instability. However, the resulting field ϕ_0 is still well below the upper bound, i.e., $\phi_0 \lll 10^{-3}$, in a comfortable agreement with the Solar System tests. Note that we have omitted some modes from the discussion, i.e. those that are unstable during radiation domination only and exit the horizon between $\eta_\times$ and η_f. One can estimate the contribution of these modes to the amplitude of the scalar fluctuations at the end of inflation by integrating Eq. (3.12) in the range of momenta $\{k_{\rm max}, k_f\}$, where $k_f|\eta_f| = 1$. We obtain the rough estimate

$$\sqrt{\langle \delta\phi^2 \rangle_{\{k_{\rm max}, k_f\}}(\eta_f)} \simeq 10^{-6} . \tag{3.14}$$

Since these modes experience the instability only during radiation domination, they will only grow by a factor of 10, and will not violate current bounds on the scalar field. Hence, we did not include them in the previous discussion. Note also that upon establishing the bounds (3.1) and (3.2) for the scalar field, we have overestimated the instability of the scalar. Indeed, each mode characterized by the wavenumber k is only unstable for $k < aH$, so the modes stop growing after re-entering the horizon, which was not taken into account. However, the scalar is able to satisfy even those overestimated bounds, which is why the calculation was not refined.

Recall that we have assumed a universal coupling of matter fields to the metric. Let us comment here on modifications of the model where the coupling is non-universal. For instance, one may consider a model with a direct coupling of the inflaton to the Einstein metric. Contrary to the situation with the universal coupling, now the scalar field ϕ does not receive an effective tachyonic potential, and thus does not undergo the instability during inflation. Hence, one may naively expect that the model is viable even in the absence of the stabilizing potential $V(\phi, \chi)$ introduced in Eq. (3.7). In this case, however, the scalar ϕ enjoys shift symmetry, and hence can take on any value. Modulo fine-tuning, this value is not small generically, leading to a large value of ϕ_0 today, and consequently to the conflict with Solar System tests. Moreover, even if the background value of ϕ is tuned to zero, the perturbations $\delta\phi$ are still too large and give

rise to $\phi_0 \gg 1$. This problem is avoided upon turning on the potential $V(\varphi, \chi)$ as in Eq. (3.7). Yet another possibility is to couple the inflaton to the Einstein metric with a conformal factor as in Eq. (1.2), but with positive $\beta_{\rm inf} > 0$ (while at the same time keeping $\beta < 0$ for the normal matter to ensure scalarization). In this case, according to Eq. (1.7), the field ϕ acquires a positive mass even if $V(\varphi, \chi) = 0$. Provided that $\beta_{\rm inf} \gg 1$, the scalar ϕ is superheavy. Hence it relaxes to zero exactly in the same way as in the model with the stabilizing potential $V(\phi, \chi)$. In fact, one can view this scenario as a variation of the model discussed in this chapter, modulo the replacement of the coupling $\sim \phi^2\chi^2$ by the coupling of the field ϕ to the trace of the inflaton energy-momentum tensor.

Conclusion to Part I

The spontaneous scalarization of compact objects is an interesting phenomenon which may arise in certain classes of scalar-tensor theories. This effects relies on the existence of a tachyonic effective mass for the scalar field which destabilizes the GR solutions. In Chapter 1, we reviewed this mechanism both in the original DEF scenario for neutron stars, but also for classes of theories where the scalar field is nonminimally coupled to the Gauss-Bonnet invariant. In this case scalarization can exist for black holes as well as stars, since the Gauss-Bonnet term is nonzero in vacuum.

In Chapter 2, we studied the stability of cosmological solutions in the latter theories. As we showed in Section 2.2, the stability of scalar perturbations on GR cosmological solutions depends on the sign of the acceleration $\ddot{a}$, see Eqs. (2.18) and (2.5). For a decelerating Universe, the mass in the equation for the scalar perturbation is real, and therefore no instability arises for the GR branch. However, the mass becomes tachyonic for an accelerated expansion, and one expects the GR cosmological solution to become unstable in that case. It turns out that this instability is very slow with respect to the current acceleration, with the time of instability being much larger than the age of the Universe, see Eq. (2.22). On the contrary, the scalar-Gauss-Bonnet coupling leads to a catastrophic instability during the inflationary epoch, due to its huge effective tachyonic mass. The characteristic instability time, at which the amplitude of a classical solution increases by the factor e, is given in Eq. (2.23). This is a tiny number compared to the time of inflation. One should take into account that classically the initial conditions of the scalar field can be tuned such that the field stays on top of the potential for an infinite time, at least in principle. However, as we explicitly showed in Section 2.3, quantum fluctuations of the scalar field are large enough to trigger this instability, making any conventional inflationary scenario impossible in the theories exhibiting scalarization which we studied. Throughout this analysis, we have assumed that the scalarization field ϕ is *not* the inflaton field. However, the Gauss-Bonnet scalar is an ultraviolet correction which naturally modifies gravity at early times. Indeed, inflation models where the Gauss-Bonnet scalar is coupled to the inflaton field according to the action (1.11) have been studied in the literature (see for instance Refs. [103–105]). However, in these works, the effective sign of the coupling function F in Eq. (1.11) is crucially required to be of the opposite sign to the one which allows for scalarization.

In Chapter 3, we proposed a way to extend the original DEF model of scalarization to cosmological scales, while retaining consistency with Solar System tests. In the cosmological context, the original model leads to a runaway solution for the relevant field ϕ, making the scenario inconsistent with existing PPN constraints unless the initial value of ϕ is tuned to zero with high precision, as we discussed in Section 3.1. We have found a modification of the original scenario in which this tuning is automatic. More precisely, we showed in Section 3.2 that if the field ϕ responsible for scalarization is coupled to the inflaton, it relaxes to zero with a high accuracy during inflation. Upon the inflaton decay, the coupling effectively vanishes, meaning that in our modified

scenario all the predictions related to neutron stars are the same as in the original DEF model. Note that the results of this part are largely insensitive to the structure of the conformal factor $A(\varphi)$. While we have focused on the simple quadratic function $\ln A(\varphi) \propto \varphi^2$, involving higher powers of φ would leave our analysis and conclusions intact. Moreover, the solution we proposed to quench the cosmological instability could be applied to other models of scalarization akin to the DEF model. Indeed, starting from the action (1.1), one can make the disformal transformation of the metric as

$$g_{\mu\nu} \to C(X) g_{\mu\nu} + D(X) \partial_\mu \varphi \partial_\nu \varphi \ ,$$

where $C(X)$ and $D(X)$ are functions of the kinetic term $X = (\partial\varphi)^2$. The transformation results in a new scalar-tensor action belonging to the DHOST class (31). In the context of scalarization, such extensions have been discussed in Refs. [67,106]. We believe that our solution to the cosmological instability presented in this paper may also work for such extensions. Another idea would be to consider the scalar-Gauss-Bonnet theories in which rapidly rotating black holes were shown to scalarize [70–72]. Crucially, this can happen for a reversed sign of the parameter λ^2 in Eq.(2.18), because the Gauss-Bonnet scalar of a rotating black hole can change sign, unlike in the spherically symmetric case. Perhaps this sign reversal could lead to a relaxation of the scalar during the inflationary phase, instead of the instability discussed in Chapter 2, and we believe that this point deserves further study.

Part II

Vainshtein screening for slowly rotating stars

Introduction to part II

One of the approaches to modify general relativity (GR) is to add extra fields mediating the gravitational force, and the simplest extensions are scalar-tensor theories with one additional scalar field. However, since GR passes all local experimental tests in the Solar System [50], it is necessary to have a mechanism that screens the effect of the scalar field (fifth force) close to the gravitational source. There have been several propositions to suppress the fifth force around matter, like the chameleon [107] or symmetron mechanisms [108, 109]. We will be interested in the Vainshtein mechanism, which was originally proposed in the context of massive gravity. The linear Fierz-Pauli theory describes a free spin-2 particle of mass m [110–112]. For nonzero m, these theories were shown to have different predictions from linearized GR, even in the limit $m \to 0$, which is related to the van-Dam-Veltman-Zakharov (vDVZ) discontinuity [113–115]. The Newtonian potential for nonrelativistic bodies in these theories is larger by a factor 4/3, and hence theories which exhibit this effect are ruled out by Solar System observations. Indeed, if this extra factor were to be reabsorbed in the definition of Newton's constant, it would manifest itself in other measurable quantities. For example the bending of light by the Sun in the massive theory would be too small to pass the current experimental bounds [50]. Shortly after this was pointed out, Vainshtein proposed that the linear theory should break down inside a certain radius r_V from the gravitational source [116], where r_V is now called the Vainshtein radius. However, he did not show that the expansions in the two different regimes could be obtained by a unique underlying solution. In addition, such nonlinear theories were shown to generically present a ghost instability [117], i.e. a degree of freedom with an energy which is unbounded from below. It was understood later that the Vainshtein screening could work in a certain limit of these theories, called the decoupling limit (DL), which isolates the dominant derivative self-interactions of the massive graviton's scalar mode [118–125]. While this limit simplifies the problem, the Vainshtein mechanism was also shown to work in the full theory of nonlinear massive gravity [119, 120]. In parallel, an analogous mechanism, dubbed k-mouflage [126], was developed in the context of scalar-tensor theories. It relies on the presence of a nonlinear scalar kinetic term, which explains the name. The covariant k-mouflage action can be written [126, 127]

$$S_{\rm k} = \frac{M_P^2}{2}\int {\rm d}^4x \left[R\left(1+\frac{\phi}{2}\right) + K_{\rm NL}[\phi]\right] + S_{\rm m}\left[g_{\mu\nu}, \psi_{\rm m}\right] \ , \tag{II.1}$$

where the term $K_{\rm NL}$ contains nonlinear self-interactions of the scalar field. The idea is to expand this action around flat space, i.e. $g_{\mu\nu} = \eta_{\mu\nu} + h_{\mu\nu}$, and keep terms up to second order in $h_{\mu\nu}$. Higher-order terms are kept in $K_{\rm NL}$ however, as they are important for the screening to work. After the following redefinition of the tensor h,

$$h_{\mu\nu} = \tilde{h}_{\mu\nu} - \phi\,\eta_{\mu\nu} \ , \tag{II.2}$$

the k-mouflage action reads

$$S_{\rm k} = \frac{M_P^2}{4}\int {\rm d}^4x \left[-\tilde{h}^{\mu\nu}E_{\mu\nu}{}^{\alpha\beta}\tilde{h}_{\alpha\beta} + 3\phi\Box\phi + 2m^2K_{\rm NL}[\phi] + \frac{2}{M_P^2}\left(\tilde{h}^{\mu\nu}T_{\mu\nu} - T\phi\right)\right] ,$$

where the tensor $E_{\mu\nu} = E_{\mu\nu}{}^{\alpha\beta}h_{\alpha\beta}$ is the linearization of the Einstein tensor around flat space, and the indices are raised with the flat metric $\eta_{\mu\nu}$ in the previous expression. The field equations which derive from this action read

$$\begin{aligned} E_{\mu\nu}{}^{\alpha\beta}\tilde{h}_{\alpha\beta} &= \frac{T_{\mu\nu}}{M_P^2} , \\ 3\Box\phi + E_{\rm NL} &= \frac{T}{M_P^2} , \end{aligned} \tag{II.3}$$

where $E_{\rm NL}$ is obtained from varying the part of the action containing $K_{\rm NL}$. The main features of the Vainshtein mechanism can be understood from these equations, as explained in Ref. [127]. There are two different regimes, depending on which term dominates in the scalar field equation:

- If $\Box\phi \gg E_{\rm NL}$, then the scalar equation is linear and we have $\phi \sim \tilde{h}_{\mu\nu}$. This means that the physical metric $h_{\mu\nu}$, given by Eq. (II.2), receives leading-order corrections and GR is modified. We will see that the linear regime corresponds to a region far away from the gravitational source.
- On the other hand, if a region exists where $\Box\phi \ll E_{\rm NL}$, then $\phi \ll \tilde{h}_{\mu\nu}$ and we recover GR, i.e. $h_{\mu\nu} \simeq \tilde{h}_{\mu\nu}$. This is called the nonlinear regime, and it generically happens inside a radius r_V which is given by the theory at hand.

The Vainshtein mechanism can be most easily demonstrated for nonrelativistic spherically symmetric static configurations outside the source. Let us give a simple illustration in the case of the cubic Galileon theory [128]. We choose the following functions in the DHOST action (31):

$$f = 1 + \alpha\phi , \qquad K = \eta X , \qquad G_3 = \beta X , \qquad A_1 = A_3 = 0 , \tag{II.4}$$

where $\{\alpha, \beta, \eta\}$ are constants. Note that upon imposing the DHOST Ia conditions (33), this leads to $A_4 = A_5 = 0$ also. We consider a static scalar field $\phi = \phi(r)$, and use the following ansatz for the metric tensor:

$${\rm d}s^2 = -e^{\nu}{\rm d}t^2 + e^{\lambda}{\rm d}r^2 + r^2\left({\rm d}\theta^2 + \sin^2\theta{\rm d}\varphi^2\right) . \tag{II.5}$$

We will use this ansatz throughout this part, but we give here the relation between the functions $\{\lambda, \nu\}$ and the potentials $\{\Phi, \Psi\}$ in the Newtonian gauge which are often used in the literature. The metric in isotropic coordinates is written

$${\rm d}s^2 = -\left(1 + 2\Phi(\bar{r})\right){\rm d}t^2 + \left(1 - 2\Psi(\bar{r})\right)\left[{\rm d}\bar{r}^2 + \bar{r}^2\left({\rm d}\theta^2 + \sin^2\theta{\rm d}\varphi^2\right)\right] , \tag{II.6}$$

and in the weak field limit, one can show that the following relations hold

$$r \simeq \bar{r}\,(1-\Psi) \simeq \bar{r}\ , \qquad \nu = 2\Phi\ , \qquad \lambda = 2r\Psi'\ .$$

In GR, the potentials in the Newtonian limit are given by

$$\Phi_{\rm GR} = \Psi_{\rm GR} = -\frac{r_S}{2r}\ , \qquad \text{or} \qquad \lambda_{\rm GR} = -\nu_{\rm GR} = \frac{r_S}{r}\ . \tag{II.7}$$

In the weak field limit [120], i.e. $\{\nu, r\nu', \lambda, r\lambda', \phi, r\phi'\} \ll 1$, the independent field equations for the theory (II.4) read

$$\begin{aligned} \frac{\mathrm{d}}{\mathrm{d}r}\left[r\lambda - \alpha r^2\phi'\right] &= r^2\rho(r)\ , \\ \lambda - r\nu' &= 2\alpha\phi'\ , \\ \frac{1}{r^2}\frac{\mathrm{d}}{\mathrm{d}r}\left[r\alpha\,(2\lambda - r\nu') - 2\eta r^2\phi' + 2\beta r\phi'^2\right] &= 0\ , \end{aligned} \tag{II.8}$$

where $\rho(r)$ is the energy density of the source, and we have neglected its pressure because it is assumed to be nonrelativistic. These correspond to the (tt), (rr) and scalar field equations, respectively. The third equation can be written in an integrated form because in the weak-field approximation, the Ricci scalar reads

$$R_{\rm weak} = \frac{1}{r^2}\frac{\mathrm{d}}{\mathrm{d}r}\left[2r\lambda - r^2\nu'\right]\ . \tag{II.9}$$

Note that upon the redefinitions $\lambda \to \tilde{\lambda} + \alpha r\phi'$ and $\nu \to \tilde{\nu} - \alpha\phi$, the previous system decouples and we obtain equations of the form (II.3). This redefinition is not necessary however, and we will keep the system as it is. We now integrate the first equation and introduces the Schwarzschild radius $r_S = 2GM$ of the object. We set the integration constant in the scalar equation to 0 (as we will see in the following, this is to have a regular scalar current at $r = 0$), and upon combining these equations we obtain an algebraic equation for the fifth force ϕ':

$$4\beta r\phi'^2 + \left(3\alpha^2 - 2\eta\right) r^2\phi' + \alpha r_S = 0\ . \tag{II.10}$$

If $\beta = 0$, the equation is linear and we obtain the following solution for ϕ' in the linear regime:

$$\phi'_{\rm lin} = \frac{\alpha r_S}{(2\eta - 3\alpha^2)r^2}\ . \tag{II.11}$$

Let us now determine the metric potentials in this region. In the linear regime, replacing the scalar profile in the field equations leads to the following expressions:

$$\begin{aligned} \lambda &= \frac{r_S}{r}\left(1 + \frac{\alpha^2}{2\eta - 3\alpha^2}\right)\ , \\ \nu &= -\frac{r_S}{r}\left(1 - \frac{\alpha^2}{2\eta - 3\alpha^2}\right)\ . \end{aligned} \tag{II.12}$$

When $\alpha \neq 0$, it is clear that GR is not recovered, and the fifth force introduces leading order corrections to the metric functions. Importantly, the corrections for λ and ν are different, meaning that they cannot be absorbed by a redefinition of Newton's constant. Hence, when $\beta = 0$, one does not recover GR unless $\alpha = 0$, in which case the scalar is trivial, i.e. $\phi' = 0$.

Let us now consider the general case $\beta \neq 0$. The fifth force is given by solving the quadratic equation above:

$$\phi' = \frac{\mu r r_S}{r_V^3}\left[1 \pm \sqrt{1 + \left(\frac{r_V}{r}\right)^3}\right] , \tag{II.13}$$

where we have defined

$$\begin{aligned} \mu &= \frac{2\alpha}{3\alpha^2 - 2\eta} , \\ r_V^3 &= -\frac{4\beta r_S \mu^2}{\alpha} . \end{aligned} \tag{II.14}$$

We can identify the two regimes from the expression (II.13) for ϕ':

- If $r \gg r_V$, then we obtain $\phi' = \phi'_{\rm lin}$, where we have chosen the minus sign in Eq. (II.13) in order for the scalar field to remain finite as $r \to \infty$. As we discussed above, the metric potentials receive leading-order corrections in this case, and we obtain deviations from GR.

- If $r_S \ll r \ll r_V$, which correspond to a region inside the Vainshtein radius but outside the nonrelativistic source, then we obtain

  $$\phi' = \frac{\mu r_S}{r^2}\left(\frac{r}{r_V}\right)^{3/2} . \tag{II.15}$$

  From this expression, it is clear that the fifth force is suppressed compared to the Newtonian force $\nu' \sim r_S/r^2$. Substituting the expression for ϕ' in the field equations, we obtain the following solutions for the metric potentials:

  $$\nu = -\frac{r_S}{r}\left[1 + \mathcal{O}\left(\frac{r}{r_V}\right)^n\right] \qquad \text{and} \qquad \lambda = \frac{r_S}{r}\left[1 + \mathcal{O}\left(\frac{r}{r_V}\right)^n\right] , \tag{II.16}$$

  where $n = 3/2$ in the present case, but generically depends on the theory considered.

We have presented a simple example belonging to the k-mouflage family and with a static scalar field. It is possible to consider more complicated setups, like for instance allowing a time dependence of the scalar field [129–131]:

$$\phi = qt + \phi(r) . \tag{II.17}$$

In this case, the previous analysis can be repeated, and we obtain the following coefficients which generalize those of Eq. (II.14):

$$\mu = \frac{2(\alpha - q^2\beta)}{(3\alpha - q^2\beta)(\alpha + q^2\beta) - 2\eta} ,$$
$$r_V^3 = -\frac{4\beta r_S \mu^2}{(\alpha - q^2\beta)} . \tag{II.18}$$

The Vainshtein screening in the cubic Galileon theory with a time-dependent scalar was studied in [130], though the scalar was coupled to the matter fields instead of the Ricci tensor. The approaches are similar, and it was shown that one must instead chose the plus sign in Eq. (II.13), which leads to de Sitter asymptotics where $\phi' \sim r$. Hence the time dependence of the scalar field can also lead to a screening of the fifth force. It is also worth noting that in some scalar-tensor theories the spin-0 and spin-2 degrees of freedom do not decouple entirely, and the field equations do not reduce to a system which has the form of Eq. (II.3) (see Ref. [127] for explicit examples). In these cases, one solves for the metric potentials in terms of the scalar field and uses the resulting expressions in the scalar equation. It is sometimes necessary to neglect part of the nonlinear terms in the metric equations, in anticipation of the Vainshtein screening, and one can check the validity of such assumptions once the solutions have been found.

The Vainshtein screening has been extensively studied in scalar tensor theories for spherically symmetric spacetimes, in particular in Horndeski [126, 130, 132–137], beyond Horndeski [138–143] and DHOST theories [54, 144–147]. However, realistic astrophysical objects typically rotate, and one may naturally ask whether rotation affects the validity of the Vainshtein mechanism. Indeed, it has been found that the chameleon screening mechanism is shape dependent [148, 149], i.e. the fifth force does depend on the deviation from spherical symmetry. In the case of the Vainshtein mechanism, the recovery of GR for nonspherical configurations in particular models has been previously considered in [136, 143, 150–153]. The aim of this part is to make a systematic study of the Vainshtein screening in scalar-tensor theories for slowly rotating bodies. Following the Hartle-Thorne formalism developed in GR [154], we will introduce a frame-dragging function ω to the line element, and include the scalar field in the discussion. In Chapter 4, we derive the equation satisfied by the frame-dragging function for a slowly rotating star, and discuss its solutions in the weak-field approximation. In Chapter 5, we study the Vainshtein screening for slowly rotating stars in DHOST Ia theories in the case of a time-dependent scalar field, i.e. when $q \neq 0$. Finally, we analyze the case of a static scalar field in Chapter 6, meaning that we set $q = 0$. We study a subclass of quadratic Horndeski theories, with an additional coupling of the scalar to the Ricci curvature which breaks shift-symmetry.

Chapter 4

Setup and weak-field approximation

It is known that in spherical symmetry, theories belonging to the DHOST class exhibit the Vainshtein screening [144], meaning that GR is recovered inside a radius r_V called the Vainshtein radius, and deviations from GR may be observed at large radii. However, for some theories beyond Horndeski, the screening is broken inside matter [138] when the scalar field depends on time, and sometimes even outside the matter source [146, 147]. Our aim is to extend these studies by deviating from spherical symmetry and examining how the Vainshtein screening is affected. Following the Hartle-Thorne formalism [154], we will introduce an additional function ω to the metric, which accounts for the slow rotation of the source. In this chapter, we derive the differential equation satisfied by the function ω, and discuss its solutions in the weak-field approximation. The three chapters in this part are based on Ref. [155].[1]

4.1 Equations of motion for slow rotation

We will consider theories belonging to the quadratic DHOST Ia class, given by the following Lagrangian density:

$$\mathcal{L} = f(\phi, X)R + K(\phi, X) - G_3(\phi, X)\Box\phi + \sum_{i=1}^{5} \mathcal{L}_i \,, \tag{4.1}$$

the densities $\mathcal{L}_i$ are given in Eq. (32) and we assume the Ia conditions (33). In addition, we assume a matter action with fields $\psi_{\rm m}$ that are minimally coupled to the metric $g_{\mu\nu}$, and an energy-momentum tensor defined by Eq. (27). We define the quantities $\mathcal{E}_{\mu\nu}$ and $\mathcal{E}_\phi$ which come from the variation of $\mathcal{L}$:

$$\mathcal{E}_{\mu\nu} = \frac{1}{\sqrt{-g}} \frac{\delta\left(\sqrt{-g}\mathcal{L}\right)}{\delta g^{\mu\nu}} \,, \qquad \text{and} \qquad \mathcal{E}_\phi = \frac{1}{\sqrt{-g}} \frac{\delta\left(\sqrt{-g}\mathcal{L}\right)}{\delta\phi} \,. \tag{4.2}$$

[1] Note that the scalar kinetic term $X = (\partial\phi)^2$ is defined differently in this reference, $X = -(\partial\phi)^2/2$, resulting in many formulas being altered.

With these definitions, the field equations for the metric and scalar field read

$$M_P^2\,\mathcal{E}_{\mu\nu} = T_{\mu\nu}\ , \tag{4.3}$$
$$\mathcal{E}_\phi = 0\ . \tag{4.4}$$

We consider a slowly rotating source of radius R modeled by a perfect fluid. We will follow the Hartle-Thorne formalism [154] developed for general relativity, and assume a uniform rotation of the fluid at angular velocity Ω. We take the same ansatz for the metric tensor as in GR:

$$\mathrm{d}s^2 = -e^{\nu(t,r)}\mathrm{d}t^2 + e^{\lambda(t,r)}\mathrm{d}r^2 + r^2\mathrm{d}\theta^2 + r^2\sin^2\theta\,[\mathrm{d}\varphi - \epsilon\omega(t,r)\mathrm{d}t]^2\ , \tag{4.5}$$

where the frame-dragging function ω is the angular velocity acquired by an observer falling freely from infinity, due to the dragging of inertial frames. The bookkeeping parameter ϵ accounts for the slow rotation of the source, and we will keep terms only up to first order in ϵ in the following. For the scalar field we take the (generically) time-dependent ansatz given by Eq. (II.17). The metric functions can *a priori* depend on time if the constant $q \neq 0$, because the Lagrangian functions generically depend on ϕ. The solutions for the metric potentials depend on these functions, meaning that they also depend on time. We assume that the star is a perfect fluid, which is described by the following energy-momentum tensor:

$$T^{\mu\nu} = (\rho + P)\,u^\mu u^\nu + P g^{\mu\nu}\ , \tag{4.6}$$

where u^μ is the 4-velocity of the fluid, given at first order in ϵ by

$$u^\mu = \left(e^{-\nu/2}, 0, 0, \epsilon\Omega e^{-\nu/2}\right)\ , \tag{4.7}$$

where the component of u along the vector ∂_φ accounts for the slow rotation. We will be interested in the differential equation for the function ω, obtained from the $(t\varphi)$ component of the metric equations:

$$M_P^2\,\mathcal{E}^t{}_\varphi = T^t{}_\varphi\ . \tag{4.8}$$

At the same time, for the other nontrivial equations, (tt), (rr) and (tr) components as well as for the scalar field equation, it is enough to keep only terms of order 0 in ϵ, i.e. to consider these equations of motion without rotation,

$$M_P^2\,\mathcal{E}^{(0)}_{tt} = T^{(0)}_{tt}\ , \tag{4.9}$$
$$M_P^2\,\mathcal{E}^{(0)}_{rr} = T^{(0)}_{rr}\ , \tag{4.10}$$
$$\mathcal{E}^{(0)}_{tr} = 0\ , \tag{4.11}$$
$$\mathcal{E}^{(0)}_{\phi} = 0\ , \tag{4.12}$$

where the superscript (0) implies that one should set $\epsilon = 0$ in the equations of motion. Note that not all of the equations (4.9)–(4.12) are independent, because of the following relation due to the diffeomorphism invariance of the action [156]:

$$\nabla^\nu \mathcal{E}_{\mu\nu} = -\frac{1}{2}\nabla_\mu \phi \, \mathcal{E}_\phi \, . \tag{4.13}$$

With the choice (4.6) for $T_{\mu\nu}$, Eq. (4.8) can be written as

$$\omega'' + K_1 \omega' + \frac{K_2}{M_P^2}(\rho + P)(\omega - \Omega) = 0 \, , \tag{4.14}$$

where the functions K_1 and K_2 depend on the specific theory considered and on the solution in the nonrotating limit,

$$K_1 = \frac{4}{r} - \frac{\lambda' + \nu'}{2} + \frac{\mathrm{d}}{\mathrm{d}r}\ln(f - XA_1) \, , \tag{4.15}$$

$$K_2 = -\frac{2e^\lambda}{f - XA_1} \, , \tag{4.16}$$

and $'$ denotes a derivative with respect to the radial coordinate. Thus the system of equations to solve is given by Eqs. (4.9)–(4.12) and (4.14) with (4.15) and (4.16), where all the functions depend on ϕ given by (II.17) and X evaluated in the spherically symmetric limit,

$$X = e^{-\lambda}\phi'^2 - e^{-\nu}q^2 \, . \tag{4.17}$$

Using the previous relation, Eq. (4.15) can be written in an expanded form, which will be useful in the following, as

$$K_1 = \frac{4}{r} - \frac{\lambda' + \nu'}{2} + \frac{(f_X - XA_{1X} - A_1)X' + \phi'(f_\phi - XA_{1\phi})}{f - XA_1} \, . \tag{4.18}$$

where

$$X' = q^2 e^{-\nu}\nu' - e^{-\lambda}\phi'(\lambda'\phi' - 2\phi'') \, . \tag{4.19}$$

Eq. (4.14) with the coefficients given by Eqs. (4.15) and (4.16) is the main equation we will focus on throughout this part.

Note that the GR case is easily obtained from the above equations. Indeed, we set $\mathcal{L} = R$, corresponding to $G_3 = K = A_i = 0$ and $f = 1$. Using Eqs. (4.15) and (4.16) in Eq. (4.14) one obtains

$$\omega'' + \left(\frac{4}{r} - \frac{\lambda' + \nu'}{2}\right)\omega' - \frac{2}{M_P^2}e^\lambda(\rho + P)(\omega - \Omega) = 0 \, , \tag{4.20}$$

which coincides with the GR equation for ω [154]. In vacuum we impose $\rho = P = 0$, which implies $\lambda' = -\nu'$ in GR, so that Eq. (4.20) becomes

$$\omega'' + \frac{4}{r}\omega' = 0 \, . \tag{4.21}$$

It was shown that this vacuum GR equation is recovered in particular classes of DHOST theories [143, 151–153]. We generalize these results in Appendix II.A, showing that it is true for any shift-symmetric quadratic Gleyzes-Langlois-Piazza-Vernizzi (GLPV) theory [44] with $G_3 = 0$. The solution to this equation, assuming that $\lim_{r\to\infty}\omega = 0$, is

$$\omega = \frac{2JG}{r^3} \,, \tag{4.22}$$

where J is the total angular momentum of the star [154, 157], which can be expressed in terms of the moment of inertia I of the star as $J = \Omega I$. In the following, we will examine the solutions for ω in DHOST Ia theories and compare them to the GR expression Eq. (4.22).

4.2 Frame-dragging function in the weak-field approximation

From now on we will employ the weak-field approximation [120], assuming that λ, ν, ϕ and their derivatives are small, which one can check once the solutions are found:

$$\{r^n\frac{\mathrm{d}^n\lambda}{\mathrm{d}r^n}, r^n\frac{\mathrm{d}^n\nu}{\mathrm{d}r^n}, r^n\frac{\mathrm{d}^n\phi}{\mathrm{d}r^n}\} \ll 1 \,, \tag{4.23}$$

where n is a positive integer. Additionally, we assume that

$$\omega \ll \Omega \,,$$

which is the appropriate approximation in the Newtonian regime [154]. Physically, the above conditions correspond to nonrelativistic sources, for which we also assume $P \ll \rho$. These assumptions considerably simplify Eq. (4.14), since it becomes a first order equation for ω':

$$\omega'' + \frac{4}{r}\left[1 + \frac{r\delta K_1}{4}\right]\omega' = \frac{K_2(r)\Omega}{M_P^2}\rho(r) \,, \tag{4.24}$$

where

$$\delta K_1 \equiv K_1 - \frac{4}{r}$$

marks the departure from the vacuum GR behavior ($\rho = 0$). The integration of Eq. (4.24) with the conditions $\omega'(0) = 0$ and $\lim_{r\to\infty}\omega = 0$ leads to

$$\omega(r) = \frac{\Omega}{M_P^2}\int_\infty^r \frac{\mathcal{I}_1(v)}{v^4}\left(\int_0^v \frac{K_2(u)\rho(u)}{\mathcal{I}_1(u)}u^4\mathrm{d}u\right)\mathrm{d}v \,, \tag{4.25}$$

where we have defined the function

$$\mathcal{I}_1(r) = e^{-\int \delta K_1 \mathrm{d}r} \,.$$

We see that the overall integration constant which appears in the expression for $\mathcal{I}_1$ is not important, as it disappears in the final result for ω. Note that Eq. (4.25) is valid even if δK_1 is not small. In order to compare a generic situation to GR, let us briefly describe the latter case, corresponding to $f = 1$ and $G_3 = K = A_i = 0$. The linearization of Eqs. (4.9) and (4.10) gives, respectively,

$$\lambda + r\lambda' = \frac{1}{M_P^2} r^2 \rho \,,$$
$$r\nu' - \lambda = \frac{1}{M_P^2} r^2 P \,.$$

In the case of nonrelativistic matter, $P \ll \rho$, we obtain from Eq. (4.20):

$$\omega'' + \frac{4}{r}\left(1 - \frac{GM'}{4}\right)\omega' = -\frac{4GM'\Omega}{r^2}\left(1 + \frac{2GM}{r}\right) \,, \tag{4.26}$$

where we have introduced the mass function

$$M(r) = 4\pi \int_0^r \rho \bar{r}^2 \mathrm{d}\bar{r} \,. \tag{4.27}$$

This is the weak-field equivalent of the relativistic GR equation found in Ref. [154]. As one can see by comparing Eqs. (4.24) and (4.26), outside the source δK_1 measures the departure from GR, while inside the source it takes into account both GR and non-GR corrections due to the presence of matter.

4.2.1 Leading term

Let us now calculate the leading term in Eq. (4.25), assuming that $\int \delta K_1 \mathrm{d}r$ is small and K_2 is almost constant. We can then write

$$\begin{aligned} \mathcal{I}_1 &= 1 + \varepsilon \delta \mathcal{I}_1 \,, \\ K_2 &= \kappa_2 \left(1 + \varepsilon \delta K_2\right) \,, \end{aligned} \tag{4.28}$$

where κ_2 is a constant, $\{\delta\mathcal{I}_1, \delta K_2\} \ll 1$, and ε is a bookkeeping parameter used to keep track of small terms.

Outside the source: In the exterior region, $r > R$, Eq. (4.25) simplifies to

$$\omega(r) = \frac{2G\tilde{J}}{r^3} + \mathcal{O}\left(\varepsilon\right) \,, \tag{4.29}$$

where we have defined an effective angular momentum

$$\tilde{J} = -\frac{4\pi\Omega}{3} \int_0^R \frac{K_2(u)\rho(u)}{\mathcal{I}_1(u)} u^4 \mathrm{d}u \,. \tag{4.30}$$

This coefficient can *a priori* be different from the GR value. However, if the density profile of the star is unknown, $\mathcal{I}_1$ and K_2 can be reabsorbed in the definition of ρ. Therefore, unless the density profile $\rho(r)$ is known, any physical effect related to frame-dragging outside the star is the same as in GR at leading order. Thus, one can say that the Vainshtein screening can be extended outside the star to the case of slowly rotating bodies in the weak-field approximation.

Inside the source: Inside the source, we have from Eq. (4.25)

$$\omega - \omega(0) = \frac{\kappa_2 \Omega}{M_P^2} \int_0^r \frac{1}{v^4} \left(\int_0^v \rho(u) u^4 \mathrm{d}u \right) \mathrm{d}v + \mathcal{O}(\varepsilon) \ . \tag{4.31}$$

The constant $\omega(0)$ is not free and it should be fixed by continuity at the surface of the star. One can see that for $\kappa_2 \neq -2$, the solution for ω differs from its GR counterpart at leading order inside the star.[2] In this case the Vainshtein mechanism is broken for rotating solutions inside the star. On the other hand, the Vainshtein screening operates for theories in which $\kappa_2 = -2$ (for instance when $A_1 = 0$ and $f = 1$). As an illustration, let us consider a star with constant density $\rho = \rho_0$ for $r < R$. From Eq. (4.31) we have

$$\omega - \omega(0) = \frac{\kappa_2 \rho_0 \Omega r^2}{10 M_P^2} + \mathcal{O}(\varepsilon) \ . \tag{4.32}$$

In order for $\tilde{J}$ to be positive at leading order in Eq. (4.30), one must have $\kappa_2 < 0$. This implies that $\omega(r)$ is everywhere decreasing (as in GR) and that it is maximal at $r = 0$.

4.2.2 Subleading terms

In this subsection, we examine the subleading terms in the solution to Eq. (4.24), when the corrections to the coefficients K_1 and K_2 are power laws. The coefficient K_2 is only relevant inside the star where $\rho \neq 0$. On the other hand we will be interested in the corrections to K_1 for all r. As we will see in the following, one can in general identify three regions of radii, and in each of those the correction δK_1 has a particular power-law behavior. These regions are $r < R$, $R \leq r \ll r_V$ and $r \gg r_V$, where r_V is the Vainshtein radius of the considered theory. Therefore, we can write approximately

$$\begin{aligned} \frac{r \delta K_1}{4} &= a_1 \left(\frac{r}{r_1} \right)^{s_1} H_{r \leq R} + a_2 \left(\frac{r}{r_2} \right)^{s_2} H_{R < r \leq r_V} + a_3 \left(\frac{r}{r_3} \right)^{s_3} H_{r > r_V} \ , \\ \delta K_2 &= a_0 \left(\frac{r}{r_0} \right)^{s_0} \ , \end{aligned}$$

[2] Note that nonrotating solutions in some theories require a renormalization of M_P. In this case one should write Eq. (4.31) in terms of the renormalized Planck mass and take into account this extra factor in the definition of κ_2.

where H is the Heaviside step function, the a_i are constants, and we assume that $(r/r_i)^{s_i} \ll 1$. The scaling exponents s_i depend on the theory at hand and should satisfy certain constraints in order for the integral (4.25) to be finite and for ω to have the correct boundary conditions. Therefore we set $s_0 + 1 > 0$, $s_1 + 1 > 0$, $s_2 \neq 0$ and $s_3 < 0$. We also assume $s_2 \neq 3$, since we did not find an example of a theory with such a behavior, although it is not difficult to consider the case $s_2 = 3$ separately. It is worth noting that in the case of a time-dependent scalar field, which we consider in Chapter 5, our analysis allows us to calculate the coefficients K_1 and K_2 up to $r \sim 1/q$. In this case, instead of imposing the boundary condition at $r = +\infty$, we set the boundary condition at $r = 1/q$, i.e. $\omega(1/q) = 0$. This does not affect the final result, due to a very weak dependence of the integral (4.25) on the upper bound. In this case, we obtain the following corrections in the region $r > R$ outside the star:

$$\begin{aligned}\frac{r^3\omega}{2G\tilde{J}} - 1 = 12\varepsilon \Bigg[& \frac{a_3}{s_3(s_3-3)} \left(\frac{r}{r_V}\right)^3 \left(\frac{r_V}{r_3}\right)^{s_3} \\ & + \frac{a_2}{s_2(s_2-3)} \left(\frac{r}{r_2}\right)^{s_2} \left(1 - \left(\frac{r}{r_V}\right)^{3-s_2}\right) \Bigg] H_{R<r\leq r_V} \\ & + \frac{12a_3\varepsilon}{s_3(s_3-3)} \left(\frac{r}{r_3}\right)^{s_3} H_{r>r_V} \,.\end{aligned}$$

Assuming $s_2 < 3$, one can write the solution in the regions $R < r \ll r_V$ and $r \gg r_V$ that we will focus on in the following:

$$\omega = \frac{2G\tilde{J}}{r^3} \left[1 + \frac{12a_2\varepsilon}{s_2(s_2-3)} \left(\frac{r}{r_2}\right)^{s_2} H_{R<r\ll r_V} + \frac{12a_3\varepsilon}{s_3(s_3-3)} \left(\frac{r}{r_3}\right)^{s_3} H_{r\gg r_V}\right] . \tag{4.33}$$

The above expression tells us how the corrections to ω outside the star can be read off from the coefficient K_1.

Inside the source: As we saw in Eq. (4.32), the leading term differs from GR inside the star when $\kappa_2 \neq -2$, meaning that the Vainshtein screening is broken. In theories for which $\kappa_2 = -2$, the leading term in the solution for ω coincides with its GR counterpart, and the corrections to the frame-dragging function come from the subleading terms. Assuming for simplicity that the star has a constant density ρ_0, the frame-dragging function inside the star can be written as follows:

$$\omega(r) - \omega(0) = -\frac{\rho_0\Omega r^2}{5M_P^2} \left[1 + \frac{10a_0\varepsilon}{(s_0+5)(s_0+2)} \left(\frac{r}{r_0}\right)^{s_0} - \frac{40a_1\varepsilon}{(s_1+5)(s_1+2)} \left(\frac{r}{r_1}\right)^{s_1}\right] , \tag{4.34}$$

where $\omega(0)$ can be determined using Eq. (4.33) by continuity of ω at the surface of the star $r = R$. Once again, the subleading terms can be read off from the coefficients K_1 and K_2.

Chapter 5

Slow rotation with a time-dependent scalar field

5.1 General equations

In this chapter, we study the slow rotation of nonrelativistic sources in DHOST Ia theories with $q \neq 0$, meaning that the scalar field is time-dependent. In addition to the weak-field assumption (4.23), we also assume that

$$\phi'^2 \ll q^2 \,, \tag{5.1}$$

i.e. that the spatial gradient of the scalar field is much smaller than the time derivative of ϕ. This can be viewed as a manifestation of the "static" Vainshtein screening and the failure of the Vainshtein mechanism for the time evolution of the scalar [158]. We will also assume that dimensionless combinations of coefficients are of $\mathcal{O}(1)$, for instance $f \sim q^2 f_X \sim q^2 A_1 \sim \mathcal{O}(1)$. Under the assumptions (4.23) and (5.1), the coefficients K_1 and K_2, Eqs. (4.15) and (4.16), read

$$K_1 = \frac{4}{r} - \frac{\lambda' + \nu'}{2} + \frac{(f_\phi + q^2 A_{1\phi})\phi' - (A_1 - f_X - q^2 A_{1X})\,(q^2\nu' + 2\phi'\phi'')}{(f + q^2 A_1)} \,, \tag{5.2}$$

$$K_2 = -\frac{2}{f + q^2 A_1}\left[1 + \mathcal{O}\left(\lambda, \frac{\phi'^2}{q^2}\right)\right] \,, \tag{5.3}$$

where we have used Eq. (4.19) in the weak-field approximation, and all the functions are evaluated at $\phi = qt$ and $X = -q^2$. The aim is to see how the solution to Eq. (4.14) for ω is modified in the case of the scalar-tensor theories, with respect to the GR solution. We can see that generically the coefficient κ_2 defined in Eq. (4.28) is not the same as in GR, signaling that the screening is broken inside the source. If the condition $r\phi'\phi''/q^2 \ll 1$ is verified, it is clear from Eq. (5.2) that the corrections to K_1 are small compared to $4/r$, in which case ω has the same form as in GR at leading order outside the star, see Section 4.2. For instance, this condition is satisfied if the solution for ϕ is

a power law, and we will see in many examples below that this is generically the case. Note that only the functions f and A_1 directly appear in these coefficients. Of course the other functions of the Lagrangian enter the expression for K_1 implicitly via the scalar and metric functions in Eq. (4.14). However, we can immediately see that in a theory for which $f_X = A_1 = 0$ and the Vainshtein mechanism is effective in spherical symmetry, the coefficient K_1 is the same as in GR up to subleading corrections. Indeed, in this case we have

$$K_1 = \frac{4}{r} - \frac{\lambda' + \nu'}{2} + \frac{f_\phi}{f}\phi' \ .$$

When the Vainshtein mechanism in spherical symmetry is operational, the fifth force is screened for $r \ll r_V$, implying $\phi' \ll \{\lambda', \nu'\}$. Also, the solutions for $\{\lambda, \nu\}$ are those of GR at leading order. Assuming $f_\phi/f \lesssim \mathcal{O}(1)$, these two conditions show that the GR expression for K_1 is recovered up to r_V suppressed corrections, which means that the subleading corrections for ω outside the star are also r_V suppressed.

The Vainshtein mechanism in spherical symmetry was studied for DHOST Ia theories in Refs. [54, 144, 146, 147]. Adopting similar notations, we define

$$x = \frac{\phi'}{r}, \quad y = \frac{\nu'}{2r}, \quad z = \frac{\lambda}{2r^2}, \quad M(r) = 4\pi \int_0^r \rho(\bar{r})\bar{r}^2 \mathrm{d}\bar{r}, \quad \mathcal{A}(r) = \frac{GM(r)}{q^2 r^3} \ .$$

Outside the source, we have $\mathcal{A} = r_S/(2q^2r^3)$, and we will define the Vainshtein radius r_V as $\mathcal{A}(r_V) \sim 1$, meaning that

$$r_V^3 \equiv \frac{r_S}{q^2} \ . \tag{5.4}$$

The functions $\{\lambda, \nu\}$ vary slowly with time in this section, and we assume:

$$\dot{z} \sim qz, \quad \dot{y} \sim qy \ ,$$

which can be checked once the solutions for $\{y, z\}$ are found. The (tt) and (rr) field equations for the metric, Eqs. (4.9) and (4.10), can be solved in terms of x and $\mathcal{A}$, and written in the form:

$$y = \alpha_1 \mathcal{A} + \beta_1 x + \gamma_1 x^2 + \delta_1 r x x' + \eta_1 \ , \tag{5.5}$$

$$z = \alpha_2 \mathcal{A} + \beta_2 x + \gamma_2 x^2 + \delta_2 r x x' + \eta_2 \ , \tag{5.6}$$

where all the time-dependent coefficients are listed in Appendix II.B. They can be expressed in terms of the Lagrangian functions evaluated on the background $\phi = qt$ and $X = -q^2$. Note that these coefficients are not necessarily dimensionless. In order to obtain Eqs. (5.5) and (5.6), we have also assumed $r \ll 1/q$. In terms of the function $\mathcal{A}$ defined above, the Vainshtein screening in the nonrotating case generally happens when $\mathcal{A} \gg 1$, which corresponds to $r \ll r_V$. However, there are deviations from GR when $\mathcal{A} \ll 1$, which we will examine in the region $r_V \ll r \ll 1/q$ where our equations are valid. The terms we neglected should be kept if we want to match to the appropriate de Sitter solution at cosmological radii $r \geq 1/q$. This is the asymptotic

condition consistent with the linear time dependence of the scalar field, as discussed in [130] for the cubic Galileon theory.

The expressions (5.5) and (5.6) for y and z can then be substituted in the scalar field equation, Eq. (4.12), yielding a cubic equation for x [144]:

$$C_3 x^3 + C_2 x^2 + \left(C_1 + \Gamma_1 \mathcal{A} + \Gamma_2 \frac{(r^3 \mathcal{A})'}{r^2} \right) x + \Gamma_0 \mathcal{A} + \eta_3 = 0 \, . \tag{5.7}$$

Similarly, using Eqs. (5.5) and (5.6) in Eq. (5.2) results in:

$$K_1 = \frac{4}{r} \Big[1 + \alpha_0 r^2 \mathcal{A} + \zeta_0 \left(r^3 \mathcal{A} \right)' + \beta_0 r^2 x + \kappa_0 r^3 x' + \gamma_0 r^2 x^2 + \delta_0 r^3 x x' + \sigma_0 r^4 \left(x x'' + x'^2 \right) + \eta_0 r^2 \Big] \, . \tag{5.8}$$

The coefficients of Eqs. (5.7) and (5.8) are listed in Appendix II.B. One can see from Eq. (5.8) that there is always a leading term in the brackets corresponding to the Minkowski limit of the metric $K_1 \simeq 4/r$ (for radii $r \ll 1/q$). We discuss below various cases of Eq. (5.7) leading to different nonrotating solutions [132, 144]. Substituting the relevant solution for x in Eq. (5.8), we will examine how the modifications of gravity affects Eq. (4.24) for ω in the slowly rotating case. We will show that the leading corrections to the coefficients K_1 and K_2 are small and take the form of power laws. In this case, we showed in Chapter 4 that ω has the GR form at leading order outside the star, up to an overall factor (which can be absorbed in the definition of the angular momentum of the star as measured by an exterior observer, unless the density distribution of the star is known). On the other hand, the screening can be broken inside the star. We will be interested in the subleading corrections to ω when the leading term is not modified, and compare them to those of GR.

5.2 Outside the Vainshtein radius

We first examine the linear regime outside the Vainshtein radius, where we have $\mathcal{A} \ll 1$. There are two different cases, depending on the coefficient η_3. In this regime the Vainshtein mechanism for nonrotating sources does not operate, and the corrections to the metric for the spherically symmetric solution are expected to be large. Therefore, we also expect that the equation for ω receives corrections larger than those inside the Vainshtein radius.

5.2.1 $\eta_3 = 0$ and $C_1 \neq 0$

Let us first consider the case $\eta_3 = 0$. A sufficient condition for this coefficient to vanish is $K = G_{3\phi} = 0$. In this case, the nonlinear terms in x in Eq. (5.7) can be neglected, and the solution for x is

$$x = -\frac{\Gamma_0}{C_1} \mathcal{A} \sim \frac{r_S}{r^3} \, .$$

Substituting this expression into Eq. (5.8), we obtain the expression for K_1,

$$K_1 = \frac{4}{r}\left[1 + \mathcal{O}\left(\frac{r_S}{r}\right)\right] . \tag{5.9}$$

This shows that the corrections due to the scalar field are not suppressed by powers of the Vainshtein radius, and are of the order of the Newtonian potential. This is expected in the region $r \gg r_V$ where the Vainshtein screening in spherical symmetry is no longer effective (meaning that we do not have $\lambda' + \nu' \simeq 0$ in Eq.(5.2)).

5.2.2 $\eta_3 \neq 0$ and $C_1 \neq 0$

If $\eta_3 \neq 0$, we have $\Gamma_0 \mathcal{A} \ll \eta_3$, since $\mathcal{A} \ll 1$. In this case Eq. (5.7) reduces to the following cubic equation for x with r-independent coefficients:

$$C_3 x^3 + C_2 x^2 + C_1 x + \eta_3 = 0 .$$

The relevant solution for x must be chosen by taking into account the asymptotic behavior of the solution at large radii, $r \gg 1/q$. Since the coefficients of the algebraic equation depend on time only, x does not depend on the radial coordinate and we have $x = x_0(t)$. Substituting this solution into Eq. (5.8), we obtain

$$K_1 = \frac{4}{r}\left[1 + \mathcal{O}\left(q^2 r^2\right)\right] . \tag{5.10}$$

Note that here the corrections have a clear physical interpretation; they arise as a backreaction on the metric due to the "weight" of the scalar field, see for instance Ref. [159]. They are present even in the simplest theory with a minimally coupled scalar field. The corrections are larger in this case than for $\eta_3 = 0$, considered above. Indeed, using Eq. (5.4), we obtain that the ratio of the corrections in Eq. (5.9) to the corrections in Eq. (5.10) are of order $(r_V/r)^3$.

In the rest of this chapter, we will consider the region $r \ll r_V$, where the Vainshtein mechanism usually operates in spherical symmetry.

5.3 Case 1: $C_3 \neq 0$ and $\Gamma_1 \neq 0$, inside the Vainshtein radius

We first consider the generic case $\Gamma_1 \neq 0$ and $C_3 \neq 0$ (see Appendix II.B for their expressions). Note that when $\Gamma_1 = 0$ then we also have $C_3 = 0$. We assume that $C_3\Gamma_1 < 0$ and we will confirm this choice later. Then the solutions to Eq. (5.7) for $r \ll r_V$ are[1]

$$x_1 = \pm\sqrt{\frac{-\Gamma_1 \mathcal{A} - \Gamma_2 \frac{(r^3\mathcal{A})'}{r^2}}{C_3}} , \tag{5.11}$$

[1]For some theories these solutions have been shown to match de Sitter asymptotics [142].

where we used $\mathcal{A} \gg 1$ to simplify the expression. The $\pm$ sign must be chosen in order to match the solution at infinity, depending on the theory. We have $(r^3\mathcal{A})' = 0$ outside the star, and therefore our choice $C_3\Gamma_1 < 0$ is indeed correct to have a real solution in the exterior region. Extra conditions should be also imposed on Γ_2 for the argument of the square root to be positive. In particular, a sufficient condition is $\Gamma_2 < 0$. We do not consider the third solution to the cubic equation, since there is no known example where it is matched to de Sitter asymptotics. (Note however that in Ref. [132] the asymptotically flat spherically symmetric solutions of this branch were found, and it was shown that the Vainshtein mechanism is not effective for this branch unless the speed of gravitational waves $c_T = 1$). Substituting the solution (5.11) for x in Eq. (5.8), we obtain

$$K_1 = \frac{4}{r}\left[1 + \frac{\mathrm{d}}{\mathrm{d}r}(\iota_0 r^3\mathcal{A} + \iota_1 r^4\mathcal{A}' + \iota_2 r^5\mathcal{A}'') + \mathcal{O}\left(q^2r^2\sqrt{\mathcal{A}}\right)\right] , \tag{5.12}$$

where we assumed $\mathcal{A} \sim r^n\mathcal{A}^{(n)}$ for the subsubleading part, and the expressions for the ι_i are listed in Appendix II.B. The above expression generically differs from its GR counterpart inside the source (see Eq. (4.26)). In particular, as can be seen from Eq. (4.26), $\iota_1 = \iota_2 = 0$ in GR. In the exterior region outside the star, $R < r \ll r_V$, we have $(r^3\mathcal{A})' = 0$ and the previous equation simplifies to

$$K_1 = \frac{4}{r}\left[1 + \mathcal{O}\left(\frac{r_S\sqrt{r}}{r_V^{3/2}}\right)\right] .$$

Hence, the corrections to the solution for ω are subdominant, as we showed in Chapter 4. Furthermore, they are suppressed by powers of r_V, in an analogous way to the screening in spherical symmetry. In fact, the screening is even more effective for ω, since one has a power r_S/r_V instead of r/r_V as in Eq. (II.16). A similar screening also happens for the third solution to Eq. (5.7) that cannot be matched to the de Sitter solution at large radii, which we do not consider here.

5.3.1 A class of shift-symmetric beyond Horndeski theories

Let us now restrict ourselves to the quadratic sector of GLPV theories [44], which corresponds to the following Lagrangian:

$$\mathcal{L} = f(X)R + K(X) - 2f_X\left[(\Box\phi)^2 - \phi_{\mu\nu}\phi^{\mu\nu}\right] + \frac{A_3(X)}{2}\varepsilon^{\mu\nu\alpha\sigma}\varepsilon^{\lambda\eta\kappa}{}_{\sigma}\phi_{\mu\lambda}\phi_{\nu\eta}\phi_\alpha\phi_\kappa , \tag{5.13}$$

where $\varepsilon^{\mu\nu\alpha\sigma}$ is the totally antisymmetric Levi-Civita tensor, and we have set

$$f = f(X), \quad A_1 = -A_2 = 2f_X + \frac{1}{2}XA_3(X), \quad K = K(X), \quad G_3 = 0 . \tag{5.14}$$

In the case of shift-symmetric beyond Horndeski theories, the Vainshtein mechanism for spherically symmetric configurations has been studied extensively. In particular, it was shown in Ref. [137] that the backreaction of the scalar field on the metric

leads to a redefinition of Newton's constant G. Also, in a subclass of the theory, the Vainshtein screening has been considered for slowly rotating sources. Indeed, the specific case of constant A_3 was studied in Refs. [142, 143] for relativistic stars. It was shown in this theory that ω satisfies the GR equation outside the star, meaning that $K_1 = 4/r$ exactly, with no subleading corrections. This result remains true for the shift symmetric theories defined above, and does not rely on the weak-field approximation, as we show in Appendix II.A.

We now discuss the equation for ω in the weak-field approximation inside the matter source. After substituting the solution for x, given by Eq. (5.11), the metric potentials read

$$\begin{aligned} y &= \tilde{G}\left(\frac{M}{r^3} - \frac{q^4 A_3^2 M''}{4r[f(-q^2A_{3X} + 2A_3 + 4f_{XX}) - q^2A_3f_X + 4f_X^2]}\right) , \\ z &= \tilde{G}\left(\frac{M}{r^3} + \frac{q^2A_3(-2q^4A_{3X} - 4f_X + 5q^2A_3 + 8q^2f_{XX})M'}{4r^2[f(-q^2A_{3X} + 2A_3 + 4f_{XX}) - q^2A_3f_X + 4f_X^2]}\right) , \end{aligned} \tag{5.15}$$

where we have defined an effective gravitational constant

$$\tilde{G} = \frac{2G}{2f + 8q^2f_X - 8q^4f_{XX} - 5q^4A_3 + 2q^6A_{3X}} .$$

The above equations show that the Vainshtein mechanism in spherical symmetry is broken inside the source [138], but that GR is recovered in the exterior region where M is constant.

Substituting the metric potentials in Eq. (4.14), with the coefficients given by Eqs. (5.3) and (5.8), the equation for ω inside the star and in the weak-field limit reads

$$\omega'' + \frac{4}{r}\left[1 - \frac{GM'}{2(2f + 4q^2f_X - q^4A_3)}\right]\omega' = -\frac{8GM'\Omega}{r^2(2f + 4q^2f_X - q^4A_3)}\left[1 + \mathcal{O}(r^2z)\right] ,$$

which is the same equation as in GR (up to the subleading term in the coefficient K_2) provided we redefine Newton's constant as:

$$G^* = \frac{2G}{2f + 4q^2f_X - q^4A_3} \neq \tilde{G} .$$

As we can see, in general the two redefined Newton constants $\tilde{G}$ and G^* do not coincide. This means that the coefficient κ_2 is not the same as in GR, and the Vainshtein screening is broken inside the star (see Eq. (4.31)). This is expected for $A_3 \neq 0$ since the Vainshtein screening for static sources is broken inside matter for these theories [138]. However, this remains true even for $A_3 = 0$ when the Vainshtein screening in the nonrotating case works inside the star (as can be seen from Eq. (5.15)). Note that the two redefinitions of G coincide in theories with $f_X = f_{XX} = A_3 = A_{3X} = 0$, but in this case $\Gamma_1 = C_3 = 0$, so the analysis of the present section is not valid.

5.4 Case 2: $C_3 = \Gamma_1 = 0$ and $C_2 \neq 0$ inside the Vainshtein radius

In this section, we consider the particular subclass of DHOST Ia theories verifying

$$2fA_{1X} + 2A_1 f_X + fA_3 = 0 \,, \tag{5.16}$$

which implies $C_3 = \Gamma_1 = 0$. In this case Eq. (5.7) is quadratic, and the general solution reads

$$x_2 = -\frac{r^2 C_1 + \Gamma_2 (r^3 \mathcal{A})' \pm \sqrt{[r^2 C_1 + \Gamma_2 (r^3 \mathcal{A})']^2 - 4r^4 \mathcal{A} C_2 \Gamma_0}}{2r^2 C_2} \,. \tag{5.17}$$

Assuming $\Gamma_0 C_2 < 0$ and neglecting C_1 in the limit $\mathcal{A} \ll 1$, the solution for x_2 in the exterior region $R < r \ll r_V$ is

$$x_{2\text{out}} = \pm \sqrt{\frac{-\mathcal{A}\Gamma_0}{C_2}} \,. \tag{5.18}$$

Substituting this expression in Eq. (5.8), we obtain

$$K_1 = \frac{4}{r}\left[1 + \xi \frac{r_S}{r} + \mathcal{O}\left(\frac{r_S \sqrt{r}}{r_V^{3/2}}\right)\right] \,, \tag{5.19}$$

where the coefficient ξ reads

$$\xi = \frac{\alpha_0}{2} + \frac{\Gamma_0}{4C_2}\left[3\left(\delta_0 - 4\sigma_0\right) - 2\gamma_0\right] \,.$$

The full expression for ξ is rather lengthy, but it can be rewritten in the form

$$\xi = \left[f + q^2 A_1\right]\left[f\left(q^2 A_{1X} + 2f_X\right) + A_1\left(-f + q^2 f_X\right)\right]\xi_0 \,, \tag{5.20}$$

where the coefficient ξ_0 is in general a time-dependent function. Several interesting observations can be made from Eq. (5.20). First of all, for theories with $A_1 = A_3 = f_X = 0$ (we also used the condition (5.16)), one automatically obtains $\xi = 0$. This means that there are only subleading (Vainshtein suppressed) corrections to the coefficient K_1, see Eq. (5.19). For example, this is the case for the cubic Galileon, which we will discuss in more detail below.

In fact, from Eq. (5.19) one can draw a conclusion for more general theories, namely those satisfying the constraint (5.16) with $f_X \neq 0$. Indeed, assuming that the Vainshtein mechanism in spherical symmetry is at work, the metric potentials approximately verify the GR relation in vacuum:

$$y - z = 0 \,.$$

This relation is valid whenever the Vainshtein mechanism in spherical symmetry operates outside the star, up to subleading corrections. Substituting Eq. (5.18) into Eqs. (5.5) and (5.6), we obtain

$$r^2\,(y-z) = -4\xi_0 f_X \left(f+q^2A_1\right)^2 \frac{r_S}{r} + \mathcal{O}\left(\frac{r_S\sqrt{r}}{r_V^{3/2}}\right) . \tag{5.21}$$

We see that if $f_X \neq 0$, one must impose $\xi_0 = 0$ to recover the Vainshtein screening in the absence of rotation (since $f+q^2A_1 \neq 0$ in the DHOST Ia class). In this case, ξ also vanishes, see Eq. (5.20). On the other hand, when Eq. (5.16) is satisfied but $f_X = 0$, the Vainshtein mechanism operates in spherical symmetry, but ξ is not necessarily zero, as we will see in an explicit example below.

5.4.1 Example 1: theory with larger corrections to the frame-dragging function in the exterior region

As we mentioned above, there are theories which allow for the spherically symmetric Vainshtein screening, but for which the corrections to the frame-dragging equation are of the order of the Newtonian potential (showing that the screening is less effective for ω than for the metric potentials). We consider such theories in detail in the present section. If Eq. (5.16) is satisfied, a necessary condition for the Vainshtein mechanism to work in spherical symmetry if $\xi_0 \neq 0$ is $f_X = 0$. This can be seen from Eq. (5.21), which shows deviations of the metric functions from the GR case. If we assume $f_X = 0$, Eq. (5.16) implies $A_3 = -2A_{1X}$. Assuming $f = f(\phi)$, the dimensionless coefficient ξ can be written

$$\xi = \frac{N_\xi}{D_\xi} ,$$

where N_ξ and D_ξ read

$$\begin{aligned} N_\xi = {} & \left(f+q^2A_1\right)\left(q^2A_{1X}-A_1\right)\left[f_\phi\left(2q^2A_1+f-q^4A_{1X}\right)\right. \\ & \left. -q^2A_{1\phi}\left(3q^2A_1+4f+q^4A_{1X}\right)+q^2\left(f+q^2A_1\right)\left(3G_{3X}+2q^2A_{1\phi X}\right)\right] , \\ D_\xi = {} & \left(3q^2A_1+2f-q^4A_{1X}\right)^2\left[f^2\left(4G_{3X}-6A_{1\phi}+4q^2A_{1\phi X}\right)+q^2A_1f_\phi\left(q^2A_{1X}-3A_1\right)\right. \\ & \left. +q^2fA_{1\phi}\left(4A_1G_{3X}-3A_1A_{1\phi}-3q^2A_{1X}A_{1\phi}+4q^2A_1A_{1\phi X}-2f_\phi A_{1X}\right)\right] . \end{aligned}$$

Note that since we consider the case $C_2 \neq 0$, we have $D_\xi \neq 0$. The metric potentials in these theories read:

$$r^2y = \iota_3\frac{r_S}{r} + \mathcal{O}\left(\frac{r_S\sqrt{r}}{r_V^{3/2}}\right) , \tag{5.22}$$

$$r^2z = \iota_3\frac{r_S}{r} + \mathcal{O}\left(\frac{r_S\sqrt{r}}{r_V^{3/2}}\right) , \tag{5.23}$$

where the coefficient ι_3 is given in Appendix II.B.

After redefining Newton's constant, the metric potentials have the GR form up to subleading corrections, meaning that the Vainshtein mechanism works in spherical symmetry. Meanwhile $\xi \neq 0$, and therefore the corrections to the frame-dragging function ω are of order r_S/r, as Eq. (5.19) shows. This implies that the screening for ω is not as effective as it is for the metric potentials λ and ν. We have thus demonstrated for a particular theory that the Vainshtein screening in spherical symmetry is not sufficient to ensure that the leading corrections to the GR expression for ω are suppressed by powers of r_V.

In order to give a simpler example, let us consider the particular case of shift-symmetric theories. We set $f = f_0 = \text{const.}$, since we must have $f_X = 0$, and we assume that the other functions depend on X only. In this case the previous expression simplify and we obtain

$$\xi^{(\mathrm{s})} = \frac{3q^2\left(f_0 + q^2 A_1\right)\left(q^2 A_{1X} - A_1\right)}{4f_0\left(2f_0 + 3q^2 A_1 - q^4 A_{1X}\right)^2} , \tag{5.24}$$

$$\iota_3^{(\mathrm{s})} = \frac{q^2 A_1\left(15 f_0 + 6q^2 A_1\right) + f_0\left(8f_0 - q^4 A_{1X}\right)}{4f_0\left(2f_0 + 3q^2 A_1 - q^4 A_{1X}\right)^2} , \tag{5.25}$$

where the subscript "(s)" refers to shift-symmetric theories. Hence, unless we have $A_1 \sim 1/X$, this provides a simple example for which the Vainshtein screening in spherical symmetry does not imply r_V suppressed corrections for the frame-dragging function.

5.4.2 Example 2: theory with $c_T = 1$ and no decay of the graviton into dark energy

Most of the DHOST Ia theories as models of dark energy [53] have been ruled out by the constraint $c_T = 1$ (i.e. the graviton propagates at the speed of light) coming from the merger of a binary neutron star system [56, 58, 59], and requiring that the graviton does not decay into dark energy [63]. The surviving theories correspond to the choice

$$A_4 = \frac{6f_X^2}{f} \qquad \text{and} \qquad A_1 = A_2 = A_3 = A_5 = 0 . \tag{5.26}$$

The Vainshtein screening in the absence of rotation for these theories was studied in Refs. [146, 147]. It was shown that the screening is broken inside the star, and that it may work in the exterior region provided the parameters of the theory are fine-tuned.

Outside the source: Outside the star, the coefficient K_1 is of the form (5.19), with

$$\xi = \frac{f_X\left[f_\phi\left(f - 10q^2 f_X\right) + q^2 f\left(3G_{3X} + 2f_{\phi X}\right)\right]}{8(f + q^2 f_X)^2(fG_{3X} - 3f_X f_\phi)} ,$$

where we used Eq. (5.26). Note that the denominator does not vanish in the case $C_2 \neq 0$. It was shown in [146, 147] that the Vainshtein mechanism can work outside the star in this theory if the parameters verify

$$f_X \left[f_\phi \left(f - 10 q^2 f_X \right) + q^2 f \left(3 G_{3X} + 2 f_{\phi X} \right) \right] = 0 \, . \tag{5.27}$$

Interestingly, this is exactly the condition for ξ to vanish, as can be seen from the above expression. This shows that if we fine-tune the parameters to recover the Newtonian potential outside the source, then the screening for ω becomes more effective, in the sense that corrections to the GR expression for ω are suppressed by powers of r_V (see Eq. (5.19)). If this condition is verified, the potentials in the exterior region read

$$r^2 y = r^2 z = \frac{r_S}{2r \left(f + q^2 f_X \right)} + \mathcal{O}\left(\frac{r_S \sqrt{r}}{r_V^{3/2}} \right) \, .$$

In this case, GR is recovered if Newton's constant is redefined according to

$$\tilde{G} = \frac{G}{f + q^2 f_X} \, . \tag{5.28}$$

Inside the source: Let us examine the $(t\varphi)$ equation inside the source, where $(r^3 \mathcal{A})' \neq 0$ and we assume $r\mathcal{A}' \sim \mathcal{A}$. We also assume

$$\Gamma_2 = -192 q^2 f^2 f_X \left(f + q^2 f_X \right) \neq 0 \, ,$$

which implies that the leading term inside the square root of Eq. (5.17) is the one containing the coefficient Γ_2. One of the branches obtained with these assumptions is physically unacceptable,[2] as argued in Ref. [146], so we focus on the second branch for which

$$r^2 x \simeq -\frac{\Gamma_0}{\Gamma_2} \frac{r^4 \mathcal{A}}{(r^3 \mathcal{A})'} \sim \mathcal{O}\left(q^2 r^2 \right) \, .$$

This expression is only valid when $(r^3 \mathcal{A})' \neq 0$ and $(r^3 \mathcal{A})' \gg 1$. We assume that the Vainshtein mechanism in spherical symmetry operates outside the source, meaning that condition (5.27) is verified. In terms of the constant $\tilde{G}$ defined in Eq. (5.28), the frame-dragging equation inside the star reads

$$\omega'' + \frac{4}{r} \left[1 + \frac{q^2 f_X \tilde{G} M}{r (f + q^2 f_X)} - \frac{(f + 2 q^2 f_X) \tilde{G} M'}{4 (f + q^2 f_X)} + \mathcal{O}\left(q^2 r^2 \right) \right] \omega' + \frac{4 (f + q^2 f_X) \tilde{G} M' \Omega}{f r^2} \left[1 + \mathcal{O}(r^2 z) \right] = 0 \, .$$

[2] In this case the potentials in the Newtonian gauge have the form $\Phi' \simeq -\Psi' \sim \frac{M' M''}{r^2} - \frac{M'^2}{r^3}$, which is far from the normal GR behavior.

On the left-hand side of this equation, there is an extra term $\propto \tilde{G}M/r$ compared to the equation in GR (see Eq. (4.26)). Note that this term is nonzero, since we study the case $\Gamma_2 \neq 0$, which implies $f_X \neq 0$ (see Appendix II.B). The screening is broken inside the star, because generically $\kappa_2 \neq -2$ when $f_X \neq 0$ as can be seen from the equation above. This behavior is not surprising, since the Vainshtein mechanism in spherical symmetry is broken inside the source. Note that the expressions for K_1 inside and outside the star were obtained in different limits ($(r^3\mathcal{A})' \gg 1$ in the former and $(r^3\mathcal{A})' = 0$ in the latter case), therefore they cannot be matched at the surface of the star. One would have to solve the full equation to obtain a continuous profile, as was done in Ref. [146].

5.4.3 Example 3: cubic Galileon

The time-dependent cubic Galileon was studied in Ref. [132], and also in Ref. [130], where the appropriate de Sitter asymptotics were discussed. To get the cubic Galileon from the general action (31), we set

$$f = 1, \quad G_3 = \beta X, \quad K = \eta X, \quad A_i = 0\,. \tag{5.29}$$

With these choices, we have that $\Gamma_2 = 0$ in Eq. (5.7), and the expression for x for $r \ll r_V$ reads

$$x = \pm q^2 \sqrt{\frac{\mathcal{A}}{2}}\,.$$

The sign should be chosen when properly examining the asymptotic behavior for large radii, but it does not affect the resulting equation for ω (since quadratic terms are dominant in Eq. (5.8) inside the Vainshtein radius) both inside and outside the star. The equation for the frame-dragging function can be written as follows:

$$\omega'' + \frac{4}{r}\left[1 - \frac{GM'}{4} + \mathcal{O}\left(q^2 r^2 \sqrt{\mathcal{A}}\right)\right]\omega' = -\frac{4GM'\Omega}{r^2}\left[1 + \frac{2GM}{r} + \mathcal{O}\left(q^2 r^2 \sqrt{\mathcal{A}}\right)\right]\,,$$

where we have assumed $\mathcal{A} \sim r\mathcal{A}'$ and $\beta q^2 \sim 1$. By comparing the above equation with Eq. (4.26) and taking into account Eq. (5.4), we can see that the corrections for ω to the GR equation are suppressed by powers of r_V inside the Vainshtein radius both inside and outside the source. Using the results of Section 4.2, we then conclude that deviations from the GR expression for ω are also suppressed by powers of r_V in a way analogous to the screening in spherical symmetry. It should also be noted that nonlinear GR corrections (which we did not take into account) may be larger than those due to modified gravity, but they are of course still smaller than the linear GR terms.

Chapter 6

Slow rotation with a static scalar field

We set $q = 0$ in this chapter, meaning that $\phi = \phi(r)$, and consider the shift-symmetric sector of the DHOST Ia class, i.e. the theories which are invariant under the transformation

$$\phi \to \phi + \text{const.}$$

This symmetry is associated with a conserved current

$$J^\mu = -\frac{\delta \mathcal{L}}{\delta(\partial_\mu \phi)} \,,$$

so that in this case the scalar field equation is simply

$$\nabla_\mu J^\mu = 0 \,.$$

It was shown in Ref. [160] that such theories generically lead to a trivial scalar field, i.e. $\phi' = 0$, in spherically symmetric configurations.[1] Because of the shift-symmetry, this is equivalent to having $\phi = 0$. In order to avoid this no-hair theorem for stars, we introduce an additional linear coupling of the scalar field to the Ricci scalar of the form $\alpha\phi R$, which breaks the shift symmetry. This coupling to the curvature provides a nontrivial scalar field configuration with rich phenomenology, including k-mouflage gravity [126], an analog of the Vainshtein mechanism. In this setup, the scalar equation can be written in the form

$$\nabla_\mu J^\mu = -\alpha R \,, \tag{6.1}$$

where J^μ is the conserved current associated with the shift symmetry of the action when $\alpha = 0$. In the following, we will focus on the quadratic Horndeski theory, i.e. we will consider the Lagrangian

$$\mathcal{L} = (f(X) + \alpha\phi)\, R + K(X) - G_3(X)\Box\phi - 2f_X \left[(\Box\phi)^2 - \phi_{\mu\nu}\phi^{\mu\nu}\right] \,. \tag{6.2}$$

[1] We do not give details about the precise hypotheses of the theorem, which can be found in [160].

For these theories, the current associated to shift-symmetry reads

$$\begin{aligned} J^\mu = {} & 4R^{\mu\nu}\phi_\nu f_X - X^\mu \left(G_{3X} + 4f_{XX}\Box\phi\right) + 4f_{XX}\phi^{\mu\nu}X_\nu \\ & - 2\phi^\mu \left[Rf_X + K_X - G_{3X}\Box\phi + 2f_{XX}\left(\phi_{\alpha\beta}\phi^{\alpha\beta} - \{\Box\phi\}^2\right)\right] . \end{aligned} \tag{6.3}$$

Interestingly, the current equation (6.1) can be integrated in the weak-field regime, and we obtain

$$\frac{1}{r^2}\frac{\mathrm{d}}{\mathrm{d}r}\left[r^2 J^r + \alpha\left(2r\lambda - r^2\nu'\right)\right] = 0 ,$$

where we have used Eq. (II.9) to express the Ricci scalar in the weak-field regime. Even though the action is not shift-symmetric if $\alpha \neq 0$, there is an effective conserved current in the weak-field limit in this particular case of a linear coupling to the Ricci scalar. In the following, we will set the integration constant to 0, in order for the norm of the current $J_\mu J^\mu = e^\lambda (J^r)^2$ to be regular at the center of the star. In this case, the scalar field equation reads

$$rJ^r + \alpha\left(2\lambda - r\nu'\right) = 0 . \tag{6.4}$$

It is clear from the above equation that the radial component of the current cannot be zero, in contrast to the shift-symmetric time-dependent case, where we have $J^r = 0$. The presence of the symmetry-breaking term, when $\alpha \neq 0$, renders J^r nonzero. This, and the fact that the ratio ϕ'^2/q^2 is no longer a small parameter in the equations, cf. Eq. (5.1), changes the results in the weak-field approximation. This means that one cannot simply set $q = 0$ in the analysis of the previous chapter, but it is instead necessary to proceed starting from square one.

6.1 K-essence

Let us first consider a k-essence theory, i.e. we take $f = 1$, $A_i = 0$ and $K = \gamma X^p$, where $p \in \mathbb{N}\backslash\{0, 1\}$ and μ is constant. Neglecting the backreaction of the energy-momentum of the scalar field on the metric, which corresponds to neglecting nonlinear scalar contributions in Eqs. (4.9) and (4.10), one can integrate Eq. (4.9) to obtain the metric potentials:

$$\begin{aligned} \lambda &= \frac{2GM(r)}{r} + \alpha r\phi' , \\ \nu' &= \frac{2GM(r)}{r^2} - \alpha\phi' . \end{aligned} \tag{6.5}$$

After combining these expressions with Eq. (6.4), we obtain the following equation for the scalar field:

$$\frac{2\alpha GM(r)}{r^2} + 3\alpha^2\phi' - 2p\gamma\phi'^{2p-1} = 0 . \tag{6.6}$$

6.1.1 Linear regime

Outside the star, we have $2GM(r) = r_S$, and in the limit $r \to \infty$ we can neglect the nonlinear term in Eq. (6.6). In that case, the solution for the scalar field can easily be found:

$$\phi'_{\rm lin} = -\frac{r_S}{3\alpha r^2} \,. \tag{6.7}$$

Note that the limit $\alpha \to 0$ is not well defined in Eq. (6.7). This is a consequence of the absence of a standard kinetic term in the considered theory. Indeed, due to the mixing term $\alpha\phi R$ the scalar degree of freedom has a kinetic term. However, it disappears in the limit $\alpha \to 0$, thus making the theory strongly coupled. Said differently, the nonlinear term is dominant for small α, and therefore the linear regime is nowhere valid.

Using Eq. (6.7) in Eqs. (6.5), one can see that in the linear regime, the GR condition $\lambda + \nu = 0$ is not satisfied even approximately. Instead, the solutions of the system (6.5) read

$$\lambda = \frac{2r_S}{3r} \qquad \text{and} \qquad \nu = -\frac{4r_S}{3r} \,, \tag{6.8}$$

meaning that deviations of the metric potentials from the GR solutions are of $\mathcal{O}(1)$. Upon substituting Eqs. (6.7) and (6.8) into Eq. (5.2) for ω, we obtain

$$\omega'' + \frac{4}{r}\left(1 - \frac{r_S}{6r}\right)\omega' = 0 \,. \tag{6.9}$$

This expression is to be compared with Eq. (4.26) in vacuum, for which $M'(r) = 0$. One can see that the term proportional to r_S has a coefficient different from the GR case. Thus, according to the results of Chapter 4, the leading term in the solution for ω is the same as in GR, unlike the metric potentials. However, the subleading corrections in the weak-field approximation are of order r_S/r. As we will see below, the screening is less effective than in the region $r \ll r_V$, where the leading corrections are suppressed by powers of r_V.

6.1.2 Inside the Vainshtein radius

The linear regime breaks down at the Vainshtein radius $r \sim r_V$, where nonlinear terms become important. Let us determine r_V by taking the solution for ϕ' at infinity and evaluating at which radius the nonlinear term becomes comparable to the linear one [126]. We find

$$r_V^2 = r_S \left(\frac{6p|\gamma|}{3^{2p}\alpha^{2p}}\right)^{\frac{1}{2p-2}} \,. \tag{6.10}$$

For $r \ll r_V$, we can neglect the linear term in Eq. (6.6), and in this range of radii the scalar field reads

$$\phi' = \mathrm{sgn}\,[\alpha\gamma] \left(\frac{|\alpha| GM(r)}{r^2 p|\gamma|}\right)^{\frac{1}{2p-1}} \,. \tag{6.11}$$

Note that the limit $\alpha \to 0$ is well defined, and in that case we have $\phi' \to 0$, in contrast to the solution in the linear regime Eq. (6.7). The limit is consistent with the solution to the scalar equation (6.6) for $\alpha = 0$. In the limit $\alpha \to 0$, the Vainshtein radius given by Eq. (6.10) is infinite; therefore, the Vainshtein mechanism operates for all distances and the linear regime is invalid.

In the region $r \ll r_V$, one can compare the strength of the fifth force with the Newtonian force $\{\lambda'_{\rm GR}, \nu'_{\rm GR}\} \sim 2GM/r^2$, obtained by setting $\phi = 0$ in Eq. (6.5):

$$\left| \frac{\phi'}{\{\lambda'_{\rm GR}, \nu'_{\rm GR}\}} \right| \sim \frac{1}{3|\alpha|} \left(\frac{r_S r^2}{2GM(r) r_V^2} \right)^{\frac{2p-2}{2p-1}} .$$

Outside the source, in the region $R \leq r \ll r_V$, we have $2GM = r_S$, and it is clear that the fifth force is screened. Inside the star, assuming it has a constant density ρ_0, we have $2GM(r) = r_S r^3/R^3$. In this case, it is clear from the above expression that the fifth force becomes dominant for radii smaller than $r_* = R^3/r_V^2 \ll R$. Meanwhile, in the region $r_* \ll r \leq R$, the fifth force is screened. To examine the effects of rotation, we substitute Eq. (6.6) into the $(t\varphi)$ metric equation. Assuming for instance that $\alpha\gamma > 0$ (the other case is analogous), the coefficients K_1 (outside and inside the star respectively) and K_2 read

$$\begin{aligned}
K_1^{\rm out} &= \frac{4}{r} \left[1 + \mathcal{O}\left(\frac{r_S}{r_V} \left(\frac{r}{r_V} \right)^{\frac{2p-3}{2p-1}} \right) \right] , \\
K_1^{\rm in} &= \frac{4}{r} \left[1 + \frac{r_S r}{8 r_V^2} \left(\frac{3-4p}{3(1-2p)} \left(\frac{r}{r_*} \right)^{\frac{1}{2p-1}} - \frac{3r}{r_*} \right) \right] , \\
K_2 &= -2 \left[1 + \frac{r_S r^2}{R^3} \left(1 + \mathcal{O}\left(\frac{r_*}{r} \right)^{\frac{2p-2}{2p-1}} \right) \right] .
\end{aligned}$$

This shows that the Vainshtein mechanism operates in the region $r_* \ll r \ll r_V$. Furthermore, corrections to the GR expression for ω are suppressed by powers of r_V in this region. On the other hand, the subleading correction to ω differs from GR in the region $r \leq r_*$, due to a different power law as compared to the GR case. Hence, the screening for ω is less effective in this region, meaning that corrections to the GR expression are not r_V suppressed. One can check that the size of the value of r_* is very small in physically relevant situations, i.e. $r_* \ll R$.

6.2 Cubic Galileon

We now discuss the cubic Galileon theory, defined by the relations (5.29). The static Vainshtein screening in this theory was studied in Ref. [130], though the authors considered both a time dependence of the scalar field and a coupling of the scalar to the matter fields. The slow rotation in this theory has already been discussed in

Ref. [136], where it was found that the correction to the $(t\varphi)$ equation coming from the Galileon term is highly suppressed. The scalar field equation (6.4) is quadratic in ϕ', and the solution reads

$$\phi' = \frac{\mu r r_S}{r_V^3}\left[1 - \sqrt{1 + \left(\frac{r_V}{r}\right)^3}\right] , \tag{6.12}$$

where we chose the solution that does not diverge at $r \to \infty$, and the constants μ and r_V are given in Eq. (II.14). We assume $\alpha\beta < 0$, in order to have $r_V > 0$. The solution for the scalar field in the linear regime, i.e. $r \gg r_V$, is similar to its counterpart in the case of k-essence, see Eq. (6.7). The difference is that in the case of the cubic Galileon we included a canonical kinetic term, and therefore the limit $\alpha \to 0$ is well defined in this regime as well. In the linear regime, the equation for the frame-dragging function is modified in a similar way to the k-essence case, Eq. (6.9), and the conclusions of the previous section about a less effective screening for ω hold. Inside the Vainshtein radius, i.e. for $r \ll r_V$, we expand the solution (6.12) and obtain

$$\phi' = \frac{2\alpha r_S}{k_2 r_V^{3/2}}\sqrt{\frac{2GM}{r_S r}} .$$

In order to study the equation for the frame-dragging function inside the star, we assume that the matter source has a constant density. It is easy to check from the above expression that the fifth force is screened everywhere in the region $r \ll r_V$, unlike in the k-essence case, where the fifth force becomes dominant for small radii inside the source (see Section 6.1). Substituting the expression for ϕ' into the $(t\varphi)$ equation, we obtain the following expressions for the coefficients K_1 (outside and inside the source) and K_2:

$$\begin{aligned} K_1^{\text{out}} &= \frac{4}{r}\left[1 + \mathcal{O}\left(\frac{r_S\sqrt{r}}{r_V^{3/2}}\right)\right] , \\ K_1^{\text{in}} &= \frac{4}{r}\left[1 - \frac{3r_S r^2}{8R^3}\left(1 + \mathcal{O}\left(\frac{R^{3/2}}{r_V^{3/2}}\right)\right)\right] , \\ K_2 &= -2\left[1 + \frac{r_S r^2}{R^3}\left(1 + \mathcal{O}\left(\frac{R^{3/2}}{r_V^{3/2}}\right)\right)\right] . \end{aligned}$$

For a star of constant density, $\rho_0 = 3r_S/R^3$, the leading corrections to the GR equation (4.26) are suppressed by powers of r_V. This means that the corrections to the GR solution for ω are also suppressed by powers of r_V, in a way analogous to the screening in spherical symmetry.

6.3 Quadratic sector of Horndeski theory

We now consider the quadratic sector of Horndeski theory, and set

$$K = G_3 = 0 \,. \tag{6.13}$$

We will treat the case $f_{XX} = 0$ separately, since the scalar equation is different in that case.

6.3.1 Case $f_{XX} \neq 0$

For now let us assume $f_{XX} \neq 0$. Neglecting nonlinear terms in the (tt) and (rr) equations, the expressions for $\{\lambda, \nu\}$ are the same as Eq. (6.5). After substituting these expressions for the metric potentials, the scalar equation reads

$$2\alpha GM(r) + 3\alpha^2 r^2 \phi' + 8\phi'^3 f_{XX} = 0 \,, \tag{6.14}$$

where f_{XX} is evaluated at $X = \phi'^2$. In the nonlinear regime outside the source, i.e. for $R \leq r \ll r_V$, the linear term in Eq. (6.14) can be neglected. In that case, the scalar field is constant and satisfies the equation

$$8\phi'^3 f_{XX} = -\alpha r_S \,,$$

unless $f(X) \propto \sqrt{X}$, in which case the nonlinear term disappears in the scalar equation. For these particular theories, solving Eq. (6.14) leads to $\phi' \sim 1/r^2$ everywhere outside the star. A similar case was studied in an application to black holes in Ref. [161]. In the general case, when $f(X)$ is not proportional to $\sqrt{X}$ and $f_{XX} \neq 0$, the derivative of the scalar field ϕ' must be constant. This allows us to simplify the equation for ω, since $\phi'' = 0$. Let us examine what happens for polynomial functions of the form

$$f(X) = 1 + \kappa X^p \,,$$

with κ a constant coefficient and $p > 1$ so that $f_{XX} \neq 0$. The spherically symmetric Vainshtein regime in such theories was discussed in Ref. [135]. For large radii, one can neglect the nonlinear term in Eq. (6.14), and the solution for ϕ' is the same as those for k-essence and the cubic Galileon discussed above. One can then define a Vainshtein radius r_V by equating the linear and nonlinear terms in Eq. (6.14), and show that in the region $r \ll r_V$ the fifth force reads

$$\phi' \sim \frac{r_S}{3\alpha r_V^2} \left(\frac{2GM(r)}{r_S} \right)^{\frac{1}{2p-1}} \,. \tag{6.15}$$

It is constant outside the source, and one can easily check that it is screened for $r \ll r_V$. Inside the source the situation is similar to the k-essence theories discussed above. Indeed, for a star of constant density the fifth force becomes larger than the

Newtonian force near the center of the star when $p > 2$ (for $p = 2$, $|\phi'|$ grows linearly and the Vainshtein screening is effective for all radii $r \ll r_V$). For $p > 2$, the fifth force becomes dominant for radii smaller than some $r_* \ll R$. A simple estimate, assuming that r_V is of the order of Neptune's distance to the Sun, gives $r_* \leq 10$ m (the case of k-essence is recovered for large p), while for more realistic Vainshtein radii, the value of r_* is much smaller. As in the k-essence theories, this small radius is not physically relevant.

Substituting the solution (6.15) into the $(t\varphi)$ equation, we obtain the following expressions for the coefficients K_1 (outside and inside the source) and K_2:

$$\begin{aligned} K_1^{\text{out}} &= \frac{4}{r}\left[1 + \mathcal{O}\left(\frac{r_S r}{r_V^2}\right)\right] , \\ K_1^{\text{in}} &= \frac{4}{r}\left[1 - \frac{3 r_S r^2}{8R^3}\left(1 + \frac{R^2}{r_V^2}\cdot\mathcal{O}\left(\frac{R}{r}\right)^{\frac{2p-4}{2p-1}}\right)\right] , \\ K_2 &= -2\left[1 + \frac{r_S r^2}{R^3}\left(1 + \frac{R^2}{r_V^2}\cdot\mathcal{O}\left(\frac{R}{r}\right)^{\frac{2p-4}{2p-1}}\right)\right] . \end{aligned} \tag{6.16}$$

Using the results of Section 6.2, one can see that for $p = 2$ the situation is similar to the cubic Galileon case. The corrections to the GR expression for ω are suppressed by powers of r_V, and the screening operates in a way analogous to the spherically symmetric mechanism. For $p > 2$, the situation is similar to the k-essence case, and the subleading terms in the solution for ω are not the same as in GR in the region $r \leq r_*$. However, as we discussed above, this region is not physically relevant.

6.3.2 Case $f_{XX} = 0$

Let us now look at the case where the Lagrangian contains a derivative coupling to the Einstein tensor $\sim \phi^\mu \phi^\nu G_{\mu\nu}$, which corresponds to

$$f(X) = 1 + \kappa X .$$

The spherically symmetric Vainshtein mechanism in this theory was discussed in Ref. [134]. The particularity of this Lagrangian in application to the Vainshtein mechanism is that the leading nonlinear term in the scalar equation (6.14) vanishes. Therefore we have to keep nonlinear terms in the metric equations, as well as the subleading term for the scalar current, since the leading term vanishes. This modifies the expression for λ (compared to Eq. (6.5)), and the metric potentials read

$$\begin{aligned} \lambda &= \frac{2GM(r)}{r} + \alpha r\phi' - 2\kappa\phi'^2 , \\ \nu' &= \frac{2GM(r)}{r^2} - 2\alpha\phi' . \end{aligned} \tag{6.17}$$

Substituting these expressions into the scalar equation, we obtain

$$2\alpha GM(r) + 3\alpha^2 r^2 \phi' \left[1 - 4\frac{\kappa\phi'}{\alpha r} + \frac{8}{3}\left(\frac{\kappa\phi'}{\alpha r}\right)^2\right] = 0 \,.$$

In the linear regime, the scalar field is given by Eq. (6.7), as in the previous case. We define the Vainshtein radius as $\kappa\phi'(r_V) \sim \alpha r_V$, which implies that both nonlinear terms are of the same order around $r \sim r_V$. Using the expression for ϕ' in the linear regime, we obtain

$$r_V^3 = \frac{|\kappa| r_S}{3\alpha^2} \,.$$

In the nonlinear regime $r \ll r_V$, the expressions (6.17) for the metric potentials imply that $\kappa r \phi'^2 \ll GM$ in order for the static Vainshtein screening to work. In this case, one can show that the cubic term dominates in the scalar equation (otherwise we find $\kappa r \phi'^2 \sim GM$, which modifies the GR expression for λ in Eq. (6.17)), and the fifth force reads

$$\phi' = -\frac{r_S}{3\alpha r_V^2}\left(\frac{GM(r)}{4r_S}\right)^{1/3} \,.$$

The above expression is similar to the one obtained for $p = 2$ in the previous section. This means that the fifth force is screened for all radii $r \ll r_V$, inside and outside the matter source. After substituting this expression in the $(t\varphi)$ metric equation, we obtain the following coefficients for the frame-dragging equation:

$$\begin{aligned}
K_1^{\rm out} &= \frac{4}{r}\left[1 + \mathcal{O}\left(\frac{r_S r}{r_V^2}\right)\right] \,, \\
K_1^{\rm in} &= \frac{4}{r}\left[1 - \frac{3 r_S r^2}{8R^3}\left(1 + \mathcal{O}\left(\frac{R^2}{r_V^2}\right) + \mathcal{O}\left(\frac{r_S r^2}{R^2 r_V}\right)\right)\right] \,, \\
K_2 &= -2\left[1 + \frac{r_S r^2}{R^3}\left(1 + \mathcal{O}\left(\frac{R}{r_V}\right)\right)\right] \,.
\end{aligned}$$

The subleading corrections depend on the value of r inside the star. In any case, however, the corrections to the GR expression for ω are screened by a power of r_V, and the conclusions are the same as for $p = 2$ in the previous section. It is worth stressing again that in addition to these corrections due to modifications of gravity, there exist nonlinear GR terms. Both types of contributions can be seen as higher-order corrections to linearized GR. We do not consider them here, though it is possible for these corrections to be larger than those coming from modified gravity.

Conclusion to Part II

We have analyzed the validity of the Vainshtein mechanism for slowly rotating stars in scalar tensor theories belonging to the DHOST Ia class. While it is usually studied for spherically symmetric objects, we have shown that, in general, slow rotation does not spoil the Vainshtein screening. We also found that in most situations, when the Vainshtein screening operates in spherical symmetry, the leading corrections to the GR expression for ω in the weak-field approximation are also suppressed by powers of the Vainshtein radius r_V. Importantly, even though the corrections to ω may receive sizable modifications (inside the star), the metric functions ν and λ are not modified. This means that if the theory exhibits the Vainshtein mechanism in spherical symmetry, slow rotation does not change the Vainshtein suppression of non-GR corrections to the "static" part of the metric ν and λ, independently of the behavior of the frame-dragging function ω. We applied the Hartle-Thorne formalism for slowly rotating stars to the scalar-tensor theories of the DHOST Ia class, and considered both a time-dependent and a static scalar field. Our main purpose was to study the equation for ω and compare the results with the standard GR case.

In the first part of Chapter 4, we found the general equation for the frame-dragging function in DHOST Ia theories, Eq. (4.14), with coefficients K_1 and K_2 given by Eqs. (4.15) and (4.16), respectively. For slowly rotating relativistic sources in a subclass of Horndeski theory, we calculated exact expressions for the coefficients K_1 and K_2 and showed that the vacuum GR equation for the frame-dragging function is fully recovered, see Appendix II.A. This result also applies to the quadratic beyond Horndeski theories, namely the theories described by the Lagrangian (5.13). It can also be extended to general shift-symmetric DHOST Ia theories, with the additional assumption that the kinetic term for the solution has the constant value $X = -q^2$.

In the rest of this part, we assumed that the weak-field approximation is valid, see Eq. (4.23). In Section 4.2, we derived the equation satisfied by the frame-dragging function in this limit, and showed that outside the star the solution is the same as in GR at leading order. Inside the source, we showed that the screening can be broken, in which case $\kappa_2 \neq -2$, see Eq. (4.28). We also computed corrections to the solution for ω, assuming that the coefficients of the frame-dragging equation acquire small modifications. In Chapter 5 we studied the equation for the frame-dragging function for various subclasses of the DHOST Ia class in the case $q \neq 0$, i.e. when the scalar is time-dependent. In Section 5.1, we found the expressions for the coefficients K_1 and K_2 of the equation for ω in this approximation, Eqs. (5.2) and (5.3). We then used the metric field equations to obtain the coefficient K_1 in terms of the scalar field only, Eq. (5.8). In Section 5.2, we showed that outside the Vainshtein radius the coefficient K_1 receives a correction suppressed by r_S/r or q^2r^2, Eqs. (5.9) and (5.10). To study the region inside the Vainshtein radius, we considered different classes of theories case by case in Sections 5.3 and 5.4. In most cases, when the Vainshtein screening works in spherical symmetry, the corrections to the GR expression for ω are screened by powers of r_V, in a way analogous to what happens in the nonrotating case. However, we have

found a particular theory for which the suppression is not as effective, in this case the leading correction is suppressed by r_S/r instead. We also studied a different class of theories for which the static metric potentials in the nonrotating case are exactly the same as in GR (possibly up to a redefinition of Newton's constant), while the screening for ω is broken inside the star.

The case of a static scalar field was discussed in Chapter 6, and we found that the results are similar to the time-dependent case. In all the examples we considered, the Vainshtein mechanism works for the frame-dragging function ω. Furthermore, the screening is more effective in regimes where the Vainshtein mechanism operates in spherical symmetry, meaning that the corrections to the GR expression are suppressed by powers of r_V. Meanwhile, outside the Vainshtein radius, the coefficients of the frame-dragging equation receive non-screened corrections, see e.g. Eq. (6.9) for k-essence. The screening still works for the frame-dragging function ω, but it is less effective in this region.

Although our results show that the deviations from GR are always small (outside the source), it is interesting to see whether local gravity tests can provide additional constraints on scalar-tensor theories coming from the sub-leading modifications to the frame-dragging function. Probably the simplest way is to check constraints on PPN parameters (although it should be noted that precisely speaking the PPN analysis does not apply). The frame-dragging function ω can be written as (see for instance section 4.4 of Ref. [50]),

$$\omega_{\rm PPN} = \left(1+\gamma+\frac{1}{4}\alpha_1\right)\frac{J}{r^3}\,.$$

We have $\omega = 2J/r^3$ in GR, and hence deviations from GR are characterized by the combination $\gamma - 1 + \alpha_1/4$. This is to be compared to our results on the frame-dragging function. Generically the deviation of ω from its GR value is of order r_S/r for non-Vainshtein suppression, and much smaller for the Vainshtein suppressed cases. Therefore the combination of PPN parameters $\gamma-1+\alpha_1/4$ is not larger than $\mathcal{O}(r_S/r)$ in our case, which gives a deviation of order 10^{-8} at Earth's orbit. This value is well within the experimental constraints on both γ and α_1, and therefore we do not get any additional constraints on the parameters of the scalar-tensor theories from this estimation.

Appendix

II.A Relativistic sources in shift-symmetric theories

In this appendix, we study the slow rotation of relativistic stars for shift-symmetric theories that are invariant under $\phi \to -\phi$, meaning we set $G_3 = 0$. We also assume slow rotation, but otherwise the equations are fully nonlinear in the metric functions λ and ν, i.e. we do not assume the weak-field approximation in this section.

II.A.1 Horndeski theories

We first consider Horndeski theories with general functions $f(X)$ and $K(X)$, in which case the Lagrangian density reads:

$$\mathcal{L} = f(X)R + K(X) - 2f_X \left[(\Box\phi)^2 - \phi_{\mu\nu}\phi^{\mu\nu}\right] . \tag{II.19}$$

The authors of Ref. [153] studied slowly rotating neutron stars in the case when $f(X)$ and $K(X)$ are linear functions of X. They showed that the equation for ω in vacuum reduced to the GR expression, meaning that we have $K_1 = 4/r$ and the term proportional to K_2 in Eq. (4.14) is absent. In fact this property was pointed out before in Refs. [151, 152], in the case of slowly rotating black holes. We now extend this result to a more general class of theories. We assume $f_{XX} \neq 0$, since the case $f_{XX} = 0$ was treated in Ref. [153]. With this assumption, the scalar field can be obtained in terms of $\{\lambda, \nu, \nu'\}$ from the equation $\mathcal{E}_{tr} = 0$:

$$\phi'^2 = \frac{e^\lambda \left[-2f_X\left(1 + r\nu' - e^\lambda\right) + r\left(4q^2 f_{XX}\nu' e^{-\nu} + rK_X e^{-\lambda}\right)\right]}{4f_{XX}\left(1 + r\nu'\right)} .$$

One then substitutes this expression into the (rr) component of the metric equations to obtain λ in terms of ν':

$$e^\lambda = \frac{2\left(1 + r\nu'\right)\left(f_X^2 + f f_{XX}\right)}{2f_X^2 + r^2 f_X K_X + f_{XX}\left(2f + r^2 K + 2r^2 P/M_P^2\right)} .$$

Using the (tt) equation one can then obtain λ' in terms of $\{\lambda, \nu, \phi', \phi'', \rho\}$. After substituting this expression in Eq. (4.18), the second derivatives of ϕ disappear and we are left with a coefficient K_1 which depends only on $\{\lambda, \nu, \nu', \phi'^2\}$. Upon substituting

the expressions for ϕ'^2 and λ the final expression for K_1 depends only $\{\rho, P, \nu, \nu'\}$. Finally, the coefficients read:

$$K_1 = \frac{4}{r} - \frac{re^{\nu}(1+r\nu')^2(f_X^2 + f f_{XX})(\rho + P)}{M_P^2 D_1} \,,$$
$$K_2 = -\frac{2e^{\lambda}}{f + 4X f_X} \,,$$

where the denominator in the first expression is given by

$$D_1 = 2q^2 f_X \left[2f_X^2 + r^2 f_X K_X + \left[2f + r^2\left(\frac{2P}{M_P^2} + K\right)\right] f_{XX}\right]$$
$$+ e^{\nu}\left[2f + r^2\left(\frac{2P}{M_P^2} + K\right)\right]\left(f_X^2 + f f_{XX}\right)(1 + r\nu') \,.$$

One can see that the GR case is recovered in vacuum, where we simply have $K_1 = 4/r$. This shows that the result of Ref. [153] can be extended to general functions f and K in Horndeski theories.

It is also worth pointing out a mistake in formulas (44) and (53) of Ref. [153]. In their notations, which are obtained from ours by $\omega \to \Omega_* - \omega$, $e^{\nu} \to b$, $q \to Q$ and $K_2 \to -K_2(\rho + P)$, these formulas should read (note also that the definition of the scalar kinetic term is different)

$$u_{\varphi} = \varepsilon \frac{r^2 \sin^2\theta \omega}{\sqrt{b}} \,,$$
$$K_2 = \frac{4(b + rb')^2(P + \rho)}{b[(Pr^2 + 4\kappa)(b + rb') - \eta Q^2]} \,.$$

With the above expression for u_{φ}, one recovers the correct expression for the 4-velocity vector [154]:

$$u^{\mu} = \left(u^0, 0, 0, \epsilon \Omega u^0\right) \,,$$

unlike in Ref. [153].

II.A.2 Quadratic GLPV theories

The above result, namely that the equation for ω reduces to the one of GR in vacuum for Horndeski theory with arbitrary $f(X)$ and $K(X)$, can be extended to quadratic Gleyzes-Langlois-Piazza-Vernizzi (GLPV) theories [44]. They are given by the Lagrangian density (5.13). The inclusion of A_3 makes $\mathcal{E}_{tr} = 0$ a quadratic equation in ϕ'^2, in contrast to the Horndeski case, where the analogous equation is linear in ϕ'^2. In order to obtain the desired result, we use the metric equations in a different order than in the previous case for Horndeski theory. First, we use $\mathcal{E}_{rr}$ to express $\phi'\phi''$ in terms of $\{\phi', \lambda, \nu, \nu'\}$. Then, we substitute this expression into $\mathcal{E}_{tt}$ to obtain λ' in

terms of $\{\phi', \lambda, \nu, \nu'\}$, which we inject into $\mathcal{E}_{tr}$. This yields a quadratic equation for ϕ'^2, and the two solutions are expressed in terms of $\{\lambda, \nu, \nu'\}$. Using the expressions for $\{\phi'\phi'', \lambda', \phi'^2\}$, one can obtain that $K_1 = 4/r$ in vacuum, which means that the GR equation for ω is fully recovered in the case of the theories (5.13) as well.

II.A.3 DHOST Ia with constant X

Assuming in addition that X is constant, i.e. $X_0 = -q^2$, the previous result can be extended to shift-symmetric DHOST theories. Indeed, when X =const., the terms containing A_4 and A_5 in the action (31) drop out of the field equations, because one can write

$$\mathcal{L}_4 \sim X_\mu X^\mu \ , \quad \mathcal{L}_5 \sim (X_\mu \phi^\mu)^2 \ .$$

Since the above expressions are quadratic in X_μ, their variation will not give any contribution to the field equations when X is constant. It immediately follows from Eq. (4.15) that

$$K_1 = \frac{4}{r} - \frac{\lambda' + \nu'}{2} \ ,$$

since $f(X_0) - X_0 A_1(X_0)$ is a constant. With the choice $X_0 = -q^2$, the scalar can be expressed in terms of $\{\lambda, \nu\}$ as

$$\phi'^2 = q^2 e^\lambda \left(e^{-\nu} - 1\right) \ . \tag{II.20}$$

Using Eq. (II.20) in the (tt), (tr) and (rr) components of the metric equations, one can show that

$$\lambda' + \nu' \sim r\,(P + \rho) \ ,$$

so once again the GR equation for ω, Eq. (4.21), is recovered in vacuum.

II.B List of coefficients

In this appendix, we list the coefficients of Eqs. (5.5), (5.6), (5.7), and (5.8). Each time a function is written, it is evaluated on the time-dependent background. For instance,

$$f \equiv f\left(qt, -q^2\right) \ .$$

The time dependence of these coefficients comes from the ϕ dependence of the functions. We will implement the constraint $A_2 = -A_1$, but in order to keep expressions light, we will not always substitute the expression for A_4 in DHOST Ia theories. Whenever A_4 appears, one must keep in mind that the following constraint holds:

$$\begin{aligned} A_4 = &\frac{1}{8(f + q^2 A_1)^2} \left\{12 f A_1^2 + 16 q^2 A_1^3 - 12 q^2 f A_1 A_3 - f A_3 \left(8f + q^4 A_3\right)\right. \\ &\left. -8 f_X \left[6 f A_1 + q^2 \left(8 A_1^2 + f A_3 + 2 q^2 A_1 A_3\right) - 2 f_X \left(3f + 4 q^2 A_1\right)\right]\right\} \ . \end{aligned}$$

The terms involving A_5 were negligible in the field equations when assuming dimensionless quantities to be of $\mathcal{O}(1)$, so this function does not appear in the following.

II.B.1 Coefficients of the metric equations

With the definition

$$C = f(2f + 2q^2 A_1 - q^4 A_4) + 4q^2 f_X (f + 2q^2 f_X) \,,$$

the coefficients for Eqs. (5.5) and (5.6) read:

$$\begin{aligned}
C\alpha_1 &= 2q^2 f \,, \\
C\alpha_2 &= 2q^2 \left(f + 2q^2 f_X\right) \,, \\
2C\beta_1 &= -2f_\phi \left(f + 4q^2 f_X\right) - q^2 \left[-2f G_X + q^2 f A_{3\phi} + \left(6f + 8q^2 f_X\right) A_{1\phi}\right] \,, \\
2C\beta_2 &= 2q^2 \left[\left(f + 2q^2 f_X\right) G_X - \left(f - 2q^2 A_1 + 6q^2 f_X + q^4 A_4\right) A_{1\phi}\right] \\
&\quad - q^4 \left(f + 2q^2 f_X\right) A_{3\phi} + 2f_\phi \left(f + 2q^2 A_1 - 2q^2 f_X - q^4 A_4\right) \,, \\
2C\gamma_1 &= 2f \left(A_1 + 2q^2 A_{1X}\right) + q^2 f \left(3A_3 + 2A_4\right) - 4f_X \left(f + 4q^2 f_X - 3q^2 A_1\right) \,, \\
2C\gamma_2 &= A_1 \left(3q^4 A_4 - 4f\right) + q^2 \left(3f A_3 + 2f A_4 - 6A_1^2\right) \\
&\quad + 2f_X \left(2f + 6q^2 A_1 + 3q^4 A_3 - 4q^2 f_X\right) + 4q^2 A_{1X} \left(f + 2q^2 f_X\right) \,, \\
2C\delta_1 &= 2\left(A_1 - 2f_X\right) \left(f + 4q^2 f_X\right) + q^2 f \left(A_3 + 2A_4\right) \,, \\
2C\delta_2 &= q^2 f \left(A_3 + 2A_4\right) - 2A_1 \left(f + 2q^2 A_1 - q^4 A_4\right) \\
&\quad + 2f_X \left(2f - 4q^2 f_X + 6q^2 A_1 + q^4 A_3\right) \,, \\
3C\eta_1 &= fK + q^2 \left[3f_X \left(K - q^2 G_\phi\right) - f\left(K_X + 2G_\phi\right)\right] \,, \\
12C\eta_2 &= K \left(3q^4 A_4 - 6q^2 A_1 - 2f\right) + q^2 \left[-4fK_X + 8f_X \left(K - q^2 K_X - 2q^2 G_\phi\right)\right. \\
&\quad \left. + G_\phi \left(6q^2 A_1 - 2f - 3q^4 A_4\right)\right] \,.
\end{aligned}$$

II.B.2 Coefficients of the scalar equation

We now list the coefficients of the scalar equation (5.7). We do not write C_1 or η_3 because the expressions are cumbersome, and we always neglect those terms in the nonlinear regime where the Vainshtein mechanism operates. The other coefficients read

$$\begin{aligned}
C_2 = 6 &\left(f + q^2 A_1\right) \left\{-12q^4 A_1^3 \left(3f_\phi + 4q^2 f_{\phi X}\right) - 4q^2 A_1 \left(-4q^2 G_{3X} \left[3f + q^2 f_X\right]\right.\right. \\
&+ q^2 \left[3A_{1\phi} + 4q^2 A_{1\phi X}\right] \left[3f + 4q^2 f_X\right] + 4q^4 A_{3\phi} \left[3f + 2q^2 f_X\right] \\
&\left. + f_\phi \left[6f - 3q^4 A_3 - 12q^4 A_{1X} + 8q^2 f_X\right] - 2q^2 f_{\phi X} \left[3q^4 A_3 + 8q^4 A_{1X} - 10f\right]\right) \\
&+ 16f^2 G_{3X} \left(2f + 2q^2 f_X - q^4 A_3 - 3q^4 A_{1X}\right) + 16q^4 f^2 f_{\phi X} \left(A_3 + 2A_{1X}\right) \\
&- f A_{1\phi} \left(16q^4 A_{1X} \left[q^4 A_3 - 8f - 12q^2 f_X\right] + \left[4f - 5q^4 A_3\right] \left[12f - q^4 A_3\right]\right. \\
&\left. + 16q^2 f_X A_{1\phi} \left[10f + 7q^2 f_X - 5q^4 A_3\right]\right) - 8q^2 f^2 A_{1\phi X} \left(4f + q^4 A_3 + 4q^2 f_X\right) \\
&- 8q^2 f^2 A_{3\phi} \left(4f - q^4 A_3 + 4q^2 f_X - 4q^4 A_{1X}\right) + 2f f_\phi \left(q^2 A_3 \left[16f - q^4 A_3\right]\right. \\
&\left. - 16 f_X \left[3f - 2q^4 A_3 + 3q^2 f_X\right] + 4q^2 A_{1X} \left[6f - q^4 A_3 + 20q^2 f_X\right]\right)
\end{aligned}$$

$$
\begin{aligned}
&+q^2A_1\left(16fG_{3X}\left[5f-q^4A_3-3q^4A_{1X}+3q^2f_X\right]+4A_{1\phi}\left[2q^2f_X(-28f\right.\right.\\
&\left.+7q^4A_3+16q^4A_{1X}-12q^2f_X)+3f(5q^4A_3+8q^4A_{1X}-8f)\right]\\
&+8fq^2A_{3\phi}\left[q^4A_3-10f+4q^4A_{1X}-8q^2f_X\right]+8ff_{\phi X}\left[5q^4A_3-4f+12q^4A_{1X}\right]\\
&-8fq^2A_{1\phi X}\left[10f+q^4A_3+12q^2f_X\right]+q^2A_3f_\phi\left[40f+3q^4A_3\right]\\
&\left.-8f_\phi f_X\left[18f-5q^4A_3+10q^2f_X\right]+8q^2f_\phi A_{1X}\left[8f+q^4A_3+12q^2f_X\right]\right)\Big\}\ ,\\
C_3 &= 24\left(f+q^2A_1\right)^2\left(2fA_{1X}+2A_1f_X+fA_3\right)\\
&\qquad\times\left(4q^2f_X-3q^4A_3+4f+6q^2A_1-8q^4A_{1X}\right)\ ,\\
\Gamma_0 &= 48q^2\left(f+q^2A_1\right)\Big\{q^2\left(q^2A_3-4f_X\right)\left(-2q^2fA_{1\phi}+f_\phi\left[q^2A_1-f\right]\right)\\
&\quad+2q^2A_1f\left(q^4A_{3\phi}+2f_\phi+6q^2f_{\phi X}-q^2G_{3X}\right)+2q^4A_1^2\left(3f_\phi+4q^2f_{\phi X}\right)\\
&\quad+2f^2\left(f_\phi+q^2\left[2A_{1\phi}+q^2A_{3\phi}+2f_{\phi X}-G_{3X}\right]\right)\Big\}\ ,\\
\Gamma_1 &= -192q^4\left(f+q^2A_1\right)^2\left(2fA_{1X}+2A_1f_X+fA_3\right)\ ,\\
\Gamma_2 &= 12q^2\left[2fA_1+q^2\left(4A_1^2-fA_3\right)-4f_X\left(f+2q^2A_1\right)\right]\\
&\qquad\times\left[f\left(4f+6q^2A_1+q^4A_3\right)+4q^2f_X\left(f+2q^2A_1\right)\right]\ .
\end{aligned}
$$

II.B.3 Coefficients of the $(t\varphi)$ equation

We now list the coefficients of Eq. (5.8), apart from β_0, κ_0, since we neglect these terms inside the Vainshtein radius. We define

$$
D = f\left(4f+6q^2A_1+q^4A_3\right)+4q^2f_X\left(f+2q^2A_1\right)\ .
$$

The remaining coefficients read

$$
\begin{aligned}
D^2\alpha_0 &= 8q^4\left(f+q^2A_1\right)\left(-fA_1+q^2fA_{1X}+f_X\left[2f+q^2A_1\right]\right)\ ,\\
D^2\zeta_0 &= -4q^2\left(f+q^2A_1\right)^2\left(f+2q^2f_X\right)\ ,\\
4D^2\gamma_0 &= \{f+q^2A_1\}\{f\left[8q^2A_{1X}\left(-2f-4q^2A_1+4q^4A_{1X}+3q^4A_3\right)+3q^6A_3^2\right.\\
&\quad\left.-12q^2\left(A_1^2+fA_3\right)-8fA_1-24q^4A_1A_3\right]\\
&\quad-16f_X\left[3q^4A_1^2-2q^6A_1A_{1X}-f^2\right]+16q^2f_X^2\left[f+2q^2A_1\right]\}\ ,\\
2D^2\delta_0 &= \left(f+q^2A_1\right)\left(2A_1+q^2A_3-4f_X\right)\left(f\left[4f+6q^2A_1+3q^4A_3+4q^4A_{1X}\right]\right.\\
&\quad\left.+4q^2f_X\left[f+3q^2A_1\right]\right)\ ,\\
4D\sigma_0 &= \left(f+q^2A_1\right)\left(2A_1+q^2A_3-4f_X\right)\ .
\end{aligned}
$$

II.B.4 Other coefficients

We define

$$B = 8\left(f+q^2A_1\right)\left(2A_1f_X+2fA_{1X}+fA_3\right) \times\left[4f+2q^2\left(3A_1+2f_X\right)-q^4\left(8A_{1X}+3A_3\right)\right] .$$

Then, the coefficients of Eq. (5.12) read

$$\begin{aligned} B\iota_0 =& 4q^2\left(f+2q^2A_1\right)\left[A_1^2-2fA_3+4f_X\left(f_X-2A_1\right)\right]+q^6A_3\left(4A_1^2+3fA_3\right) \\ &+8q^2A_{1X}\left[f\left(-2f-4q^2A_1+3q^4A_3\right)+4q^4\left(fA_{1X}+A_1f_X\right)\right] , \\ B\iota_1 =& -q^2\left(2A_1-4f_X+q^2A_3\right)\left[2fA_1-4f_X\left(f+3q^2A_1\right)\right. \\ &\left.+q^2\left(4A_1^2-3fA_3-4fA_{1X}\right)\right] , \\ 2B\iota_2 =& -q^2\left(2A_1-4f_X+q^2A_3\right)\left[2fA_1-4f_X\left(f+2q^2A_1\right)+q^2\left(4A_1^2-fA_3\right)\right] . \end{aligned}$$

The coefficient of Eqs. (5.22) and (5.23) reads

$$\iota_3 = \frac{N_{\iota_3}}{D_{\iota_3}} ,$$

where the numerator and denominator are given by

$$\begin{aligned} N_{\iota_3} =& f_\phi\left\{A_1\left(f^2-2q^2fA_1-5q^4A_1^2\right)+q^2A_{1X}\left(-3f^2-3q^2fA_1+4q^4A_1^2\right.\right. \\ &\left.\left.+q^4A_{1X}\left[f-q^2A_1\right]\right)\right\}-2A_{1\phi}\left\{6f^3+14q^2f^2A_1+10q^4fA_1^2+3q^6A_1^3\right. \\ &\left.+q^4A_{1X}\left(2f^2+5q^2fA_1+q^4A_1^2-q^4fA_{1X}\right)\right\} \\ &+\left\{f+q^2A_1\right\}\left\{G_{3X}\left(8f^2+15q^2fA_1+6q^4A_1^2-q^4fA_{1X}\right)\right. \\ &\left.+2q^2A_{1\phi X}\left(4f^2+7q^2fA_1+2q^4A_1^2-q^4fA_{1X}\right)\right\} , \\ D_{\iota_3} =& \left(2f+3q^2A_1-q^4A_{1X}\right)^2\left\{q^2f_\phi\left(A_{1X}\left[q^2A_1-2f\right]-3A_1^2\right)\right. \\ &\left.+f\left(4\left[f+q^2A_1\right]\left[G_{3X}+q^2A_{1\phi X}\right]-3A_{1\phi}\left[2f+q^2A_1+q^4A_{1X}\right]\right)\right\} . \end{aligned}$$

Part III

Disforming the Kerr metric

Introduction to Part III

In 1916, a few months after Einstein proposed his general theory of relativity (GR), Schwarzschild discovered a static solution to the vacuum field equations. This solution possesses an intriguing property, namely there exists a surface of no return, from the interior of which it is impossible for matter or even light to escape. For this reason, the term "black hole" was introduced by Wheeler in 1967 to describe such objects. Though the metric of a static black hole was found rather quickly, the quest to find a rotating counterpart to the Schwarzschild solution remained fruitless for decades. In 1963, Kerr derived the expression for a rotating black hole depending on two parameters [11], its mass M and angular momentum $J = aM$, and which reduced to the Schwarzschild spacetime in the limit $a = 0$. It was later shown that the Kerr metric is the unique stationary and axisymmetric vacuum black hole in GR [162], making it essential from a theoretical point of view. While black holes were for a long time believed to be of mathematical interest only, proof of their existence in Nature has started to arise in later years.

Einstein's theory has been extensively tested in the Solar System in the last century, passing all weak-field tests with great success (see Ref. [50] for a review). The study of binary pulsars has provided a window into the strong gravity regime in GR [6], but the spacetime around black holes remains largely untested. At the center of the Milky Way, there exists a bright source of radio and infrared emissions called Sagittarius A, and in which lies Sagittarius A* (Sgr A*). The current understanding is that this region coincides with a supermassive black hole (SMBH) of mass $M \sim 4 \times 10^6 M_\odot$ (see Ref. [163] and references within). In fact, a SMBH (meaning $M \gtrsim 10^6 M_\odot$) is expected to exist in the center of almost every large galaxy. Recently, the Event Horizon Telescope collaboration produced an image of M87* [164], which is the SMBH at the center of Messier 87, a galaxy in the Virgo cluster. Furthermore, gravitational waves from the distant merger of binary black holes have been detected by ground-based interferometers for the first time in 2015 [12]. Stars orbiting around Sgr A* have been observed for more than two decades, and this led to the determination of its mass. In addition, the GRAVITY collaboration was able to measure the gravitational redshift and pericenter precession of the star S2 [165, 166], which agree with the GR predictions. In the future, more precise measurements will be able to determine the spin and quadrupole moment of Sgr A* [167], providing a test of the no-hair theorem in general relativity [168–170] (which states that higher-order multipole moments of the Kerr black hole are determined by its mass and spin only). This could in particular be achieved if a binary pulsar orbiting close enough to the black hole is discovered, by studying the time of arrival of pulses. Hence, Sgr A* provides a promising avenue to test GR in the vicinity of a black hole [171].

In this context of increasing efforts aimed at probing the spacetime around black holes, it is natural to construct alternatives to the Kerr metric. Given the difficulty of finding metrics describing rotating black holes, several numerical solutions have been constructed (see Refs. [172–175] and references therein). However, there have also been

efforts to construct analytical solutions, the usual approach consisting in adopting a theory-agnostic point of view, while focusing on the phenomenological signatures of the spacetime. Even though the underlying theory is unknown in these cases, the Kerr deformations are usually chosen in order to preserve some properties of the GR spacetime [176–178], like the possibility to integrate the geodesic equation for instance [179]. These *ad hoc* deformations were sometimes shown to possess pathologies like closed timelike curves [177]. Another approach is to construct a metric which is a solution to a specific theory of gravity, and we will present such examples in the following chapters: the disformed Kerr metrics. These spacetimes are constructed in the context of degenerate higher-order scalar-tensor (DHOST) theories, by applying a disformal transformation [41] to the Kerr metric using a geodesic scalar field. While the resulting metrics present some similarities to the Kerr spacetime, we will see that they are distinct in many interesting ways.

In Chapter 7, we will review the (uncharged[2]) black hole solutions of general relativity, by presenting the properties of the Schwarzschild and Kerr solutions. In Chapter 8, we will present the construction of the disformed Kerr metrics, and analyze their properties, highlighting the differences with the Kerr spacetime. Finally, in Chapter 9 we will study the orbit of stars around a disformed Kerr black hole, showing that in general the no-hair theorem of GR is violated. Furthermore, we will use the current experimental measurements to put a bound on the parameter arising from the disformal transformation.

[2]There exists a charged version of the Kerr metric, the Kerr-Newman black hole [180]. However, since such an object would rapidly neutralize due to the influence of a surrounding plasma, it is reasonable to assume that astrophysical black holes are uncharged.

Chapter 7

Black holes in general relativity

This chapter is devoted to black holes in general relativity. We start by presenting the static Schwarzschild black hole, and define some important terms that we will use in the following. We then review the main properties of the Kerr spacetime in GR, which will provide a reference point to which we will compare those of the disformed Kerr metric in the following chapter.

7.1 Schwarzschild black hole and definitions

In 1916, Schwarzschild found a metric which satisfies the vacuum Einstein equations

$$R_{\mu\nu} = 0 \, . \tag{7.1}$$

In geometric units, where $G = c = 1$, the line element reads

$$\mathrm{d}s^2 = -\left(1 - \frac{2M}{r}\right)\mathrm{d}t^2 + \left(1 - \frac{2M}{r}\right)^{-1}\mathrm{d}r^2 + r^2\left(\mathrm{d}\theta^2 + r^2\sin^2\theta\mathrm{d}\varphi^2\right) \, , \tag{7.2}$$

where M is a constant parameter. Let us consider a freely-falling particle in this spacetime with a 4-velocity $u^\mu = \mathrm{d}x^\mu/\mathrm{d}\tau$, where the proper time τ is defined as $\mathrm{d}\tau^2 = -\mathrm{d}s^2$. The particle's motion is given by the geodesic equation

$$u^\mu\nabla_\mu u^\nu = \frac{\mathrm{d}^2x^\nu}{\mathrm{d}\tau^2} + \Gamma^\nu_{\mu\alpha}\frac{\mathrm{d}x^\alpha}{\mathrm{d}\tau}\frac{\mathrm{d}x^\mu}{\mathrm{d}\tau} = 0 \, . \tag{7.3}$$

Let us now examine the Newtonian limit of this equation, by assuming that the particle is nonrelativistic, i.e. $\mathrm{d}x^i/\mathrm{d}t \ll 1$. With this approximation, the spatial components of the geodesic equation can be written

$$\frac{\mathrm{d}^2x^i}{\mathrm{d}t^2} = -\frac{Mx^i}{r^3} + \mathcal{O}\left(\frac{M^2}{r^3}\right) \, . \tag{7.4}$$

This is simply the Newtonian force created by an object of mass M located at $r = 0$. The constant M is hence interpreted as the mass of the central object. From the

expression (7.2), the metric seems singular at $r = 2M$. However, an explicit calculation of the Kretschmann scalar for this metric yields

$$R_{\mu\nu\alpha\beta}R^{\mu\nu\alpha\beta} = \frac{48M^2}{r^6} \,, \tag{7.5}$$

which suggests that $r = 2M$ is not a curvature singularity. To see this explicitly, one can introduce the coordinates

$$v = t + r_* \,, \tag{7.6}$$
$$u = t - r_* \,, \tag{7.7}$$

where the tortoise coordinate r_* is given by

$$r_* = r + 2M \ln \left| \frac{r}{2M} - 1 \right| \,. \tag{7.8}$$

In these coordinates, ingoing light rays correspond to $v = \text{const.}$, while outgoing light rays are given by $u = \text{const.}$. In terms of the coordinate v, the Schwarzschild metric reads

$$\mathrm{d}s^2 = -\left(1 - \frac{2M}{r}\right)\mathrm{d}v^2 + 2\mathrm{d}v\mathrm{d}r + r^2\left(\mathrm{d}\theta^2 + \sin^2\theta\mathrm{d}\varphi^2\right) \,. \tag{7.9}$$

These are called ingoing Eddington-Finkelstein (EF) coordinates, and one can obtain an analogous line element for outgoing coordinates u by the substitution $\mathrm{d}v \to -\mathrm{d}u$. It is clear from this expression that the only singularity of the Schwarzschild spacetime lies at $r = 0$. In terms of the coordinates v, outgoing null geodesics verify the equation

$$\frac{\mathrm{d}r}{\mathrm{d}v} = \frac{1}{2}\left(1 - \frac{2M}{r}\right) \,. \tag{7.10}$$

Hence, for $r < 2M$, even future oriented outgoing light rays travel to decreasing r [181]. Because of this peculiar property, the surface $r = 2M$ is called the event horizon of the Schwarzschild spacetime. Once a timelike or null observer has entered the region $r < 2M$, it can no longer escape to infinity, and in order to stay on the surface $r = 2M$, it is necessary to travel at the speed of light. This property has led to this object being called a black hole, since not even light can escape its gravitational pull, and hence it looks black to an observer on the outside. Notice that in terms of the coordinate u, the same reasoning shows that infalling light rays move towards increasing r when $r < 2M$. In this case we obtain a "white hole", since all light rays must escape the interior region and the object looks bright to an observer in the exterior region.

We will now see that the event horizon surface $r = 2M$ is different from the other constant r surfaces in the Schwarzschild spacetime. A hypersurface is a 3-dimensional surface Σ that can be defined by a constraint on the spacetime coordinates

$$\Sigma \quad : \quad F(x^\mu) = 0 \,. \tag{7.11}$$

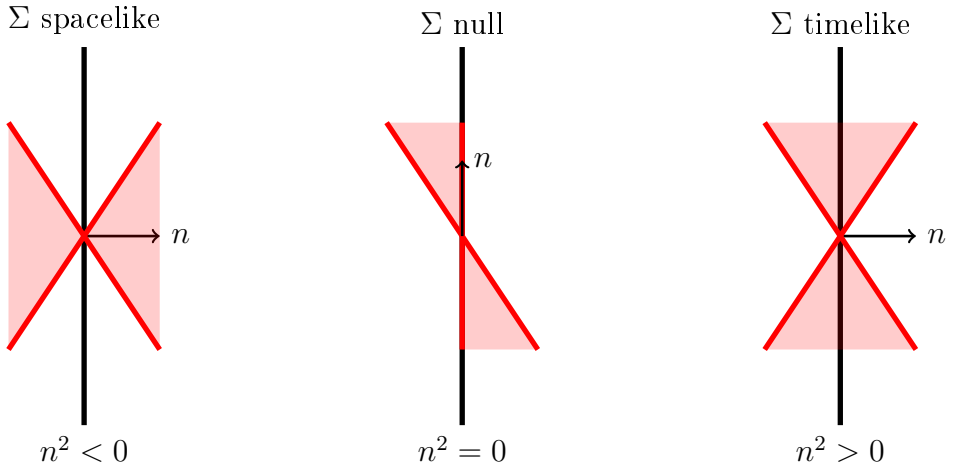

Figure 1: Different types of hypersurfaces, depending on the norm of the normal vector n.

The normal vector n to this surface has covariant components which are given by the gradient of the function F:

$$n_\mu = \partial_\mu F \ . \tag{7.12}$$

We now define the nature of the hypersurface depending on the norm of n:

$$n^2 = g^{\mu\nu}\partial_\mu F \partial_\nu F \ . \tag{7.13}$$

There are 3 different cases, which are represented on Fig. 1:

- if n is spacelike, i.e. $n^2 > 0$: Σ is a timelike hypersurface, and the light cone at a point of Σ overlaps the surface, meaning a timelike observer can cross the surface in both directions.
- if n is null $n^2 = 0$: Σ is null, and a the light cone is tangent to the surface. This means that a light ray can skim the surface, but a future-oriented timelike observer has to cross the surface in a future-pointing direction.
- if n is timelike, i.e. $n^2 < 0$: Σ is a spacelike hypersurface, and the light cone at a given point is oriented in a specific direction which both light and timelike observers must follow.

Let us now determine the nature of the hypersurfaces Σ_0 defined by the equation $r = r_0$, where r_0 is a constant. The normal vector to such a surface is simply $n^\mu = g^{r\mu}$, and its norm is given by

$$n^2 = g^{rr} = 1 - \frac{2M}{r} \ . \tag{7.14}$$

From the definitions that we gave above, we see that there are 3 different cases: Σ_0 is timelike i timelike when $r_0 > 2M$, null for $r_0 = 2M$ and spacelike for $0 < r_0 < 2M$.

Hence if a timelike observer crosses the surface $r = 2M$, they will continue falling inwards until they reach the singularity at $r = 0$. The surface $r = 2M$ is the event horizon of the Schwarzschild spacetime, and it separates the singularity at $r = 0$ from the exterior region $r > 2M$.

We now discuss the symmetries of the Schwarzschild solution. If the metric tensor is invariant under the flow of a vector V, i.e.

$$\mathcal{L}_V\, g = V^\alpha \partial_\alpha g_{\mu\nu} + 2 g_{\alpha(\mu}\partial_{\nu)} V^\alpha = 0 \,, \tag{7.15}$$

where $\mathcal{L}$ is the Lie derivative, then V is called a Killing vector. It generates a continuous isometry of spacetime, and using the previous expression we obtain the Killing equation

$$\nabla_{(\mu} V_{\nu)} = 0 \,, \tag{7.16}$$

where the brackets denote a symmetrization of the indices. Each Killing vector corresponds to a conserved quantity along geodesics. Indeed, for a geodesic vector u^μ, we have

$$u^\alpha \nabla_\alpha \left(u^\mu V_\mu\right) = u^\alpha u^\mu \nabla_\alpha V_\mu + V_\mu u^\alpha \nabla_\alpha u^\mu \,. \tag{7.17}$$

The two terms on the right-hand side both vanish, the first because of the Killing equation, and the second because u is geodesic. This implies that $u^\mu V_\mu$ is a constant of motion.

A spacetime is said to be *stationary* if it possesses an asymptotically timelike Killing vector ξ, i.e. $\xi^2 < 0$ for $r \to \infty$. For the Schwarzschild metric, the vector $\xi = \partial_t$ is timelike in the region $r > 2M$, and hence the spacetime is stationary. A stationary spacetime is *static* if the timelike Killing vector is irrotational, in which case the spacetime can be foliated by spacelike hypersurfaces orthogonal to the Killing field ξ. One can show that the Schwarzschild metric is indeed static. An important theorem by Birkhoff [182][1] states that any spherically symmetric solution to the vacuum Einstein equations must be static and asymptotically flat (in the sense that we recover the Minkowski metric when $r \to \infty$[2]). In other words, the exterior metric of any spherically symmetric star is isomorphic to the Schwarzschild spacetime.

Now that we have defined Killing vectors, we introduce the notion of Killing horizon. A Killing horizon is a null hypersurface which possesses a normal Killing vector. Hence, the Killing vector has a vanishing norm on the surface, and is normal to it. In the Schwarzschild spacetime, the timelike Killing vector becomes null on the surface $r = 2M$, which corresponds to the event horizon. Let us now show that this vector is also normal to the surface. In Eddington-Finkelstein coordinates, one can choose the timelike Killing vector $\xi_{(v)} = \partial_v$, which has contravariant components $\xi^\mu_{(v)} = (1, 0, 0, 0)$. The normal vector to the horizon surface has covariant components $n_\mu = (0, 1, 0, 0)$.

[1] The theorem was in fact formulated two years before Birkhoff, in 1921, by the Norwegian physicist J. Jebsen, see Ref. [183] for an English translation of the paper.

[2] For a more precise definition of asymptotic flatness, see chapter 11 of Wald's book [184].

The covariant components of the Killing vector read

$$g_{\mu\nu}\xi^{\nu}_{(v)} = \left(-1 + \frac{2M}{r}, 1, 0, 0\right) \ , \tag{7.18}$$

and it is clear that this vector is normal to the horizon surface, upon evaluating it at $r = 2M$. Hence the event horizon of the Schwarzschild spacetime is also a Killing horizon. In fact, the rigidity theorem, due to Hawking, states [51]:

Rigidity theorem: *The event horizon of a real analytic, stationary, regular vacuum spacetime is a Killing horizon.*

One can define the notion of surface gravity κ of the Killing horizon, which is given by the inaffinity of the Killing field

$$\xi^{\mu}_{(v)} \nabla_{\mu} \xi^{\nu}_{(v)} = \kappa \xi^{\nu}_{(v)} \ , \tag{7.19}$$

where the equality is evaluated on the horizon surface. The term "inaffinity" is due to the resemblance of the previous equation to the one verified by a non-affine geodesic field. An explicit calculation for the Schwarzschild metric yields

$$\kappa = \frac{1}{4M} \ . \tag{7.20}$$

It can be shown that the surface gravity is constant on a Killing horizon. More details can be found in Wald's book [184], along with other definitions of the surface gravity (which provide the same result in GR). In the context of black hole thermodynamics, the surface gravity is related to the Hawking temperature T_H of the black hole, through the relation $T_H = \kappa/(2\pi)$ [185, 186].

7.2 The Kerr spacetime

7.2.1 Properties and symmetries

The Schwarzschild solution for a static black hole was found within a year of the publication of Einstein's general theory of relativity. In 1918, Lense and Thirring, derived the exterior metric of a rotating body up to first order in the angular momentum, but an exact rotating black hole solution was not found until 1963. The Kerr metric was originally written in the following form [11]:

$$\begin{aligned} \mathrm{d}s^2_{\mathrm{K}} = &- \left(1 - \frac{2Mr}{r^2 + a^2\cos^2\theta}\right) \left(\mathrm{d}v + a\sin^2\theta\,\mathrm{d}\Phi\right)^2 \\ &+ 2\left(\mathrm{d}v + a\sin^2\theta\,\mathrm{d}\Phi\right)\left(\mathrm{d}r + a\sin^2\theta\,\mathrm{d}\Phi\right) \\ &+ \left(r^2 + a^2\cos^2\theta\right)\left(\mathrm{d}\theta^2 + \sin^2\theta\,\mathrm{d}\Phi^2\right) \ , \end{aligned} \tag{7.21}$$

where the parameters M and a represent the black hole's mass and spin (or angular momentum per unit mass), respectively. When $a = 0$, the above line element reduces to the Schwarzschild metric written in ingoing EF coordinates, and for this reason they are sometimes referred to as generalized ingoing EF coordinates. It is clear that they are regular everywhere except when:

$$r = 0 \qquad \text{and} \qquad \theta = \frac{\pi}{2} \,. \tag{7.22}$$

The Kretschmann scalar for the Kerr metric is given by:

$$R_{\mu\nu\alpha\beta}R^{\mu\nu\alpha\beta} = \frac{48M^2(r^2 - a^2\cos\theta)[(r^2 + a^2\cos^2\theta)^2 - 16r^2a^2\cos^2\theta]}{(r^2 + a^2\cos^2\theta)^6} \,, \tag{7.23}$$

which shows that the above relations correspond to a curvature singularity. It is referred to as a ring singularity, which can be understood by performing the following coordinate transformation [11]:

$$\begin{aligned} \tilde{t} &= v - r \,, \\ \tilde{z} &= r\cos\theta \,, \\ \tilde{x} + i\tilde{y} &= (r - ia)\, e^{i\Phi}\sin\theta \,. \end{aligned} \tag{7.24}$$

Indeed, in these coordinates the singularity lies at $\tilde{z} = 0$ and $\tilde{x}^2 + \tilde{y}^2 = a^2$, hence the name *ring* singularity. The Kerr metric was written by Boyer and Lindquist [187] in a form that contains only one off-diagonal term, and hence usually simplifies calculations. The coordinate transformation to Boyer-Lindquist (BL) coordinates starting from the metric (7.21) is given by:

$$\begin{aligned} t &= v - r - \int \frac{2Mr}{r^2 + a^2 - 2Mr}\mathrm{d}r \,, \\ \varphi &= -\Phi - a\int \frac{\mathrm{d}r}{r^2 + a^2 - 2Mr} \,, \end{aligned} \tag{7.25}$$

resulting in the following line element:

$$\begin{aligned} \mathrm{d}s^2_{\mathrm{K}} = &-\left(1 - \frac{2Mr}{\rho^2}\right)\mathrm{d}t^2 - \frac{4Mar\sin^2\theta}{\rho^2}\mathrm{d}t\mathrm{d}\varphi \\ &+ \frac{\rho^2}{\Delta}\mathrm{d}r^2 + \rho^2\mathrm{d}\theta^2 + \frac{\sin^2\theta}{\rho^2}\left[\left(r^2 + a^2\right)^2 - a^2\Delta\sin^2\theta\right]\mathrm{d}\varphi^2 \,. \end{aligned} \tag{7.26}$$

In order to lighten the notation, we have defined the following functions:

$$\begin{aligned} \Delta(r) &= r^2 + a^2 - 2Mr \,, \\ \rho^2(r,\theta) &= r^2 + a^2\cos^2\theta \,. \end{aligned}$$

These coordinates are singular when $\Delta = 0$ or $\rho = 0$. We have seen that $\rho = 0$ corresponds to a curvature singularity, since the Kretschmann scalar diverges. On the other hand, $\Delta = 0$ is a coordinate singularity, and it is clear from the line element written in the original Kerr coordinates that the metric is well defined at these points. When $a = 0$, the metric (7.26) reduces to the Schwarzschild metric in the usual Schwarzschild coordinates.

The Kerr metric is a stationary spacetime, as the vector $\xi = \partial_t$ is an asymptotically timelike Killing vector. Furthermore, the metric is axially symmetric, and the associated Killing field $\eta = \partial_\varphi$ is spacelike (and vanishes on the axis of symmetry $\theta = 0$ [188]). Furthermore, one says that the spacetime is axisymmetric if the action of these fields commutes, i.e.

$$\xi^\mu \nabla_\mu \eta^\nu - \eta^\mu \nabla_\mu \xi^\nu = 0 \,,$$

which can easily be checked for the Kerr metric. In addition to being independent of t and φ, the line element (7.26) also enjoys the reflection symmetry $(t, \varphi) \to (-t, -\varphi)$. In other words, the metric is invariant under the simultaneous reversal of the time and azimuthal angle coordinates. This can be formulated in terms of the Killing fields as follows [189]:

$$\xi_{[\mu}\eta_\nu \nabla_\alpha \xi_{\beta]} = \xi_{[\mu}\eta_\nu \nabla_\alpha \eta_{\beta]} = 0 \,,$$

where the square brackets denote the antisymmetrization of indices. With a slight abuse of notation, we refer to the associated 1-forms to the Killing vectors with the same letter, i.e. $\xi = g_{t\mu}\mathrm{d}x^\mu$ and $\eta = g_{\varphi\mu}\mathrm{d}x^\mu$. The previous conditions can then be rewritten as

$$\xi \wedge \eta \wedge \mathrm{d}\xi = \xi \wedge \eta \wedge \mathrm{d}\eta = 0 \,, \tag{7.27}$$

where the $\wedge$ is the exterior product on the space of forms. A spacetime which verifies the previous conditions is said to be *circular*. This is the case for black hole solutions in GR. Indeed, it can be shown [190] that a Ricci-circular spacetime, i.e. a spacetime verifying:

$$\xi^\mu R_\mu{}^{[\nu}\xi^\alpha \eta^{\beta]} = \eta^\mu R_\mu{}^{[\nu}\xi^\alpha \eta^{\beta]} = 0 \,, \tag{7.28}$$

is circular as long as the conditions (7.27) hold at one point of the spacetime. For axisymmetric spacetimes, the spacelike Killing vector $\eta^\mu = 0$ on the symmetry axis [188], so the relations (7.27) are satisfied there. It follows that vacuum axisymmetric spacetimes in GR are circular, as Ricci-circularity is immediate from $R_{\mu\nu} = 0$.

In addition to the two Killing vectors, the Kerr metric possesses a nontrivial Killing tensor, i.e. a symmetric 2-tensor K verifying the generalized Killing equation:

$$\nabla_{(\alpha} K_{\mu\nu)} = 0 \,. \tag{7.29}$$

We say nontrivial in the sense that K is neither the metric tensor (which trivially verifies this identity if one assumes the Levi-Civita connection, i.e. $\nabla g = 0$), nor any tensor product combination of the Killing vectors ξ and η. The Killing tensor is

associated to a conserved quantity $K_{\mu\nu}u^\mu u^\nu$ along the geodesic u^μ, as can be seen by calculating:

$$u^\alpha \nabla_\alpha \left(K_{\mu\nu}u^\mu u^\nu\right) = u^\alpha u^\mu u^\nu \nabla_\alpha K_{\mu\nu} + 2K_{\mu\nu}u^\mu u^\alpha \nabla_\alpha u^\nu = 0 \,. \tag{7.30}$$

The two terms on the right-hand-side of the previous expression vanish separately. The first term is zero because of the relation (7.29), while the second vanishes because u is a geodesic vector. The same argument can be used to show that the quantities

$$E = -\xi^\mu u_\mu \qquad \text{and} \qquad L = \eta^\mu u_\mu \tag{7.31}$$

are also conserved along the geodesic defined by the vector u, as we saw in the previous section. These correspond to the energy and angular momentum of the particle, respectively. The meaning of the conserved quantity associated to the Killing tensor is not very clear, in the sense that it is not immediately associated to spacetime symmetries as in the case of the Killing vectors. It is said to correspond to a "hidden symmetry" of the Kerr spacetime.

It should be noted that the existence of a nontrivial Killing tensor for vacuum spacetimes in GR is a generic feature of type D metrics [191], according to the Petrov classification [192–194]. In this case the Killing tensor can be expressed in terms of the metric and the two repeated principal null directions of the spacetime (see Theorem 35.3 in Ref. [195] for an exception). For the Kerr spacetime, the Killing tensor can be written [191]

$$K^{\mu\nu} = 2\rho^2(r,\theta)k_0^{(\mu}l_0^{\nu)} + r^2 g^{\mu\nu} \,, \tag{7.32}$$

where the repeated principal null directions in Boyer-Lindquist coordinates read

$$\begin{aligned} k_0 &= \frac{r^2+a^2}{\Delta}\partial_t + \partial_r + \frac{a}{\Delta}\partial_\varphi \,, \\ l_0 &= \frac{\Delta}{2\rho^2}\left(\frac{r^2+a^2}{\Delta}\partial_t - \partial_r + \frac{a}{\Delta}\partial_\varphi\right) \,. \end{aligned} \tag{7.33}$$

This extra conserved quantity makes it possible to integrate the geodesic equations and write them as a first-order system. This was first discovered by Carter when he realized that the Hamilton-Jacobi equation for geodesics was separable [179], and was later related to the existence of a nontrivial Killing tensor [191]. To see this explicitly, let us write the Hamilton-Jacobi equation for geodesics in the Kerr spacetime:

$$\frac{\partial S}{\partial \tau} + \frac{1}{2}g^{\mu\nu}\partial_\mu S \partial_\nu S = 0 \,, \tag{7.34}$$

where S is the Hamilton-Jacobi potential. We now search for separable solutions of the form

$$S = \frac{1}{2}m^2\tau - Et + L\varphi + S_r(r) + S_\theta(\theta) \,, \tag{7.35}$$

where m, E, and L are respectively the mass, energy and angular momentum of a geodesic particle. For the Kerr spacetime, the equation does separate, and we obtain the relation

$$\begin{aligned} &- \left[m^2 r^2 - \frac{\left[aL - E\left(r^2+a^2\right)\right]^2}{\Delta} + \Delta \left(\frac{\partial S_r}{\partial r}\right)^2 \right] \\ &= a^2 m^2 \cos^2\theta + \sin^2\theta \left(aE - \frac{L}{\sin^2\theta} \right)^2 + \left(\frac{\partial S_\theta}{\partial \theta}\right)^2 \\ &= \mathcal{K} \,, \end{aligned} \tag{7.36}$$

where $\mathcal{K}$ is a separation constant which must be positive for timelike and null geodesics, as can be seen from the second line in the previous expression. This constant is in fact the conserved quantity associated to the Killing tensor $K_{\mu\nu}$ defined above. After integrating the previous relations, we obtain the final expression for the Hamilton-Jacobi potential

$$S = \frac{1}{2} m^2 \tau - Et + L\varphi \pm \int \frac{\sqrt{\mathcal{R}(r)}}{\Delta} \mathrm{d}r \pm \int \sqrt{\Theta(\theta)} \mathrm{d}\theta \,, \tag{7.37}$$

where the functions $\mathcal{R}$ and Θ are given by:

$$\begin{aligned} \mathcal{R} &= \left[aL - E\left(r^2+a^2\right)\right]^2 - \Delta\left(\mathcal{K} + m^2 r^2\right) \,, \\ \Theta &= \mathcal{K} - a^2 m^2 \cos^2\theta - \sin^2\theta \left(aE - \frac{L}{\sin^2\theta} \right)^2 \,. \end{aligned} \tag{7.38}$$

The following combination of conserved quantities is often used:

$$\mathcal{Q} = \mathcal{K} - (aE - L)^2 \,, \tag{7.39}$$

and either $\mathcal{K}$ or $\mathcal{Q}$ are called Carter's constant, depending on the reference. Each has its own advantage. As we discussed, $\mathcal{K} \geq 0$ for timelike and null geodesics, and it can be shown that $\mathcal{K} = 0$ only for principal null geodesics. On the other hand, the constant $\mathcal{Q}$ has a clearer geometrical interpretation. For instance, any geodesic which approaches the ring singularity must have $\mathcal{Q} = 0$. For a detailed study of Kerr geodesics, see for example Refs. [181, 196].

7.2.2 Timelike observers in the Kerr spacetime

In this section, we will discuss the important hypersurfaces and regions of the Kerr spacetime. We will start in the region $r \gg M$, and describe what happens as r decreases progressively. In the asymptotic region, the metric (7.26) reads

$$\begin{aligned} \mathrm{d}s^2_{\mathrm{K}} = &- \left[1 - \frac{2M}{r} + \mathcal{O}\left(\frac{Ma^2}{r^3}\right) \right] \mathrm{d}t^2 - \left[\frac{4aM}{r^3} + \mathcal{O}\left(\frac{Ma^3}{r^5}\right) \right] \left[x\mathrm{d}y - y\mathrm{d}x \right] \mathrm{d}t \\ &+ \left[\delta_{ij} + \mathcal{O}\left(\frac{M}{r}\right) \right] \mathrm{d}x^i \mathrm{d}x^j \,, \end{aligned} \tag{7.40}$$

where we have introduced the Cartesian coordinates

$$\begin{aligned} x &= r\cos\varphi\sin\theta\ , \\ y &= r\sin\varphi\sin\theta\ , \\ z &= r\cos\theta\ . \end{aligned}$$

The mass and spin of the black hole are obtained from the leading corrections to flat space: the mass is given by the g_{tt} term, while we obtain the spin from the g_{ti} terms [48].

We now decrease the radial coordinate, starting from infinity. To understand the structure of the spacetime, it is instructive to study the trajectories of timelike observers. We assume $a \leq M$ and focus on stationary observers, meaning that the coordinates r and θ are constant. The 4-velocity $l_{\rm S}$ of such observers is hence given by:

$$l_{\rm S} = \partial_t + \omega\partial_\varphi\ , \tag{7.41}$$

where ω corresponds to the angular velocity in the φ direction. The vector $l_{\rm S}$ is timelike, $l_{\rm S}^2 \leq 0$, which implies the following condition for the function ω:

$$g_{tt} + 2\omega g_{t\varphi} + \omega^2 g_{\varphi\varphi} \leq 0\ . \tag{7.42}$$

The metric component $g_{\varphi\varphi} > 0$ for large enough r, in which case the condition above is satisfied for $\omega \in [\omega_-, \omega_+]$, where the $\omega_\pm$ are given by:

$$\omega_\pm = -\frac{g_{t\varphi}}{g_{\varphi\varphi}}\left(1 \pm \sqrt{1 - \frac{g_{tt}g_{\varphi\varphi}}{g_{t\varphi}^2}}\right)\ . \tag{7.43}$$

While $g_{tt} < 0$, which is true asymptotically, it is possible to have $\omega < 0$. However, there exists a hypersurface $r = r_E(\theta)$ inside which $g_{tt} > 0$. Solving the equation $\rho^2 = 2Mr$, we obtain:

$$r_E(\theta) = M + \sqrt{M^2 - a^2\cos^2\theta}\ . \tag{7.44}$$

This surface is called the ergosurface, or *static limit*. The latter name stems from the fact that when $g_{tt} > 0$, a timelike or null vector must have $\omega > 0$, since $\omega_- > 0$. Hence, such observers necessarily co-rotate with the black hole, or in other words the frame-dragging effect from the rotating source can no longer be countered, even with a powerful engine. Hence this surface is the endpoint of static observers located at constant $\{r, \theta, \varphi\}$. It can be shown that the ergosurface is a timelike hypersurface, meaning that it is possible to cross it in both directions (increasing or decreasing r). Although the Killing vector ξ is null on this surface, we do not have a Killing horizon since ξ is not normal to the ergosurface. The Killing vector ξ becomes spacelike when $g_{tt} > 0$, but it is still possible to construct a timelike Killing vector of the form (7.41) with a constant angular velocity.

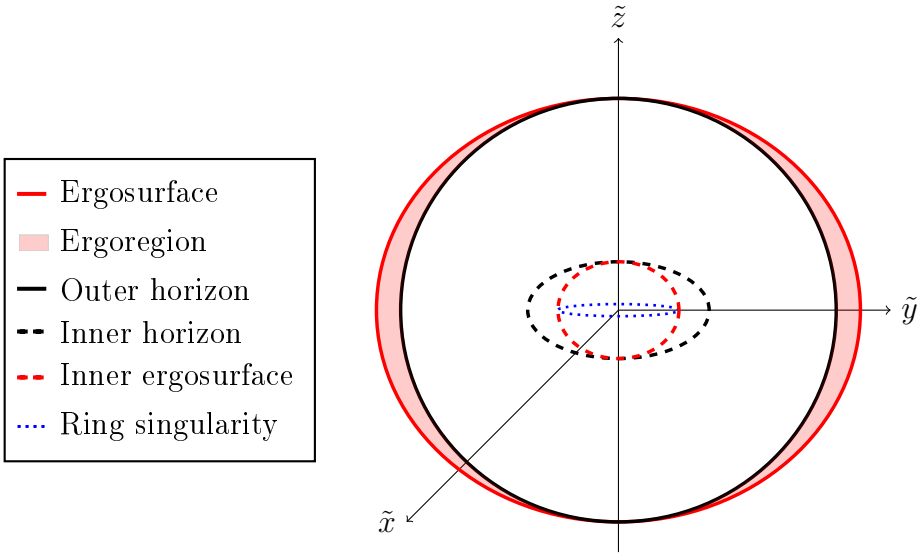

Figure 2: Schematic structure of the Kerr spacetime in the Cartesian coordinates (7.24). The ergoregion (in red), lies between the ergosurface (red) and the outer event horizon (black). Inside the outer horizon lies the inner horizon (dashed black), the inner ergosurface (dashed red) and the ring singularity (dotted blue).

By going deeper towards the interior of the ergosurface, one reaches a point where the condition (7.42) can no longer be satisfied. The limiting surface, which we call the *stationary limit*,[3] verifies

$$g_{tt}g_{\varphi\varphi} - g_{t\varphi}^2 = 0 \, . \tag{7.45}$$

For the Kerr metric, this is equivalent to solving the equation $\Delta = 0$, which admits the roots

$$r_\pm = M \pm \sqrt{M^2 - a^2} \, . \tag{7.46}$$

In between these two constant r surfaces, timelike stationary observers of the form (7.41) cannot exist, as this would correspond to an imaginary angular velocity ω. The stationary limit is the surface corresponding to the outer root $r = r_+$. These two surfaces are in fact null hypersurfaces, and correspond to the outer and inner event horizon of the Kerr spacetime, respectively. When $a = 0$, we obtain the Schwarzschild horizon located at $r = 2M$, as we discussed in the previous section. When $a > M$, the equation $\Delta = 0$ has no real solutions, and hence the ring singularity is not shielded by an event horizon [197]. However, the cosmic censorship hypothesis states that no such naked singularity can exist in Nature [198]. In the special case $a = M$, the equation $\Delta = 0$ has a double root and we obtain the extremal Kerr metric, with an event horizon at $r = M$. Let us discuss the nature of the surfaces Σ_0 defined by $r = r_0$ in the Kerr spacetime. It is easy to show that such surfaces are timelike

[3] Note that some authors use this term to refer to the ergosurface.

for $r_0 > r_+$ and $0 < r_0 < r_-$, spacelike for $r_- < r_0 < r_+$ and null for $r_0 = r_\pm$. When $a = M$, in the case of the extremal Kerr metric, we have $r_+ = r_-$ and the surfaces Σ_0 are timelike both in the interior and the exterior of the horizon. Hence, unlike for the Schwarzschild spacetime, a timelike observer can avoid the ring singularity, as the motion towards increasing r is permitted in the region $r < r_-$. For details about the global structure of the Kerr spacetime, see for instance Ref. [196].

According to Hawking's rigidity theorem [51], which we wrote in the previous section, the event horizons are also Killing horizons. Their Killing generators $k_\pm$ are co-linear to the principal null directions (7.33) of the Kerr spacetime on the Killing horizon, and read

$$k_\pm = \partial_t + \frac{a}{a^2 + r_\pm^2}\partial_\varphi \,. \tag{7.47}$$

When $a = 0$ we recover the Killing generator of the Schwarzschild horizon, and in the general case this can be interpreted as a rotation of the event horizons with constant angular velocities

$$\Omega_\pm = \frac{a}{a^2 + r_\pm^2} = \frac{a}{2Mr_\pm} \,. \tag{7.48}$$

The inaffinity of the Killing generators $k_\pm$ leads to the expression of the surface gravities $\kappa_\pm$ of the Killing horizons

$$\kappa_\pm = \frac{r_\pm - r_\mp}{2Mr_\pm} \,. \tag{7.49}$$

For a review of black hole thermodynamics, see for instance Ref. [199].

We end this section by discussing an interesting property of the ergoregion in the Kerr spacetime, i.e. the region between the ergosurface and the outer event horizon. Remarkably, it is possible to extract rotational energy from the black hole in this region by the Penrose process [198, 200]. The mechanism can be understood by considering a particle with 4-momentum p^μ coming from infinity with an energy $E_0 = -p \cdot \xi$. We assume that in the ergoregion, this particle decays into 2 other particles having momenta p_1^μ and p_2^μ. Since the Killing vector ξ is spacelike in this region, it is possible to choose $E_1 < 0$ for instance. The particle (1) has a negative energy as seen from an observer at infinity, and will fall inside the black hole. On the other hand, the particle (2) can escape to infinity, and the conservation of energy gives $E_2 > E_0$. In this way, rotational energy has been extracted from the black hole. Though this is an interesting theoretical property, it has been shown that the efficiency of this process for realistic astrophysical scenarios is rather low [201]. A similar process exists for the amplification of waves in the ergoregion [202–207], which is called superradiance (see Ref. [208] for a review). These effects are part of a wide class of physical phenomena, which also include the quantum laser effects of black holes [209–211] (and their acoustic counterparts [212]).

Chapter 8

The disformed Kerr metrics

In this chapter, which is based on Ref. [213], we present the construction of the disformed Kerr metrics and compare their properties to those of the GR spacetime. We will see that they constitute interesting counterexamples to many of the properties exhibited by the Kerr black hole. Some important features are the following: the disformed metrics are noncircular and not Ricci-flat; their event horizon does not lie at constant r; the event horizon is not a Killing horizon; there is no nontrivial Killing tensor. On the other hand, we will see that the asymptotic form of the disformed metrics is very similar to Kerr, and that they are regular everywhere except on the ring singularity.

8.1 Construction of the disformed Kerr metrics

The starting point of our construction is the stealth-Kerr black hole solution of Ref. [214]. In a particular class of DHOST theories, the authors showed that there exist solutions of the form:

$$g_{\mu\nu} = g^K_{\mu\nu} \,,$$
$$\phi = -Et + L\varphi \pm \int \frac{\sqrt{\mathcal{R}(r)}}{\Delta}\mathrm{d}r \pm \int \sqrt{\Theta(\theta)}\mathrm{d}\theta \,,$$

where the expressions for $\mathcal{R}$ and Θ are given by Eq. (7.38). This type of solution, where a nontrivial scalar field has no backreaction on the GR metric, is called a *stealth* solution. There are examples of static stealth solutions, like for instance that of Ref. [131], but the stealth-Kerr solution of [214] is the first to describe a rotating black hole. The scalar field is assumed to posses a constant kinetic term X, which implies that it defines a geodesic direction ϕ^μ, since we have

$$\phi^\mu \phi_{\nu\mu} = \phi^\mu \phi_{\mu\nu} = 0 \,. \tag{8.1}$$

This justifies the previous ansatz for the scalar field, in which it is identified with the Hamilton-Jacobi potential S. The constants E and L represent the two conserved

quantities along the geodesic, the energy and angular momentum. They are associated to the Killing vectors ξ^μ and η^μ respectively. It was shown in Ref. [214] that in order for the solution to be regular at the poles, i.e. $\partial\phi/\partial\theta \to 0$ when $\theta \to 0$, one must set $L = 0$ and $\mathcal{K} = m^2a^2$. In this case the expressions for $\mathcal{R}$ and Θ become

$$\begin{aligned} \mathcal{R} &= m^2\left(a^2+r^2\right)\left[\sigma^2\left(r^2+a^2\right)-\Delta\right] \ , \\ \Theta &= m^2a^2\sin^2\theta\left(1-\sigma^2\right) \ , \end{aligned} \tag{8.2}$$

where $\sigma = E/m$. Furthermore, in order for both $\mathcal{R}$ and Θ to be positive from the outer Kerr horizon to spatial infinity, one must set $\sigma = 1$.[1] In this case, our starting solution reads

$$g_{\mu\nu} = g^K_{\mu\nu} \ , \tag{8.3}$$

$$\phi = q_0\left(t + \int \frac{\sqrt{2Mr(a^2+r^2)}}{\Delta}\mathrm{d}r\right) \ , \tag{8.4}$$

where we have defined $q_0 = -m$ and g^K is the Kerr metric. The scalar kinetic term is constant and reads

$$X_0 = -q_0^2 \ ,$$

which shows that the vector ϕ^μ is timelike. The relative sign in the expression for the scalar field was chosen so that it is regular from the outer horizon of the Kerr metric to spatial infinity. This becomes clear when writing the scalar field in the generalized ingoing EF coordinates, as we will do in the following.

The theory which contains this solution belongs to the shift-symmetric DHOST Ia class [45, 46], i.e. those described by Eq. (31) with functions that depend on X only. The authors of Ref. [214] chose to consider theories in which the graviton propagates at the speed $c_T = 1$, as in GR. This is motivated by the measurement of gravitational waves along with the electromagnetic counterpart coming from the merger of two neutron stars [56]. Assuming that the scalar field is cosmologically dominant, one must set $A_1 = A_2 = 0$ in the action (31) in order to satisfy this constraint. In the absence of a cosmological constant, one must set $K(X_0) = K'(X_0) = 0$, so we choose $K = 0$ for simplicity. We also set $G_3 = 0$ as in Ref. [214]. Since the scalar field has a constant kinetic term, the terms proportional to A_4 and A_5 in the Lagrangian do not enter the equations of motion. This is easily understood by writing

$$\mathcal{L}_4 = \frac{A_4}{4}X_\mu X^\mu \ , \quad \mathcal{L}_5 = \frac{A_5}{4}\left(X_\mu\phi^\mu\right)^2 \ .$$

Since these terms are quadratic in X^μ, any contribution to the field equations will contain at least one derivative of X, which vanishes on-shell. Hence these terms are

[1] Note that in Ref. [215], the authors considered Kerr-de Sitter solutions with a nonzero cosmological constant, and in these cases the condition $\sigma = 1$ is not necessary.

irrelevant in the present case, and one can omit them from the discussion. Another condition that we must enforce for the equations of motion to be verified is

$$A_3(X_0) = 0 \ . \tag{8.5}$$

The disformed Kerr metrics $\tilde{g}$ are constructed by performing a disformal transformation [41] of the Kerr metric using the geodesic scalar of Eq. (8.3), namely:

$$\tilde{g}_{\mu\nu} = g^K_{\mu\nu} + B(X)\partial_\mu\phi\partial_\nu\phi \ , \tag{8.6}$$

where the function B is chosen to be a function of X only in the context of shift-symmetric theories. Since the kinetic term is constant on-shell, $X = X_0$, we take the function B to be a constant, and set:

$$B(X) = -\frac{D}{q_0^2} \ . \tag{8.7}$$

The parameter D is the disformal parameter, and the rescaling by q_0^2 is simply done to lighten the expressions in the following. The scalar kinetic term transforms as $\tilde{X} = -q_0^2/(1+D)$, which shows that ϕ^μ is again a (timelike) geodesic vector for the disformed metrics.

The DHOST Ia class, given by Eq. (33), is stable under the disformal map [42, 43, 47], which means that the metrics (8.6) are solutions to specific DHOST theories labeled by the constant B. The transformation (8.6) modifies the functions in the Lagrangian such that we have $\tilde{S}[\tilde{g}] = S[g]$, where S represents the DHOST action (31). However, we couple the matter fields to the metric minimally in each case (either to $\tilde{g}_{\mu\nu}$ or $g_{\mu\nu}$), which ensures that we indeed have different theories. For a constant disformal parameter, the transformation rule for the Lagrangian functions [47] is simplified, and we obtain:

$$\begin{aligned}
f &= \tilde{f}\sqrt{1+BX} \ , \\
A_1 &= \frac{\tilde{A}_1 + B(1+BX)\tilde{f}}{(1+BX)^{3/2}} \ , \\
A_2 &= \frac{\tilde{A}_2 - B(1+BX)\tilde{f}}{(1+BX)^{3/2}} \ , \\
A_3 &= \frac{\tilde{A}_3 - 2B(1+BX)\tilde{A}_2 - 4B(1+BX)^3\tilde{f}_X}{(1+BX)^{7/2}} \ , \\
A_4 &= \frac{\tilde{A}_4 - 2B(1+BX)\tilde{A}_1 + 4B(1+BX)^3\tilde{f}_X}{(1+BX)^{7/2}} \ , \\
A_5 &= \frac{\tilde{A}_5 + B(1+BX)\left[B(1+BX)(\tilde{A}_1+\tilde{A}_2) - (\tilde{A}_3+\tilde{A}_4)\right]}{(1+BX)^{11/2}} \ ,
\end{aligned} \tag{8.8}$$

where $\tilde{f}_X = \partial\tilde{f}/\partial X$. The functions of $\tilde{X}$ can be seen as functions of X through the transformation

$$\tilde{X} = \frac{X}{1+BX} \,. \tag{8.9}$$

As we argued above, we will only be interested in the functions $\{\tilde{f}, \tilde{A}_1, \tilde{A}_3\}$ in the following. Indeed, $\{A_4, A_5\}$ are irrelevant for a constant scalar kinetic density, and we impose $\tilde{A}_2 = -\tilde{A}_1$, which is one of the conditions to avoid the Ostrogradsky ghost in DHOST Ia theories. Assuming $A_1 = A_2 = G_3 = K = 0$ [214], we invert the relations (8.8) and obtain:

$$\begin{aligned}
\tilde{f} &= f\sqrt{1-B\tilde{X}}, \\
\tilde{A}_1 &= -\frac{B}{\sqrt{1-B\tilde{X}}} f \,, \\
\tilde{A}_3 &= \frac{A_3}{(1-B\tilde{X})^{7/2}} + \frac{4Bf_{\tilde{X}}}{\sqrt{1-B\tilde{X}}} \,.
\end{aligned} \tag{8.10}$$

It should be noted that $\tilde{A}_1 \neq 0$ in this case, which means that the constraint $c_T = 1$ is not satisfied in these theories. However, we will see that these disformed solutions present some interesting properties which are worth studying in their own right.

Starting from the Kerr metric (7.26) in BL coordinates, the explicit expression for the disformed metric (8.6) is

$$\begin{aligned}
\mathrm{d}\tilde{s}^2 = &-\left(1-\frac{2\tilde{M}r}{\rho^2}\right)\mathrm{d}t^2 - \frac{4\sqrt{1+D}\tilde{M}ar\sin^2\theta}{\rho^2}\mathrm{d}t\mathrm{d}\varphi - 2D\frac{\sqrt{2\tilde{M}r(a^2+r^2)}}{\Delta}\mathrm{d}t\mathrm{d}r \\
&+ \frac{\rho^2\Delta - 2\tilde{M}(1+D)rD(a^2+r^2)}{\Delta^2}\mathrm{d}r^2 + \rho^2\mathrm{d}\theta^2 + \frac{\sin^2\theta}{\rho^2}\left[\left(r^2+a^2\right)^2 - a^2\Delta\sin^2\theta\right]\mathrm{d}\varphi^2 \,,
\end{aligned} \tag{8.11}$$

where we have rescaled the time coordinate as $t \to t/\sqrt{1+D}$ and defined a new mass $\tilde{M} = M/(1+D)$. As we discussed above, the choice of $B = -D/q_0^2$ parametrizes a class of DHOST theories of which this metric, along with the scalar field (8.3), are solutions. Hence this does not correspond to an extra parameter of the metric, since changing D modifies the theory, unless q_0 is chosen so that B remains the same. However, from a phenomenological point of view, one may consider D as an extra parameter, and study the disformed metric for different values of D, which is an approach that we will adopt in the following.

Before discussing the properties of the disformed Kerr metric in the general case, let us briefly consider the case $a = 0$, for which the off-diagonal term $\tilde{g}_{tr}$ in Eq. (8.11) can be removed by the following coordinate transformation:

$$\mathrm{d}t = \mathrm{d}T - \frac{D\sqrt{2\tilde{M}r^3}}{\Delta\left(1-\frac{2\tilde{M}}{r}\right)}\mathrm{d}r \,. \tag{8.12}$$

The resulting metric is nothing but the Schwarzschild spacetime with a rescaled mass:

$$\mathrm{d}\tilde{s}^2 = -\left(1-\frac{2\tilde{M}}{r}\right)\mathrm{d}T^2 + \left(1-\frac{2\tilde{M}}{r}\right)^{-1}\mathrm{d}r^2 + r^2\mathrm{d}\Omega^2 \,. \tag{8.13}$$

Hence, in the static case, the net effect of the disformal transformation is only to rescale the mass parameter. Note that a similar observation has been noted in the case of the Schwarzschild-de Sitter metric in Ref. [216–218]. In Ref. [219], the authors claim that the disformation of Schwarzschild leads to a different metric, i.e. not Schwarzschild with mass $\tilde{M}$, but the previous coordinate redefinition shows that it is the case.

8.2 Properties of the disformed Kerr metrics

In this section, we analyze the properties of the disformed Kerr metric (8.11), and treat D as a parameter, keeping in mind that it does not actually correspond to extra hair, as discussed above.

8.2.1 Symmetries of the disformed Kerr metric

We start by discussing the singularities of the disformed metric. One can start by calculating some scalar quantities, which include

$$\begin{aligned}
\tilde{R} &= -\frac{Da^2Mr[1+3\cos(2\theta)]}{(1+D)\rho^6}\,, \\
\tilde{R}_{\mu\nu}\tilde{R}^{\mu\nu} &= \frac{D^2a^4M^2Q_1(r,\theta)}{4\rho^{12}(r^2+a^2)(1+D)^2}\,, \\
\tilde{R}_{\mu\nu\alpha\beta}\tilde{R}^{\mu\nu\alpha\beta} &= \frac{M^2Q_2(r,\theta)}{\rho^{12}(r^2+a^2)(1+D)^2}\,,
\end{aligned} \tag{8.14}$$

where the functions Q_1 and Q_2 can be found in Appendix III.A. These expressions show that the disformed metric is not Ricci-flat, i.e. $\tilde{R}_{\mu\nu} \neq 0$, which is an important property. Furthermore, the expressions suggest that the disformed metric does not present new singularities compared to the Kerr metric, meaning that the only singularity lies at $\rho = 0$. To check this explicitly, it is enough to find a coordinate system in which $\rho = 0$ is the only apparent singular point. We apply the coordinate transformation (7.25), and rescale the coordinate $v \to v/\sqrt{1+D}$, as we did for the coordinate t in order to obtain the line element (8.11). This leads to the following expressions for the metric and scalar in the generalized ingoing Eddington-Finkelstein coordinates:

$$\mathrm{d}\tilde{s}^2 = -\left(1-\frac{2\tilde{M}r}{\rho^2}\right)\mathrm{d}v^2 + 2\sqrt{1+D}\left(1-\frac{D}{(1+D)(1+\sqrt{\frac{r^2+a^2}{2Mr}})}\right)\mathrm{d}v\mathrm{d}r \tag{8.15}$$

$$- D\left(1-\frac{1}{1+\sqrt{\frac{a^2+r^2}{2Mr}}}\right)^2 \mathrm{d}r^2 \tag{8.16}$$

$$+\frac{4a\tilde{M}r\sin^2\theta\sqrt{1+D}}{\rho^2}\mathrm{d}v\mathrm{d}\varphi + 2a\sin^2\theta\mathrm{d}r\mathrm{d}\varphi + \rho^2\mathrm{d}\theta^2 \tag{8.17}$$

$$+\frac{\sin^2\theta\left(2a^4\cos^2\theta + 4a^2Mr\sin^2\theta + a^2r^2\left[3+2\cos(2\theta)\right] + 2r^4\right)}{2\rho^2}\mathrm{d}\varphi^2\,, \tag{8.18}$$

$$\phi = -m\left(\frac{v}{\sqrt{1+D}} - r + \int\frac{\mathrm{d}r}{1+\sqrt{\frac{r^2+a^2}{2Mr}}}\right)\,. \tag{8.19}$$

These expressions show that the disformed metric does not contain any singularity other than the ring singularity of the Kerr spacetime. In particular, the metric and scalar are regular at the Kerr horizon given by $\Delta = 0$. In Ref. [219], the authors chose the other relative sign for the scalar field in Eq. (8.3). This means that their scalar field is not regular in the ingoing coordinates, but rather in outgoing ones, which represent a white hole instead of a black hole.

Let us now discuss the symmetries of the disformed Kerr metrics. It is clear from the line element (8.11) that the vectors $\xi = \partial_t$ and $\eta = \partial_\varphi$ are still Killing vectors of these spacetimes. One can check that their action commutes, so that the disformed Kerr metrics are stationary and axisymmetric spacetimes. However, the circularity conditions are no longer verified in the generic case, and we have:

$$\begin{aligned}
\xi\wedge\eta\wedge\mathrm{d}\xi &= -\frac{4Da^2\tilde{M}r\sqrt{2\tilde{M}r(a^2+r^2)}\cos\theta\sin^3\theta}{\rho^4}\mathrm{d}t\wedge\mathrm{d}r\wedge\mathrm{d}\theta\wedge\mathrm{d}\varphi\,,\\
\xi\wedge\eta\wedge\mathrm{d}\eta &= \frac{4Da^3\tilde{M}r\sqrt{2\tilde{M}r(1+D)(a^2+r^2)}\cos\theta\sin^5\theta}{\rho^4}\mathrm{d}t\wedge\mathrm{d}r\wedge\mathrm{d}\theta\wedge\mathrm{d}\varphi\,.
\end{aligned} \tag{8.20}$$

This means that it is not possible in the generic case to write the disformed metric in a way that exhibits the reflection symmetry $(t,\varphi)\to(-t,-\varphi)$. In particular, the $\tilde{g}_{tr}$ term in Eq. (8.11) cannot be eliminated without introducing other off-diagonal components that break circularity. When $D = 0$, we recover the Kerr metric and the circularity conditions are verified. Similarly, when $a = 0$, the disformal metric is simply Schwarzschild with a rescaled mass, as we discussed already, and the conditions are satisfied in this case also.

This is an interesting property, as circularity is usually assumed as a starting point when discussing stationary solutions in the literature. Indeed, as we discussed above this is a feature of black hole solutions in GR. However, noncircular spacetimes may arise in physical situations, and hence it is important to understand their properties. This choice of ansatz can prove to be too restrictive in some situations, as was shown for example in for the numerical simulation of black holes in the cubic Galileon

theory [175]. There have been efforts to develop numerical schemes to study such spacetimes [220], but there is nonetheless very little work on this subject in the literature. Such conditions can arise in the presence of toroidal magnetic fields, or with a convective fluid having a meridional flow [221, 222]. Noncircularity has an impact on the symmetries of the disformed Kerr metrics. In a spacetime with a separability structure, and hence with a nontrivial Killing tensor, it was shown that circularity could be made manifest with a particular choice of coordinates [223–225]. Since circularity is a coordinate independent property (as long as the coordinates are adapted to the Killing vectors), one concludes that noncircular spacetimes in 4 dimensions do not possess a nontrivial Killing tensor, and hence the integrability of the geodesic equation is lost in this case. In fact, the most general Kerr deformation which is compatible with the separability condition was given in [176].

This kind of approach is usually followed in the literature when constructing deformations of the Kerr metric. One retains a certain amount of properties of the Kerr metric, while performing the deformations which are compatible with the hypotheses. This point of view has been used to propose alternatives to the Kerr metric [176–178]. Even though this method provides testable deviations from the GR spacetime, the underlying theory is unknown, and deformations often possess pathologies like closed timelike curves [177]. Such pathologies also exist in GR, for instance in the Kerr spacetime with $a > M$ [197], which describes a naked singularity.

One can show that the disformed Kerr metric is stably causal, meaning that it remains causal under a small perturbation of the light cone. It is argued in Wald's book, Ref. [184], that stable causality is sufficient to avoid pathologies such as closed timelike curves. We will use the following theorem from this reference:

Theorem [184]: *A spacetime is stably causal if and only if there exists a differentiable function f such that $\nabla^\mu f$ is a past directed timelike vector field.*

This function can be thought of as a global time, and in our case there exists such a function by construction, the scalar field $\phi(t, r)$ itself. We have already seen that the vector ϕ^μ is timelike[2] According to Eq. (8.15), the scalar is regular for $r > 0$. Therefore our spacetime is globally causal, provided that the region of the spacetime for some positive r (in particular outside the event horizon) is causally disconnected from the region $r < 0$ (where closed timelike curves are present, similarly to the Kerr case).

8.2.2 Spacetime structure and analytical constraints

We will now follow a similar approach to that of Section 7.2.2, namely we will start at spatial infinity and slowly uncover important hypersurfaces as as the radial coordinate

[2]The same argument was used in Ref. [226] to show that a black hole with an accreting k-essence field [227] has no closed timelike curves. Similarly to our case, the k-essence field was identified as a global time function in Ref. [226].

decreases. As we saw in the case $a = 0$, a coordinate change was necessary in order to put the metric in the Schwarzschild form. Similarly, we perform the following coordinate transformation in the general case:

$$\mathrm{d}t = \mathrm{d}T - D\frac{\sqrt{2\tilde{M}r(a^2+r^2)}}{\Delta(1-\frac{2\tilde{M}}{r})}\mathrm{d}r\ . \tag{8.21}$$

Though this redefinition does not eliminate the $\tilde{g}_{tr}$ in the metric, it makes it smaller asymptotically. In fact, in these coordinates the Schwarzschild solution (8.13) is recovered for large r, contrary to what is claimed in Ref. [219]. We thus obtain a coordinate system which is closer to the BL coordinates for the Kerr metric, which we will call Boyer-Lindquist-like coordinates. In these coordinates the disformal Kerr metric for large r reads

$$\begin{aligned}\mathrm{d}\tilde{s}^2 = &-\left[1-\frac{2\tilde{M}}{r}+\mathcal{O}\left(\frac{\tilde{a}^2\tilde{M}}{r^3}\right)\right]\mathrm{d}T^2-\left[\frac{4\tilde{a}\tilde{M}}{r^3}+\mathcal{O}\left(\frac{\tilde{a}^3\tilde{M}}{r^5}\right)\right][x\mathrm{d}y-y\mathrm{d}x]\,\mathrm{d}T\\ &+\left[\delta_{ij}+\mathcal{O}\left(\frac{\tilde{M}}{r}\right)c_{ij}\right]\mathrm{d}x^i\mathrm{d}x^j\\ &+\frac{D}{1+D}\left[\mathcal{O}\left(\frac{\tilde{a}^2\tilde{M}}{r^3}\right)\mathrm{d}t^2+\mathcal{O}\left(\frac{\tilde{a}^2\tilde{M}^{3/2}}{r^{7/2}}\right)b_i\mathrm{d}t\mathrm{d}x^i+\mathcal{O}\left(\frac{\tilde{a}^2}{r^2}\right)d_{ij}\mathrm{d}x^i\mathrm{d}x^j\right]\ ,\end{aligned} \tag{8.22}$$

where $\tilde{a} = a\sqrt{1+D}$, $\{b_i, c_{ij}, d_{ij}\} \sim \mathcal{O}(1)$, and Cartesian coordinates have been introduced as in Eq. (7.40). From this expansion, we see that at leading order the disformed metric is the same as Kerr, with a mass and angular momentum given by

$$\tilde{M} = \frac{M}{1+D} \qquad \text{and} \qquad \tilde{a} = a\sqrt{1+D}\ . \tag{8.23}$$

The effect of disformality appears at higher orders, and notice in particular the unusual half-integer power of r in the cross terms $\mathrm{d}t\mathrm{d}x^i$. In the rest of this section, we will keep using the parameter a for simplicity, but one must keep in mind that the spin of the black hole, as determined by the asymptotic expansion, is $\tilde{a}$.

As the radial coordinate decreases, we reach the surface where the timelike Killing vector ξ becomes null, which is determined by $\tilde{g}_{tt} = 0$. As in the case of Kerr, this surface $r = \tilde{r}_{\mathrm{E}}(\theta)$ is called the static limit, or ergosurface, and is defined by

$$\tilde{r}_{\mathrm{E}}(\theta) = \tilde{M} + \sqrt{\tilde{M}^2 - a^2\cos^2\theta}\ . \tag{8.24}$$

Note that there is nonetheless a difference compared to the Kerr spacetime, since the spin a enters the previous expression, and not $\tilde{a}$. Inside this surface, static observers no longer exist and stationary observers of the form (7.41) must have $\omega > 0$. As we

go deeper inside the ergoregion, we reach a surface inside which timelike stationary observers no longer exist, which we defined as the stationary limit. This surface is obtained by solving the equation:

$$P(r,\theta) \equiv r^2 + a^2 - 2\tilde{M}r + \frac{2\tilde{M}Da^2 r \sin^2\theta}{r^2 + a^2\cos^2\theta} = 0\,. \tag{8.25}$$

It can be seen as a fourth order polynomial in the variable r, which has at most four roots. The outermost one, which we call $R_{\rm S}(\theta)$, defines the stationary limit

$$\Sigma_{\rm S}: \quad r - R_{\rm S}(\theta) = 0 \tag{8.26}$$

In the limit $D = 0$, this would correspond to the outer event horizon of the Kerr metric. In general, this surface does not lie at constant r, and it meets the ergosurface at the poles. We now show that $\Sigma_{\rm S}$ cannot be an event horizon, since such a surface is necessarily null. To determine the nature of $\Sigma_{\rm S}$ we write the covariant components of the normal vector N to this surface:

$$N_\mu = (0, 1, -R'_{\rm S}(\theta), 0)\ , \tag{8.27}$$

where a $'$ denotes a derivative with respect to θ. We now calculate the norm of this vector, and obtain

$$N^2 = \tilde{g}^{\mu\nu}N_\mu N_\nu = \tilde{g}^{\theta\theta}\left[R'^2_{\rm S}(\theta) + P(r,\theta)\right]\ . \tag{8.28}$$

By evaluating this expression on the surface $r = R_{\rm S}(\theta)$, where we have $P = 0$, we obtain

$$N^2|_{r=R_{\rm S}} = \tilde{g}^{\theta\theta}R'^2_{\rm S}(\theta) > 0\ .$$

This shows that unless $D = 0$ (in which case $R_{\rm S}$ is constant and we have $R'_{\rm S} = 0$), the normal vector N is spacelike, meaning that $\Sigma_{\rm S}$ is a timelike hypersurface. Hence it cannot correspond to an event horizon. This confusion is common in the literature, and many authors have associated the solutions of Eq. (7.45) to event horizons, regardless of the θ-dependent profile. Hence, if an event horizon does exist for the disformed Kerr spacetime, it must lie in the interior of $\Sigma_{\rm S}$. A notable feature of the interior of $\Sigma_{\rm S}$ is that all of the Killing vectors, i.e. of the form $\mu_1\partial_t + \mu_2\partial_\varphi$ with $\{\mu_1, \mu_2\}$ constants, are spacelike in this region. Indeed, by factorizing μ_1, one can write these vectors in a form that is proportional to the vector (7.41), and we showed that such vectors are spacelike inside $\Sigma_{\rm S}$. This implies that if an event horizon is found in the interior of the stationary limit, it cannot be a Killing horizon, as this would require a Killing vector to be null on the surface. This is impossible, since the Killing vectors are spacelike in this region. This property is a notable difference form the GR spacetimes. In our case Hawking's rigidity theorem does not hold since the spacetime is not Ricci flat.

We now search for a candidate event horizon in the interior of the stationary limit surface $\Sigma_{\rm S}$, which must be a null hypersurface. The usual assumption is to look for a

horizon located at constant r. Requiring that the normal vector to such a surface be null, we obtain the equation $\tilde{g}^{rr} = 0$. It can be shown that in the present case

$$\tilde{g}^{rr} = \frac{P(r,\theta)}{\rho^2(r,\theta)} ,$$

so that the equation $\tilde{g}^{rr} = 0$ does not admit constant r solutions when $D \neq 0$. This means that our starting assumption is wrong, and a potential event horizon cannot be located at constant r. As we already stated, this error is common in the literature, as the link between solving $\tilde{g}^{rr} = 0$ and the hypothesis of a constant r surface is often forgotten.

Since the event horizon cannot be a constant r surface, we look for more general hypersurface $\mathcal{H}$ defined by

$$\mathcal{H}: \quad r - R(\theta) = 0 . \tag{8.29}$$

We introduce the vector n normal to $\mathcal{H}$, which has the following covariant components:

$$n_\mu = (0, 1, -R'(\theta), 0) \ . \tag{8.30}$$

We now ask for this vector to be null, which is a necessary condition for $\mathcal{H}$ to be a horizon. After dividing by $\tilde{g}^{\theta\theta}$, which is strictly positive outside of the ring singularity $\rho = 0$, the condition $n^2 = 0$ leads to

$$R'^2(\theta) + P(R(\theta),\theta) = 0 , \tag{8.31}$$

which constitutes the equation for the horizon surface. This type of horizon equation was also obtained in Refs. [177, 178, 228].

Let us now discuss some analytical properties of the solution to Eq. (8.31). First of all, a solution exists only if $P(R(\theta),\theta) \leq 0$, which is consistent with the fact that we're looking for a horizon in the interior of Σ_S. It is a first-order differential equation which admits two branches in which R is monotonous:

$$R'(\theta) = \pm\sqrt{-P(R(\theta),\theta))} . \tag{8.32}$$

We will see that the branch must be chosen depending on the value of D and the interval of θ. The function $R(\pi - \theta)$ satisfies the same equation because P is invariant under the transformation $\theta \to \pi - \theta$. This is consistent with the fact that our solution should be symmetric with respect to the equator. In order for the solution to be smooth, its derivative must vanish at the poles, i.e. $R'(0) = R'(\pi) = 0$. Furthermore, a smooth solution with the symmetry $\theta \to \pi - \theta$ must also satisfy $R'(\pi/2) = 0$. Hence, we are looking for a solution to Eq. (8.32) which satisfies the conditions:

$$R'(0) = R'\left(\frac{\pi}{2}\right) = 0 . \tag{8.33}$$

The condition $R'(\pi) = 0$ follows from the symmetry with respect to the equator. Note that if these conditions are verified, the surfaces $\mathcal{H}$ and Σ_S must touch at the poles

and equator.[3] Since we are solving a first-order differential equation, it is *a priori* only possible to specify one of the boundary conditions given by Eq. (8.33). We will see by solving the equation numerically that this indeed becomes a problem for some ranges of parameters, in the sense that upon imposing one of the conditions, the second one is not necessarily verified. In the following, we will express distances in units of $\tilde{M}$ to simplify the expressions, and for this we define

$$h(\theta) = \frac{R(\theta)}{\tilde{M}} , \quad h_{\rm S}(\theta) = \frac{R_{\rm S}(\theta)}{\tilde{M}} \quad \text{and} \quad \chi = \frac{a}{\tilde{M}} . \tag{8.34}$$

In terms of these variables, the horizon equation (8.31) becomes

$$h'^2(\theta) + h^2 + \chi^2 - 2h + \frac{2D\chi^2 h \sin^2\theta}{h^2 + \chi^2\cos^2\theta} = 0 . \tag{8.35}$$

It is possible to derive necessary conditions on the parameters χ and D for both of the conditions (8.33) to be verified. Let us assume that the function h is twice differentiable at the points $\theta = 0$ and $\theta = \pi/2$, which should be verified for a smooth solution. In this case, a Taylor expansion around the point $\theta = \pi/2$ yields the condition

$$\left(h^3(\frac{\pi}{2}) - h^2(\frac{\pi}{2}) - D\chi^2\right)^2 + 8D\chi^2 h(\frac{\pi}{2})\left(h^2(\frac{\pi}{2}) + \chi^2\right) \geq 0 , \tag{8.36}$$

in order for the second derivative $h''(\pi/2)$ to be real.[4] This condition is trivially verified for $D \geq 0$, but it constrains the parameters $\{\chi, D\}$ in the case $D < 0$. The horizon equation evaluated at $\theta = \pi/2$ gives the following polynomial equation for $h(\pi/2)$:

$$h^3(\frac{\pi}{2}) - 2h^2(\frac{\pi}{2}) + \chi^2 h(\frac{\pi}{2}) + 2D\chi^2 = 0 . \tag{8.37}$$

Let us assume that $D < 0$ is fixed and χ may vary. Then, at the critical point $\chi = \chi_{\rm c}$ for which the inequality (8.36) is saturated, it is possible to eliminate h using the expressions (8.36) and (8.37). We obtain a polynomial equation that must be satisfied by the critical parameter $\chi_{\rm c}$:

$$\begin{aligned} 0 = &-256D^2 + 32D\left[39 + D\left(50 - 13D\right)\right]\chi_{\rm c}^2 \\ &+ \left[15 + D\left(-2076 + D\left(562 + 7D\left(332 + 49D\right)\right)\right)\right]\chi_{\rm c}^4 \\ &- \left[30 - 2D\left(414 + 517D\right)\right]\chi_{\rm c}^6 + 15\chi_{\rm c}^8 . \end{aligned} \tag{8.38}$$

This can be seen as a fourth order polynomial in $\chi_{\rm c}^2$, and one can show that only one of the four roots is a positive number in the interval $D \in [-1, 0]$. Hence for each D we

[3] More precisely, the surface $\mathcal{H}$ must touch one of the surfaces corresponding to a root of P. However, one can check numerically that the surface is indeed $\Sigma_{\rm S}$.

[4] Higher orders of the Taylor expansion around $\theta = \pi/2$ do not give additional conditions. Indeed, if we assume that $h^{(2p+1)}(\pi/2) = 0$, then the order $2p$ in the Taylor expansion is linear in $h^{(2p)}$ when $p > 1$. So we do not have additional constraints to ensure that $h^{(4)}, h^{(6)}$, etc. are real at $\theta = \pi/2$. The same is true for the expansion around $\theta = 0$.

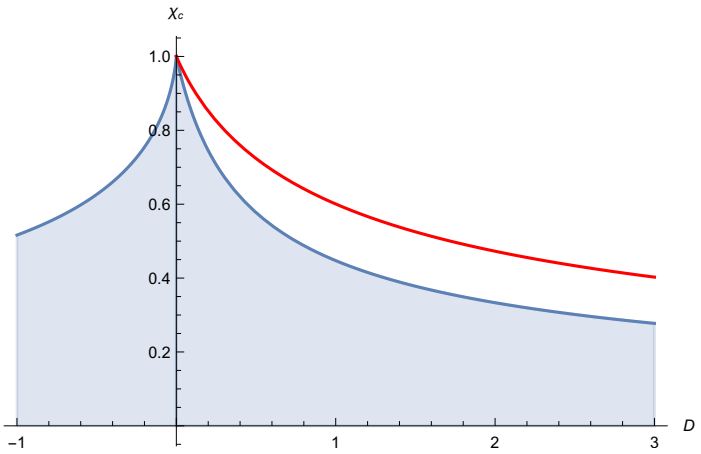

Figure 1: Critical value χ_c as a function of D (in blue). For $\chi > \chi_c$, we have $h'(\pi/2) \neq 0$ when $D < 0$, and $h'(0) \neq 0$ when $D > 0$. For points in the shaded region, $h'(0) = h'(\pi/2) = 0$ is allowed. The red curve is an existence condition for the horizon at the equator, which gives a milder constraint.

obtain an upper bound for the parameter χ, in the sense that for $\chi > \chi_c$ the horizon surface cannot be smooth. Note that the condition $\chi \leq \chi_c$ is not a sufficient condition for the smoothness of $\mathcal{H}$, but it is necessary.

We now proceed similarly at the point $\theta = 0$, where it is easy to see that

$$h(0) = 1 + \sqrt{1 - \chi^2}\,, \tag{8.39}$$

assuming that $\chi \leq 1$. We have chosen this root in order for the horizon to coincide with the ergosphere at the poles, as in the Kerr spacetime. We now perform a Taylor expansion and set $h'(0) = 0$. Then, the necessary condition for $h''(0)$ to be real translates to

$$1 - (1 + 4D)\,\chi^2 \geq 0. \tag{8.40}$$

This is trivially verified when $D \leq 0$, since we assume $\chi < 1$. However, when $D > 0$ we obtain the following upper bound on the parameter χ:

$$\chi_c = \frac{1}{\sqrt{1 + 4D}}\,. \tag{8.41}$$

Hence, if we ask for both conditions (8.33) to be verified, in order to have a smooth horizon we obtain a necessary upper bound for the parameter χ for each value of $D \in [-1, \infty)$. It is worth noting that there exists an additional bound linked to the existence of a real positive root to Eq. (8.37). As we saw, this is a necessary condition for the horizon to be smooth, as it must touch the stationary limit at the equator and poles. An analysis of the polynomial gives another upper bound on χ when $D > 0$, but this constraint is milder than the one derived above, i.e. Eq. (8.41). The results

are summarized in Fig. 1. Let us now comment on the implications of these bounds on the physical spin parameter $\tilde{a}$, to which we associate the dimensionless parameter

$$\tilde{\chi} = \frac{\tilde{a}}{\tilde{M}} = \chi\sqrt{1+D} \, . \tag{8.42}$$

Using the condition (8.41), we obtain that solutions with a smooth horizon verify $\tilde{\chi} < 1$ for $D \neq 0$. This means that the smooth disformed Kerr black holes look like a sub-extremal Kerr solution to an observer at infinity.

Another method to find the horizon equation (8.31) is to introduce an adapted radial coordinate of the form

$$\mathrm{d}\zeta = \mathrm{d}r - R'(\theta)\,\mathrm{d}\theta \, , \tag{8.43}$$

such that the null hypersurface is now located at some constant value of ζ. In terms of these coordinates, Eq. (8.31) is found by solving $\tilde{g}^{\zeta\zeta} = 0$, which is analogous to solving $g^{rr} = 0$ for the Kerr spacetime, when searching for a horizon at $r = \text{const}$. As we discussed in the previous chapter, the constant r surfaces in the Kerr spacetime are timelike when $r > r_+$, spacelike in between the two event horizons, i.e. for $r_- < r < r_+$, while the event horizon $r = r_+$ is a null hypersurface providing a transition between these two regions. Using a similar argument in the case of the disformed Kerr metrics, we argue that if a smooth solution to Eq. (8.31) is found, it indeed represents an event horizon. In this case, we introduce the one-parameter family of surfaces defined as

$$R_\zeta(\theta) = R(\theta) + \zeta \, , \tag{8.44}$$

where $R_0(\theta) = R(\theta)$ is the candidate event horizon. We now examine the nature of such a surface by calculating the norm of its normal vector n_ζ. We obtain

$$n_\zeta^2 = R'^2(\theta) + P(R_\zeta(\theta), \theta) \, . \tag{8.45}$$

For $\zeta = 0$, we have $n_\zeta^2 = 0$, while $n_\zeta^2 > 0$ for $\zeta > 0$, since the surface $r = R(\theta)$ is the outermost surface which satisfies Eq. (8.31). We now assume $|\zeta| \ll 1$, so that one can write

$$n_\zeta^2 = \zeta \frac{\partial P}{\partial r}\left(R(\theta), \theta\right) + \mathcal{O}\left(\zeta^2\right) \, . \tag{8.46}$$

If one can show that $\partial P/\partial r > 0$ when evaluated at the horizon surface, then this proves the existence of some ζ_0 for which $n_\zeta^2 < 0$ in the interval $\zeta \in [\zeta_0, 0)$, which is precisely what we wish to establish. Note that one cannot have $\partial P/\partial r < 0$, as this would contradict the result that $n_\zeta^2 > 0$ for any $\zeta > 0$. Hence, it is enough to prove that $\partial P/\partial r \neq 0$ when evaluated at the horizon surface.

In terms of the dimensionless variables, an explicit calculation shows that this is equivalent to determining the sign of

$$P_1 = (h-1)\left(h^2 + \chi^2\cos^2\theta\right)^2 - D\chi^2\sin^2\theta\left(h^2 - \chi^2\cos^2\theta\right) \, . \tag{8.47}$$

Let us now prove that this polynomial is positive at the horizon surface. We first prove that $h \geq 1$. We will show in the next section that depending on the sign of D, a different branch must be chosen in Eq. (8.32). When $D < 0$, the increasing branch $h' > 0$ must be chosen in the interval $[0, \pi/2]$, so that $h \geq h(0) \geq 1$. When $D > 0$, the minimum h_m of the function h is reached at the equator, and it is the outermost root of the polynomial (8.37). By evaluating this polynomial at $h = 1$ and enforcing the constraint (8.41), we obtain a negative number. Since P is positive for large r, this means that the outermost root is larger than 1, i.e. $h_m \geq 1$. Hence we have $h \geq 1$ in all cases. Note that the inequality is strict unless $\chi = 1$, and hence $D = 0$, in which case we simply recover the extremal Kerr black hole. This shows in particular that $h^2 \geq \chi^2 \sin^2\theta$, since $\chi \leq 1$. Hence, it is clear that $P_1 > 0$ for $D < 0$. It remains to show that this is also the case when $D > 0$. It is clearly the case for $\theta = 0$, but one can show that it is true for any angle by solving $P_1 = 0$ numerically. The solution does not satisfy the horizon equation at any point, and hence $P_1 > 0$ for $D > 0$ also. Hence, for any $D \neq 0$, we have shown that for a regular horizon surface h, i.e. verifying the necessary conditions (8.33), we have

$$\frac{\partial P}{\partial r}(R(\theta), \theta) \neq 0 \, . \tag{8.48}$$

This signifies that the surfaces $r = R_\zeta$ are indeed timelike for $\zeta > 0$, null for $\zeta = 0$, and spacelike in an interval $[\zeta_0, 0)$ for some constant ζ_0. Because of this property, and in analogy with the Kerr spacetime, we will say that the surface $r = R(\theta)$ verifying Eq. (8.31) is an event horizon for the disformed Kerr metrics.

8.2.3 Numerical integration and approximate solutions

As we already mentioned, one cannot integrate the horizon equation (8.32) analytically. In this section, we discuss the numerical integration of this equation, along with an approximate solution when the disformal parameter D is small. The numerical integration is performed using the Runge-Kutta method with a specified boundary condition. Depending on the sign of D, we integrate the horizon equation (8.32) with different initial conditions. For $D < 0$, the integration is performed in the interval $\theta \in [0, \pi/2]$ with the initial condition $h'(0) = 0$, while for $D > 0$ we integrate in the interval $\theta \in [\pi/2, \pi]$ with the condition $h'(\pi/2) = 0$. In the latter case, we use the symmetry $\theta \to \pi - \theta$ to plot the solution in the interval $[0, \pi/2]$. If the wrong interval is chosen, the integration is unsuccessful, and we believe that this is caused by a growth of the numerical error. Furthermore, the right branch must be chosen in Eq. (8.32). For $D > 0$, one must choose $h' \leq 0$ in the interval $[0, \pi/2]$, and the other branch is not physical. Hence, we have $h \leq h(0)$ in this case, and the minimum is reached at the equator. It is the opposite for $D < 0$, i.e. one must choose the branch where $h' \geq 0$ and we have $h \geq h(0)$, so that the maximum is reached at the equator.

Different profiles for $\chi = 0.9$ are represented in Fig. 2. Some of the solutions are manifestly not smooth at $\theta = \pi/2$. In fact, only the cases $D = -0.1$ and $D = 0.05$

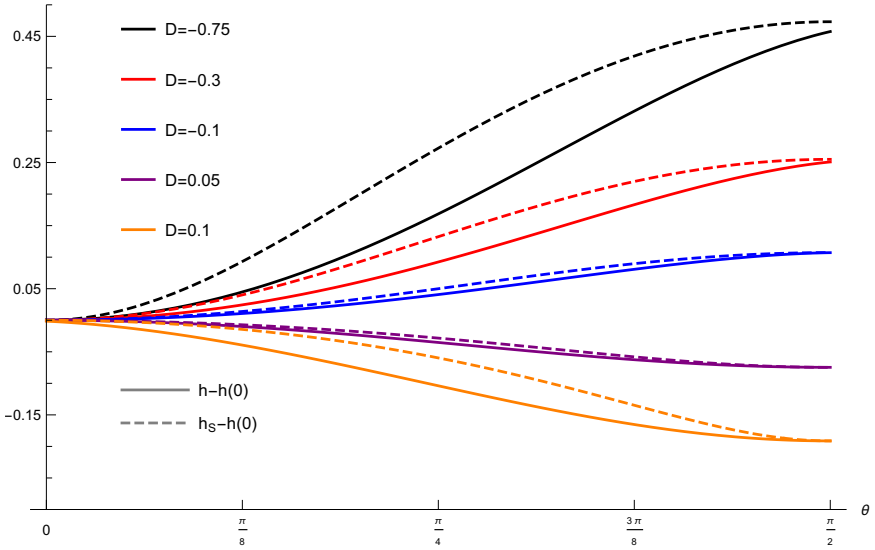

Figure 2: Numerical integration of $h - h(0)$ and $h_S - h(0)$ for $\chi = 0.9$ and varying D, respectively $D = -0.75$ (black), $D = -0.3$ (red), $D = -0.1$ (blue), $D = 0.05$ (purple) and $D = 0.1$ (orange). The solution becomes unphysical when $|D|$ becomes large.

in Fig. 2 represent smooth solutions. The other cases do not satisfy the necessary conditions given by Eqs. (8.38) and (8.41). This can be seen from the fact that h' is nonzero at the equator, which also means that the horizon surface and the stationary limit do not touch at this point. This is very clear from Fig. 2 in the case $D = -0.75$ for instance. In the cases where the horizon is smooth, the surfaces $\mathcal{H}$ and Σ_S are very close to each other in the whole interval $[0, \pi/2]$, and touch at the poles and equator. They are nevertheless distinct, and it is possible for a timelike observer to escape the region in between these two surfaces. Using the numerical integration, it is possible to check the necessary condition $\chi \leq \chi_c$. Depending on the sign of D, we specify one of the conditions (8.33) and integrate in the corresponding interval as discussed previously. For each case, we determine the value of h' at the end point of the interval, and check if it is consistent with $h' = 0$. Some examples are shown in Fig. 3 for $D < 0$, though analogous results hold for $D > 0$. By increasing the numerical precision, we obtain that $h' \to 0$ if the condition $\chi \leq \chi_c$ is verified. This numerical argument seems to indicate that the condition $\chi \leq \chi_c$ is in fact also a sufficient condition to have a smooth horizon surface, though we have not yet found an analytical proof of this claim.

Another way to gain some insight on the solutions to Eq. (8.35) is to solve it perturbatively. The term containing D can be thought of as a perturbation, and for $D\chi^2 \ll 1$ we write

$$h(\theta) = h(0) + \sum_{n=1}^{\infty} (D\chi^2)^n \delta h_n(\theta) \, . \tag{8.49}$$

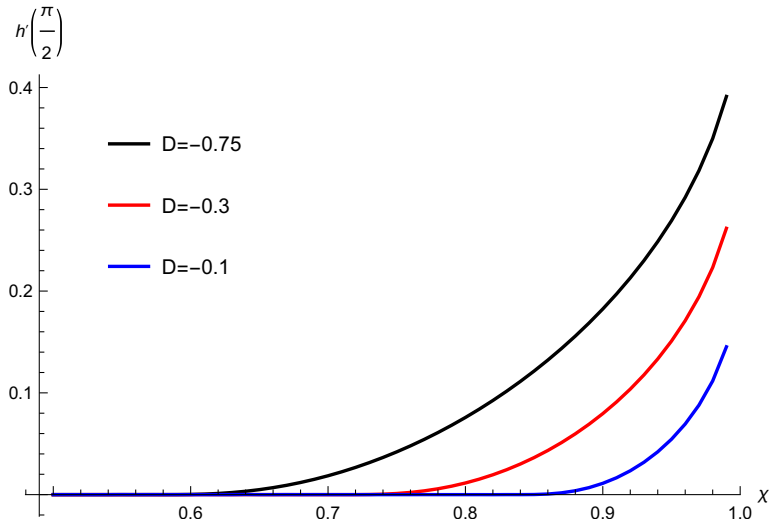

Figure 3: Numerical value of $h'(\pi/2)$ for $D = -0.75$ (black), $D = -0.3$ (red) and $D = -0.1$ (blue).

Using Eq. (8.35), we can obtain δh_1 algebraically. Then, higher orders in the expansion give δh_n in terms of δh_{n-i} and $\delta h'_{n-i}$, where $i \in [\![1, n-1]\!]$. One can hence obtain the solution as a perturbative series to the desired order. The first-order term reads

$$\delta h_1(\theta) = -\frac{\chi \sin^2\theta \left(1+\sqrt{1-\chi^2}\right)}{2\left(1-\chi^2\right)+\sqrt{1-\chi^2}\left(2-\chi^2\sin^2\theta\right)} \,. \tag{8.50}$$

The deviations from the Kerr solution are maximal at the equator, and are of order $h(\pi/2) \sim |Da^2|$ (for small Da^2). Notice that $\delta h_1 < 0$, meaning that the sign of the first order correction is opposite to the sign of D. This is in accordance with the choice of the branch for the numerical integration depending on the sign of D. As we discussed above, we have $h - h(0) > 0$ (resp. $h - h(0) < 0$) when $D < 0$ (resp. $D > 0$).

Another way to find an approximate solution is to expand around the stationary limit surface $r = R_{\rm S}(\theta)$. As we discussed, for smooth solutions the surfaces $\mathcal{H}$ and $\Sigma_{\rm S}$ meet at the poles and equator, and remain very close to each other in the interval $\theta \in [0, \pi/2]$. This motivates the search for approximate solutions of the form

$$R_{n+1}(\theta) = R_n(\theta) + F_n(\theta) \,, \tag{8.51}$$

where we start with $R_0 = R_{\rm S}$, and $F_n \ll R_n$. To determine the function F_n at each order, we Taylor expand Eq. (8.31) and obtain

$$R_n'^2 + 2R'_nF'_n + F_n'^2 + P(R_n,\theta) + F_n\frac{\partial P}{\partial r}(R_n,\theta) = 0 \,. \tag{8.52}$$

We also assume $F'_n \ll R'_n$, which should be checked numerically, and in this case the

solution at each order reads

$$R_{n+1}(\theta) = R_n(\theta) - \left(R_n'^2 + P(R_n,\theta)\right)\left(\frac{\partial P}{\partial r}(R_n,\theta)\right)^{-1} . \tag{8.53}$$

This provides an alternative method to integrate the horizon equation, and we have checked numerically that both methods converge towards the same solution when the necessary condition $\chi \leq \chi_c$ is satisfied.

8.3 Interesting limiting cases

In this section, we examine some interesting limits of the disformed Kerr metrics (8.11), namely $D \to -1$ and $D \to \infty$. They constitute simple examples of noncircular metrics, and their study could be helpful to understand the properties of such spacetimes.

8.3.1 Limit $D \to -1$: the quasi-Weyl metric

We first examine the limit $D \to -1$, which is *a priori* singular, since the metric (8.11) was written after the redefinition $t \to t/\sqrt{1+D}$, and in these coordinates the scalar field reads:

$$\phi = \frac{q_0}{\sqrt{1+D}}\left[t + (1+D)\int \frac{\sqrt{2\tilde{M}r(a^2+r^2)}}{\Delta}\mathrm{d}r\right] .$$

In order to make sense of the limit, we redefine the scalar field and the corresponding kinetic density as

$$\psi = \frac{\sqrt{1+D}}{q_0}\phi \quad \text{and} \quad \tilde{Y} = \tilde{g}^{\mu\nu}\partial_\mu\psi\partial_\nu\psi . \tag{8.54}$$

After taking the limit $D \to -1$, we simply have $\psi = t$ in this case. In the same limit, the line element (8.11) becomes

$$\mathrm{d}\tilde{s}^2_{\mathrm{QW}} = -\left(1 - \frac{2\tilde{M}r}{\rho^2}\right)\mathrm{d}t^2 + \frac{\rho^2}{r^2+a^2}\mathrm{d}r^2 + 2\sqrt{\frac{2\tilde{M}r}{r^2+a^2}}\mathrm{d}t\mathrm{d}r + \rho^2\mathrm{d}\theta^2 + \left(r^2+a^2\right)\sin^2\theta\mathrm{d}\varphi^2 . \tag{8.55}$$

The $\tilde{g}_{t\varphi}$ term disappears in this limit, but the metric isn't static because of the $\tilde{g}_{tr}$ term which cannot be eliminated because of noncircularity. In the absence of the $\tilde{g}_{tr}$ term the above line-element would be a Weyl metric, in essence a static and axially symmetric circular metric, and because of this we call it a quasi-Weyl (QW) metric. In the limit $a = 0$, one recovers the Schwarzschild metric in Gullstrand-Painlevé coordinates.

Interestingly, in this case the ergosurface coincides with the stationary limit Σ_{S}. However, as we discussed above the event horizon is located further in the interior of these surfaces, even though they meet at the poles and equator. This is an interesting property, since the ergoregion is usually a feature of rotating black holes. In the

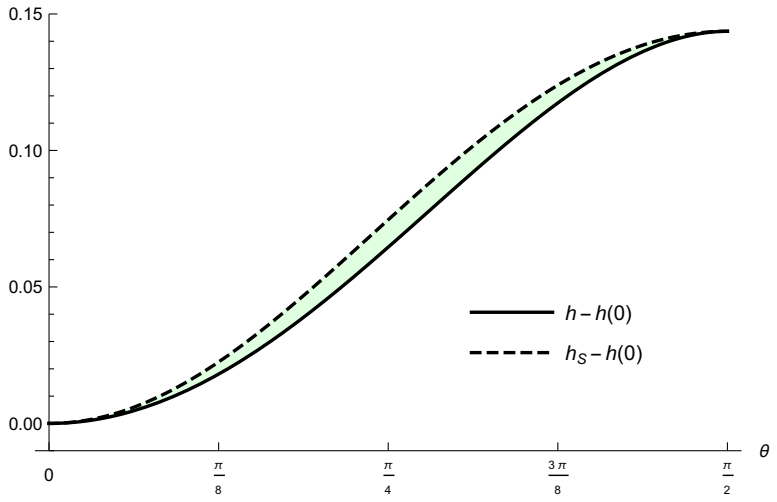

Figure 4: Stationary limit (dashed black line) and event horizon (black) for the quasi-Weyl metric with the critical parameter $\chi = 2/\sqrt{15}$. In the green region, the Killing vector ξ is spacelike. The ergosurface coincides with the stationary limit in this case.

present case, the object is not spinning in the φ direction, and yet there exists a region outside the horizon where the Killing vector ξ is spacelike. This will force timelike observers to move along the radial direction in this region. Indeed, by setting $\mathrm{d}r = 0$ in the line element above, we obtain $\mathrm{d}\tilde{s}^2_{\mathrm{QW}} > 0$ in this region, which is impossible for a timelike curve. However, such a timelike observer can still escape to infinity, since they haven't yet crossed the null surface $\mathcal{H}$. In terms of the adapted coordinate ζ defined in Eq. (8.43), it is still possible to move towards increasing ζ in this region.

In this limit, the polynomial (8.38) determining the critical parameter $\chi = a/\tilde{M}$ simplifies, and we obtain

$$\chi_{\mathrm{c}} = \frac{2}{\sqrt{15}} \,. \tag{8.56}$$

The horizon equation for this metric is obtained by setting $D = -1$ in Eq. (8.35), which still cannot be integrated analytically. The different surfaces (obtained numerically) for $\chi = \chi_{\mathrm{c}}$ are represented in Fig. 4. For values of $\chi < \chi_{\mathrm{c}}$, the green region in Fig. 4 would be thinner.

We now discuss the theory corresponding to this solution. We take the same limit in the general action given by the functions (8.10), and express everything in terms of the field ψ, resulting in:

$$S_{\mathrm{QW}}[\tilde{g}] = \frac{M_P^2}{2}\int \mathrm{d}^4x\sqrt{-\tilde{g}}\left(\sqrt{-\tilde{Y}}f(\tilde{Y})\tilde{R} - \frac{f}{\sqrt{-\tilde{Y}}}\left[\psi_{\mu\nu}\psi^{\mu\nu} - (\Box\psi)^2\right] + \frac{4f_{\tilde{Y}}}{\sqrt{-\tilde{Y}}}\psi^{\mu}\psi_{\mu\nu}\psi^{\nu}\Box\psi\right) \,, \tag{8.57}$$

where f has also been redefined as $f \to f\sqrt{1+D}$ to absorb a residual infinite factor. One can check that the above action admits the QW metric (9.35) and $\psi = t$ as a solution. If we consider a constant f, the theory belongs to the Horndeski class, i.e. it leads to second-order field equations.

8.3.2 Limit $D \to \infty$: the noncircular Schwarzschild metric

Let us now consider the limit of an infinite disformal parameter, i.e. $D \to \infty$, while at the same time keeping the physical spin of the black hole $\tilde{a} = a\sqrt{1+D}$ finite. This implies $a \to 0$ but as we discussed above, the observable quantity is $\tilde{a}$ rather than a. This limit applied to the disformed metric (8.11) leads to the following line element:

$$\begin{aligned} \mathrm{d}\tilde{s}^2_{\mathrm{NCS}} = &-\left(1-\frac{2\tilde{M}}{r}\right)\mathrm{d}t^2 + \sqrt{\frac{2r}{\tilde{M}}}\mathrm{d}t\mathrm{d}r - \frac{4\tilde{\chi}\tilde{M}^2\sin^2\theta}{r}\mathrm{d}t\mathrm{d}\varphi - \frac{r}{2\tilde{M}}\mathrm{d}r^2 \\ &+ r^2\mathrm{d}\theta^2 + r^2\sin^2\theta\left(1+\frac{2\tilde{\chi}^2\tilde{M}^3\sin^2\theta}{r^3}\right)\mathrm{d}\varphi^2 \,. \end{aligned}$$

From this expression, it is clear that the metric is only singular at the point $r = 0$. We can put the metric in a Schwarzschild-like form by trading the (tr) term for an $(r\varphi)$ term through the coordinate change (8.21), assuming the limit $D \to \infty$ and $a \to 0$:

$$\mathrm{d}t = \mathrm{d}T + \frac{r^{3/2}\mathrm{d}r}{\sqrt{2\tilde{M}}(r-2\tilde{M})} \,.$$

In terms of these new coordinates, we obtain the following line element:

$$\begin{aligned} \mathrm{d}\tilde{s}^2_{\mathrm{NCS}} = &-\left(1-\frac{2\tilde{M}}{r}\right)\left(\mathrm{d}T + \frac{2\tilde{\chi}\tilde{M}^2\sin^2\theta}{r-2\tilde{M}}\mathrm{d}\varphi\right)^2 \\ &+\left(1-\frac{2\tilde{M}}{r}\right)^{-1}\left(\mathrm{d}r - \sqrt{\frac{2\tilde{M}^3}{r}}\tilde{\chi}\sin^2\theta\mathrm{d}\varphi\right)^2 + r^2\left(\mathrm{d}\theta^2+\sin^2\theta\mathrm{d}\varphi^2\right) \,. \end{aligned} \tag{8.58}$$

This noncircular metric reduces to the Schwarzschild line element in the limit $\tilde{\chi} = 0$, so we call it the noncircular Schwarzschild metric (NCS). Despite the name, the properties of the above metric are quite different from the static GR case. For a start the metric is stationary and spinning : from the $(t\varphi)$ term we can read off the value of the spin $\tilde{\chi}$, when compared to an asymptotic expansion of the Kerr spacetime. The necessary condition (8.41) for this black hole to have a smooth outer horizon translates to

$$\tilde{\chi} \leq \frac{1}{2} \,, \tag{8.59}$$

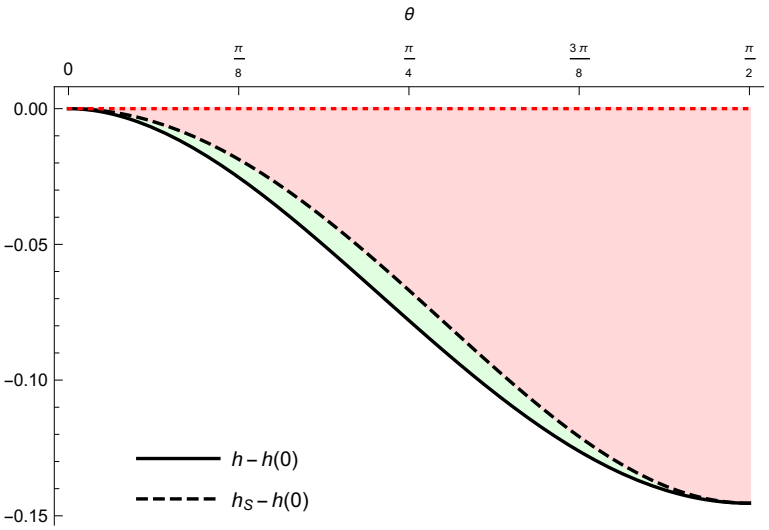

Figure 5: Ergosurface (dotted red line), stationary limit (dashed black line) and numerical integration of the horizon surface (black) for the NCS metric with critical spin $\tilde{\chi} = 1/2$.

in terms of the physical spin parameter. The surface $r = 2\tilde{M}$ corresponding to the Schwarzschild event horizon in the limit $\tilde{\chi} = 0$ is now the static limit of the spinning black hole, while the stationary limit and event horizon lie inside this surface. The horizon equation (8.31) simplifies in this limit, and we obtain

$$h'^2(\theta) + h^2 - 2h + \frac{2\tilde{\chi}^2 \sin^2\theta}{h} = 0 \,. \tag{8.60}$$

Even though this equation simplifies a lot, one still cannot solve it analytically. A numerical integration for the critical spin $\tilde{\chi} = 1/2$ is represented in Fig. 5.

We now discuss the theory corresponding to the NCS metric and its associated scalar field. We perform the same field redefinition as in Eq. (8.54), and obtain in this case

$$\psi = T + 2\sqrt{2\tilde{M}r} - 4\tanh^{-1}\sqrt{\frac{r}{2\tilde{M}}} \,. \tag{8.61}$$

The resulting action in terms of ψ and $\tilde{Y}$ reads, in the limit $D \to \infty$,

$$\begin{aligned} S_{D\to\infty}[\tilde{g}] = \frac{M_P^2}{2}\int \mathrm{d}^4x\sqrt{-\tilde{g}}\Bigg(&\sqrt{1+\tilde{Y}}f(\tilde{Y})\tilde{R} + \frac{f}{\sqrt{1+\tilde{Y}}}\left[\psi_{\mu\nu}\psi^{\mu\nu} - (\Box\psi)^2\right] \\ &- \frac{4f_{\tilde{Y}}}{\sqrt{1+\tilde{Y}}}\psi^\mu\psi_{\mu\nu}\psi^\nu\Box\psi\Bigg) \,. \end{aligned} \tag{8.62}$$

In this limit, we have $\tilde{Y} \to -1$, which leads to diverging terms in the equations of motion. However, by inspecting the equations of motion following from the above

action, one can notice that the first and third terms give subdominant contributions with respect to the second one, in the limit $\tilde{Y} \to -1$. As a result, upon redefining the function f as $F = f/\sqrt{1+\tilde{Y}}$, we obtain the action

$$S_{\rm NCS}[\tilde{g}] = \frac{M_P^2}{2}\int \mathrm{d}^4x\sqrt{-\tilde{g}}F(\tilde{Y})\left[\psi_{\mu\nu}\psi^{\mu\nu} - (\Box\psi)^2\right]. \tag{8.63}$$

One can check that the equations of motion deriving from this action are satisfied by the NCS metric (8.58) and scalar field (8.61). This theory belongs to both the Ia and IIIa DHOST classes [45, 46], due to the absence of an Einstein-Hilbert term.

8.4 Petrov type of the disformed metrics

In this section, we use the NCS metric (8.58) to comment on the Petrov type of the disformed metrics. As we discussed, the Kerr metric is algebraically special and has a Petrov type D, meaning that it possesses the two repeated principal null directions given in Eq. (7.33). We will show that the NCS metric is of general Petrov type I, meaning that it is not not algebraically special. This is a generic feature of all the disformed metrics, but we choose to perform the calculations for the NCS metric for simplicity. However, even for type D metrics, most of the useful theorems apply only for vacuum solutions. For instance, in this case the Goldberg-Sachs theorem [229] states that the repeated principal null directions are geodesic (and shear-free). One can also prove the existence of a nontrivial Killing tensor in this case [191]. However, since the disformed Kerr metrics are not Ricci flat, these theorems wouldn't apply anyway, so determining the Petrov type is not crucial. The authors of [219] constructed deformed versions of the principal directions of the Kerr spacetime of the form

$$\tilde{k}^\mu = k_0^\mu + \alpha_1(r)\,\phi^\mu \qquad \text{and} \qquad \tilde{l}^\mu = l_0^\mu + \alpha_2(r)\,\phi^\mu. \tag{8.64}$$

We show here that these objects cannot be considered as repeated principal null directions of the disformed spacetime, since the Petrov type D is not conserved through the disformal transformation. Instead, these are simply null vectors which are not geodesic, and have no link to the Weyl tensor in the generic case $D \neq 0$.

The NCS metric written in Schwarzschild-like coordinates is a good starting point for applying the Newman-Penrose (NP) formalism [230]. Indeed, the line element (8.58) can be written

$$\mathrm{d}\tilde{s}^2 = \eta_{ab}\, e^a_\mu\, e^b_\nu\, \mathrm{d}x^\mu\, \mathrm{d}x^\nu\,, \tag{8.65}$$

where η_{ab} is the Minkowski metric and the 1-forms e^a read

$$e^0 = \left(1 - \frac{2\tilde{M}}{r}\right)^{1/2}\left(\mathrm{d}T + \frac{2\tilde{\chi}\tilde{M}^2\sin^2\theta}{r-2\tilde{M}}\mathrm{d}\varphi\right)\,,$$

$$
\begin{aligned}
e^1 &= \left(1-\frac{2\tilde{M}}{r}\right)^{-1/2}\left(\mathrm{d}r-\sqrt{\frac{2\tilde{M}^3}{r}}\tilde{\chi}\sin^2\theta\mathrm{d}\varphi\right)\ ,\\
e^2 &= r\,\mathrm{d}\theta\ ,\\
e^3 &= r\sin\theta\,\mathrm{d}\varphi\ .
\end{aligned}
$$

We assume that we are in the region $r > 2\tilde{M}$ in order for the previous expressions to be valid. From this real tetrad, we can construct a complex null tetrad $\{k, l, m, \bar{m}\}$ according to

$$
k=\frac{e^0+e^1}{\sqrt{2}}\ ,\qquad l=\frac{e^0-e^1}{\sqrt{2}}\ ,\qquad m=\frac{e^2-i\,e^3}{\sqrt{2}}\ ,\qquad \bar{m}=\frac{e^2+i\,e^3}{\sqrt{2}}\ . \tag{8.66}
$$

In this formalism, the metric can be written

$$
\tilde{g}_{\mu\nu}=-k_\mu l_\nu-l_\mu k_\nu+m_\mu\bar{m}_\nu+\bar{m}_\mu m_\nu\ \ .
$$

In terms of the Riemann and Ricci tensors, the Weyl tensor in four dimensions reads

$$
C_{\mu\nu\alpha\beta}=R_{\mu\nu\alpha\beta}-g_{\mu[\alpha}R_{\beta]\nu}+g_{\nu[\alpha}R_{\beta]\mu}+\frac{1}{3}R\,g_{\mu[\alpha}g_{\beta]\nu}\ . \tag{8.67}
$$

It is the trace-free component of the Riemann tensor, as can be checked easily by contracting any two indices in the previous expression. We can now construct five Weyl scalars through contractions with the vectors of the null tetrad:

$$
\begin{aligned}
\psi_0 &= C_{\mu\nu\alpha\beta}k^\mu m^\nu k^\alpha m^\beta\ ,\\
\psi_1 &= C_{\mu\nu\alpha\beta}k^\mu l^\nu k^\alpha m^\beta\ ,\\
\psi_2 &= C_{\mu\nu\alpha\beta}k^\mu m^\nu \bar{m}^\alpha l^\beta\ ,\\
\psi_3 &= C_{\mu\nu\alpha\beta}l^\mu k^\nu l^\alpha \bar{m}^\beta\ ,\\
\psi_4 &= C_{\mu\nu\alpha\beta}l^\mu \bar{m}^\nu l^\alpha \bar{m}^\beta\ .
\end{aligned} \tag{8.68}
$$

The Weyl scalars completely determine the Petrov type of a given spacetime [230]. In terms of the null tetrad (8.66), an explicit calculation for the NCS metric yields

$$
\begin{aligned}
\psi_0 &= \frac{\tilde{M}^3\tilde{\chi}^2\sin^2\theta\left(\sqrt{r}-\sqrt{2\tilde{M}}\right)^2}{r^5\left(r-2\tilde{M}\right)}\ ,\\
\psi_1 &= -\frac{\tilde{M}^2\tilde{\chi}\sin\theta\left(\sqrt{r}-\sqrt{2\tilde{M}}\right)\left(7\tilde{M}\tilde{\chi}\cos\theta-6ir\right)}{4r^5\sqrt{r-2\tilde{M}}}\ ,\\
\psi_2 &= -\frac{\tilde{M}}{r^3}\left[1-\frac{\tilde{M}^2\tilde{\chi}^2\left(1+3\cos 2\theta\right)}{3r^2}+\frac{3i\tilde{M}\tilde{\chi}\cos\theta}{r}\right]\ ,
\end{aligned}
$$

$$\psi_3 = \frac{\tilde{M}^2\tilde{\chi}\sin\theta\left(\sqrt{r}+\sqrt{2\tilde{M}}\right)\left(7\tilde{M}\tilde{\chi}\cos\theta-6ir\right)}{4r^5\sqrt{r-2\tilde{M}}}\,,$$
$$\psi_4 = \frac{\tilde{M}^3\tilde{\chi}^2\sin^2\theta\left(\sqrt{r}+\sqrt{2\tilde{M}}\right)^2}{r^5\left(r-2\tilde{M}\right)}\,. \tag{8.69}$$

The Weyl scalars are modified by a rotation of the tetrad. For example, in the case of a type D spacetime, one can find a null tetrad for which only the Weyl scalar $\psi_2 \neq 0$. This is the case when $\tilde{\chi} = 0$ in the previous expressions, which corresponds to the Schwarzschild metric. We have in this case $\psi_0 = \psi_1 = \psi_3 = \psi_4 = 0$, while $\psi_2 = -\tilde{M}/r^3$. It is possible to construct scalars which are invariant under the rotation off the tetrad, among which [195]

$$\mathcal{I} = \psi_0\psi_4 - 4\psi_1\psi_3 + 3\psi_2^2\,,$$
$$\mathcal{J} = \psi_0\psi_2\psi_4 - \psi_1^2\psi_4 - \psi_0\psi_3^2 + 2\psi_1\psi_2\psi_3 - \psi_2^3\,. \tag{8.70}$$

It can be shown that an algebraically special spacetime (i.e. not of Petrov type I) satisfies $27\mathcal{J}^2 = \mathcal{I}^3$ (see for instance Ref. [195]). One can define the following speciality index $\mathscr{S}$ in order to quantify the deviations from an algebraically special spacetime [231]:

$$\mathscr{S} = \frac{27\mathcal{J}^2}{\mathcal{I}^3}\,. \tag{8.71}$$

For the NCS metric, one can check explicitly that $\mathscr{S} \neq 1$, indicating that the spacetime is of generic Petrov type I. Furthermore, in the case $\tilde{\chi} \ll 1$ we obtain

$$\mathscr{S}_{\rm NCS} = 1 - \frac{3\tilde{M}^4\tilde{\chi}^4\sin^4\theta}{4r^4} + \mathcal{O}\left(\tilde{\chi}^5\right)\,. \tag{8.72}$$

The limit $\tilde{\chi} = 0$ corresponds to the Schwarzschild metric, which is of Petrov type D, so we recover $\mathscr{S} = 1$ in that case. This calculation can be performed for the disformed Kerr metric (8.11) in the general case, and we obtain the same result $\mathscr{S} \neq 1$, unless $D = 0$ or $a = 0$ (which both correspond to vacuum GR black holes that are of type D).[5] However, since the expressions are much heavier in the general case, the case of the NCS metric was presented for simplicity. An analogous calculation for the quasi-Weyl metric (8.55) outside the ergosurface yields the same result as Eq. (8.72) in the case $\chi \ll 1$, with the substitution $\tilde{\chi} \to \chi$. The next-to-leading correction is of order $\mathcal{O}(\chi^6)$ for that spacetime.

[5] After the submission of this thesis, Ref. [232] appeared, in which the authors study the effect of the disformal transformation on the Petrov type. They also find that the disformed metric is generically of Petrov type I.

Chapter 9

Orbit of stars in the disformed Kerr spacetime

In this chapter, which is based on Ref. [233], we study the post-Newtonian (PN) motion of stars around a disformed Kerr black hole. We will study different limits of the disformal parameter D, showing that generically the no-hair theorem of GR is violated. In a specific limit, we will be able to put a lower bound on the disformal parameter in order to satisfy the current experimental constraints from the GRAVITY collaboration [165, 166]. We start by comparing the second post-Newtonian (2PN) expansion of the disformed metric to various rotating spacetimes in the literature, and discuss the violation of the no-hair theorem. We then present the two-timescale analysis which is used to compute the secular variation of orbital parameters, closely following the analysis of Ref. [234]. Finally we calculate the secular shifts of orbital parameters for various cases of the constant D and discuss experimental constraints.

9.1 Comparison of different metrics asymptotically

Our goal is to study the post-Newtonian motion of stars in the vicinity of a disformed Kerr spacetime. In the Newtonian limit, the trajectory of a star forms an ellipse with the black hole located at one of its foci. In order to describe the post-Newtonian motion, we introduce the following dimensionless parameter:

$$\varepsilon = \frac{\tilde{M}}{A} \,, \tag{9.1}$$

where A is the semimajor axis of the ellipse. We consider the case where the star is far away from the black hole, and write the metric up to 2PN order, meaning that we keep terms up to order $\mathcal{O}(\varepsilon^3)$. We write the metric in terms of the physical spin $\tilde{\chi} = \tilde{a}/\tilde{M}$, which we assume is of order $\mathcal{O}(1)$. After the coordinate change (8.21), which we perform so that the asymptotic form of the metric is closer to Kerr in BL

coordinates, the line element up to 2PN order reads:

$$\begin{aligned} \mathrm{d}\tilde{s}^2_{\rm 2PN} = &-\left(1-\frac{2\tilde{M}}{r}+\frac{2\tilde{M}^3\chi^2\cos^2\theta}{(1+D)r^3}\right)\mathrm{d}T^2+\left(1+\frac{2\tilde{M}}{r}+\frac{4\tilde{M}^2}{r^2}-\frac{\tilde{M}^2\chi^2\sin^2\theta}{(1+D)r^2}\right)\mathrm{d}r^2 \\ &+r^2\left(1+\frac{\tilde{M}^2\chi^2\cos^2\theta}{(1+D)r^2}\right)\mathrm{d}\theta^2+r^2\sin^2\theta\left(1+\frac{\tilde{M}^2\chi^2}{(1+D)r^2}\right)\mathrm{d}\varphi^2 \\ &-\frac{4\tilde{M}^2\chi\sin^2\theta}{r}\mathrm{d}T\mathrm{d}\varphi\ . \end{aligned} \tag{9.2}$$

Note that we keep terms up to $\mathcal{O}(\varepsilon^3)$ in the $\tilde{g}_{tt}$ component, and lower-order terms in ε in other components because the motion of stars is assumed to be nonrelativistic. Indeed, in this case the spatial variation is suppressed with respect to the time variation along the trajectory by the 3-velocity $v\sim\sqrt{\varepsilon}$, i.e. $\mathrm{d}x^i\sim\sqrt{\varepsilon}\mathrm{d}t$, and therefore one only needs to keep lower-order terms in the spatial components of the metric. At this PN order, the metric is circular (meaning it is unchanged under the reflection $(t,\varphi)\to(-t,-\varphi)$), and the expansion is very similar to that of the Kerr metric. One can also check that the Ricci tensor for the metric (9.2) is nonzero only at ε^3 order, i.e. $R_{\mu\nu}\sim\mathcal{O}(\varepsilon^3)$ (in these coordinates). This can be seen by evaluating the Ricci tensor for the full metric (8.11). Thus one can say that the metric (9.2) is Ricci-flat up to the order ε^2.

Once we have read off the mass and spin of the black hole from the $\tilde{g}_{tt}$ and $\tilde{g}_{t\varphi}$ terms, the disformal factor D only enters the quadrupole terms proportional to χ^2 in Eq. (9.2). These terms correspond to the leading-order contributions of the Newtonian quadrupole moment, even though we will refer to them as 2PN in the context of a large r expansion. In other words, the disformal metric is equivalent to the Kerr metric up to 1.5PN order for generic D. To better understand the form of deviations at higher PN orders, it is instructive to compare the metric (9.2) to a non-Kerr metric at that order. A particularly interesting example is the Butterworth-Ipser (BI) metric [235, 236], which was constructed to model a rapidly rotating star. It is usually expressed using the ansatz of Ref. [237] for a circular and axisymmetric metric in quasi-isotropic coordinates:

$$\mathrm{d}s^2=-e^{2\nu}\mathrm{d}t^2+e^{2\Psi}\left(\mathrm{d}\varphi-\tilde{\omega}\mathrm{d}t\right)^2+e^{2\mu}\left(\mathrm{d}R^2+R^2\mathrm{d}\theta^2\right)\ ,$$

where ν, Ψ, $\tilde{\omega}$ and μ are functions of R and θ. The BI metric at 2PN order is given by the following expressions (see for instance Ref. [238][1]):

$$\nu=-\frac{\tilde{M}}{R}+\left[-\frac{1}{12}+a_0-(4a_0+q)\,P_2(\cos\theta)\right]\frac{\tilde{M}^3}{R^3}+\mathcal{O}(R^{-4})\ ,$$

[1] There is a typo in Eq. (3.29c) of this reference, where the quantity μ_S should be added to the right-hand-side.

$$\mu = \frac{\tilde{M}}{R} - \left[\frac{1}{4} + a_0 - 4a_0 P_2(\cos\theta)\right]\frac{\tilde{M}^2}{R^2} + \mathcal{O}(R^{-3}) ,$$
$$\Psi = \log(R\sin\theta) + \frac{\tilde{M}}{R} + \left[3a_0 - \frac{1}{4}\right]\frac{\tilde{M}^2}{R^2} + \mathcal{O}(R^{-3}) ,$$
$$\tilde{\omega} = \frac{2\chi\tilde{M}^2}{R^3} + +\mathcal{O}(R^{-4}) , \tag{9.3}$$

where a_0 and q are quadrupole parameters, and $P_2(x) = (3x^2-1)/2$ is a Legendre polynomial. We adopt here the notations of Ref. [238] (but we use a_0 instead of their a to avoid confusion with the Kerr spin parameter). With these conventions, the parameter q corresponds to the coordinate invariant quadrupole moment, as pointed out in Ref. [239] (see also Ref. [240]). In order to compare the asymptotic expansions of the disformed Kerr and the BI metrics, we write the 2PN order expansion of the BI metric in BL-like coordinates. One can show that the disformed metric can be written in quasi-isotropic coordinates up to 2PN order by the coordinate transformation

$$r = R\left[1 + \frac{\tilde{M}}{2R}\left(1 + \frac{\tilde{\chi}}{\sqrt{1+D}}\right)\right]\left[1 + \frac{\tilde{M}}{2R}\left(1 - \frac{\tilde{\chi}}{\sqrt{1+D}}\right)\right] . \tag{9.4}$$

When $D = 0$, this coordinate redefinition brings the full Kerr metric in BL coordinates to quasi-isotropic ones [241]. However, for the disformed metric this is true only up to 2PN order. By inverting this relation, we obtain the BI metric in BL-like coordinates at 2PN order:

$$\begin{aligned} \mathrm{d}s^2_{\rm BI} = &-\left(1 - \frac{2\tilde{M}}{r} + \frac{2\tilde{M}^3}{r^3}\left[q + 6a_0 + \frac{\tilde{\chi}^2}{2(1+D)} - 3(4a_0+q)\cos^2\theta\right]\right)\mathrm{d}t^2 \\ &+\left(1 + \frac{2\tilde{M}}{r} + \frac{4\tilde{M}^2}{r^2} + \frac{\tilde{M}^2}{r^2}\left[6a_0\cos 2\theta - \frac{\tilde{\chi}^2}{2(1+D)}\right]\right)\mathrm{d}r^2 \\ &+r^2\left(1 + \frac{\tilde{M}^2}{r^2}\left[6a_0\cos 2\theta + \frac{\tilde{\chi}^2}{2(1+D)}\right]\right)\mathrm{d}\theta^2 \\ &-\frac{4\tilde{M}^2\tilde{\chi}\sin^2\theta}{r}\mathrm{d}t\mathrm{d}\varphi + r^2\sin^2\theta\left(1 + \frac{\tilde{M}^2}{r^2}\left[6a_0 + \frac{\tilde{\chi}^2}{2(1+D)}\right]\right)\mathrm{d}\varphi^2 , \end{aligned} \tag{9.5}$$

One can see that the disformed Kerr and the BI metrics can indeed be matched at 2PN order. A direct comparison of the above line element to the metric (9.2) gives the following identification of the parameters for the disformed metric in the case of generic D:

$$a_0^{(D)} = \frac{\tilde{\chi}^2}{12(1+D)} , \qquad q^{(D)} = -\frac{\tilde{\chi}^2}{1+D} , \tag{9.6}$$

It may seem surprising that such a matching exists, taking into account the completely different nature of the disformed Kerr and BI metrics, and given that there are only

two free parameters at hand. It should be noted however, that at higher PN orders, where the noncircularity of the disformed metric (re)appears, such a matching cannot be done as the BI metric is circular (see for example Refs. [238, 242]). Furthermore, for some limiting cases of D that we will consider below, the matching does not exist, i.e. the disformed metric does not fall in the BI form, even at 2PN order.

In GR, the higher multipole moments M_l and S_l of the Kerr metric are uniquely determined as a function of the mass $\tilde{M}$ and spin $\tilde{a}$ of the black hole according to the formula [243, 244]

$$M_l + iS_l = \tilde{M}(i\tilde{a})^l \,. \tag{9.7}$$

We have $M_0 = \tilde{M}$, $S_1 = \tilde{M}\tilde{a}$ and $M_2 = -\tilde{M}\tilde{a}^2$. Hence, for the Kerr metric, the dimensionless quadrupole moment q reads

$$q^{(K)} = -\tilde{\chi}^2 \,. \tag{9.8}$$

For generic D we have $q^{(K)} \neq q^{(D)}$, which means that the no-hair theorem is violated for the disformed Kerr spacetime. In the future, the spin and quadrupole moment of Sgr A* will be measured, providing a test of the previous theorem.

It is instructive to compare the Kerr disformation to other metrics presented in the literature in the asymptotic regime, i.e. for large r. The main challenge here is that normally line elements are written in different coordinates, which makes a direct comparison impossible. We will write all of the metrics in Boyer-Lindquist-like coordinates, so that we can see a connection to our asymptotic expansion of the disformed Kerr metric, given by Eq. (9.2).

A well-known example of an axisymmetric and stationary spacetime is the Hartle-Thorne (HT) metric [245], which was constructed to model slowly rotating stars. Note that the "quasi-Kerr" metric [246], sometimes used as an alternative to the Kerr metric, is exactly the HT metric up to 2PN order. The HT metric for slowly rotating stars can be written in a form which reduces to BL coordinates in the Kerr limit. At 2PN order, this metric reads

$$\begin{aligned} \mathrm{d}s^2_{\mathrm{HT}} = &-\left(1 - \frac{2\tilde{M}}{r} - \frac{\tilde{M}^3}{r^3}\left[q_{\mathrm{HT}} - \tilde{\chi}^2 + (\tilde{\chi}^2 - 3q_{\mathrm{HT}})\cos^2\theta\right]\right)\mathrm{d}t^2 \\ &+ \left(1 + \frac{2\tilde{M}}{r} + \frac{\tilde{M}^2(4 - \tilde{\chi}^2\sin^2\theta)}{r^2}\right)\mathrm{d}r^2 + r^2\left(1 + \frac{\tilde{M}^2\tilde{\chi}^2\cos^2\theta}{r^2}\right)\mathrm{d}\theta^2 \\ &+ r^2\sin^2\theta\left(1 + \frac{\tilde{M}^2\tilde{\chi}^2}{r^2}\right)\mathrm{d}\varphi^2 - \frac{4\tilde{M}^2\tilde{\chi}\sin^2\theta}{r}\mathrm{d}t\mathrm{d}\varphi \,. \end{aligned} \tag{9.9}$$

We have used the expression of the metric in the appendix of Ref. [245][2] with the identification $Q = q_{\mathrm{HT}}\tilde{M}^3$ and $J = \tilde{\chi}\tilde{M}^2$. The HT metric up to 2PN order is a

[2]Notice a typo in the coordinate transformation to BL-like coordinates (as pointed out in Ref. [246]).

subclass of the BI metric. This can be seen by comparing Eqs. (9.9) and (9.5) (where one sets $D = 0$) with the identification $q = -q_{\rm HT}$ and $a_0 = \tilde{\chi}^2/12$. The disformed metric given by Eq. (9.2) cannot be matched with Eq. (9.9), as can be seen from a direct comparison. The other variants of Kerr disformations that we will consider in the following cannot be matched to the HT metric either.

Another spacetime worth considering is the Johannsen metric [178], which describes a rotating black hole, unlike the HT metric. Using the notations of Ref. [178], the line element at 2PN order in BL coordinates reads:

$$\begin{aligned} \mathrm{d}s^2_{\rm J} = &-\left(1-\frac{2\tilde{M}}{r}+\frac{\tilde{M}^3}{r^3}\left[2\alpha_{13}-\epsilon_3-2\tilde{\chi}^2\cos^2\theta\right]\right)\mathrm{d}t^2 \\ &+\left(1+\frac{2\tilde{M}}{r}+\frac{\tilde{M}^2(4-\alpha_{52}-\tilde{\chi}^2\sin^2\theta)}{r^2}\right)\mathrm{d}r^2+r^2\left(1+\frac{\tilde{M}^2\tilde{\chi}^2\cos^2\theta}{r^2}\right)\mathrm{d}\theta^2 \\ &+r^2\sin^2\theta\left(1+\frac{\tilde{M}^2\tilde{\chi}^2}{r^2}\right)\mathrm{d}\varphi^2-\frac{4\tilde{M}^2\tilde{\chi}\sin^2\theta}{r}\mathrm{d}t\mathrm{d}\varphi\ . \end{aligned} \tag{9.10}$$

Note that the Johannsen metric is circular by construction. The Kerr metric at this order is obtained by setting $\alpha_{13} = \alpha_{52} = \epsilon_3 = 0$ in the above expression. In general, the metric (9.10) does not match the BI metric at 2PN order. It only happens for a special combination of the parameters, i.e. $q = -\tilde{\chi}^2$, $a_0 = \tilde{\chi}^2/12$, $\alpha_{52} = 0$ and $\epsilon_3 = 2\alpha_{13}$. In this case the coordinate invariant quadrupole is the same as for Kerr and the no-hair theorem is not violated at this order. The Johannsen metric can also be mapped to other Kerr-like metrics, see Ref. [178] for details. One can also verify by comparing Eqs. (9.10) and (9.2) that the disformed metric in the generic case does not match the Johannsen metric at this order. The same conclusion holds for the other variants of the disformed metric.

9.2 Two-timescale analysis for the secular variation of orbital elements

In this section, we present the two-timescale analysis that we will use to calculate the secular variation of orbital parameters, closely following Ref. [234]. We will use the standard osculating orbit method, see for instance Ref. [247]. In general, the 3-dimensional acceleration of a test body can be written in the following form:

$$\mathbf{a} = -\frac{\tilde{M}}{r^3}\mathbf{x}+\mathbf{F}\ , \tag{9.11}$$

where the first term on the right-hand side corresponds to the Newtonian acceleration, $\mathbf{F}$ is the perturbation of the Newtonian acceleration and $\mathbf{x}$ is the position vector in space, so that $r = |\mathbf{x}|$. We need to calculate the projections of the acceleration (9.11)

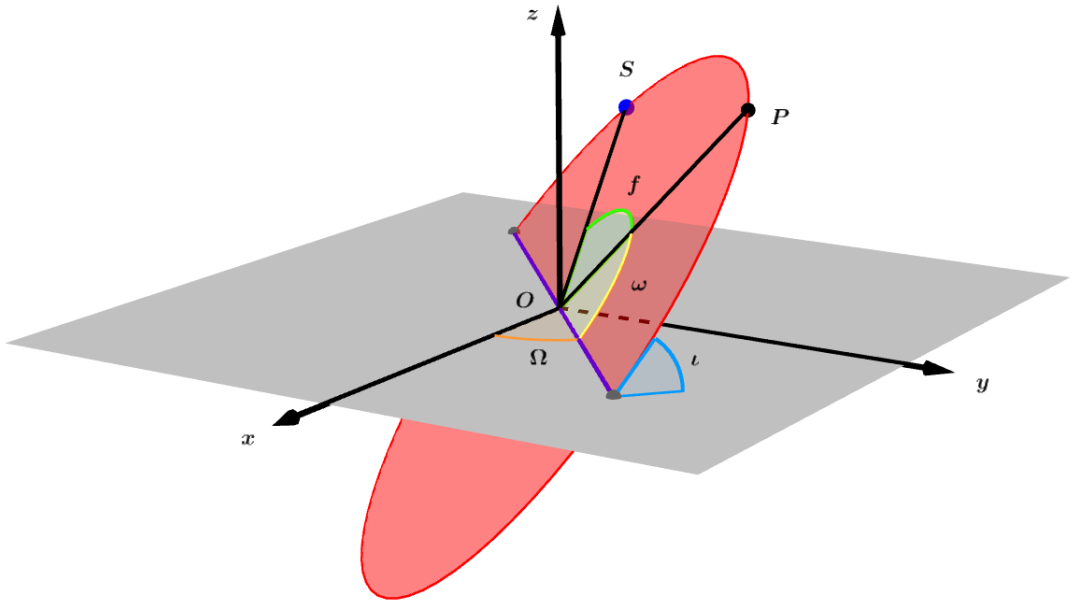

Figure 1: Kepler orbit of a star S around the black hole located at O. The purple line is called the line of nodes, and it is defined by the intersecting points of the star's trajectory with the (Oxy) reference plane. The nodal angle Ω gives the position of this line with respect to the (Ox) axis. Starting from the line of nodes, the pericenter P of the trajectory is given by the pericenter angle ω, while ι represents the inclination angle of the ellipse with respect to the (Oxy) plane. Finally, the true anomaly f gives the position of the star S with respect to the pericenter P.

along the orthogonal directions $\mathbf{x}$, $\mathbf{h} = \mathbf{x} \times \mathbf{v}$, and $\mathbf{h} \times \mathbf{x}$, where $\mathbf{v} = \mathrm{d}\mathbf{x}/\mathrm{d}t$ is the 3-velocity of the star. These projections are given by

$$\mathcal{S} = \frac{1}{r}\mathbf{x} \cdot \mathbf{F} \,, \qquad \mathcal{T} = \frac{1}{hr}(\mathbf{h} \times \mathbf{x}) \cdot \mathbf{F} \,, \qquad \mathcal{W} = \frac{1}{h}\mathbf{h} \cdot \mathbf{F} \,,$$

where $h = |\mathbf{h}|$. The expressions for the components of $\mathbf{x}$ in Cartesian coordinates (see Fig. 1) with respect to the orbital elements read

$$\begin{aligned} x &= r\left[\cos\Omega\cos u - \sin\Omega\cos\iota\sin u\right] \,, \\ y &= r\left[\sin\Omega\cos u + \cos\Omega\cos\iota\sin u\right] \,, \\ z &= r\sin\iota\sin u \,, \end{aligned}$$

where $u = \omega + f$. To obtain the components of $\mathbf{v}$ one differentiates the above expression assuming that all the angles are constant except for u. In the following, we use the standard relations

$$r = \frac{p}{1 + e\cos f} \,, \qquad \frac{dr}{dt} = \frac{eh}{p}\sin f \,, \qquad h = \sqrt{\tilde{M}p} \,, \qquad p = A\left(1 - e^2\right) \,, \tag{9.12}$$

where A and e are respectively the semi-major axis and eccentricity of the ellipse. In order for the limit $e \to 0$ to be well defined, the alternative orbit parameters $\alpha = e\cos\omega$ and $\beta = e\sin\omega$ are introduced [248]. With the above definitions, we can write the Gauss equations for the evolution of the orbital parameters:[3]

$$\begin{aligned}
\frac{\mathrm{d}p}{\mathrm{d}t} &= 2r\sqrt{\frac{p}{\tilde{M}}}\mathcal{T}\ , \\
\frac{\mathrm{d}\alpha}{\mathrm{d}t} &= \sqrt{\frac{p}{\tilde{M}}}\left[\mathcal{S}\sin u + \left(\frac{\alpha r}{p} + \left(1+\frac{r}{p}\right)\cos u\right)\mathcal{T} + \frac{\beta r\mathcal{W}}{p}\cot\iota\sin u\right]\ , \\
\frac{\mathrm{d}\beta}{\mathrm{d}t} &= \sqrt{\frac{p}{\tilde{M}}}\left[-\mathcal{S}\cos u + \left(\frac{\beta r}{p} + \left(1+\frac{r}{p}\right)\sin u\right)\mathcal{T} - \frac{\alpha r\mathcal{W}}{p}\cot\iota\sin u\right]\ , \\
\frac{\mathrm{d}\iota}{\mathrm{d}t} &= \frac{r\mathcal{W}\cos u}{\sqrt{\tilde{M}p}}\ , \\
\frac{\mathrm{d}\Omega}{\mathrm{d}t} &= \frac{r\mathcal{W}\sin u}{\sqrt{\tilde{M}p}\sin\iota}\ , \\
\frac{\mathrm{d}u}{\mathrm{d}t} &= \frac{h}{r^2} - \cos\iota\frac{\mathrm{d}\Omega}{\mathrm{d}t}\ .
\end{aligned} \tag{9.13}$$

Using this system, we follow the analysis of Ref. [234] to obtain the secular variation of orbital elements. We perform a two-timescale analysis [234, 248–251] by introducing a second variable $\Theta = \epsilon u$, where ϵ is a bookkeeping parameter that is useful to keep track of small terms. Since Θ varies on longer timescales, in the following we treat u and Θ as independent variables. This approach allows us to make an average over a period using the variable u, while keeping Θ as a slow varying (almost constant) variable. First, we use the last equation of the system (9.13) to trade dt for du in all other equations and write them in the form,

$$\frac{\mathrm{d}X_k}{\mathrm{d}u} = \epsilon Q_k\left(X_l(u), u\right)\ , \tag{9.14}$$

where the X_k stands for the orbital parameters p, α, β, ι and Ω. In the two-timescale approach, we have

$$\frac{\mathrm{d}}{\mathrm{d}u} = \frac{\partial}{\partial u} + \epsilon\frac{\partial}{\partial\Theta} \tag{9.15}$$

We define the average $\langle\cdot\rangle$ and average-free part $\mathcal{AF}$ as

$$\begin{aligned}
\langle C\rangle &= \frac{1}{2\pi}\int_0^{2\pi} C(\Theta, u)\,\mathrm{d}u\ , \\
\mathcal{AF}\left(C\right) &= C(\Theta, u) - \langle C(\Theta, u)\rangle\ .
\end{aligned} \tag{9.16}$$

[3] See for instance Ref. [234], though notice a typo in the expressions for $\mathrm{d}\alpha/\mathrm{d}t$ and $\mathrm{d}\beta/\mathrm{d}t$.

and each orbital parameter is decomposed as:

$$X_k(\Theta, u) = \bar{X}_k(\Theta) + \epsilon Z_k(\bar{X}_l, u) \ , \tag{9.17}$$

$$\bar{X}_k(\Theta) = \langle X_k(\Theta, u) \rangle \ , \tag{9.18}$$

$$\langle Z_k(\bar{X}_k(\Theta), u) \rangle = 0 \ . \tag{9.19}$$

This analysis is not necessary to obtain leading-order terms in the variation of orbital parameters, but the periodic contributions which appear in the Z_k must be taken into account if one calculates higher-order terms in ϵ. Let us now derive the formula that we will use to calculate the secular variation of orbital parameters, following Ref. [234]. By using the previous decomposition with the evolution equations (9.14), we obtain the following expressions:

$$\frac{\mathrm{d}\bar{X}_k}{\mathrm{d}\Theta} = \langle Q_k \left(\bar{X}_l + \epsilon Z_l, u \right) \rangle \ , \tag{9.20}$$

$$\frac{\partial Z_k}{\partial u} = \mathcal{AF} \left[Q_k \left(\tilde{X}_l + \epsilon Z_l, u \right) \right] - \epsilon \frac{\partial Z_k}{\partial \bar{X}_m} \frac{\mathrm{d}\bar{X}_m}{\mathrm{d}\Theta} \tag{9.21}$$

We want to obtain the corrections up to order ϵ^2 in Eq. (9.14), so we must calculate them up to order ϵ in terms of Θ derivatives. At the end, we sill replace $\Theta = \epsilon u$ to obtain the desired result. We expand the functions Z_k as

$$Z_k = Z_k^{(0)} + \epsilon Z_k^{(1)} + \dots \ , \tag{9.22}$$

and we perform a Taylor expansion of Eq. (9.21). The result is

$$\frac{\mathrm{d}\bar{X}_k}{\mathrm{d}\Theta} = \langle Q_k^{(0)} \rangle + \epsilon \langle Q_{k,l}^{(0)} Z_l^{(0)} \rangle + \mathcal{O}(\epsilon^2) \ , \tag{9.23}$$

where $Q_k^{(0)} = Q_k(\bar{X}_l, u)$ and $Q_{k,l}^{(0)} = (\partial Q_k / \partial \bar{X}_l)(\bar{X}_l, u)$. We must now determine $Z^{(0)}$, in order to obtain the final formula for the secular shifts. Using Eq. (9.21), we obtain that

$$\frac{\mathrm{d}Z_k^{(0)}}{\mathrm{d}u} = \mathcal{AF} \left[Q_k^{(0)} \right] \ , \tag{9.24}$$

and one can show that the solution reads [234]

$$Z_k^{(0)} = \int_0^u Q_k^{(0)} \mathrm{d}u' - (u + \pi) \langle Q_k^{(0)} \rangle + \langle u Q_k^{(0)} \rangle \ . \tag{9.25}$$

Finally, injecting this solution into Eq. (9.23) and multiplying by ϵ yields

$$\frac{\mathrm{d}\bar{X}_k}{\mathrm{d}u} = \epsilon \langle Q_k^0 \rangle + \epsilon^2 \left[\langle Q_{k,l}^0 \int_0^u Q_l^0 \mathrm{d}u' \rangle + \langle Q_{k,l}^0 \rangle \langle u Q_l^0 \rangle - \langle (u + \pi) \, Q_{k,l}^0 \rangle \langle Q_l^0 \rangle \right] + \mathcal{O}\left(\epsilon^3\right) \ , \tag{9.26}$$

In the following section, we will use this formula to find the secular variation of orbital parameters for different ranges of the disformal parameter D.

9.3 Orbital perturbations for the disformed Kerr metric

In this section, we use the technique described above to calculate the secular shifts of orbital parameters for different cases involving the disformal parameter D. We will start with a generic D, and then consider limiting cases that provide interesting phenomenology. As is common in the literature, we work with Kerr harmonic coordinates, i.e. coordinates verifying $\Box x^\mu_{\rm H} = 0$, where the $\Box$ operator is associated to the Kerr metric with rescaled Kerr parameters $\tilde{M}$ and $\tilde{a}$. It should be made clear that one has $\tilde{\Box} x^\mu_{\rm H} \neq 0$, which means that these coordinates are *not* harmonic for the disformed metric. The idea, however, is to use the same coordinates that one uses when assuming the Kerr black hole and GR, in order to better gauge the differences arising from the disformed spacetime. This is also the reason why we work with the black hole parameters $\{\tilde{a}, \tilde{M}\}$ determined from the asymptotic expansion. Therefore, this choice of coordinates makes it easier to link our results to observations.

In the following, we first consider the case of generic D in Section 9.3.1, and then study different limits of the parameter D. In particular, we investigate the noncircular Schwarzschild and quasi-Weyl metrics presented in the previous chapter. In addition, we study the limit of small but finite $(1+D)$, for which deviations from the Kerr geometry are enhanced, and consequently the corrections to orbital shifts become larger. We consider two different regimes separately: $(1+D) \sim \varepsilon$ in Section 9.3.4, and $(1+D) \sim \sqrt{\varepsilon}$ in Section 9.3.5.

9.3.1 Disformal Kerr: generic case

We start with the generic case, where D is arbitrary, but not too large or too close to -1. In terms of the BL coordinates $\{t, r, \theta, \varphi\}$, the harmonic coordinates $x^\mu_{\rm H}$ can be written as [234, 252]

$$\begin{aligned} t_{\rm H} &= t \,, \\ x_{\rm H} &= \sqrt{\tilde{R}^2 + a^2}\cos\tilde{\psi}\sin\theta \,, \\ y_{\rm H} &= \sqrt{\tilde{R}^2 + a^2}\sin\tilde{\psi}\sin\theta \,, \\ z_{\rm H} &= \tilde{R}\cos\theta \,, \end{aligned} \tag{9.27}$$

where $\tilde{R}$ and $\tilde{\psi}$ are defined as

$$\begin{aligned} \tilde{R} &= r - \tilde{M} \,, \\ \tilde{\psi} &= \varphi + \tan^{-1}\left(\frac{\tilde{a}}{r-\tilde{M}}\right) + \int \frac{\tilde{a}}{\Delta}\mathrm{d}r \,. \end{aligned} \tag{9.28}$$

We now invert these relations up to $\mathcal{O}(\varepsilon^3)$, and replace the BL-like coordinates of Eq. (9.2) by harmonic coordinates (we drop the index "H" in the following). The

result is:

$$\begin{aligned}
\tilde{g}_{00} &= -1 + \frac{2\tilde{M}}{r} - \frac{2\tilde{M}^2}{r^2} + \frac{2\tilde{M}^3}{r^3} + \frac{\tilde{M}^3\tilde{\chi}^2}{r^3}\left[1 - \frac{3+D}{1+D}\left(\mathbf{n}\cdot\mathbf{s}\right)^2\right] + \mathcal{O}\left(\varepsilon^4\right) \ , \\
\tilde{g}_{0j} &= \frac{2\tilde{M}^2\tilde{\chi}}{r^2}\left(\mathbf{n}\times\mathbf{s}\right)_j + \mathcal{O}\left(\varepsilon^3\right) \ , \\
\tilde{g}_{ij} &= \left[1 + \frac{2\tilde{M}}{r} + \frac{\tilde{M}^2}{r^2}\left(1 - \frac{D\tilde{\chi}^2}{1+D}\right)\right]\delta_{ij} + \frac{\tilde{M}^2}{r^2}n_i n_j \\
&\quad + \frac{D\tilde{M}^2\tilde{\chi}^2}{(1+D)r^2}\left[2n_i n_j + s_i s_j - 2s_{(i}n_{j)}(\mathbf{n}\cdot\mathbf{s})\right] + \mathcal{O}\left(\varepsilon^{5/2}\right) \ ,
\end{aligned} \tag{9.29}$$

where $\mathbf{n} = \mathbf{x}/r$, $\mathbf{s} = \mathbf{J}/J = \mathbf{e}_z$, and $r = r(x,y,z)$ is now the radial coordinate in the old metric expressed in harmonic coordinates. When $D = 0$, the expressions (9.29) reduce to the Kerr metric components in harmonic coordinates (see Ref. [234]).

We now apply the method described in Section 9.2 to the metric (9.29). For generic values of D, the secular variation of orbit elements up to 2PN order is given by,

$$\begin{aligned}
\frac{\mathrm{d}\bar{p}}{\mathrm{d}u} &= 0 \ , \\
\frac{\mathrm{d}\bar{\alpha}}{\mathrm{d}u} &= -\frac{3\tilde{M}\bar{\beta}}{\bar{p}} + 6\tilde{\chi}\bar{\beta}\cos\bar{\iota}\left(\frac{\tilde{M}}{\bar{p}}\right)^{3/2} + \frac{3\tilde{M}^2\bar{\beta}}{4\bar{p}^2}\left(10 - \bar{\alpha}^2 - \bar{\beta}^2\right) - \frac{3\tilde{M}^2\bar{\beta}\tilde{\chi}^2(5\cos^2\bar{\iota} - 1)}{4\bar{p}^2(1+D)} \ , \\
\frac{\mathrm{d}\bar{\beta}}{\mathrm{d}u} &= \frac{3\tilde{M}\bar{\alpha}}{\bar{p}} - 6\tilde{\chi}\bar{\alpha}\cos\bar{\iota}\left(\frac{\tilde{M}}{\bar{p}}\right)^{3/2} - \frac{3\tilde{M}^2\bar{\alpha}}{4\bar{p}^2}\left(10 - \bar{\alpha}^2 - \bar{\beta}^2\right) + \frac{3\tilde{M}^2\bar{\alpha}\tilde{\chi}^2(5\cos^2\bar{\iota} - 1)}{4\bar{p}^2(1+D)} \ , \\
\frac{\mathrm{d}\bar{\iota}}{\mathrm{d}u} &= 0 \ , \\
\frac{\mathrm{d}\bar{\Omega}}{\mathrm{d}u} &= 2\tilde{\chi}\left(\frac{\tilde{M}}{\bar{p}}\right)^{3/2} - \frac{3\tilde{M}^2\tilde{\chi}^2\cos\bar{\iota}}{2\bar{p}^2(1+D)} \ .
\end{aligned} \tag{9.30}$$

The corresponding relations for $\bar{\omega}$ and $\bar{e}$ read:

$$\begin{aligned}
\frac{\mathrm{d}\bar{\omega}}{\mathrm{d}u} &= \frac{3\tilde{M}}{\bar{p}} - 6\tilde{\chi}\cos\bar{\iota}\left(\frac{\tilde{M}}{\bar{p}}\right)^{3/2} - \frac{3\tilde{M}^2(10 - \bar{e}^2)}{4\bar{p}^2} + \frac{3\tilde{M}^2\tilde{\chi}^2(5\cos^2\bar{\iota} - 1)}{4\bar{p}^2(1+D)} \ , \\
\frac{\mathrm{d}\bar{e}}{\mathrm{d}u} &= 0 \ .
\end{aligned} \tag{9.31}$$

The expressions for the Kerr metric are obtained by setting $D = 0$ in the above equations. Note that terms of order $\mathcal{O}(\varepsilon^{n+1})$ in the metric correspond to $\mathcal{O}(\varepsilon^n)$ order in the equations for the secular shifts (9.30). In particular, in the Newtonian approximation, the right-hand sides of the equations in the system (9.30) are identically zero, so that there are no shifts in any of the orbital parameters. The leading-order PN corrections

of $\mathcal{O}(\varepsilon)$ lead to a variation of α and β, which correspond to the standard pericenter precession as in GR. The Lense-Thirring (or frame-dragging) effect is due to the term $\mathcal{O}(\varepsilon^{3/2})$, corresponding to 1.5PN order in the last equation of (9.30), which results in a variation of Ω. Similar terms also enter the corrections to the shifts of α and β. The higher-order Schwarzschild corrections at 2PN order in the variation of α and β (the third term on right-hand side of (9.30)), are unaffected by the modification of gravity in this case. Crucially however, quadrupole corrections proportional to $\tilde{\chi}^2$ now get corrected by the factor $(1+D)^{-1}$. As expected, the secular variation of the orbital parameters remains unchanged up to the Lense-Thirring terms when compared to Kerr, while the quadrupole terms are modified.

9.3.2 Case of the noncircular Schwarzschild metric

We now consider the noncircular Schwarzschild metric (8.58), which we presented in Section 8.3. Similarly to the generic case considered above, we change coordinates to those that are harmonic for the Kerr metric, and expand in ε to obtain:

$$\begin{aligned}
\tilde{g}_{00}^{\rm NCS} &= -1 + \frac{2\tilde{M}}{r} - \frac{2\tilde{M}^2}{r^2} + \frac{2\tilde{M}^3}{r^3} + \frac{\tilde{M}^3\tilde{\chi}^2}{r^3}\left[1-(\mathbf{n}\cdot\mathbf{s})^2\right] + \mathcal{O}\left(\varepsilon^4\right) \,, \\
\tilde{g}_{0j}^{\rm NCS} &= \frac{2\tilde{M}^2\tilde{\chi}}{r^2}\left(\mathbf{n}\times\mathbf{s}\right)_j + \mathcal{O}\left(\varepsilon^3\right) \,, \\
\tilde{g}_{ij}^{\rm NCS} &= \left[1 + \frac{2\tilde{M}}{r} + \frac{\tilde{M}^2}{r^2}\left(1-\tilde{\chi}^2\right)\right]\delta_{ij} + 2\sqrt{2}\tilde{\chi}\left(\mathbf{n}\times\mathbf{s}\right)_{(i}\,n_{j)}\left(\frac{\tilde{M}}{r}\right)^{3/2} + \frac{\tilde{M}^2}{r^2}n_i n_j \\
&\quad + \frac{\tilde{M}^2\tilde{\chi}^2}{r^2}\left[2n_i n_j + s_i\varepsilon s_j - 2s_{(i}n_{j)}(\mathbf{n}\cdot\mathbf{s})\right] + \mathcal{O}\left(\varepsilon^{5/2}\right) \,. \qquad (9.32)
\end{aligned}$$

where r is now the radial harmonic coordinate relevant for the PN expansion. This metric is almost identical to the $D\to\infty$ limit of Eq. (9.29), the only difference being the term $\sim\mathcal{O}(\varepsilon^{3/2})$ in the $\tilde{g}_{ij}^{(\rm NCS)}$ components. This term comes from the $\tilde{g}_{r\varphi}$ component of Eq. (8.58), meaning that the metric is already noncircular at this PN order (unlike in the case of generic D discussed above). In particular, this implies that the NCS metric cannot be matched to the BI metric (9.5) at this PN order. It can be shown that the Ricci tensor for the NCS metric is nonzero only at ε^3 order, as in the case of generic D.

We now perform the two-timescale analysis described in Section 9.2, and obtain:

$$\begin{aligned}
\frac{\mathrm{d}\bar{p}}{\mathrm{d}u} &= 0 \,, \\
\frac{\mathrm{d}\bar{\alpha}}{\mathrm{d}u} &= -\frac{3\tilde{M}\bar{\beta}}{\bar{p}} + 6\tilde{\chi}\bar{\beta}\cos\bar{\iota}\left(\frac{\tilde{M}}{\bar{p}}\right)^{3/2} + \frac{3\tilde{M}^2\bar{\beta}}{4\bar{p}^2}\left(10-\bar{\alpha}^2-\bar{\beta}^2\right) \,, \\
\frac{\mathrm{d}\bar{\beta}}{\mathrm{d}u} &= \frac{3\tilde{M}\bar{\alpha}}{\bar{p}} - 6\tilde{\chi}\bar{\alpha}\cos\bar{\iota}\left(\frac{\tilde{M}}{\bar{p}}\right)^{3/2} - \frac{3\tilde{M}^2\bar{\alpha}}{4\bar{p}^2}\left(10-\bar{\alpha}^2-\bar{\beta}^2\right) \,,
\end{aligned}$$

$$\frac{\mathrm{d}\bar{\iota}}{\mathrm{d}u} = 0 \,,$$
$$\frac{\mathrm{d}\bar{\Omega}}{\mathrm{d}u} = 2\tilde{\chi}\left(\frac{\tilde{M}}{\bar{p}}\right)^{3/2} \,. \tag{9.33}$$

The above expressions can be alternatively found by taking the limit $D \to \infty$ in in Eq. (9.30). Hence, the noncircular terms in the spatial components of Eq. (9.32) do not influence the secular shifts at this PN order, as their effect averages to 0 over an orbital period. As we can see by comparing Eqs. (9.33) and (9.30) where we set $D = 0$, the variation of the orbit elements are modified at 2PN order, while the 1PN and Lense-Thirring terms remain the same. The difference appearing at 2PN order is in the quadrupole terms. In the present case they do not appear at this order, while they are present for Kerr. In terms of $\bar{\omega}$, we obtain the following expression at 2PN order:

$$\frac{\mathrm{d}\bar{\omega}}{\mathrm{d}u} = \frac{3\tilde{M}}{\bar{p}} - 6\chi\cos\bar{\iota}\left(\frac{\tilde{M}}{\bar{p}}\right)^{3/2} - \frac{3\tilde{M}^2(10-\bar{e}^2)}{4\bar{p}^2} \,. \tag{9.34}$$

In comparison to the Kerr case, the quadrupole term is absent in the above expression, while other terms are the same as Kerr, namely the 1PN and 2PN Schwarzschild corrections and the Lense-Thirring term are recovered. This means that the no-hair theorem is violated for this spacetime.

9.3.3 Case of the quasi-Weyl metric

We now consider the quasi-Weyl metric (8.55), which was introduced in Section 8.3. After the coordinate change (8.21), the metric reads

$$\begin{aligned}\mathrm{d}\tilde{s}^2_{\mathrm{QW}} = &-\left(1-\frac{2\tilde{M}r}{\rho^2}\right)\mathrm{d}T^2 - \frac{4a^2\sqrt{2\tilde{M}^3 r}\cos^2\theta}{\rho^2(r-2\tilde{M})\sqrt{a^2+r^2}}\mathrm{d}T\mathrm{d}r \\ &+ \frac{r^5(r-2\tilde{M}) + 2a^2r^3\cos^2\theta(r-3\tilde{M}) + a^4\cos^4\theta(r-2\tilde{M})^2}{\rho^2(r-2\tilde{M})^2(r^2+a^2)}\mathrm{d}r^2 \\ &+ \rho^2\mathrm{d}\theta^2 + \left(r^2+a^2\right)\sin^2\theta\mathrm{d}\varphi^2 \,.\end{aligned} \tag{9.35}$$

We saw that in this case, one must keep the parameter $\chi = a/\tilde{M}$ instead of the physical spin $\tilde{\chi}$. The 2PN expression of the above metric can be obtained from Eq. (9.2) by setting $\tilde{\chi} = \chi\sqrt{1+D}$ and taking the limit $D \to -1$. Note that we also assume $\chi \sim \mathcal{O}(1)$ in order to perform the expansion. At this PN order, the quasi-Weyl metric can also be matched to the BI metric (9.5), with the BI parameters $q = -\chi^2$ and $a_0 = \chi^2/12$. The resulting 2PN metric does not contain the Lense-Thirring term, which could be anticipated since the physical rotation parameter $\tilde{\chi} = 0$ in this case. Meanwhile, the metric still contains a free quadrupole parameter χ. As in the two previous cases, the Ricci tensor for the metric (9.35) is nonzero only at ε^3 order.

Similarly to the generic case described above, we change to Kerr harmonic coordinates and calculate the secular variations of orbital parameters, following the method of Section 9.2. We obtain the following results up to 2PN order:

$$\begin{aligned}
\frac{\mathrm{d}\bar{p}}{\mathrm{d}u} &= 0 \,, \\
\frac{\mathrm{d}\bar{\alpha}}{\mathrm{d}u} &= -\frac{3\tilde{M}\bar{\beta}}{\bar{p}} + \frac{3\tilde{M}^2\bar{\beta}}{4\bar{p}^2}\left(10 - \bar{\alpha}^2 - \bar{\beta}^2\right) - \frac{3\tilde{M}^2\bar{\beta}\chi^2}{4\bar{p}^2}\left(5\cos^2\bar{\iota} - 1\right) \,, \\
\frac{\mathrm{d}\bar{\beta}}{\mathrm{d}u} &= \frac{3\tilde{M}\bar{\alpha}}{\bar{p}} - \frac{3\tilde{M}^2\bar{\alpha}}{4\bar{p}^2}\left(10 - \bar{\alpha}^2 - \bar{\beta}^2\right) + \frac{3\tilde{M}^2\bar{\alpha}\chi^2}{4\bar{p}^2}\left(5\cos^2\bar{\iota} - 1\right) \,, \\
\frac{\mathrm{d}\bar{\iota}}{\mathrm{d}u} &= 0 \,, \\
\frac{\mathrm{d}\bar{\Omega}}{\mathrm{d}u} &= -\frac{3\tilde{M}^2\chi^2\cos\bar{\iota}}{2\bar{p}^2} \,.
\end{aligned} \tag{9.36}$$

The above expressions can also be obtained from the system (9.30) by the substitution $\tilde{\chi} = \chi\sqrt{1+D}$ as explained above. As one can see from Eq. (9.36), the Lense-Thirring terms drop out in this limit, which is consistent with the absence of a $(t\varphi)$ term in the metric. However, the quadrupole terms appear at 2PN order, similarly to the Kerr case. While the structure of these terms is the same as for Kerr, the free parameter χ entering the quadrupole terms is not related to the black hole spin, which is zero in the quasi-Weyl case. Hence, the no-hair theorem is violated in this case also.

9.3.4 Enhanced Kerr disformation

Finally, for the two last variants of the Kerr disformation we examine the situation when $(1+D)$ is small but finite. As we saw above, the generic values of D result in a rather mild effect on the secular shifts, i.e. only quadrupole terms in Eq. (9.30) are modified. The limit $D \to -1$ (quasi-Weyl) yields stronger modifications, since $\tilde{\chi} = 0$ in this case, and hence the frame-dragging terms are also modified with respect to Kerr. In contrast to the quasi-Weyl case, here we assume that D has a small finite offset from -1, so that the physical spin remains finite, while the corrections to the Kerr metric are enhanced with respect to the generic case. Indeed, if we take $1 + D \sim \varepsilon$, the terms proportional to $(1+D)^{-1}$ in the metric expansion (9.2) become one order lower in ε. More precisely, we assume the following form for the constant disformal factor:

$$D = -1 + \frac{\tilde{\chi}^2}{\lambda}\varepsilon \,, \qquad \{\lambda, \tilde{\chi}\} \sim \mathcal{O}(1) \,, \tag{9.37}$$

where the factor $\tilde{\chi}^2/\lambda$ is chosen for convenience and we introduced a new parameter λ here. Similarly to the case of generic D discussed above, we perform the coordinate transformation (8.21) in the disformal metric (8.11), and expand the line element to

$\mathcal{O}(\varepsilon^3)$, assuming $\mathrm{d}x^i \sim \sqrt{\varepsilon}\,\mathrm{d}t$. The result is:

$$\begin{aligned}
\mathrm{d}\tilde{s}^2_{\rm EKD} \simeq &-\left(1-\frac{2A\varepsilon}{r}+\frac{2A^3\varepsilon^2\lambda}{r^3}\cos^2\theta-\frac{2A^5\varepsilon^3\lambda^2\cos^4\theta}{r^5}\right)\mathrm{d}t^2\\
&+\left(1+\frac{A\varepsilon(2r-A\lambda\sin^2\theta)}{r^2}+\frac{A^2\varepsilon^2(4r^2-2Ar\lambda+A^2\lambda^2\sin^2\theta)}{r^4}\right)\mathrm{d}r^2\\
&+r^2\left(1+\frac{\varepsilon\lambda A^2}{r^2}\cos^2\theta\right)\mathrm{d}\theta^2+r^2\sin^2\theta\left(1+\frac{\varepsilon\lambda A^2}{r^2}\right)\mathrm{d}\varphi^2\\
&-\frac{4\sqrt{2}A^{7/2}\varepsilon^{5/2}\lambda\cos^2\theta}{r^{7/2}}\mathrm{d}t\mathrm{d}r-\frac{4A^2\varepsilon^2\tilde{\chi}\sin^2\theta}{r}\mathrm{d}t\mathrm{d}\varphi\,. \qquad (9.38)
\end{aligned}$$

We call this metric the Enhanced Kerr disformation (EKD). Note that the above expression cannot be obtained by substituting Eq. (9.37) in the asymptotic expansion (9.2). This is because in Eq. (9.2) we neglected, in particular, terms of the form $\sim(1+D)^{-2}\mathcal{O}(\varepsilon^5)$ in the (tt) component of the metric, which become $\sim\mathcal{O}(\varepsilon^3)$ for values of the disformal parameter given by Eq. (9.37). Similarly, terms $\sim(1+D)^{-1}\mathcal{O}(\varepsilon^{7/2})$ in the (tr) components and $\sim(1+D)^{-1}\mathcal{O}(\varepsilon^3)$ or $\sim(1+D)^{-2}\mathcal{O}(\varepsilon^4)$ in spatial components were neglected in (9.2). However, they become important for the case considered here.

The metric (9.38) is noncircular and its Ricci curvature is nonzero already at ε^2 order, which is one order lower than all other cases considered above. As one of the consequences of noncircularity, the EKD metric cannot be matched to the BI metric (9.5) at this order. Also, due to noncircularity in the generic case (9.2), the off-diagonal term (tr) cannot be eliminated in Eq. (9.38), since $\tilde{g}_{tt}$ depends on θ now. To recover the asymptotic Kerr metric at $\mathcal{O}(\varepsilon^3)$ one replaces $\lambda=\tilde{\chi}^2\varepsilon$ in Eq. (9.38), which corresponds to setting $D=0$. By inverting the relations (9.27) to the right order, the asymptotic expansion (9.38) can be written in the Kerr harmonic coordinates,

$$\begin{aligned}
\tilde{g}^{\rm EKD}_{00} &= -1+\frac{2\tilde{M}}{r}-\frac{2\tilde{M}^2}{r^2}\left[1+\frac{\tilde{A}\,(\mathbf{n}\cdot\mathbf{s})^2}{r}\right]\\
&\quad+\frac{\tilde{M}^3}{r^3}\left[2+\left(1-(\mathbf{n}\cdot\mathbf{s})^2\right)\tilde{\chi}^2+\frac{6\tilde{A}(\mathbf{n}\cdot\mathbf{s})^2}{r}+\frac{2\tilde{A}^2(\mathbf{n}\cdot\mathbf{s})^4}{r^2}\right]+\mathcal{O}\left(\varepsilon^4\right)\,, \qquad (9.39)\\
\tilde{g}^{\rm EKD}_{0j} &= \frac{2\tilde{M}^2\tilde{\chi}}{r^2}\left(\mathbf{n}\wedge\mathbf{s}\right)_j-\frac{2\sqrt{2}\tilde{A}\tilde{M}^{5/2}(\mathbf{n}\cdot\mathbf{s})}{r^{7/2}}n_j+\mathcal{O}\left(\varepsilon^3\right)\,, \qquad (9.40)\\
\tilde{g}^{\rm EKD}_{ij} &= \left[1+\frac{\tilde{M}}{r}\left(2+\frac{\tilde{A}}{r}\right)+\frac{\tilde{M}^2}{r^2}\left(1-\tilde{\chi}^2\right)\right]\delta_{ij}-\frac{2\tilde{A}\tilde{M}}{r^2}n_in_j\\
&\quad+\frac{\tilde{M}^2}{r^2}\left[1+2\tilde{\chi}^2-\frac{2\tilde{A}(\mathbf{n}\cdot\mathbf{s})^2}{r}+\frac{\tilde{A}^2}{r^2}\left(1-(\mathbf{n}\cdot\mathbf{s})^2\right)\right]n_in_j\\
&\quad+\frac{\tilde{A}\tilde{M}}{r^2}\left[1-\frac{\tilde{M}\tilde{\chi}^2}{\tilde{A}}\right]\left[2s_{(i}n_{j)}(\mathbf{n}\cdot\mathbf{s})-s_is_j\right]+\mathcal{O}\left(\varepsilon^{5/2}\right)\,, \qquad (9.41)
\end{aligned}$$

where $\tilde{A} = \lambda A$. The asymptotic expansion of the Kerr metric in harmonic coordinates is recovered by setting $\tilde{A} \to \tilde{M}\tilde{\chi}^2$ and keeping terms up to 2PN order (one can check that the Kerr metric is indeed recovered by comparing to Ref. [234] for instance).

We now apply the osculating orbit method starting with the metric (9.39), and calculate the secular shifts up to 2PN order. The final expressions are quite heavy, and can be found in Appendix III.B. Setting $\lambda = \tilde{\chi}^2\varepsilon$, our results up to 2PN order coincide with Ref. [234] for the Kerr spacetime. Using the expressions for the secular variations of $\{\bar{\alpha}, \bar{\beta}\}$ in Eq. (III.1), one can obtain the secular variations of $\bar{\omega}$ and $\bar{e}$:

$$\frac{\mathrm{d}\bar{\omega}}{\mathrm{d}u} = \frac{3\tilde{M}}{\bar{p}}\left[1 + \frac{\lambda}{4(1-\bar{e}^2)}\left(5\cos^2\bar{\iota} - 1\right)\right] - 6\tilde{\chi}\cos\bar{\iota}\left(\frac{\tilde{M}}{\bar{p}}\right)^{3/2} + \mathcal{O}\left(\varepsilon^2\right) , \tag{9.42}$$

$$\begin{aligned}\frac{\mathrm{d}\bar{e}}{\mathrm{d}u} = {} & \frac{\lambda\tilde{M}^2\sin^2\bar{\iota}}{8\bar{p}^2(1-\bar{e}^2)^2}[\bar{e}\sin 2\bar{\omega}\left(17 + 183\bar{e}^2 + 40\bar{e}^4\right) \\ & + 16\sqrt{2}\left(1-\bar{e}^2\right)^2\langle\sin 2u\sin(u-\bar{\omega})\left(1+\bar{e}\cos(u-\bar{\omega})\right)^{3/2}\rangle] \\ & + \frac{\bar{e}\lambda^2\tilde{M}^2\sin^2\bar{\iota}}{64\bar{p}^2(1-\bar{e}^2)^2}\left[4\bar{e}^2\sin^2\bar{\iota}\sin 4\bar{\omega}\right. \\ & \left. + 2\sin 2\bar{\omega}\left(-39 + 5\bar{e}^2 + \bar{e}^4 + \cos^2\bar{\iota}\left(-81 - 25\bar{e}^2 + \bar{e}^4\right)\right)\right] .\end{aligned} \tag{9.43}$$

In this case, the leading-order term in the secular variation of $\bar{\omega}$ receives corrections due to disformality. Additionally, we see that $\bar{e}$ has a secular corrections of 2PN order, which is one ε order lower than the GR value. The same is true for the parameters $\{\bar{p}, \bar{\iota}\}$, as one can check using the expressions in Appendix III.B. This naively suggests possible strong secular effects in the case of the disformed metric, meaning that the parameters $\{\bar{p}, \bar{\iota}, \bar{e}\}$ could change considerably over a long period of time, when compared to the Kerr predictions. However, one can show that over long timescales these contributions average out to 0. Indeed, the characteristic timescale over which the pericenter angle $\bar{\omega}$ varies is shorter than for other parameters, as the leading secular shift for $\bar{\omega}$ appears at 1PN order. Hence, one can average the secular variations of orbital parameters over $\bar{\omega}$, while keeping other parameters fixed. It is not necessary to perform another 2-timescale analysis since the terms containing $\bar{\omega}$ are already of 2PN order, which means such an analysis would only be relevant if we were interested in higher-order PN terms (see Ref. [234]). From Eq. (9.42), one can easily see that

$$\frac{1}{2\pi}\int_0^{2\pi}\frac{\mathrm{d}\bar{e}}{\mathrm{d}u}\mathrm{d}\bar{\omega} = 0 \tag{9.44}$$

at this PN order, and hence the variation of eccentricity averages out to 0 over a long timescale. One can check that the same is true for the parameters $\{\bar{p}, \bar{\iota}\}$, using the expressions given in Appendix III.B.

By combining the expression for the secular variation of $\bar{\Omega}$ (found in Appendix III.B) with the variation of $\bar{\omega}$, we obtain the following formula after multiplication by 2π:

$$\Delta\bar{\varpi} \equiv \Delta\bar{\omega} + \cos\bar{\iota}\,\Delta\bar{\Omega} = \frac{6\pi\tilde{M}}{\bar{p}}\left[1 + \frac{\lambda}{4(1-\bar{e}^2)}\left(3\cos^2\bar{\iota} - 1\right)\right] + \mathcal{O}\left(\varepsilon^{3/2}\right) , \tag{9.45}$$

where $\bar{\varpi}$ is the precession of the pericenter relative to the fixed reference direction (the (Ox) axis in our case, see Fig. 1). As expected from the asymptotic expression Eq. (8.22), there are leading-order corrections to the secular pericenter shift. In Appendix III.C, we derive this leading term with the standard textbook method using equatorial geodesics. One can check that the two methods are compatible by setting $\bar{\iota} = 0$ in Eq. (9.45), which corresponds to an orbit in the equatorial plane of the black hole. While the leading-order terms are the same, one must be careful when comparing the higher-order corrections of the different methods, as explained in Ref. [253].

9.3.5 *e*nhanced Kerr disformation

We now examine another case of small and finite deviation of D from -1, similarly to the previous case. We study larger (but still small) deviations of order $\sqrt{\varepsilon}$:

$$D = -1 + \frac{\tilde{\chi}^2}{\lambda_2}\sqrt{\varepsilon}\,, \qquad \lambda_2 \sim \mathcal{O}(1)\,. \tag{9.46}$$

We call this the *e*nhanced Kerr disformation (*e*KD), in order to differentiate it from the EKD spacetime. Since the offset is larger than in the previous case, one expects that the modified gravity effects are smaller than those for EKD, while still larger than in the generic case. The metric in this limit can be obtained by replacing the relation (9.46) in the line element (9.29). Unlike in the EKD case, the metric is circular at 2PN order, and we have $R_{\mu\nu} \sim \varepsilon^{5/2}$. The resulting metric cannot be matched to the BI metric (9.5), since by replacing the disformal parameter according to Eq. (9.46), one introduces fractional powers of the mass in the metric. The secular variation of orbital parameters reads

$$\begin{aligned}
\frac{\mathrm{d}\bar{p}}{\mathrm{d}u} &= 0\,,\\
\frac{\mathrm{d}\bar{\alpha}}{\mathrm{d}u} &= -\frac{3\tilde{M}\bar{\beta}}{\bar{p}} + \frac{3\bar{\beta}}{4}\left(8\tilde{\chi}\cos\bar{\iota} - \frac{\lambda_2(5\cos^2\bar{\iota}-1)}{\sqrt{1-\bar{\alpha}^2-\bar{\beta}^2}}\right)\left(\frac{\tilde{M}}{\bar{p}}\right)^{3/2} + \frac{3\tilde{M}^2\bar{\beta}}{4\bar{p}^2}\left(10-\bar{\alpha}^2-\bar{\beta}^2\right)\,,\\
\frac{\mathrm{d}\bar{\beta}}{\mathrm{d}u} &= \frac{3\tilde{M}\bar{\alpha}}{\bar{p}} - \frac{3\bar{\alpha}}{4}\left(8\tilde{\chi}\cos\bar{\iota} - \frac{\lambda_2(5\cos^2\bar{\iota}-1)}{\sqrt{1-\bar{\alpha}^2-\bar{\beta}^2}}\right)\left(\frac{\tilde{M}}{\bar{p}}\right)^{3/2} - \frac{3\tilde{M}^2\bar{\alpha}}{4\bar{p}^2}\left(10-\bar{\alpha}^2-\bar{\beta}^2\right)\,,\\
\frac{\mathrm{d}\bar{\iota}}{\mathrm{d}u} &= 0\,,\\
\frac{\mathrm{d}\bar{\Omega}}{\mathrm{d}u} &= 2\left(\tilde{\chi} - \frac{3\lambda_2\cos\bar{\iota}}{4\sqrt{1-\bar{\alpha}^2-\bar{\beta}^2}}\right)\left(\frac{\tilde{M}}{\bar{p}}\right)^{3/2}\,.
\end{aligned} \tag{9.47}$$

The above expressions can be obtained by replacing Eq. (9.46) in the expressions (9.30) for the generic case. As one can see from the above equations, the Kerr quadrupole terms drop out in this case, similarly to the NCS case. However, for the *e*KD secular

corrections appear at lower order, at the level of the Lense-Thirring terms. This happens because the quadrupole (2PN) corrections of the generic case become 1.5PN order corrections here, due to the presence of the small value of $(1 + D)$ given by Eq. (9.46). The 1PN order is not modified for the eKD case unlike in the EKD case considered above.

9.3.6 Summary, observational constraints and predictions

We now summarize the main results of this section, and discuss how the current experimental measurements can constrain the disformed Kerr metric. For the values of D that we considered, deviations from GR appear at different PN orders in the metric or the secular variation of orbital parameters. We summarize the different cases in Table 1.

One can show that the orbital shifts up to 2PN order in the generic case (9.30) can be matched to the orbital shifts for the HT metric (9.9), by the identification $q_{\rm HT} = \tilde{\chi}^2/(1 + D)$. Similarly, the secular variations for the NCS metric at 2PN are identical to those for HT metric when setting $q_{\rm HT} = 0$. In order to recover the 2PN secular shifts of the QW metric, Eq. (9.36), one sets $q_{\rm HT} = \chi^2$ and $\tilde{\chi} = 0$ in the metric (9.9). In the case of the Johannsen metric (9.10), the 2PN Schwarzschild terms are modified with respect to the Kerr case in the secular variation of orbital parameters. On the other hand, the quadrupole terms proportional to $\tilde{\chi}^2$ are the same as in the Kerr case (i.e. the terms are those of Eq. (9.30) with $D = 0$). Note that this is different from the generic case of the disformal parameter, where we found that the terms proportional to $\tilde{\chi}^2$ are modified with respect to the Kerr case.

The observation of the star S2 in the center of our galaxy provides an opportunity to test GR by measuring its redshift [165] and pericenter precession [166]. The redshift includes the Newtonian Doppler effect and relativistic corrections. The measured combination of the leading corrections, the gravitational redshift and relativistic transverse Doppler effect, was found to be in agreement with GR [165]. Note, however, that the gravitational redshift at this observational precision is due to the Newtonian potential in the $\tilde{g}_{tt}$ component of the metric. This means that the current observations of the S2's redshift do not allow to test the Sgr A* metric beyond Newtonian order. Taking into account that all the variants of the disformed Kerr metric agree with GR at this order, these observations do not put any constraints on the considered Kerr deformations.

On the other hand, one can use the pericenter precession experienced by the star S2 when orbiting around Sgr A*. It was found to be in agreement with GR [166] with the accuracy $f_{\rm SP} \simeq 1.1 \pm 0.2$, where $f_{\rm SP}$ defines the ratio of the orbital pericenter precession (per period) of S2 to its GR value. For GR one has $f_{\rm SP} = 1$ while for Newtonian gravity $f_{\rm SP} = 0$. Since the pericenter precession is a 1PN effect, the only case we can constrain using the observed pericenter precession [166] is the Enhanced

Deviations from Kerr					
Value of D	Metric	Secular evolution	$R_{\mu\nu}$	Circularity at 2PN order	BI form at 2PN order
Generic D	2PN	2PN	$\mathcal{O}(\varepsilon^3)$	✓	✓
NCS ($D \to \infty$)	1.5PN	2PN	$\mathcal{O}(\varepsilon^3)$	✗	✗
QW ($D \to -1$)	1.5PN	1.5PN	$\mathcal{O}(\varepsilon^3)$	✓	✓
EKD ($D+1 \sim \varepsilon$)	1PN	1PN	$\mathcal{O}(\varepsilon^2)$	✗	✗
eKD ($D+1 \sim \sqrt{\varepsilon}$)	1.5PN	1.5PN	$\mathcal{O}(\varepsilon^{5/2})$	✓	✗

Table 1: Summary of the different regimes considered for the disformal parameter D and some properties of the resulting metrics at 2PN order. In the first column, we report the PN order at which the metric differs from Kerr in each case. The second column shows the PN order at which the secular variation of orbital parameters start to deviate from Kerr. The third column contains the order of the Ricci tensor. In the fourth column, we specify if the 2PN metric in each case is circular, and in the last column if the 2PN metric can be identified with the Butterworth-Ipser metric.

Kerr Disformation studied in Section 9.3.4.[4] All other deformations give corrections to the orbital shifts at higher PN orders (see Table 1), and therefore they automatically pass this observational test.[5] For the EKD metric, on the other hand, it is possible to constrain the disformal parameter D using the pericenter precession of the star S2. In order to stay within the experimental bounds of Ref. [166], the correction to the Schwarzschild precession in Eq. (9.45) must satisfy

$$\left| \frac{\lambda \left(3\cos^2 \bar{\iota} - 1\right)}{4(1-\bar{e}^2)} \right| \lesssim 0.2 \,. \tag{9.48}$$

If we assume $|3\cos^2 \bar{\iota} - 1| \sim 1$, and replace the eccentricity $\bar{e} = 0.87$ of the star S2, the inequality is saturated for $\lambda_0 \sim 0.2$. Using the relation (9.37), we deduce a lower

[4]Note that since the pericenter precession is sensitive to 1PN order terms, its measurement also allows to constrain spherically symmetric deformations of the Schwarzschild metric in DHOST theory. In particular Refs. [254, 255] constrained a particular solution of Horndeski theory given in [161].

[5]Note also that for stronger Kerr deformations than EKD, for instance when $1 + D \sim \varepsilon^{3/2}$, the correction to the pericenter shift is larger than the leading GR correction, which is already ruled out by the GRAVITY observations [166].

bound for the disformal parameter, $D \geq D_0$, which verifies:

$$D_0 = -1 + \frac{\tilde{\chi}^2 \varepsilon_0}{\lambda_0} \,, \tag{9.49}$$

where $\varepsilon_0 = \tilde{M}/A_0$, A_0 being the semi-major axis of S2's orbit. Taking the parameter $D = D_0$, in order to maximize the effects of disformality, we consider another star with $\varepsilon \neq \varepsilon_0$ in general. The leading pericenter precession reads, from Eq. (9.45),

$$\Delta\bar{\varpi} = \frac{6\pi\tilde{M}}{\bar{p}} \left[1 + \frac{\varepsilon\lambda_0}{\varepsilon_0} \frac{(3\cos^2\bar{\iota} - 1)}{4(1-\bar{e}^2)}\right] . \tag{9.50}$$

Note the factor $\varepsilon\lambda_0/\varepsilon_0$ in the second term of the brackets, since $\varepsilon/\lambda = \varepsilon_0/\lambda_0$. The above expression is correct as long as ε stays in the range,

$$\varepsilon^2 \lesssim 10^{-3} \lesssim \sqrt{\varepsilon} \,, \tag{9.51}$$

which implies that the perturbative expansion in ε is valid.[6] In the future, the pericenter precession of other stars orbiting around Sgr A* will be observed. If some of them have high eccentricities, the effect of modified gravity in the case of the EKD metric will be detected by the correction to the pericenter precession, as suggested by Eq. (9.50). This is correct for a generic inclination angle $\bar{\iota}$, but it is worth noting that for a specific value $\bar{\iota} = \arccos(1/\sqrt{3})$ the contribution coming from the disformal metric vanishes completely. Note also that depending on the value of $\bar{\iota}$, it is in principle possible to obtain a negative pericenter precession at leading order. This is a notable difference from the Kerr spacetime, as argued in Ref. [256], where the authors showed that a negative precession can arise in the case of a naked singularity in the Johannsen-Psaltis spacetime [257].

[6] To see this explicitly, we need to inspect the sub-leading terms in Eq. (9.50), which have the structure $\mathcal{O}\left((1+\lambda)\varepsilon^{3/2}\right) + \mathcal{O}\left((1+\lambda)^2\varepsilon^2\right)$. The first inequality in Eq. (9.51) comes from the requirement that $\mathcal{O}\left((1+\lambda)^2\varepsilon^2\right)$ be sub-leading with respect to Eq. (9.50), i.e. $(\lambda\varepsilon)^2 \lesssim (\lambda\varepsilon)$. The second inequality comes from the comparison of Eq. (9.50) with $\mathcal{O}\left((1+\lambda)\varepsilon^{3/2}\right)$ for small λ. One must ensure that the corrections are subdominant, resulting in $\varepsilon^{3/2} \lesssim \lambda\varepsilon$. After replacing the values $\lambda_0 \sim 10^{-1}$ and $\varepsilon_0 \sim 10^{-4}$ we obtain Eq. (9.51).

Conclusion to Part III

There has been increasing evidence in recent years for the existence of black holes in Nature. Hence it is important to understand these objects from a theoretical point of view. Rotating (uncharged) black holes in GR are described by the Kerr metric, and we reviewed its main properties in Chapter 7. It is a remarkably simple spacetime which depends on two parameters only: the mass M and spin a of the black hole. In particular, the quadrupole moment of a Kerr black hole is determined by these two parameters only, and constitutes the no-hair theorem (in fact all higher-order multipoles are uniquely determined). It is interesting to construct alternatives to the Kerr metric, both theoretically, but also in the aim of predicting testable differences from the GR spacetime.

In Chapter 8, starting from a stealth-Kerr solution in scalar-tensor theory, we constructed the disformed Kerr metrics. This construction relies on the disformal transformation, which is an internal map of DHOST Ia theories. The Kerr metric is deformed along the gradient of the Hamilton-Jacobi potential, which is a geodesic vector. The integration constants are chosen so that the scalar field is regular from the outer Kerr horizon up to spatial infinity. We start from $c_T = 1$ theories where our spacetime is identical to the GR Kerr solution [214], and map to a disformed Kerr metric which is solution to some DHOST Ia theory [47]. Such theories are constrained from gravity wave tests, assuming that the scalar is varying at vast cosmological scales, i.e. a dark energy field. The solutions we have discussed here are asymptotically flat and locally influence the speed of gravity waves for these particular scalar tensor theories. Independently of gravity wave constraints, the solutions discussed here go beyond the interest of these particular theories and we believe that they are interesting in their own right as simple, analytic, benchmark alternatives to the prototype Kerr solution. The resulting spacetimes remain axisymmetric and present some interesting features which we will summarize here. First of all, the disformed metrics are regular everywhere except at $\rho = 0$, which is the ring singularity of the original Kerr spacetime. Furthermore, an asymptotic expansion reveals that the metrics look like sub-extremal Kerr spacetimes for large radii, with a rescaled mass $\tilde{M}$ and spin $\tilde{a}$ given by Eq. (8.23). However, the disformed metrics present some notable differences in the strong field regime close to the black hole. The most interesting feature is perhaps noncircularity, i.e. the fact that the metric cannot be cast in a form which exhibits the reflection symmetry $(t, \varphi) \to (-t, -\varphi)$. Noncircular spacetimes are rarely studied in the literature, and usually a circular ansatz is assumed when studying rotating objects. However, in some situations this assumption fails and one must consider noncircular metrics. An example is when considering neutron stars with strong toroidal magnetic fields. Noncircularity has consequences on the separable structure of the spacetimes, and the disformed metrics do not possess a nontrivial Killing tensor, which means that the geodesic equations cannot be integrated so easily. Importantly, the disformed metrics are stably causal, since the scalar field has a timelike gradient, and can be interpreted as a global time. This allows to avoid pathologies like closed timelike curves, which

are know to arise in certain *ad hoc* deformations of the Kerr metric.

By analyzing the fate of timelike observers in the disformed spacetime, we have found that there exists an ergosurface where the Killing vector ∂_t becomes null, similarly to the Kerr case. In the ergoregion, one finds a limiting surface for stationary observers, inside which all Killing vectors are spacelike. This stationary limit surface does not lie at constant r and can be shown to be timelike, and hence cannot correspond to an event horizon when the disformal parameter D is nonzero. Hence a candidate event horizon must lie in the interior of this surface. We have shown that it is necessary to consider a θ-dependent profile of the surface in the generic case $D \neq 0$. We have derived the equation satisfied by the candidate horizon surface, and argued by an analogy with the constant r surfaces of the Kerr spacetime that it indeed corresponds to an event horizon. Though the horizon equation cannot be solved analytically, we have performed a numerical integration of the horizon profile, and given necessary analytical conditions for the surface to be smooth at the poles and equator. We have also studied the disformed metric in the limits $D \to -1$ (quasi-Weyl) and $D \to \infty$ (noncircular Schwarzschild), which provide very interesting examples of noncircular metrics and could be helpful in understanding the properties of such spacetimes. We have shown explicitly that the NCS metric is of Petrov type I. This result applies to the generic case $D \neq 0$ and $a \neq 0$, but we only wrote explicitly in this simple case.

In Chapter 9, we searched for experimental signatures of the disformed metrics. In GR, a Kerr black hole is completely determined its mass and angular momentum. All higher-order multipoles depend on these two parameters only, and this property is know as the no-hair theorem. In Section 9.1, we established that the no-hair theorem of GR is generically violated in the case of a disformed Kerr black hole. Instead, the gauge independent quadrupole moment depends on the disformal parameter D according to Eq. (9.6). This expression was obtained by comparing the asymptotic expansion of the disformed metric to the Butterworth-Ipser metric (9.5). We then studied the orbit of stars around a disformed back hole, using a two-timescale analysis reviewed in Section 9.2. In Section 9.3, we calculated the secular variation of orbital parameters for different cases of the disformal parameter. We summarized the results in Section 9.3.6, and discussed the experimental signatures of the disformed spacetimes. In the case of the EKD metric (9.39), the measurement of the Schwarzschild precession of the star S2 around Sgr A* [166] allows us to set a lower bound on the disformal parameter D.

While all the other variants of the Kerr deformations automatically satisfy the current observational bounds coming from the star S2, future experiments will be able to probe these Kerr deformations as well. Indeed, none of the deformations of Kerr presented here verify the no-hair theorem. Therefore, future observations aiming at testing the no-hair theorem for the Kerr spacetime will probe all the deformations of Kerr. More precisely, the observation of high-eccentricity stars with short periods orbiting Sgr A* can in principle lead to the determination of the spin and quadrupole moment by measuring the secular variation of the nodal and inclination angles $\{\Omega, \iota\}$

[167] (see also Ref. [171] for a review). Another promising method to test the no hair theorem is to use pulsar timing, which could allow the determination of the spin and quadrupole moment of Sgr A* if a binary pulsar orbiting closely enough to the black hole is discovered (see the review [171] and references therein). The authors of Ref. [258] calculated the second-order Shapiro delay for the BI metric. These results can be applied to the disformed Kerr metric in the cases where the line element can be put in the BI form (see Table 1).

There are numerous questions which we have left unanswered, starting with the global causal structure of the disformed spacetime (8.11), which is a rather nontrivial question and requires a separate study. Furthermore, we have shown that unlike in the case of GR, the event horizon of the disformed spacetimes fails to be a Killing horizon. The possibility of extending the notion of surface gravity for horizons which are no longer Killing has been studied by several authors in different contexts (see Ref. [259] and references therein). Hence, it would be interesting to study the thermodynamics of the disformed solutions using these different definitions for surface gravity. As we have discussed, the disformed metrics do not possess a nontrivial Killing tensor, making the study of geodesics around such objects more involved. This task is nonetheless made possible by numerically integrating the equations, and in this way the shadows of disformed Kerr black holes have been computed in Ref. [260]. Finally, as we have shown the stationary limit in the disformed spacetime generically lies outside of the event horizon. Even though these two surfaces almost coincide, it would be interesting to understand what the properties of the region separating them, if any. For instance, in the example of the quasi-Weyl metric (8.55), there seems to exist an ergoregion without any rotation of the black hole along the azimuthal direction, which is an intriguing feature.

Appendix

III.A Polynomials Q_i

We give here the full expressions of the functions Q_1 and Q_2 appearing in the expressions (8.14) for the curvature invariants of the disformed Kerr metric:

$$
\begin{aligned}
Q_1(r,\theta) &= \left[127 + 56\cos(2\theta) + 9\cos(4\theta)\right] r^4 + 4a^2\left[33 + 14\cos(2\theta) + \cos(4\theta)\right] r^2 \\
&\quad + 18a^4 \sin^2(2\theta)\,, \\
Q_2(r,\theta) &= 48\left(r^2+a^2\right)\left(r^6 - 15a^2r^4\cos^2\theta + 15a^4r^2\cos^4\theta - a^6\cos^6\theta\right) \\
&\quad - \frac{Da^2}{2}\{160\left[4 + 3\cos(2\theta)\right] r^6 \\
&\quad - a^2\left[3\left(52+3D\right)\cos(4\theta) + 4\left(48+25D\right)\cos(2\theta) - 124 + 243D\right] r^4 \\
&\quad + a^4\left[3\cos(6\theta) + \left(D-138\right)\cos(4\theta) - \left(627+100D\right)\cos(2\theta) - 486 - 253D\right] r^2 \\
&\quad + 12a^6\cos^2\theta\left[\cos(4\theta) + \left(4+6D\right)\cos(2\theta) + 3 - 6D\right]\}\,.
\end{aligned}
$$

III.B Secular shifts for the EKD metric

In this appendix, we provide the expressions for the secular perturbations of orbital parameters up to 2PN order in the case of the EKD metric, $D+1 \sim \mathcal{O}(\varepsilon)$, see Section 9.3.4. Since the EKD metric (9.39) does not fall in the class of generic D, we cannot use the results of Section 9.3.1 to find the variation of orbital parameters. We present the results obtained by applying the osculating orbit method described in Section 9.2 to the metric (9.39). We obtain:

$$
\begin{aligned}
\frac{\mathrm{d}\bar{p}}{\mathrm{d}u} &= \frac{\lambda\tilde{M}^2\sin^2\bar{\iota}}{\bar{p}(1-\bar{\alpha}^2-\bar{\beta}^2)^2}\left[5\bar{\alpha}\bar{\beta}\left(5+2\bar{\alpha}^2+2\bar{\beta}^2\right) + \mathcal{I}_1(\bar{\alpha},\bar{\beta})\right] \\
&\quad - \frac{\lambda^2\tilde{M}^2\bar{\alpha}\bar{\beta}\sin^2\bar{\iota}}{8\bar{p}(1-\bar{\alpha}^2-\bar{\beta}^2)^3}[-72 + \left(\bar{\alpha}^2+\bar{\beta}^2\right)^2 + 6\bar{\alpha}^2 - 2\bar{\beta}^2 \\
&\qquad\qquad + \left(84 + (\bar{\alpha}^2+\bar{\beta}^2)^2 - 6\bar{\beta}^2 - 14\bar{\alpha}^2\right)\cos^2\bar{\iota}]\,, \\
\frac{\mathrm{d}\bar{\iota}}{\mathrm{d}u} &= \frac{\lambda\tilde{M}^2\sin 2\bar{\iota}}{4\bar{p}^2(1-\bar{\alpha}^2-\bar{\beta}^2)^2}\left[5\bar{\alpha}\bar{\beta}\left(5+2\bar{\alpha}^2+2\bar{\beta}^2\right) + \mathcal{I}_1(\bar{\alpha},\bar{\beta})\right]
\end{aligned}
$$

$$
\begin{aligned}
&+\frac{\lambda^2\tilde{M}^2\bar{\alpha}\bar{\beta}\sin 2\bar{\iota}}{32\bar{p}^2(1-\bar{\alpha}^2-\bar{\beta}^2)^3}[176+3\left(\bar{\alpha}^2+\bar{\beta}^2\right)^2+86\bar{\beta}^2+78\bar{\alpha}^2\\
&\qquad\qquad -\left(84+(\bar{\alpha}^2+\bar{\beta}^2)^2-6\bar{\beta}^2-14\bar{\alpha}^2\right)\cos^2\bar{\iota}]\,,\\
\frac{\mathrm{d}\bar{\Omega}}{\mathrm{d}u}&=-\frac{3\tilde{M}\lambda\cos\bar{\iota}}{2\bar{p}(1-\bar{\alpha}^2-\bar{\beta}^2)}+2\tilde{\chi}\left(\frac{\tilde{M}}{\bar{p}}\right)^{3/2}\\
&+\frac{\lambda\tilde{M}^2\cos\bar{\iota}}{4\bar{p}^2(1-\bar{\alpha}^2-\bar{\beta}^2)^2}\left[48+37\bar{\alpha}^4+57\bar{\beta}^4-35\bar{\alpha}^2+15\bar{\beta}^2+94\bar{\alpha}^2\bar{\beta}^2+\mathcal{I}_2(\bar{\alpha},\bar{\beta})\right]\\
&+\frac{\lambda^2\tilde{M}^2\cos\bar{\iota}}{32\bar{p}^2(1-\bar{\alpha}^2-\bar{\beta}^2)^3}[174+\bar{\alpha}^4\left(6\bar{\beta}^2-79\right)+6\bar{\alpha}^2\left(13-\bar{\beta}^2+2\bar{\beta}^4\right)\\
&\qquad\qquad +\bar{\beta}^2\left(570+89\bar{\beta}^2+6\bar{\beta}^4\right)]\\
&+\frac{\lambda^2\tilde{M}^2\cos^3\bar{\iota}}{32\bar{p}^2(1-\bar{\alpha}^2-\bar{\beta}^2)^3}[-66+2\bar{\alpha}^6-554\bar{\beta}^2+207\bar{\beta}^4\\
&\qquad\qquad +\bar{\alpha}^4\left(191+4\bar{\beta}^2\right)+2\bar{\alpha}^2\left(\bar{\beta}^4+207\bar{\beta}^2-123\right)]\,,\\
\frac{\mathrm{d}\bar{\alpha}}{\mathrm{d}u}&=-\frac{3\tilde{M}\bar{\beta}}{4\bar{p}(1-\bar{\alpha}^2-\bar{\beta}^2)}\left[4\left(1-\bar{\alpha}^2-\bar{\beta}^2\right)+\lambda\left(5\cos^2\bar{\iota}-1\right)\right]+6\bar{\beta}\tilde{\chi}\cos\bar{\iota}\left(\frac{\tilde{M}}{\bar{p}}\right)^{3/2}\\
&+\frac{3\tilde{M}^2\bar{\beta}(10-\bar{\alpha}^2-\bar{\beta}^2)}{4\bar{p}^2}\\
&+\frac{\lambda\tilde{M}^2}{16\bar{p}^2(1-\bar{\alpha}^2-\bar{\beta}^2)^2}[2\bar{\beta}\left(-53+199\bar{\alpha}^2+34\bar{\alpha}^4-19\bar{\beta}^2(5+2\bar{\alpha}^2)-72\bar{\beta}^4\right)\\
&\qquad\qquad +\sin^2\bar{\iota}\,\mathcal{I}_3(\bar{\alpha},\bar{\beta})+\mathcal{J}_1(\bar{\alpha},\bar{\beta},\bar{\iota})]\\
&+\frac{\lambda\tilde{M}^2\bar{\beta}\cos^2\bar{\iota}}{8\bar{p}^2(1-\bar{\alpha}^2-\bar{\beta}^2)^2}\left[253+48\bar{\alpha}^4+194\bar{\beta}^4-27\bar{\beta}^4+\bar{\alpha}^2(242\bar{\beta}^2-421)\right]\\
&-\frac{\lambda^2\tilde{M}^2\bar{\beta}}{64\bar{p}^2(1-\bar{\alpha}^2-\bar{\beta}^2)^3}[585+2\bar{\alpha}^2\left(2\bar{\alpha}^4-18\bar{\alpha}^2-147\right)+2\bar{\beta}^2\left(693+34\bar{\alpha}^2+4\bar{\alpha}^4\right)\\
&\qquad\qquad +4\bar{\beta}^4\left(46+\bar{\alpha}^2\right)]\\
&-\frac{\lambda^2\tilde{M}^2\bar{\beta}\cos^2\bar{\iota}}{32\bar{p}^2(1-\bar{\alpha}^2-\bar{\beta}^2)^3}[-729+\bar{\alpha}^2\left(290+295\bar{\alpha}^2+6\bar{\alpha}^4\right)\\
&\qquad\qquad +2\bar{\beta}^2\left(6\bar{\alpha}^4+315\bar{\alpha}^2-733\right)+\bar{\beta}^4\left(239+6\bar{\alpha}^2\right)]\\
&+\frac{\lambda^2\tilde{M}^2\bar{\beta}\cos^4\bar{\iota}}{64\bar{p}^2(1-\bar{\alpha}^2-\bar{\beta}^2)^3}[-585+2\bar{\alpha}^2\left(-209+321\bar{\alpha}^2+4\bar{\alpha}^4\right)\\
&\qquad\qquad +2\bar{\beta}^2\left(8\bar{\alpha}^4+936\bar{\alpha}^2-941\right)+2\bar{\beta}^4\left(559+4\bar{\alpha}^2\right)]\,,\\
\frac{\mathrm{d}\bar{\beta}}{\mathrm{d}u}&=\frac{3\tilde{M}\bar{\alpha}}{4\bar{p}(1-\bar{\alpha}^2-\bar{\beta}^2)}\left[4\left(1-\bar{\alpha}^2-\bar{\beta}^2\right)+\lambda\left(5\cos^2\bar{\iota}-1\right)\right]-6\bar{\alpha}\tilde{\chi}\cos\bar{\iota}\left(\frac{\tilde{M}}{\bar{p}}\right)^{3/2}
\end{aligned}
$$

$$
\begin{aligned}
&- \frac{3\tilde{M}^2\bar{\alpha}(10-\bar{\alpha}^2-\bar{\beta}^2)}{4\bar{p}^2} \\
&+ \frac{\lambda\tilde{M}^2}{16\bar{p}^2(1-\bar{\alpha}^2-\bar{\beta}^2)^2}[2\bar{\alpha}\left(87+46\bar{\alpha}^4+461\bar{\beta}^2+\bar{\alpha}^2(167+198\bar{\beta}^2)+152\bar{\beta}^4\right) \\
&\qquad\qquad - \sin^2\bar{\iota}\,\mathcal{I}_4(\bar{\alpha},\bar{\beta}) - \mathcal{J}_2(\bar{\alpha},\bar{\beta},\bar{\iota})] \\
&- \frac{\lambda\tilde{M}^2\bar{\alpha}\cos^2\bar{\iota}}{8\bar{p}^2(1-\bar{\alpha}^2-\bar{\beta}^2)^2}\left[287+128\bar{\alpha}^4+339\bar{\beta}^2+274\bar{\beta}^4+\bar{\alpha}^2\left(-55+402\bar{\beta}^2\right)\right] \\
&- \frac{\lambda^2\tilde{M}^2\bar{\alpha}}{64\bar{p}^2(1-\bar{\alpha}^2-\bar{\beta}^2)^3}[-429+102\bar{\alpha}^2+68\bar{\alpha}^4+2\bar{\beta}^2\left(-773-18\bar{\alpha}^2+2\bar{\alpha}^4\right) \\
&\qquad\qquad + 8\bar{\beta}^4\left(\bar{\alpha}^2-23\right)+4\bar{\beta}^6] \\
&+ \frac{\lambda^2\tilde{M}^2\bar{\alpha}\cos^2\bar{\iota}}{32\bar{p}^2(1-\bar{\alpha}^2-\bar{\beta}^2)^3}[-813+298\bar{\alpha}^2+371\bar{\alpha}^4+6\bar{\alpha}^6+2\bar{\beta}^2\left(-713+375\bar{\alpha}^2+6\bar{\alpha}^4\right) \\
&\qquad\qquad + \bar{\beta}^4\left(283+6\bar{\alpha}^2\right)] \\
&- \frac{\lambda^2\tilde{M}^2\bar{\alpha}\cos^4\bar{\iota}}{64\bar{p}^2(1-\bar{\alpha}^2-\bar{\beta}^2)^3}[-909-210\bar{\alpha}^2+762\bar{\alpha}^4+4\bar{\alpha}^6+2\bar{\beta}^2\left(-821+2\bar{\alpha}^2(520+\bar{\alpha}^2)\right) \\
&\qquad\qquad + 2\bar{\beta}^4\left(603-2\bar{\alpha}^2\right)-4\bar{\beta}^6]\,, \qquad \text{(III.1)}
\end{aligned}
$$

where we defined the following functions to make the previous expressions lighter (and we use the average $\langle\cdot\rangle$ as defined in Eq. (9.16)):

$$
\begin{aligned}
H^{(\kappa)}(u,\bar{\alpha},\bar{\beta}) &= 4\sqrt{2}\left(1-\bar{\alpha}^2-\bar{\beta}^2\right)\left(1+\bar{\alpha}\cos u+\bar{\beta}\sin u\right)^{\kappa}\,, \\
\mathcal{I}_1(\bar{\alpha},\bar{\beta}) &= \langle\sin 2u\left(\bar{\beta}\cos u-\bar{\alpha}\sin u\right)H^{(3/2)}(u,\bar{\alpha},\bar{\beta})\rangle\,, \\
\mathcal{I}_2(\bar{\alpha},\bar{\beta}) &= 4\langle\sin^2 u\left(\bar{\beta}\cos u-\bar{\alpha}\sin u\right)H^{(3/2)}(u,\bar{\alpha},\bar{\beta})\rangle\,, \\
\mathcal{I}_3(\bar{\alpha},\bar{\beta}) &= 16\langle\cos u\sin^2 u\,H^{(7/2)}(u,\bar{\alpha},\bar{\beta})\rangle\,, \\
\mathcal{I}_4(\bar{\alpha},\bar{\beta}) &= 16\langle\cos^2 u\sin u\,H^{(7/2)}(u,\bar{\alpha},\bar{\beta})\rangle\,, \\
\mathcal{J}_1(\bar{\alpha},\bar{\beta},\bar{\iota}) &= 4\langle\left(\bar{\beta}\cos u-\bar{\alpha}\sin u\right)H^{(3/2)}(u,\bar{\alpha},\bar{\beta})\{4\bar{\beta}\cos^2\bar{\iota}\sin^2 u \\
&\qquad + \sin^2\bar{\iota}\sin 2u(3\bar{\alpha}+4\cos u+\bar{\alpha}\cos 2u+\bar{\beta}\sin 2u)\}\rangle\,, \\
\mathcal{J}_2(\bar{\alpha},\bar{\beta},\bar{\iota}) &= 4\langle\left(\bar{\beta}\cos u-\bar{\alpha}\sin u\right)H^{(3/2)}(u,\bar{\alpha},\bar{\beta})\{4\bar{\alpha}\cos^2\bar{\iota}\sin^2 u \\
&\qquad + \sin^2\bar{\iota}\sin 2u\left(-3\bar{\beta}-4\sin u+\bar{\beta}\cos 2u-\bar{\alpha}\sin 2u\right)\}\rangle\,.
\end{aligned}
$$

III.C Leading-order pericenter precession using the textbook method

In this appendix, we apply the textbook method to derive the leading term for the pericenter precession for the EKD metric considered in Section 9.3.4, and compare it with the result obtained in Eq. (9.45). Assuming that the trajectory is in the equatorial plane $\theta = \pi/2$, one can write first-order geodesic equations. This is not the case for the

general motion outside of the equatorial plane, because of the absence of a nontrivial Killing tensor for the disformed Kerr metric. The orbit of stars around the central black hole of the galaxy is approximately an ellipse, for which the energy and angular momentum can be written:

$$E^2 \simeq 1 - \frac{\tilde{M}}{A} \,,$$
$$L^2 \simeq A\tilde{M}(1-e^2) \,,$$

where A and e are respectively the semi-major axis and eccentricity of the Kepler orbit. We now combine the geodesic equations for the variables $\{r, \varphi\}$, and use the standard variable $U \equiv 1/r$. By substituting the above values for energy and angular momentum in the geodesic equations, a second-order equation follows:

$$U''(\varphi) + F(U, \tilde{M}, a, D) = 0 \,, \tag{III.2}$$

where F is a complicated expression which also depends on A and e. Following the standard procedure (see for instance Ref. [261]), we introduce a small parameter

$$\eta = \frac{3\tilde{M}^2}{L^2} \simeq \frac{3}{(1-e^2)}\varepsilon \,, \tag{III.3}$$

where $\varepsilon = \tilde{M}/A$ is the small parameter used throughout the main text. We again assume $\tilde{a} = \tilde{\chi}\tilde{M}$ with $\tilde{\chi} \sim \mathcal{O}(1)$, so that we can also express a in terms of η. We look for a solution to Eq. (III.2) of the form

$$U = \frac{1 + e\cos\varphi}{A(1-e^2)} + \eta\, \delta U(\varphi) \,,$$

where the first part corresponds to the Kepler orbit, and the second term is the leading correction in η. For the Schwarzschild metric ($a = 0$), this leads to the equation:

$$\delta U_S'' + \delta U_S = \frac{(1 + e\cos\varphi)^2}{A(1-e^2)} \,.$$

The above equation can be solved to write down the solution for U at first order in η:

$$U_S \simeq \frac{1 + e\cos\left[\varphi(1-\eta)\right]}{A(1-e^2)} \,.$$

From this expression, one can calculate the precession of the pericenter $\Delta\Phi_S$ as:

$$\Delta\Phi_S = 2\pi\left(\frac{1}{1-\eta} - 1\right) \simeq 2\pi\eta = \frac{6\pi\tilde{M}}{A(1-e^2)} \tag{III.4}$$

The asymptotic expression of the disformed metric suggests that for the EKD metric, i.e. when $D+1 \sim \mathcal{O}(\varepsilon)$, corrections from higher-order terms in ε become of 1PN order,

i.e. comparable to the leading Schwarzschild corrections. To check this, we rewrite Eq. (9.37) in terms of η:

$$D = -1 + \frac{(1-e^2)\tilde{\chi}^2}{3\lambda}\eta \,.$$

Assuming this form for D in Eq. (III.2) and expanding up to $\mathcal{O}(\eta)$, we obtain the following equation for the correction to the Kepler orbit:

$$\delta U'' + \delta U = \frac{(1+e\cos\varphi)^2}{A(1-e^2)} + \frac{\lambda(1+e\cos\varphi)(2+e\cos\varphi+e^2-2e^2\cos(2\varphi))}{3A(1-e^2)^2} \,.$$

Solving this equation and keeping only the terms of the form $\varphi\sin\varphi$ which provide a secular shift, the standard procedure gives,

$$\Delta\Phi = \Delta\Phi_S\left(1+\frac{\lambda}{2(1-e^2)}\right) \,. \tag{III.5}$$

Thus for a spinning EKD black hole the corrections to the pericenter precession due to modifications of gravity are of the same order as the leading GR effect. Eq. (III.5) provides a useful check for our calculations in the main text, where we obtained secular shifts for the EKD black hole by the orbital perturbation method. In particular, we obtained the expression for the pericenter precession in Eq. (9.45). The two expressions agree after setting $\bar{\iota} = 0$ in Eq. (9.45), which corresponds to an orbit in the equatorial plane, as assumed in this appendix.

Summary

In this thesis, I have presented various topics in the context of scalar-tensor theories of gravitation. The first part of the thesis was devoted to the cosmology of theories exhibiting spontaneous scalarization. I described the scalarization mechanism in Chapter 1, both in the context of standard scalar-tensor theories and in the case of a coupling to the Gauss-Bonnet scalar. It relies on a tachyonic effective mass for the scalar field, and I showed in Chapter 2 that this generically leads to an instability of scalar modes during inflation. This is true in both of the cases we consider, i.e. the DEF model and the scalar-Gauss-Bonnet theories. A mechanism to quench this instability in the case of the DEF model, relying on a coupling of the scalar to the inflaton field, was proposed in Chapter 3. This coupling acts as an effective mass term for the scalar, which stabilizes it around 0 by the end of inflation. Although the scalar grows in the subsequent phases of the expansion of the Universe (as in the DEF model), its value today is sufficiently small to pass current experimental tests of GR.

In the second part, I examined the Vainshtein screening for slowly rotating stars in scalar-tensor theories. The tests of gravity in the Solar System are all compatible with GR. Hence it is important for a modified theory of gravity to have a mechanism that restores GR close to gravitational sources, and the Vainshtein screening is one way to achieve this. It has been extensively studied in the case of spherical symmetry, but realistic astrophysical objects typically rotate, and our aim was to study this effect in the case of slowly rotating stars. Note that in some cases the GR equations are fully recovered in vacuum, even for relativistic stars, which I show in Appendix II.A. In Chapter 4, I derived the equation satisfied by the frame-dragging function ω accounting for slow rotation. I then assumed the weak-field approximation and discussed the solutions for ω in this case, showing that the screening mechanism can be extended to ω outside the source in general. However, it is possible for ω to receive leading-order corrections inside the source. In Chapter 5, I studied the screening in the case of a time-dependent scalar field, and gave examples in different classes of theories. It was shown that even if the Vainshtein screening is operational in spherical symmetry, it is not necessary for the corrections to ω to be suppressed by powers of the Vainshtein radius r_V. In these cases, while the screening works also for ω, it is less effective than for the metric potentials. The screening in the case of a static scalar field was studied in Chapter 6. I considered shift-symmetric Horndeski theories with an additional coupling of the scalar field to curvature, in order to escape the no-hair theorem for

stars. In this case the results are similar to the time-dependent case.

The final part of the thesis dealt with black holes, and I started by reviewing the (uncharged) GR solutions in Chapter 7, discussing some important properties of the Schwarzschild and Kerr solutions. In Chapter 8, rotating black hole solutions in scalar-tensor theories were constructed by performing a disformal transformation of the Kerr metric, and I discussed the properties of these spacetimes. These axisymmetric solutions are similar to Kerr in some ways: only one singularity at $\rho = 0$; same asymptotic expansion with the rescaled parameters $\tilde{M}$ and $\tilde{a}$ given by Eq. (8.23); existence of an ergoregion. However, they are very different from the Kerr spacetime in other aspects: they are noncircular; not Ricci-flat; they do not possess a nontrivial Killing tensor; the stationary limit is distinct from the event horizon; the horizon is not a Killing horizon and has a θ-dependent profile. Importantly, the spacetimes were shown to be stably causal, which allows to avoid pathologies like closed timelike curves in the region outside the horizon. Interesting examples of noncircular black hole metrics were obtained in the limits $D \to -1$ (quasi-Weyl) and $D \to \infty$ (noncircular Schwarzschild), where D is the disformal parameter. Because of their simplicity compared to the generic case, a detailed analysis of these metrics could be useful in understanding the properties of noncircular spacetimes. After introducing the noncircular Schwarzschild metric, I showed that it is of generic Petrov type I. Though the explicit calculation was presented only in this simple case, the result holds for generic $D \neq 0$ and $a \neq 0$. The orbit of stars around a disformed Kerr black hole was analyzed in Chapter 9. Using the osculating orbit method and a two-timescale analysis, I calculated the secular variation of orbital parameters up to the second post-Newtonian order for different limits of the disformal parameter D. It was shown that generically the disformed metrics violate the no-hair theorem of GR, which states that higher-order multipoles are uniquely determined by the mass and spin of the black hole. In particular, the simultaneous measurement of the spin and quadrupole of Sgr A*, which is expected in the future, will provide a test of this property. In one particular limit of D, namely the EKD metric, the first order post-Newtonian term is modified for the secular pericenter precession. This constitutes a signature of modified gravity, and allows to constrain the disformed metric using the current observational bounds coming from the orbit of the star S2 around Sgr A*.

Bibliography

[1] A. Einstein, *The Foundation of the General Theory of Relativity*, *Annalen Phys.* **49** (1916) 769–822.

[2] C. M. Will, *Henry Cavendish, Johann von Soldner, and the deflection of light*, *American Journal of Physics* **56** (1988) 413–415.

[3] F. W. Dyson, A. S. Eddington and C. Davidson, *A Determination of the Deflection of Light by the Sun's Gravitational Field, from Observations Made at the Total Eclipse of May 29, 1919*, *Phil. Trans. Roy. Soc. Lond. A* **220** (1920) 291–333.

[4] P. Coles, *Einstein, Eddington and the 1919 eclipse*, *ASP Conf. Ser.* **252** (2001) 21, [astro-ph/0102462].

[5] R. A. Hulse and J. H. Taylor, *Discovery of a pulsar in a binary system*, *Astrophys. J. Lett.* **195** (1975) L51–L53.

[6] N. Wex and M. Kramer, *Gravity Tests with Radio Pulsars*, *Universe* **6** (2020) 156.

[7] E. Hubble, *A relation between distance and radial velocity among extra-galactic nebulae*, *Proc. Nat. Acad. Sci.* **15** (1929) 168–173.

[8] Supernova Search Team collaboration, A. G. Riess et al., *Observational evidence from supernovae for an accelerating universe and a cosmological constant*, *Astron. J.* **116** (1998) 1009–1038, [astro-ph/9805201].

[9] Supernova Cosmology Project collaboration, S. Perlmutter et al., *Measurements of Ω and Λ from 42 high redshift supernovae*, *Astrophys. J.* **517** (1999) 565–586, [astro-ph/9812133].

[10] Planck collaboration, N. Aghanim et al., *Planck 2018 results. VI. Cosmological parameters*, *Astron. Astrophys.* **641** (2020) A6, [1807.06209].

[11] R. P. Kerr, *Gravitational field of a spinning mass as an example of algebraically special metrics*, *Phys. Rev. Lett.* **11** (1963) 237–238.

[12] LIGO Scientific, Virgo collaboration, B. Abbott et al., *Observation of Gravitational Waves from a Binary Black Hole Merger*, *Phys. Rev. Lett.* **116** (2016) 061102, [1602.03837].

[13] J. H. Taylor and J. M. Weisberg, *A new test of general relativity - Gravitational radiation and the binary pulsar PSR 1913+16*, *Astrophys. J.* **253** (1982) 908–920.

[14] J. Martin, *Everything You Always Wanted To Know About The Cosmological Constant Problem (But Were Afraid To Ask)*, *Comptes Rendus Physique* **13** (2012) 566–665, [1205.3365].

[15] A. A. Starobinsky, *Spectrum of relict gravitational radiation and the early state of the universe*, *JETP Lett.* **30** (1979) 682–685.

[16] A. A. Starobinsky, *A New Type of Isotropic Cosmological Models Without Singularity*, *Phys. Lett. B* **91** (1980) 99–102.

[17] A. H. Guth, *The Inflationary Universe: A Possible Solution to the Horizon and Flatness Problems*, *Phys. Rev. D* **23** (1981) 347–356.

[18] A. D. Linde, *A New Inflationary Universe Scenario: A Possible Solution of the Horizon, Flatness, Homogeneity, Isotropy and Primordial Monopole Problems*, *Phys. Lett. B* **108** (1982) 389–393.

[19] A. Albrecht and P. J. Steinhardt, *Cosmology for Grand Unified Theories with Radiatively Induced Symmetry Breaking*, *Phys. Rev. Lett.* **48** (1982) 1220–1223.

[20] S. W. Hawking, *The Development of Irregularities in a Single Bubble Inflationary Universe*, *Phys. Lett. B* **115** (1982) 295.

[21] A. A. Starobinsky, *Dynamics of Phase Transition in the New Inflationary Universe Scenario and Generation of Perturbations*, *Phys. Lett. B* **117** (1982) 175–178.

[22] A. H. Guth and S. Y. Pi, *Fluctuations in the New Inflationary Universe*, *Phys. Rev. Lett.* **49** (1982) 1110–1113.

[23] A. Arbey and F. Mahmoudi, *Dark matter and the early Universe: a review*, *Prog. Part. Nucl. Phys.* **119** (2021) 103865, [2104.11488].

[24] D. Lovelock, *The Einstein tensor and its generalizations*, *J. Math. Phys.* **12** (1971) 498–501.

[25] D. Lovelock, *The four-dimensionality of space and the einstein tensor*, *J. Math. Phys.* **13** (1972) 874–876.

[26] ATLAS collaboration, G. Aad et al., *Observation of a new particle in the search for the Standard Model Higgs boson with the ATLAS detector at the LHC*, *Phys. Lett. B* **716** (2012) 1–29, [1207.7214].

[27] M. Grana, *Flux compactifications in string theory: A Comprehensive review*, *Phys. Rept.* **423** (2006) 91–158, [hep-th/0509003].

[28] T. Clifton, P. G. Ferreira, A. Padilla and C. Skordis, *Modified Gravity and Cosmology*, *Phys. Rept.* **513** (2012) 1–189, [1106.2476].

[29] L. Heisenberg, *A systematic approach to generalisations of General Relativity and their cosmological implications*, *Phys. Rept.* **796** (2019) 1–113, [1807.01725].

[30] C. Brans and R. H. Dicke, *Mach's principle and a relativistic theory of gravitation*, *Phys. Rev.* **124** (1961) 925–935.

[31] P. Jordan, *The present state of Dirac's cosmological hypothesis*, *Z. Phys.* **157** (1959) 112–121.

[32] R. V. Wagoner, *Scalar tensor theory and gravitational waves*, *Phys. Rev. D* **1** (1970) 3209–3216.

[33] G. W. Horndeski, *Second-order scalar-tensor field equations in a four-dimensional space*, *Int. J. Theor. Phys.* **10** (1974) 363–384.

[34] A. Nicolis, R. Rattazzi and E. Trincherini, *The Galileon as a local modification of gravity*, *Phys. Rev. D* **79** (2009) 064036, [0811.2197].

[35] C. Deffayet, G. Esposito-Farese and A. Vikman, *Covariant Galileon*, *Phys. Rev.* **D79** (2009) 084003, [0901.1314].

[36] C. Deffayet, S. Deser and G. Esposito-Farese, *Generalized Galileons: All scalar models whose curved background extensions maintain second-order field equations and stress-tensors*, *Phys. Rev.* **D80** (2009) 064015, [0906.1967].

[37] C. Deffayet, X. Gao, D. A. Steer and G. Zahariade, *From k-essence to generalised Galileons*, *Phys. Rev. D* **84** (2011) 064039, [1103.3260].

[38] T. Kobayashi, M. Yamaguchi and J. Yokoyama, *Generalized G-inflation: Inflation with the most general second-order field equations*, *Prog. Theor. Phys.* **126** (2011) 511–529, [1105.5723].

[39] M. Ostrogradsky, *Mémoires sur les équations différentielles, relatives au problème des isopérimètres*, *Mem. Acad. St. Petersbourg* **6** (1850) 385–517.

[40] R. P. Woodard, *Ostrogradsky's theorem on Hamiltonian instability*, *Scholarpedia* **10** (2015) 32243, [1506.02210].

[41] J. D. Bekenstein, *The Relation between physical and gravitational geometry*, *Phys. Rev. D* **48** (1993) 3641–3647, [gr-qc/9211017].

[42] D. Bettoni and S. Liberati, *Disformal invariance of second order scalar-tensor theories: Framing the Horndeski action*, *Phys. Rev. D* **88** (2013) 084020, [1306.6724].

[43] M. Zumalacárregui and J. García-Bellido, *Transforming gravity: from derivative couplings to matter to second-order scalar-tensor theories beyond the Horndeski Lagrangian*, *Phys. Rev. D* **89** (2014) 064046, [1308.4685].

[44] J. Gleyzes, D. Langlois, F. Piazza and F. Vernizzi, *Healthy theories beyond Horndeski*, *Phys. Rev. Lett.* **114** (2015) 211101, [1404.6495].

[45] M. Crisostomi, K. Koyama and G. Tasinato, *Extended Scalar-Tensor Theories of Gravity*, *JCAP* **1604** (2016) 044, [1602.03119].

[46] D. Langlois and K. Noui, *Degenerate higher derivative theories beyond Horndeski: evading the Ostrogradski instability*, *JCAP* **02** (2016) 034, [1510.06930].

[47] J. Ben Achour, D. Langlois and K. Noui, *Degenerate higher order scalar-tensor theories beyond Horndeski and disformal transformations*, *Phys. Rev.* **D93** (2016) 124005, [1602.08398].

[48] C. W. Misner, K. Thorne and J. Wheeler, *Gravitation*. W. H. Freeman, San Francisco, 1973.

[49] R. V. Pound and G. A. Rebka, *Gravitational Red-Shift in Nuclear Resonance*, *Phys. Rev. Lett.* **3** (1959) 439–441.

[50] C. M. Will, *The Confrontation between General Relativity and Experiment*, *Living Rev. Rel.* **17** (2014) 4, [1403.7377].

[51] S. Hawking and G. Ellis, *The Large Scale Structure of Space-Time*. Cambridge Monographs on Mathematical Physics. Cambridge University Press, 2, 2011, 10.1017/CBO9780511524646.

[52] J. Ben Achour, M. Crisostomi, K. Koyama, D. Langlois, K. Noui and G. Tasinato, *Degenerate higher order scalar-tensor theories beyond Horndeski up to cubic order*, *JHEP* **12** (2016) 100, [1608.08135].

[53] D. Langlois, M. Mancarella, K. Noui and F. Vernizzi, *Effective Description of Higher-Order Scalar-Tensor Theories*, *JCAP* **1705** (2017) 033, [1703.03797].

[54] D. Langlois, R. Saito, D. Yamauchi and K. Noui, *Scalar-tensor theories and modified gravity in the wake of GW170817*, *Phys. Rev. D* **97** (2018) 061501, [1711.07403].

[55] D. Langlois, *Dark energy and modified gravity in degenerate higher-order scalar–tensor (DHOST) theories: A review*, *Int. J. Mod. Phys.* **D28** (2019) 1942006, [1811.06271].

[56] LIGO Scientific, Virgo collaboration, B. P. Abbott et al., *GW170817: Observation of Gravitational Waves from a Binary Neutron Star Inspiral*, *Phys. Rev. Lett.* **119** (2017) 161101, [1710.05832].

[57] LIGO Scientific, Virgo, Fermi-GBM, INTEGRAL collaboration, B. P. Abbott et al., *Gravitational Waves and Gamma-rays from a Binary Neutron Star Merger: GW170817 and GRB 170817A*, *Astrophys. J. Lett.* **848** (2017) L13, [1710.05834].

[58] J. M. Ezquiaga and M. Zumalacárregui, *Dark Energy After GW170817: Dead Ends and the Road Ahead*, *Phys. Rev. Lett.* **119** (2017) 251304, [1710.05901].

[59] P. Creminelli and F. Vernizzi, *Dark Energy after GW170817 and GRB170817A*, *Phys. Rev. Lett.* **119** (2017) 251302, [1710.05877].

[60] T. Baker, E. Bellini, P. G. Ferreira, M. Lagos, J. Noller and I. Sawicki, *Strong constraints on cosmological gravity from GW170817 and GRB 170817A*, *Phys. Rev. Lett.* **119** (2017) 251301, [1710.06394].

[61] J. Sakstein and B. Jain, *Implications of the Neutron Star Merger GW170817 for Cosmological Scalar-Tensor Theories*, *Phys. Rev. Lett.* **119** (2017) 251303, [1710.05893].

[62] C. de Rham and S. Melville, *Gravitational Rainbows: LIGO and Dark Energy at its Cutoff*, *Phys. Rev. Lett.* **121** (2018) 221101, [1806.09417].

[63] P. Creminelli, M. Lewandowski, G. Tambalo and F. Vernizzi, *Gravitational Wave Decay into Dark Energy*, *JCAP* **1812** (2018) 025, [1809.03484].

[64] T. Damour and G. Esposito-Farese, *Nonperturbative strong field effects in tensor - scalar theories of gravitation*, *Phys. Rev. Lett.* **70** (1993) 2220–2223.

[65] D. D. Doneva and S. S. Yazadjiev, *New Gauss-Bonnet Black Holes with Curvature-Induced Scalarization in Extended Scalar-Tensor Theories*, *Phys. Rev. Lett.* **120** (2018) 131103, [1711.01187].

[66] H. O. Silva, J. Sakstein, L. Gualtieri, T. P. Sotiriou and E. Berti, *Spontaneous scalarization of black holes and compact stars from a Gauss-Bonnet coupling*, *Phys. Rev. Lett.* **120** (2018) 131104, [1711.02080].

[67] N. Andreou, N. Franchini, G. Ventagli and T. P. Sotiriou, *Spontaneous scalarization in generalised scalar-tensor theory*, *Phys. Rev. D* **99** (2019) 124022, [1904.06365].

[68] G. Ventagli, A. Lehébel and T. P. Sotiriou, *Onset of spontaneous scalarization in generalized scalar-tensor theories*, *Phys. Rev. D* **102** (2020) 024050, [2006.01153].

[69] C. A. R. Herdeiro, E. Radu, N. Sanchis-Gual and J. A. Font, *Spontaneous Scalarization of Charged Black Holes*, *Phys. Rev. Lett.* **121** (2018) 101102, [1806.05190].

[70] A. Dima, E. Barausse, N. Franchini and T. P. Sotiriou, *Spin-induced black hole spontaneous scalarization*, *Phys. Rev. Lett.* **125** (2020) 231101, [2006.03095].

[71] C. A. R. Herdeiro, E. Radu, H. O. Silva, T. P. Sotiriou and N. Yunes, *Spin-induced scalarized black holes*, *Phys. Rev. Lett.* **126** (2021) 011103, [2009.03904].

[72] E. Berti, L. G. Collodel, B. Kleihaus and J. Kunz, *Spin-induced black-hole scalarization in Einstein-scalar-Gauss-Bonnet theory*, *Phys. Rev. Lett.* **126** (2021) 011104, [2009.03905].

[73] T. Damour and G. Esposito-Farese, *Tensor - scalar gravity and binary pulsar experiments*, *Phys. Rev. D* **54** (1996) 1474–1491, [gr-qc/9602056].

[74] G. Esposito-Farese, *Tests of Alternative Theories of Gravity*, *eConf* **C0507252** (2005) T025.

[75] T. Damour and G. Esposito-Farese, *Tensor multiscalar theories of gravitation*, *Class. Quant. Grav.* **9** (1992) 2093–2176.

[76] B. Bertotti, L. Iess and P. Tortora, *A test of general relativity using radio links with the Cassini spacecraft*, *Nature* **425** (2003) 374–376.

[77] P. C. Freire, N. Wex, G. Esposito-Farese, J. P. Verbiest, M. Bailes, B. A. Jacoby et al., *The relativistic pulsar-white dwarf binary PSR J1738+0333 II. The most stringent test of scalar-tensor gravity*, *Mon. Not. Roy. Astron. Soc.* **423** (2012) 3328, [1205.1450].

[78] L. Shao, N. Sennett, A. Buonanno, M. Kramer and N. Wex, *Constraining nonperturbative strong-field effects in scalar-tensor gravity by combining pulsar timing and laser-interferometer gravitational-wave detectors*, *Phys. Rev. X* **7** (2017) 041025, [1704.07561].

[79] L. Sampson, N. Yunes, N. Cornish, M. Ponce, E. Barausse, A. Klein et al., *Projected Constraints on Scalarization with Gravitational Waves from Neutron Star Binaries*, *Phys. Rev. D* **90** (2014) 124091, [1407.7038].

[80] T. A. de Pirey Saint Alby and N. Yunes, *Cosmological Evolution and Solar System Consistency of Massive Scalar-Tensor Gravity*, *Phys. Rev. D* **96** (2017) 064040, [1703.06341].

[81] D. Anderson, N. Yunes and E. Barausse, *Effect of cosmological evolution on Solar System constraints and on the scalarization of neutron stars in massless scalar-tensor theories*, *Phys. Rev.* **D94** (2016) 104064, [1607.08888].

[82] D. D. Doneva and S. S. Yazadjiev, *Neutron star solutions with curvature induced scalarization in the extended Gauss-Bonnet scalar-tensor theories*, *JCAP* **04** (2018) 011, [1712.03715].

[83] G. Antoniou, A. Bakopoulos and P. Kanti, *Evasion of No-Hair Theorems and Novel Black-Hole Solutions in Gauss-Bonnet Theories*, *Phys. Rev. Lett.* **120** (2018) 131102, [1711.03390].

[84] G. Antoniou, A. Bakopoulos and P. Kanti, *Black-Hole Solutions with Scalar Hair in Einstein-Scalar-Gauss-Bonnet Theories*, *Phys. Rev.* **D97** (2018) 084037, [1711.07431].

[85] A. Bakopoulos, G. Antoniou and P. Kanti, *Novel Black-Hole Solutions in Einstein-Scalar-Gauss-Bonnet Theories with a Cosmological Constant*, 1812.06941.

[86] W. Buell and B. A. Shadwick, *Potentials and bound states*, *American Journal of Physics - AMER J PHYS* **63** (03, 1995) 256–258.

[87] J. L. Blázquez-Salcedo, D. D. Doneva, J. Kunz and S. S. Yazadjiev, *Radial perturbations of the scalarized Einstein-Gauss-Bonnet black holes*, *Phys. Rev.* **D98** (2018) 084011, [1805.05755].

[88] M. Minamitsuji and T. Ikeda, *Scalarized black holes in the presence of the coupling to Gauss-Bonnet gravity*, *Phys. Rev. D* **99** (2019) 044017, [1812.03551].

[89] H. O. Silva, C. F. B. Macedo, T. P. Sotiriou, L. Gualtieri, J. Sakstein and E. Berti, *Stability of scalarized black hole solutions in scalar-Gauss-Bonnet gravity*, *Phys. Rev. D* **99** (2019) 064011, [1812.05590].

[90] T. Anson, E. Babichev, C. Charmousis and S. Ramazanov, *Cosmological instability of scalar-Gauss-Bonnet theories exhibiting scalarization*, *JCAP* **06** (2019) 023, [1903.02399].

[91] V. Mukhanov, *Physical Foundations of Cosmology*. Cambridge University Press, Oxford, 2005.

[92] A. Y. Morozov, *Anomalies in Gauge Theories*, *Sov. Phys. Usp.* **29** (1986) 993–1039.

[93] K. Kajantie, M. Laine, K. Rummukainen and Y. Schroder, *The Pressure of hot QCD up to g6 ln(1/g)*, *Phys. Rev. D* **67** (2003) 105008, [hep-ph/0211321].

[94] H. Davoudiasl, R. Kitano, G. D. Kribs, H. Murayama and P. J. Steinhardt, *Gravitational baryogenesis*, *Phys. Rev. Lett.* **93** (2004) 201301, [hep-ph/0403019].

[95] T. S. Bunch and P. C. W. Davies, *Quantum Field Theory in de Sitter Space: Renormalization by Point Splitting*, *Proc. Roy. Soc. Lond. A* **360** (1978) 117–134.

[96] C. F. Macedo, J. Sakstein, E. Berti, L. Gualtieri, H. O. Silva and T. P. Sotiriou, *Self-interactions and Spontaneous Black Hole Scalarization*, *Phys. Rev. D* **99** (2019) 104041, [1903.06784].

[97] G. Antoniou, L. Bordin and T. P. Sotiriou, *Compact object scalarization with general relativity as a cosmic attractor*, *Phys. Rev. D* **103** (2021) 024012, [2004.14985].

[98] T. Anson, E. Babichev and S. Ramazanov, *Reconciling spontaneous scalarization with cosmology*, *Phys. Rev. D* **100** (2019) 104051, [1905.10393].

[99] A. L. Erickcek, N. Barnaby, C. Burrage and Z. Huang, *Chameleons in the Early Universe: Kicks, Rebounds, and Particle Production*, *Phys. Rev. D* **89** (2014) 084074, [1310.5149].

[100] A. Belokon and A. Tokareva, *Light scalar dark matter coupled to a trace of energy-momentum tensor*, *Phys. Rev. D* **101** (2020) 103535, [1812.04065].

[101] D. Polarski and A. A. Starobinsky, *Isocurvature perturbations in multiple inflationary models*, *Phys. Rev. D* **50** (1994) 6123–6129, [astro-ph/9404061].

[102] T. M. Dunster, *Bessel functions of purely imaginary order, with an application to second-order linear differential equations having a large parameter*, *SIAM Journal on Mathematical Analysis* **21** (1990) 995–1018, [https://doi.org/10.1137/0521055].

[103] P. Kanti, R. Gannouji and N. Dadhich, *Gauss-Bonnet Inflation*, *Phys. Rev.* **D92** (2015) 041302, [1503.01579].

[104] P. Kanti, R. Gannouji and N. Dadhich, *Early-time cosmological solutions in Einstein-scalar-Gauss-Bonnet theory*, *Phys. Rev.* **D92** (2015) 083524, [1506.04667].

[105] G. Hikmawan, J. Soda, A. Suroso and F. P. Zen, *Comment on "Gauss-Bonnet inflation"*, *Phys. Rev.* **D93** (2016) 068301, [1512.00222].

[106] M. Minamitsuji and H. O. Silva, *Relativistic stars in scalar-tensor theories with disformal coupling*, *Phys. Rev. D* **93** (2016) 124041, [1604.07742].

[107] J. Khoury and A. Weltman, *Chameleon cosmology*, *Phys. Rev. D* **69** (2004) 044026, [astro-ph/0309411].

[108] K. Hinterbichler and J. Khoury, *Symmetron Fields: Screening Long-Range Forces Through Local Symmetry Restoration*, *Phys. Rev. Lett.* **104** (2010) 231301, [1001.4525].

[109] K. Hinterbichler, J. Khoury, A. Levy and A. Matas, *Symmetron Cosmology*, *Phys. Rev. D* **84** (2011) 103521, [1107.2112].

[110] W. Pauli and M. Fierz, *On Relativistic Field Equations of Particles With Arbitrary Spin in an Electromagnetic Field*, *Helv. Phys. Acta* **12** (1939) 297–300.

[111] M. Fierz, *Force-free particles with any spin*, *Helv. Phys. Acta* **12** (1939) 3–37.

[112] M. Fierz and W. Pauli, *On relativistic wave equations for particles of arbitrary spin in an electromagnetic field*, *Proc. Roy. Soc. Lond. A* **173** (1939) 211–232.

[113] H. van Dam and M. J. G. Veltman, *Massive and massless Yang-Mills and gravitational fields*, *Nucl. Phys. B* **22** (1970) 397–411.

[114] V. I. Zakharov, *Linearized gravitation theory and the graviton mass*, *JETP Lett.* **12** (1970) 312.

[115] Y. Iwasaki, *Consistency condition for propagators*, *Phys. Rev. D* **2** (1970) 2255–2256.

[116] A. Vainshtein, *To the problem of nonvanishing gravitation mass*, *Phys. Lett. B* **39** (1972) 393–394.

[117] D. G. Boulware and S. Deser, *Can gravitation have a finite range?*, *Phys. Rev. D* **6** (1972) 3368–3382.

[118] E. Babichev, C. Deffayet and R. Ziour, *The Vainshtein mechanism in the Decoupling Limit of massive gravity*, *JHEP* **05** (2009) 098, [0901.0393].

[119] E. Babichev, C. Deffayet and R. Ziour, *Recovering General Relativity from massive gravity*, *Phys. Rev. Lett.* **103** (2009) 201102, [0907.4103].

[120] E. Babichev, C. Deffayet and R. Ziour, *The Recovery of General Relativity in massive gravity via the Vainshtein mechanism*, *Phys. Rev. D* **82** (2010) 104008, [1007.4506].

[121] K. Koyama, G. Niz and G. Tasinato, *Analytic solutions in non-linear massive gravity*, *Phys. Rev. Lett.* **107** (2011) 131101, [1103.4708].

[122] K. Koyama, G. Niz and G. Tasinato, *Strong interactions and exact solutions in non-linear massive gravity*, *Phys. Rev. D* **84** (2011) 064033, [1104.2143].

[123] G. Chkareuli and D. Pirtskhalava, *Vainshtein Mechanism In Λ_3 - Theories*, *Phys. Lett. B* **713** (2012) 99–103, [1105.1783].

[124] M. S. Volkov, *Hairy black holes in the ghost-free bigravity theory*, *Phys. Rev. D* **85** (2012) 124043, [1202.6682].

[125] E. Babichev and M. Crisostomi, *Restoring general relativity in massive bigravity theory*, *Phys. Rev. D* **88** (2013) 084002, [1307.3640].

[126] E. Babichev, C. Deffayet and R. Ziour, *k-Mouflage gravity*, *Int. J. Mod. Phys.* **D18** (2009) 2147–2154, [0905.2943].

[127] E. Babichev and C. Deffayet, *An introduction to the Vainshtein mechanism*, *Class. Quant. Grav.* **30** (2013) 184001, [1304.7240].

[128] M. A. Luty, M. Porrati and R. Rattazzi, *Strong interactions and stability in the DGP model*, *JHEP* **09** (2003) 029, [hep-th/0303116].

[129] E. Babichev, *Galileon accretion*, *Phys. Rev. D* **83** (2011) 024008, [1009.2921].

[130] E. Babichev and G. Esposito-Farèse, *Time-Dependent Spherically Symmetric Covariant Galileons*, *Phys. Rev. D* **87** (2013) 044032, [1212.1394].

[131] E. Babichev and C. Charmousis, *Dressing a black hole with a time-dependent Galileon*, *JHEP* **08** (2014) 106, [1312.3204].

[132] R. Kimura, T. Kobayashi and K. Yamamoto, *Vainshtein screening in a cosmological background in the most general second-order scalar-tensor theory*, *Phys. Rev.* **D85** (2012) 024023, [1111.6749].

[133] A. De Felice, R. Kase and S. Tsujikawa, *Vainshtein mechanism in second-order scalar-tensor theories*, *Phys. Rev. D* **85** (2012) 044059, [1111.5090].

[134] K. Koyama, G. Niz and G. Tasinato, *Effective theory for the Vainshtein mechanism from the Horndeski action*, *Phys. Rev.* **D88** (2013) 021502, [1305.0279].

[135] R. Kase and S. Tsujikawa, *Screening the fifth force in the Horndeski's most general scalar-tensor theories*, *JCAP* **08** (2013) 054, [1306.6401].

[136] J. Chagoya, K. Koyama, G. Niz and G. Tasinato, *Galileons and strong gravity*, *JCAP* **1410** (2014) 055, [1407.7744].

[137] E. Babichev and G. Esposito-Farèse, *Cosmological self-tuning and local solutions in generalized Horndeski theories*, *Phys. Rev.* **D95** (2017) 024020, [1609.09798].

[138] T. Kobayashi, Y. Watanabe and D. Yamauchi, *Breaking of Vainshtein screening in scalar-tensor theories beyond Horndeski*, *Phys. Rev.* **D91** (2015) 064013, [1411.4130].

[139] R. Kase, S. Tsujikawa and A. De Felice, *Cosmology with a successful Vainshtein screening in theories beyond Horndeski*, *Phys. Rev. D* **93** (2016) 024007, [1510.06853].

[140] K. Koyama and J. Sakstein, *Astrophysical Probes of the Vainshtein Mechanism: Stars and Galaxies*, *Phys. Rev. D* **91** (2015) 124066, [1502.06872].

[141] R. Saito, D. Yamauchi, S. Mizuno, J. Gleyzes and D. Langlois, *Modified gravity inside astrophysical bodies*, *JCAP* **06** (2015) 008, [1503.01448].

[142] E. Babichev, K. Koyama, D. Langlois, R. Saito and J. Sakstein, *Relativistic Stars in Beyond Horndeski Theories*, *Class. Quant. Grav.* **33** (2016) 235014, [1606.06627].

[143] J. Sakstein, E. Babichev, K. Koyama, D. Langlois and R. Saito, *Towards Strong Field Tests of Beyond Horndeski Gravity Theories*, *Phys. Rev.* **D95** (2017) 064013, [1612.04263].

[144] A. Dima and F. Vernizzi, *Vainshtein Screening in Scalar-Tensor Theories before and after GW170817: Constraints on Theories beyond Horndeski*, *Phys. Rev.* **D97** (2018) 101302, [1712.04731].

[145] M. Crisostomi and K. Koyama, *Vainshtein mechanism after GW170817*, *Phys. Rev. D* **97** (2018) 021301, [1711.06661].

[146] S. Hirano, T. Kobayashi and D. Yamauchi, *Screening mechanism in degenerate higher-order scalar-tensor theories evading gravitational wave constraints*, *Phys. Rev.* **D99** (2019) 104073, [1903.08399].

[147] M. Crisostomi, M. Lewandowski and F. Vernizzi, *Vainshtein regime in Scalar-Tensor gravity: constraints on DHOST theories*, *Phys. Rev.* **D100** (2019) 024025, [1903.11591].

[148] C. Burrage, E. J. Copeland, A. Moss and J. A. Stevenson, *The shape dependence of chameleon screening*, *JCAP* **01** (2018) 056, [1711.02065].

[149] C. Burrage, E. J. Copeland and J. Stevenson, *Ellipticity Weakens Chameleon Screening*, *Phys. Rev. D* **91** (2015) 065030, [1412.6373].

[150] T. Hiramatsu, W. Hu, K. Koyama and F. Schmidt, *Equivalence Principle Violation in Vainshtein Screened Two-Body Systems*, *Phys. Rev. D* **87** (2013) 063525, [1209.3364].

[151] A. Maselli, H. O. Silva, M. Minamitsuji and E. Berti, *Slowly rotating black hole solutions in Horndeski gravity*, *Phys. Rev.* **D92** (2015) 104049, [1508.03044].

[152] A. Cisterna, M. Cruz, T. Delsate and J. Saavedra, *Nonminimal derivative coupling scalar-tensor theories: odd-parity perturbations and black hole stability*, *Phys. Rev. D* **92** (2015) 104018, [1508.06413].

[153] A. Cisterna, T. Delsate, L. Ducobu and M. Rinaldi, *Slowly rotating neutron stars in the nonminimal derivative coupling sector of Horndeski gravity*, *Phys. Rev.* **D93** (2016) 084046, [1602.06939].

[154] J. B. Hartle, *Slowly rotating relativistic stars. 1. Equations of structure*, *Astrophys. J.* **150** (1967) 1005–1029.

[155] T. Anson and E. Babichev, *Vainshtein screening for slowly rotating stars*, *Phys. Rev. D* **102** (2020) 044046, [2005.05990].

[156] E. Babichev, C. Charmousis and M. Hassaine, *Charged Galileon black holes*, *JCAP* **05** (2015) 031, [1503.02545].

[157] A. Papapetrou, *Einstein's theory of gravitation and flat space*, *Proc. Roy. Irish Acad.(Sect. A)* **52A** (1948) 11–23.

[158] E. Babichev, C. Deffayet and G. Esposito-Farèse, *Constraints on Shift-Symmetric Scalar-Tensor Theories with a Vainshtein Mechanism from Bounds on the Time Variation of G*, *Phys. Rev. Lett.* **107** (2011) 251102, [1107.1569].

[159] E. Babichev and A. Lehébel, *The sound of DHOST*, *JCAP* **12** (2018) 027, [1810.09997].

[160] A. Lehébel, E. Babichev and C. Charmousis, *A no-hair theorem for stars in Horndeski theories*, *JCAP* **1707** (2017) 037, [1706.04989].

[161] E. Babichev, C. Charmousis and A. Lehébel, *Asymptotically flat black holes in Horndeski theory and beyond*, *JCAP* **1704** (2017) 027, [1702.01938].

[162] D. Robinson, *Uniqueness of the Kerr black hole*, *Phys. Rev. Lett.* **34** (1975) 905–906.

[163] A. Ghez et al., *The Galactic Center: A Laboratory for Fundamental Astrophysics and Galactic Nuclei*, 0903.0383.

[164] Event Horizon Telescope collaboration, K. Akiyama et al., *First M87 Event Horizon Telescope Results. I. The Shadow of the Supermassive Black Hole*, *Astrophys. J.* **875** (2019) L1, [1906.11238].

[165] GRAVITY collaboration, R. Abuter et al., *Detection of the gravitational redshift in the orbit of the star S2 near the Galactic centre massive black hole*, *Astron. Astrophys.* **615** (2018) L15, [1807.09409].

[166] GRAVITY collaboration, R. Abuter et al., *Detection of the Schwarzschild precession in the orbit of the star S2 near the Galactic centre massive black hole*, *Astron. Astrophys.* **636** (2020) L5, [2004.07187].

[167] C. M. Will, *Testing the general relativistic no-hair theorems using the Galactic center black hole SgrA**, *Astrophys. J. Lett.* **674** (2008) L25–L28, [0711.1677].

[168] W. Israel, *Event horizons in static vacuum space-times*, *Phys. Rev.* **164** (1967) 1776–1779.

[169] W. Israel, *Event horizons in static electrovac space-times*, *Commun. Math. Phys.* **8** (1968) 245–260.

[170] B. Carter, *Axisymmetric Black Hole Has Only Two Degrees of Freedom*, *Phys. Rev. Lett.* **26** (1971) 331–333.

[171] T. Johannsen, *Sgr A* and General Relativity*, *Class. Quant. Grav.* **33** (2016) 113001, [1512.03818].

[172] C. A. R. Herdeiro and E. Radu, *Kerr black holes with scalar hair*, *Phys. Rev. Lett.* **112** (2014) 221101, [1403.2757].

[173] F. H. Vincent, E. Gourgoulhon, C. Herdeiro and E. Radu, *Astrophysical imaging of Kerr black holes with scalar hair*, *Phys. Rev. D* **94** (2016) 084045, [1606.04246].

[174] F. H. Vincent, Z. Meliani, P. Grandclement, E. Gourgoulhon and O. Straub, *Imaging a boson star at the Galactic center*, *Class. Quant. Grav.* **33** (2016) 105015, [1510.04170].

[175] K. Van Aelst, E. Gourgoulhon, P. Grandclément and C. Charmousis, *Hairy rotating black holes in cubic Galileon theory*, *Class. Quant. Grav.* **37** (2020) 035007, [1910.08451].

[176] G. O. Papadopoulos and K. D. Kokkotas, *Preserving Kerr symmetries in deformed spacetimes*, *Class. Quant. Grav.* **35** (2018) 185014, [1807.08594].

[177] T. Johannsen, *Systematic Study of Event Horizons and Pathologies of Parametrically Deformed Kerr Spacetimes*, *Phys. Rev. D* **87** (2013) 124017, [1304.7786].

[178] T. Johannsen, *Regular Black Hole Metric with Three Constants of Motion*, *Phys. Rev. D* **88** (2013) 044002, [1501.02809].

[179] B. Carter, *Hamilton-Jacobi and Schrodinger separable solutions of Einstein's equations*, *Commun. Math. Phys.* **10** (1968) 280–310.

[180] E. T. Newman, R. Couch, K. Chinnapared, A. Exton, A. Prakash and R. Torrence, *Metric of a Rotating, Charged Mass*, *J. Math. Phys.* **6** (1965) 918–919.

[181] S. Chandrasekhar, *The mathematical theory of black holes*. Oxford Univ. Press, Oxford, 2002.

[182] G. D. Birkhoff and R. E. Langer, *Relativity and modern physics*. Harvard University Press, 1923.

[183] J. T. Jebsen, *On the general spherically symmetric solutions of einstein's gravitational equations in vacuo*, *General Relativity and Gravitation* **37** (2005) 2253–2259.

[184] R. M. Wald, *General Relativity*. Chicago Univ. Pr., Chicago, USA, 1984.

[185] S. W. Hawking, *Black hole explosions*, *Nature* **248** (1974) 30–31.

[186] J. D. Bekenstein, *Black holes and entropy*, *Phys. Rev. D* **7** (1973) 2333–2346.

[187] R. H. Boyer and R. W. Lindquist, *Maximal analytic extension of the Kerr metric*, *J. Math. Phys.* **8** (1967) 265.

[188] B. Carter, *The commutation property of a stationary, axisymmetric system*, *Commun. Math. Phys.* **17** (1970) 233–238.

[189] M. Heusler, *Black Hole Uniqueness Theorems*. Cambridge University Press, 1996.

[190] A. Papapetrou, *Champs gravitationnels stationnaires a symetrie axiale*, *Ann. Inst. H. Poincare Phys. Theor.* **4** (1966) 83–105.

[191] M. Walker and R. Penrose, *On quadratic first integrals of the geodesic equations for type [22] spacetimes*, *Commun. Math. Phys.* **18** (1970) 265–274.

[192] A. Z. Petrov, *The Classification of spaces defining gravitational fields*, *Gen. Rel. Grav.* **32** (2000) 1661–1663.

[193] F. A. E. Pirani, *Invariant formulation of gravitational radiation theory*, *Phys. Rev.* **105** (1957) 1089–1099.

[194] R. Penrose, *A Spinor approach to general relativity*, *Annals Phys.* **10** (1960) 171–201.

[195] H. Stephani, D. Kramer, M. A. H. MacCallum, C. Hoenselaers and E. Herlt, *Exact solutions of Einstein's field equations*. Cambridge Monographs on Mathematical Physics. Cambridge Univ. Press, Cambridge, 2003, 10.1017/CBO9780511535185.

[196] B. O'Neill, *The Geometry of Kerr Black Holes*. A K Peters, Wellesley, Massachusetts, 1995.

[197] B. Carter, *Global structure of the Kerr family of gravitational fields*, *Phys. Rev.* **174** (1968) 1559–1571.

[198] R. Penrose, *Gravitational collapse: The role of general relativity*, *Riv. Nuovo Cim.* **1** (1969) 252–276.

[199] R. M. Wald, *The thermodynamics of black holes*, *Living Rev. Rel.* **4** (2001) 6, [gr-qc/9912119].

[200] R. Penrose and R. M. Floyd, *Extraction of rotational energy from a black hole*, *Nature* **229** (1971) 177–179.

[201] R. M. Wald, *Energy Limits on the Penrose Process*, *Astrophys. J.* **191** (1974) 231.

[202] Y. B. Zel'Dovich, *Generation of Waves by a Rotating Body*, *Soviet Journal of Experimental and Theoretical Physics Letters* **14** (1971) 180.

[203] Y. B. Zel'Dovich, *Amplification of Cylindrical Electromagnetic Waves Reflected from a Rotating Body*, *Soviet Journal of Experimental and Theoretical Physics* **35** (1972) 1085.

[204] A. A. Starobinsky, *Amplification of waves reflected from a rotating "black hole"*, *Sov. Phys. JETP* **37** (1973) 28–32.

[205] A. A. Starobinskil and S. M. Churilov, *Amplification of electromagnetic and gravitational waves scattered by a rotating "black hole"*, *Sov. Phys. JETP* **65** (1974) 1–5.

[206] N. Deruelle and R. Ruffini, *Quantum and classical relativistic energy states in stationary geometries*, *Phys. Lett. B* **52** (1974) 437–441.

[207] N. Deruelle and R. Ruffini, *Klein Paradox in a Kerr Geometry*, *Phys. Lett. B* **57** (1975) 248–252.

[208] R. Brito, V. Cardoso and P. Pani, *Superradiance: New Frontiers in Black Hole Physics*, *Lect. Notes Phys.* **906** (2015) pp.1–237, [1501.06570].

[209] S. Corley and T. Jacobson, *Black hole lasers*, *Phys. Rev. D* **59** (1999) 124011, [hep-th/9806203].

[210] U. Leonhardt and T. G. Philbin, *Black Hole Lasers Revisited*, 3, 2008, 0803.0669.

[211] A. Coutant and R. Parentani, *Black hole lasers, a mode analysis*, *Phys. Rev. D* **81** (2010) 084042, [0912.2755].

[212] S. Finazzi and R. Parentani, *Black-hole lasers in Bose-Einstein condensates*, *New J. Phys.* **12** (2010) 095015, [1005.4024].

[213] T. Anson, E. Babichev, C. Charmousis and M. Hassaine, *Disforming the Kerr metric*, *JHEP* **01** (2021) 018, [2006.06461].

[214] C. Charmousis, M. Crisostomi, R. Gregory and N. Stergioulas, *Rotating Black Holes in Higher Order Gravity*, *Phys. Rev. D* **100** (2019) 084020, [1903.05519].

[215] C. Charmousis, M. Crisostomi, D. Langlois and K. Noui, *Perturbations of a rotating black hole in DHOST theories*, *Class. Quant. Grav.* **36** (2019) 235008, [1907.02924].

[216] E. Babichev, C. Charmousis, G. Esposito-Farèse and A. Lehébel, *Stability of Black Holes and the Speed of Gravitational Waves within Self-Tuning Cosmological Models*, *Phys. Rev. Lett.* **120** (2018) 241101, [1712.04398].

[217] E. Babichev, C. Charmousis, G. Esposito-Farèse and A. Lehébel, *Hamiltonian unboundedness vs stability with an application to Horndeski theory*, *Phys. Rev. D* **98** (2018) 104050, [1803.11444].

[218] J. Ben Achour, H. Liu and S. Mukohyama, *Hairy black holes in DHOST theories: Exploring disformal transformation as a solution-generating method*, *JCAP* **02** (2020) 023, [1910.11017].

[219] J. Ben Achour, H. Liu, H. Motohashi, S. Mukohyama and K. Noui, *On rotating black holes in DHOST theories*, *JCAP* **11** (2020) 001, [2006.07245].

[220] E. Gourgoulhon and S. Bonazzola, *Noncircular axisymmetric stationary spacetimes*, *Phys. Rev. D* **48** (Sept., 1993) 2635–2652.

[221] K. Ioka and M. Sasaki, *Grad-Shafranov equation in noncircular stationary axisymmetric space-times*, *Phys. Rev. D* **67** (2003) 124026, [gr-qc/0302106].

[222] K. Ioka and M. Sasaki, *Relativistic stars with poloidal and toroidal magnetic fields and meridional flow*, *Astrophys. J.* **600** (2004) 296–316, [astro-ph/0305352].

[223] S. Benenti and M. Francaviglia, *Remarks on certain separability structures and their applications to general relativity*, *General Relativity and Gravitation* **10** (1979) 79–92.

[224] S. Benenti and M. Francaviglia, *The Theory of Separability of the Hamilton-Jacobi Equation and its Applications to General Relativity*, in *General Relativity and Gravitation. Vol. 1. One hundred years after the birth of Albert Einstein. Edited by A. Held. New York*, vol. 1, p. 393, Jan., 1980.

[225] S. Benenti and M. Francaviglia, *Canonical forms for separability structures with less than five killing tensors*, *Annales de l'I.H.P. Physique théorique* **34** (1981) 45–64.

[226] E. Babichev, V. Mukhanov and A. Vikman, *k-Essence, superluminal propagation, causality and emergent geometry*, *JHEP* **02** (2008) 101, [0708.0561].

[227] E. Babichev, V. F. Mukhanov and A. Vikman, *Escaping from the black hole?*, *JHEP* **09** (2006) 061, [hep-th/0604075].

[228] A. Anabalon, N. Deruelle, D. Tempo and R. Troncoso, *Remarks on the Myers-Perry and Einstein Gauss-Bonnet Rotating Solutions*, *Int. J. Mod. Phys. D* **20** (2011) 639–647, [1009.3030].

[229] J. N. Goldberg and R. K. Sachs, *Republication of: A theorem on petrov types*, *General Relativity and Gravitation* **41** (2009) 433–444.

[230] E. Newman and R. Penrose, *An Approach to gravitational radiation by a method of spin coefficients*, *J. Math. Phys.* **3** (1962) 566–578.

[231] J. G. Baker and M. Campanelli, *Making use of geometrical invariants in black hole collisions*, *Phys. Rev. D* **62** (2000) 127501, [gr-qc/0003031].

[232] J. B. Achour, A. De Felice, M. A. Gorji, S. Mukohyama and M. C. Pookkillath, *Disformal map and Petrov classification in modified gravity*, 2107.02386.

[233] T. Anson, E. Babichev and C. Charmousis, *Deformed black hole in Sagittarius A*, *Phys. Rev. D* **103** (2021) 124035, [2103.05490].

[234] C. M. Will and M. Maitra, *Relativistic orbits around spinning supermassive black holes. Secular evolution to 4.5 post-Newtonian order*, *Phys. Rev. D* **95** (2017) 064003, [1611.06931].

[235] E. M. Butterworth and J. R. Ipser, *Rapidly rotating fluid bodies in general relativity*, *Astrophys. J.* **200** (1975) L103–L106.

[236] E. M. Butterworth and J. R. Ipser, *On the structure and stability of rapidly rotating fluid bodies in general relativity. I. The numerical method for computing structure and its application to uniformly rotating homogeneous bodies*, *Astrophys. J.* **204** (1976) 200–223.

[237] J. M. Bardeen and R. V. Wagoner, *Relativistic Disks. I. Uniform Rotation*, *Astrophys. J.* **167** (1971) 359.

[238] J. L. Friedman and N. Stergioulas, *Rotating Relativistic Stars*. Cambridge Monographs on Mathematical Physics. Cambridge University Press, 3, 2013, 10.1017/CBO9780511977596.

[239] G. Pappas and T. A. Apostolatos, *Revising the multipole moments of numerical spacetimes, and its consequences*, *Phys. Rev. Lett.* **108** (2012) 231104, [1201.6067].

[240] V. Paschalidis and N. Stergioulas, *Rotating Stars in Relativity*, *Living Rev. Rel.* **20** (2017) 7, [1612.03050].

[241] A. Lanza, *Multigrid in general relativity. II. Kerr spacetime*, *Classical and Quantum Gravity* **9** (1992) 677–696.

[242] E. Gourgoulhon, *An Introduction to the theory of rotating relativistic stars*, in *CompStar 2010: School and Workshop on Computational Tools for Compact Star Astrophysics*, 3, 2010, 1003.5015.

[243] R. P. Geroch, *Multipole moments. II. Curved space*, *J. Math. Phys.* **11** (1970) 2580–2588.

[244] R. O. Hansen, *Multipole moments of stationary space-times*, *J. Math. Phys.* **15** (1974) 46–52.

[245] J. B. Hartle and K. S. Thorne, *Slowly Rotating Relativistic Stars. II. Models for Neutron Stars and Supermassive Stars*, *Astrophys. J.* **153** (1968) 807.

[246] K. Glampedakis and S. Babak, *Mapping spacetimes with LISA: Inspiral of a test-body in a 'quasi-Kerr' field*, *Class. Quant. Grav.* **23** (2006) 4167–4188, [gr-qc/0510057].

[247] M. H. Soffel and W.-B. Han, *Applied General Relativity*. Springer, 2019, 10.1007/978-3-030-19673-8.

[248] C. W. Lincoln and C. M. Will, *Coalescing Binary Systems of Compact Objects to (Post)5/2 Newtonian Order: Late Time Evolution and Gravitational Radiation Emission*, *Phys. Rev. D* **42** (1990) 1123–1143.

[249] T. Hinderer and E. E. Flanagan, *Two timescale analysis of extreme mass ratio inspirals in Kerr. I. Orbital Motion*, *Phys. Rev. D* **78** (2008) 064028, [0805.3337].

[250] C. M. Bender and S. A. Orszag, *Advanced mathematical methods for scientists and engineers I: Asymptotic methods and perturbation theory*. Springer Science & Business Media, 2013.

[251] T. Mora and C. M. Will, *A PostNewtonian diagnostic of quasiequilibrium binary configurations of compact objects*, *Phys. Rev. D* **69** (2004) 104021, [gr-qc/0312082].

[252] C. Jiang and W. Lin, *Harmonic metric for Kerr black hole and its post-Newtonian approximation*, *General Relativity and Gravitation* **46** (Feb., 2014) 1671.

[253] A. Tucker and C. M. Will, *Pericenter advance in general relativity: Comparison of approaches at high post-Newtonian orders*, *Class. Quant. Grav.* **36** (2019) 115001, [1809.05163].

[254] A. F. Zakharov, *Tests of gravity theories with Galactic Center observations*, *Int. J. Mod. Phys. D* **28** (2019) 1941003, [1901.08343].

[255] A. F. Zakharov, *Constraints on tidal charge of the supermassive black hole at the Galactic Center with trajectories of bright stars*, *Eur. Phys. J. C* **78** (2018) 689, [1804.10374].

[256] P. Bambhaniya, D. Dey, A. B. Joshi, P. S. Joshi, D. N. Solanki and A. Mehta, *Shadows and negative precession in non-Kerr spacetime*, 2101.03865.

[257] T. Johannsen and D. Psaltis, *A Metric for Rapidly Spinning Black Holes Suitable for Strong-Field Tests of the No-Hair Theorem*, *Phys. Rev. D* **83** (2011) 124015, [1105.3191].

[258] P. Christian, D. Psaltis and A. Loeb, *Shapiro Delays at the Quadrupole Order for Tests of the No-Hair Theorem Using Pulsars around Spinning Black Holes*, 1511.01901.

[259] B. Cropp, S. Liberati and M. Visser, *Surface gravities for non-Killing horizons*, *Class. Quant. Grav.* **30** (2013) 125001, [1302.2383].

[260] F. Long, S. Chen, M. Wang and J. Jing, *Shadow of a disformal Kerr black hole in quadratic degenerate higher-order scalar–tensor theories*, *Eur. Phys. J. C* **80** (2020) 1180, [2009.07508].

[261] R. d'Inverno, *Introducing Einstein's relativity*. Clarendon Press, Oxford, 1992.

université PARIS-SACLAY

ÉCOLE DOCTORALE
Physique en île-de-France (EDPIF)

Titre: Trous noirs, étoiles et cosmologie dans les théories tenseur-scalaire

Mots clés: Gravité modifiée, théories tenseur-scalaire, trous noirs, écrantage de Vainshtein, cosmologie

Résumé: En 1915, Einstein proposait sa théorie de la relativité générale. Bien que celle-ci ait passé tous les tests expérimentaux durant ce dernier siècle, il reste néanmoins certains mystères de la nature qui ont poussé les scientifiques à étudier des théories alternatives de la gravitation. Les modifications les plus simples sont obtenues en ajoutant un champ scalaire dans la description de l'interaction gravitationnelle, en plus du tenseur déjà présent en relativité générale. La première partie de cette thèse est consacrée à la cosmologie dans le cadre de théories tenseur-scalaire présentant le phénomène de scalarisation spontanée. Nous montrons que la masse effective tachyonique responsable de la scalarisation déstabilise en général la phase d'inflation au début de l'histoire de l'Univers, mais que ce problème peut être résolu dans un modèle particulier. La deuxième partie porte sur l'écrantage de Vainsthein, un mécanisme permettant de restaurer la relativité générale près d'une source gravitationnelle. Il s'applique en général à des configurations à symétrie sphérique, mais nous étudions ses extensions pour des sources en rotation lente. Dans la dernière partie, nous construisons une classe de trous noirs en rotation dans une certaine catégorie de théories tenseur-scalaire. Ces solutions sont obtenues en réalisant une transformation disforme à partir de la solution de Kerr, et présentent de nombreuses propriétés intéressantes que nous analysons. Nous étudions ensuite les orbites d'étoiles autour de tels objets, dans l'optique de contraindre ces solutions à l'aide d'expériences présentes et futures.

Title: Black holes, stars and cosmology in scalar-tensor theories

Keywords: Modified gravity, scalar-tensor theories, black holes, Vainshtein screening, cosmology

Abstract: It has been more than 100 years since Einstein proposed his general theory of relativity. Even though it has passed all experimental tests, there remain some mysteries in the current understanding of Nature which motivate the study of alternative theories of gravitation. The simplest modifications are obtained by considering a scalar field in addition to the tensor of general relativity. The first part of the thesis is devoted to the cosmology of scalar-tensor theories exhibiting spontaneous scalarization. We show that the tachyonic effective mass responsible for scalarization generically spoils the inflationary stage of the Universe, and argue that this instability can be cured in a particular class of theories. The second part is about the Vainshtein screening, which is a mechanism allowing the recovery of general relativity near gravitational sources. While spherical symmetry is usually assumed for the Vainshtein mechanism, we discuss its extension to slowly rotating stars. In the final part, we construct a class of rotating black holes in scalar-tensor theories. They are obtained by performing a disformal transformation of the Kerr solution along geodesic directions, and present many interesting properties which we analyze. We then study the orbit of stars around such objects, and discuss the present and future experimental tests which will allow us to constrain these solutions.

Université Paris-Saclay
Espace Technologique / Immeuble Discovery
Route de l'Orme aux Merisiers RD 128 / 91190 Saint-Aubin, France